Summer 2009

High-frequency sensing of Clear Creek water quality: mechanisms of dissolved oxygen and turbidity dynamics, and nutrient transport

John Vincent Loperfido
University of Iowa

HIGH-FREQUENCY SENSING OF CLEAR CREEK WATER QUALITY: MECHANISMS OF DISSOLVED OXYGEN AND TURBIDITY DYNAMICS, AND NUTRIENT TRANSPORT

by

John Vincent Loperfido

An Abstract

Of a thesis submitted in partial fulfillment
of the requirements for the Doctor of
Philosophy degree in Civil and Environmental Engineering
in the Graduate College of
The University of Iowa

July 2009

Thesis Supervisors: Professor Jerald L. Schnoor
Adjunct Assistant Professor Craig L. Just

ABSTRACT

The runoff of suspended solids and nutrients from land into the nation's lakes and rivers can have severe impacts on the health of these systems and their uses. High-frequency environmental data from sensors can provide insight into fundamental biogeochemical processes that dictate water quality and provide regulators with valuable knowledge on how to manage critical resources. The goal of this research was to utilize sensor technology, telemetry hardware, cyberinfrastructure, and water quality models to create a sensing system that will allow the investigation of the fate and transport of dissolved oxygen, suspended solids, nutrients, and other water quality parameters throughout a watershed dominated by agricultural activity. Deploying these sensors at multiple locations along the stream enabled the investigation of these processes from the fine scale to the larger watershed scale.

Results from this research addressed both fundamental science and resource management issues regarding water quality. Using high-frequency data, a dramatic diel cycle in dissolved oxygen was observed with nonlinear dynamics which was successfully modeled mathematically, and excursions in water quality criteria were observed. In addition, a diel pattern in turbidity was discovered with higher levels at night likely caused by bioturbation (i.e. nocturnal activity of bottom feeding fishes) which resulted in higher suspended solids loadings during nighttime. Furthermore, the QUAL2K model was successfully calibrated for water quality using sensor measurements and grab samples from volunteer, IOWATER data. Nutrient loading rates (nitrate–N, orthophosphate, and total dissolved solids) were estimated along the entire creek and were similar to other Iowa streams. Volunteer environmental data were found to be helpful in model calibration for some parameters (e.g. TSS and nitrate).

The construction and operation of a sensing system in Clear Creek contributed to water quality science and engineering. Findings from the configuration and field testing

of sensing station components such as water quality sensors, power systems and communication hardware will aid the design of future sensing systems and environmental observatories. Integrating the methodology of this research with future observing systems will further our understanding of water quality processes and help maintain the health and value of our nation's water environment.

Abstract Approved: _____
Thesis Supervisor

_____
Title and Department

_____
Date

_____
Thesis Supervisor

_____
Title and Department

_____
Date

HIGH-FREQUENCY SENSING OF CLEAR CREEK WATER QUALITY: MECHANISMS OF DISSOLVED OXYGEN AND TURBIDITY DYNAMICS, AND NUTRIENT TRANSPORT

by

John Vincent Loperfido

A thesis submitted in partial fulfillment
of the requirements for the Doctor of
Philosophy degree in Civil and Environmental Engineering
in the Graduate College of
The University of Iowa

July 2009

Thesis Supervisors: Professor Jerald L. Schnoor
Adjunct Assistant Professor Craig L. Just

Graduate College
The University of Iowa
Iowa City, Iowa

CERTIFICATE OF APPROVAL

PH.D. THESIS

This is to certify that the Ph.D. thesis of

John Vincent Loperfido

has been approved by the Examining Committee
for the thesis requirement for the Doctor of Philosophy
degree in Civil and Environmental Engineering at the July 2009 graduation.

Thesis Committee: _____
Jerald L. Schnoor, Thesis Supervisor

_____
Craig L. Just, Thesis Supervisor

_____
Athanasios N. Papanicolaou

_____
Larry J. Weber

_____
David A. Bennett

To Mom, Dad, and Kim for your love and support

"We abuse land because we regard it as a commodity belonging to us. When we see land as a community to which we belong, we may begin to use it with love and respect."

Aldo Leopold
A Sand County Almanac

ACKNOWLEDGMENTS

With deepest gratitude I would like to thank my advisors Jerry Schnoor and Craig Just for their scientific wisdom and expertise. In addition to exceptional teachers, they have been fantastic professional mentors and during my time at the University of Iowa have become dear friends. Thank you for all of your support.

This research would not have been possible without the assistance from Dr. Papanicolaou and his research group including Ozan Abaci and Chris Wilson with whom I was fortunate enough to spend many days wading through Clear Creek with. I would like to thank Dr. Papanicolaou, Dr. Weber, and Dr. Bennett for their insight and guidance, and for serving on my committee. I would like to acknowledge the help of Jean Ross at the Central Microscopy Research Facility for her help in obtaining images of particle in Clear Creek.

I feel truly fortunate to have had the opportunity to study in the Environmental Engineering and Sciences (EES) Program at the University of Iowa over the past five years. In addition to Dr. Schnoor and Dr. Just, I would like to thank the faculty in the EES Program including Dr. Hornbuckle, Dr. Mattes, Dr. Parkin, Dr. Scherer, and Dr. Valentine for their dedication to teaching and research. It is your commitment that made my time in this program an outstanding learning experience. The dedication of Judy Holland, Ginny Miller, Angie Schenkel, and Collin Just also cannot be overstated in making this program a great learning environment. I would like to thank all of my peers in the EES Program and in IIHR Hydroscience and Engineering for their friendship in the classroom, laboratory, and outside of school. You have made studying at the University of Iowa and living in Iowa City a once in a lifetime experience. Robert, Chris G., Drew, and Chris M. deserve special thanks for their assistance with this research.

Finally, I would like to acknowledge the support from family and friends in Iowa, Minnesota, and beyond whose patience and encouragement have been instrumental in

allowing me to follow my aspirations. To my parents, I am grateful for your unwavering love and support in everything I have done and am truly thankful. To my wife, Kim, I cannot imagine a more perfect partner to have shared the graduate school experience with and I am grateful for your tireless love and support through late nights of lab work, writing, and studying. I feel truly blessed to have you in my life.

This work was funded by the grants from the National Science Foundation's CLEANER and WATERS Network Project Offices, the Iowa Water Center, the University of Iowa Graduate College, the Center for Global and Regional Environmental Research, and by the Neil B Fisher Fellowship Committee.

ABSTRACT

The runoff of suspended solids and nutrients from land into the nation's lakes and rivers can have severe impacts on the health of these systems and their uses. High-frequency environmental data from sensors can provide insight into fundamental biogeochemical processes that dictate water quality and provide regulators with valuable knowledge on how to manage critical resources. The goal of this research was to utilize sensor technology, telemetry hardware, cyberinfrastructure, and water quality models to create a sensing system that will allow the investigation of the fate and transport of dissolved oxygen, suspended solids, nutrients, and other water quality parameters throughout a watershed dominated by agricultural activity. Deploying these sensors at multiple locations along the stream enabled the investigation of these processes from the fine scale to the larger watershed scale.

Results from this research addressed both fundamental science and resource management issues regarding water quality. Using high-frequency data, a dramatic diel cycle in dissolved oxygen was observed with nonlinear dynamics which was successfully modeled mathematically, and excursions in water quality criteria were observed. In addition, a diel pattern in turbidity was discovered with higher levels at night likely caused by bioturbation (i.e. nocturnal activity of bottom feeding fishes) which resulted in higher suspended solids loadings during nighttime. Furthermore, the QUAL2K model was successfully calibrated for water quality using sensor measurements and grab samples from volunteer, IOWATER data. Nutrient loading rates (nitrate–N, orthophosphate, and total dissolved solids) were estimated along the entire creek and were similar to other Iowa streams. Volunteer environmental data were found to be helpful in model calibration for some parameters (e.g. TSS and nitrate).

The construction and operation of a sensing system in Clear Creek contributed to water quality science and engineering. Findings from the configuration and field testing

of sensing station components such as water quality sensors, power systems and communication hardware will aid the design of future sensing systems and environmental observatories. Integrating the methodology of this research with future observing systems will further our understanding of water quality processes and help maintain the health and value of our nation's water environment.

TABLE OF CONTENTS

LIST OF TABLES iv

LIST OF FIGURES vii

CHAPTER 1: INTRODUCTION 1

Perspective 1
Research Objectives 2
Thesis Organization 3

CHAPTER 2: LITERATURE REVIEW AND SITE DESCRIPTION 5

Environmental Observatories for the Advancement of Water Science 5
Nutrient Discharge from the Agricultural Midwest and Associated Water Quality Issues 6
Water Quality Modeling 9
Review of Water Quality Models 9
QUAL2K Description 13
Hydraulic Modeling 14
Heat Balance 14
Constituents Modeled 14
Operation of the QUAL2K Model 19
Site Description 20
Current Research Efforts in the Clear Creek Watershed 21
Summary 21

CHAPTER 3: DESIGN, CONSTRUCTION, AND PERFORMANCE OF THE SENSING STATIONS IN THE CLEAR CREEK WATERSHED* 30

Abstract 30
Introduction 30
Materials and Methods 31
Deployment History of Water Quality Sensors in the Clear Creek Watershed 31
Construction of the SAC Sensing Station 32
Configuration of Hardware and Cyberinfrastructure for Data Transmission from the SAC Sensing Station 33
Results and Discussion 35
Powering an Environmental Sensing Station 35
Transmission of Water Quality Data in Near-Real Time 36
Water Quality Sensor Performance 36
Water Science Advances from High-frequency Clear Creek Water Quality Data 39
Conclusions 40

CHAPTER 4: HIGH-FREQUENCY DISSOLVED OXYGEN STREAM DATA TO INVESTIGATE DIEL PROCESSES AND WATER QUALITY CRITERION EXCURSIONS* 51

Abstract 51
Introduction 52

Materials and Methods....54
Site Description....54
Dissolved Oxygen Modeling....56
High-frequency Sensing of DO Water Quality Criteria....58
Results and Discussion....59
Temperature and Dissolved Oxygen Data....59
Temperature Effect on Modeling Results....60
Watershed Scaling of Model Parameters....62
Watershed Scaling of P/R Ratio....64
Excursions of DO Water Quality Criteria....65
Conclusions....67

CHAPTER 5: HIGH FREQUENCY SENSING TO UNDERSTAND DIEL TURBIDITY CYCLES, SUSPENDED SOLIDS AND NUTRIENT TRANSPORT IN CLEAR CREEK, IOWA*....79

Abstract....79
Introduction....79
Materials and Methods....80
Site Description....80
Field Study Methods....81
Laboratory Methods....81
Results and Discussion....82
Characterization of the Diel Turbidity Cycle....82
Mechanism for Diel Turbidity Cycles....84
Influence of Diel Turbidity on Suspended Solids and Nutrient Transport....88
Conclusions....89

CHAPTER 6: GEOSPATIAL INTERPRETATION OF PHYSICOCHEMICAL DATA FOR THE CLEAR CREEK WATERSHED....104

Abstract....104
Introduction....104
Material and Methods....105
Channel Width/Drainage Area Relationship....105
Average Annual Discharge/Drainage Area Relationship....105
Watershed Scaling of Chloride....106
Results and Discussion....107
Channel Width/Drainage Area Relationship....107
Average Annual Discharge/Drainage Area Relationship....108
Watershed Scaling of Chloride Concentrations....108
Conclusions....109

CHAPTER 7: WATER QUALITY MODELING OF HIGH-FREQUENCY SENSOR DATA AND VOLUNTEER DATA USING QUAL2K*....117

Abstract....117
Introduction....118
Materials and Methods....120
Water Quality Data Collection....120
Instream Modeling....120
Physical Model Inputs....121
Hydraulic Model Inputs....121

Chemical and Biological Model Inputs 121
Atmospheric, Light, and Heat Inputs 122
Results and Discussion 123
Comparison of IOWATER Volunteer Data to QUAL2K Modeling Results 123
Dissolved Solids 127
Conclusions 129

CHAPTER 8: ENGINEERING AND SCIENTIFC SIGNIFCANCE 147

Summary of Findings 147
Future Research 149
Conclusions 150

APPENDIX A: CLEAR CREEK WATER QUALITY DATA 2006-2008 151

2006 Water Quality Data 151
2007 Water Quality Data 160
2008 Water Quality Data 171

APPENDIX B: QUAL2K MODEL INPUT AND PARAMETER SETTINGS 176

REFERENCES 186

LIST OF TABLES

Table 2.1 Location of the first group of WATERS Network Test Beds and the participating universities. 27

Table 2.2 Water quality parameters simulated in the QUAL2K model....28

Table 2.3 Kinetic processes and mass transfer processes incorporated in the QUAL2K model....29

Table 3.1 Deployment history of data sondes deployed in the Clear Creek Watershed. 49

Table 3.2 Number of successful hourly connections between the data server in the EES Laboratory and the SAC sensing station per month from 4/20/2007 to 10/15/2007. 49

Table 3.3 Performance and maintenance attributes of water quality sensors deployed at the SAC sensing station. 50

Table 4.1 Drainage area, distance from headwaters, channel width, water depth, mean discharge, and calculated mean velocity at the SAC, Oxford, and Coralville sensing stations in the Clear Creek Watershed. 78

Table 4.2 Reaeration rate constants, respiration rates, and average primary production rates at a reference temperature of 20° Celsius determined from optimization of Model M1. 78

Table 4.3 Fraction of surface light energy available at the creek bed in the Clear Creek Watershed. 78

Table 5.1 Coefficient of determination (R^2) values from linear regression analyses between $\log_{10}$ turbidity and $\log_{10}$ TSS, $\log_{10}$ fixed suspended solids, and $\log_{10}$ volatile suspended solids from grab samples in Figure 5.3 collected on 9/18/2007 and 9/19/2007. 102

Table 5.2 Comparison of estimated TSS loading from the SAC under different conditions: daytime versus nighttime loading during base flow (9/12/2007 – 10/2/2007), storm event versus base flow loading (9/12/2007 – 10/15/2007), and sampling strategy using high-frequency sensors versus daily noon grab samples (9/12/2007 – 10/15/2007). 102

Table 5.3 Total suspended phosphorus (as PO_4^{3-}) concentrations and loading from the SAC during daytime and nighttime from 10:34 on 9/18/2007 to 10:34 on 9/19/2007. 103

Table 6.1 Predicted values of average annual discharge at the two Clear Creek gaging stations compared to the measured average annual discharges. 116

Table 7.1 Data sources used to describe physical feature model inputs to model Clear Creek using QUAL2K. 141

Table 7.2 Discharge values prescribed to tributaries entering Clear Creek between the SAC and Oxford sensing stations based on tributary drainage area. 142

Table 7.3 Discharge values prescribed to tributaries entering Clear Creek between the Oxford and Coralville sensing stations based on tributary drainage area. 143

Table 7.4 Chemical and biological upstream boundary conditions at the SAC sensing station and tributaries along the main channel used for QUAL2K modeling of Clear Creek. 144

Table 7.5 Water yield, areal nitrate loading rate, and areal orthophosphate loading rate during May, 2008 calculated for Clear Creek (this study) and for other Iowan Watersheds. 145

Table 7.6 Average daily water yield, nitrate areal loading rate, and orthophosphate areal loading rate for Iowan Watersheds from 1980 to 1996. 146

Table A.1 Water quality samples collected at the SAC sensing station during 2006 157

Table A.2 Water quality measurements taken at the SAC sensing station during 2006 using a Hach Quanta G data sonde. 158

Table A.3 Water quality measurements from sensors placed at the SAC sensing station from 8/03/2006 to 8/04/2006 159

Table A.4 Water quality samples collected at the SAC sensing station during 2007[a]. 166

Table A.5 Water quality samples collected at the SAC sensing station during the 28-hour study on 9/18/2007 and 9/19/2007. 167

Table A.6 Phytoplankton enumeration and identification from grab samples collected on 9/18/2007 and 9/19/2007 at the SAC sensing station. 168

Table A.7 Zooplankton enumeration and identification from grab samples collected on 9/18/2007 and 9/19/2007 at the SAC sensing station. 169

Table A.8 Water quality measurements from sensors placed at the SAC sensing station from 9/18/2007 to 9/19/2007 170

Table B.1 Physical parameters of Clear Creek reaches modeled in QUAL2K. 176

Table B.2 Temperature, specific conductivity, DO, and pH boundary conditions for QUAL2K modeling of Clear Creek at the SAC sensing station and all tributaries (T1-T14) based on instream sensor measurements collected at the SAC sensing station. 177

Table B.3 Inorganic suspended solids and detritus boundary conditions for QUAL2K modeling of Clear Creek at the SAC sensing station and all tributaries (T1-T14). 178

Table B.4 Nitrate boundary conditions and assumptions for QUAL2K modeling of Clear Creek at the SAC sensing station and all tributaries (T1-T14). 179

Table B.5 Stoichiometry, phytoplankton and bottom algae rates prescribed for QUAL2K modeling of Clear Creek. 180

Table B.6 Chemical and suspended solids rates prescribed for QUAL2K modeling of Clear Creek. 181

Table B.7 Oxygen and CBOD rates prescribed for QUAL2K modeling of Clear Creek. 182

Table B.8 Air temperature, dew point, and wind speed input for QUAL2K modeling of Clear Creek. 183

Table B.9 Light parameters and surface heat transfer models prescribed for QUAL2K modeling of Clear Creek. 184

Table B.10 Creek shading inputs for each hour throughout the modeling period for QUAL2K modeling of Clear Creek. Shading values were determined by calibrating QUAL2K temperature results to instream sensor measurements. 185

LIST OF FIGURES

Figure 2.1 QUAL2K DO simulated profiles for various CBOD point loads with restrictions of 0.3 mg L^{-1} TN from point sources, 1 m^3 s^{-1} flow augmentation and weirs at 12.5 km, 13.5 km and 14.5 km (Source: Kannel et al. 2007). 23

Figure 2.2 Transformation of a hypothetical river (A) into the QUAL2K representation of that river (B) (Adapted from Chapra et al. 2006). 24

Figure 2.3 Processes included in the general mass balance in the modeling of QUAL2K water quality parameters for a segment without a tributary (Adapted from Chapra et al. 2006). 25

Figure 2.4 The Clear Creek Watershed located in east-central Iowa. USGS Gaging stations are present in the middle of the watershed and at the outlet which drains to the Iowa River. 26

Figure 3.1 Locations of sensing stations used for deployment of high-frequency water quality sensors in the Clear Creek Watershed for this research. 42

Figure 3.2 The SAC Sensing Station located in the headwaters of the Clear Creek Watershed during 2006 (A) and 2007/2008 (B). 43

Figure 3.3 Hydrolab DS5X data sonde deployed at the SAC sensing station 44

Figure 3.4 Battery voltage at the SAC sensing station during 2006 and 2007 when powering a Hydrolab DS5X data sonde, CR1000 Data logger, Redwing 100 CMDA Cellular Modem, and a CH100 12 Volt Charger/Regulator. The addition of the DTS-12 Turbidity Sensor in September 2007 resulted in a decreasing trend in battery voltage. 45

Figure 3.5 Average monthly (A) and daily (B) successful connection rates between the data server in the EES Laboratory and the SAC sensing station from 4/21/2007 to 10/15/2007 46

Figure 3.6 High-frequency DO measurements collected at the SAC sensing station during 2006 (A) exemplify the ability of an environmental observatory to transform the understanding of fundamental hydrologic processes (B) and inform water resources management decisions (C). 47

Figure 3.7 Dissolved oxygen measurements collected at the SAC, Oxford and Coralville sensing stations from 5/9/2008 to 5/12/2008. 48

Figure 4.1 Location of the South Amana Catchment sensing stations during 2006 (SAC-2006) and 2007/2008 (SAC), and the Oxford, and Coralville sensing stations in the Clear Creek Watershed. 69

Figure 4.2 High-frequency air temperature ——, water temperature (A), and DO (B) data collected at the SAC, Oxford and Coralville sensing stations every 15 minutes. 70

Figure 4.3 DO modeling results from Model M1 ——— and Model M2 ——— compared to high-frequency DO measurements ○ and DO saturation concentrations – – – at the SAC (A), Oxford (B), and Coralville (C) sensing stations in the Clear Creek Watershed. 71

Figure 4.4 DO mass rates into the Clear Creek water column due to primary production ———, reaeration ———, and respiration ——— rates determined from high-frequency measurements and optimized with Model M1 using temperature change factors for sensing stations at the SAC (A), Oxford (B), and Coralville (C) in the Clear Creek Watershed. 72

Figure 4.5 Scaling of reaeration rate constant, average primary production and respiration rates at a reference temperature of 20°C from Model M1 versus drainage area in the Clear Creek Watershed. Average primary production values are averages of values for day 1 and day 2 of the model simulation. 73

Figure 4.6 Scaling of $\overline{P}_{av} / \overline{R}$ ratio (average primary production rate to respiration rate) at a reference temperature of 20°C versus drainage area in the Clear Creek Watershed. Average primary production values are averages of values for day 1 and day 2 of the model simulation.....74

Figure 4.7 DO data collected during 2006 and 2007 (●) statistically sampled to simulate daily noon grab samples (○). Iowa DNR water quality criterion excursions were frequently observed in 2006 whereas, DO excursions were only observed during one event in 2007. 75

Figure 4.8 Dissolved oxygen measurements from 9/7/06 to 9/10/06 in Clear Creek show periods of super-saturation and violations of Iowa DNR water quality criteria. 76

Figure 4.9 Box plot showing the average annual discharges at the Coralville and Oxford USGS gaging stations in the Clear Creek Watershed with 10^{th} and 90^{th} percentiles (whiskers), 5^{th} and 95^{th} percentiles (○), and average annual discharge values from 2006, 2007, and 2008 (◊). Data source: USGS (2008a).....77

Figure 5.1 Location of the Clear Creek HUC 10 study area with respect to Iowa and the Iowa River. Experiments in this study were performed at the environmental sensing station (▲) at the outlet of the SAC (shaded area). 91

Figure 5.2 High-frequency turbidity (A) and discharge (B) data from the SAC sensing station observed from 9/11/2007 to 10/16/2007 by in situ water quality sensors. The diel cycling in turbidity during base flow periods is shown by the inset with high turbidity at night and low turbidity values during the day. Storm events on 10/2/2007 and 10/14/2007 led to the highest turbidity and discharge measurements during the monitoring period. 92

Figure 5.3 Sensor (○) and grab sample (Δ) measurements of turbidity (A), fixed suspended solids (B), and volatile suspended solids (C) from 11:00 on 9/18/2007 to 14:00 on 9/19/2007. Averages of duplicate suspended solids samples are shown for data points at 11:00 on 9/18 and 00:10, 6:10, and 13:59 on 9/19.....93

Figure 5.4 SEM images of Clear Creek TSS filtered from grab samples during periods of low (A) and high (B) turbidity collected at 13:03 and 19:59 on 9/18/2007, respectively.....94

Figure 5.5 EDX images of TSS filtered from Clear Creek during daytime and nighttime on 9/18/2007 indicated the particles are largely comprised of silicon, aluminum, iron, and oxygen. 95

Figure 5.6 Turbidity measurements from 9/11/2007 to 10/2/2007 averaged for each measurement in the daily cycle. Error bars indicate one standard deviation for each set of measurements. The vertical gray bars indicate the range of sunrise and sunset times during the data period (sunrise/sunset data source: AAD (2008)).....96

Figure 5.7. Turbidity measured in Clear Creek (○) and in plexiglass boxes deployed in Clear Creek on 11/15/2007 and 11/16/2007. 97

Figure 5.8 XRD analysis of Clear Creek bed sediment indicated a large presence of quartz (SiO_2).....98

Figure 5.9 Linear regression (—) and 95% prediction intervals (— — —) of log transformed TSS and turbidity data from the Clear Creek Watershed (○) and the Iowa River (□). 99

Figure 5.10 Estimated TSS loading rates from the SAC from 9/11/2007 to 10/16/2007. 100

Figure 5.11 Total suspended phosphorus concentrations in Clear Creek on 9/18/2007 and 9/19/2007. 101

Figure 6.1 SAC and Conroy branches of Clear Creek included in regression models relating distance upstream from the Coralville USGS gaging station to mean May IOWATER measurements from 2004 to 2007.....110

Figure 6.2 Channel width measurements in the Clear Creek Watershed on 4/28/2008 when the average daily discharge at the USGS gaging station in Coralville near the mouth of the watershed was 9.1 $m^3 s^{-1}$.....111

Figure 6.3 Linear regression model predicting channel width in the Clear Creek Watershed on 4/28/2008 based on drainage area to that point (n = 23). The average daily discharge measured at the USGS gaging station in Coralville was 9.1 $m^3 s^{-1}$. 112

Figure 6.4 Linear regression of $\log_{10}$ drainage area versus $\log_{10}$ average annual discharge at 83 USGS gaging stations in eastern Iowa.....113

Figure 6.5 Average chloride concentrations (mg L^{-1}) from available May IOWATER Snapshot sampling events during 2004 to 2007 in the Clear Creek Watershed during May. 114

Figure 6.6 Average chloride concentration (mg L-1) from available May IOWATER Snapshot sampling events during 2004 to 2007 versus distance upstream from the Coralville sensing station in the main channel of Clear Creek and the Conroy tributary. 115

Figure 7.1 High-frequency sensors were deployed at three sensing stations (▲) on 5/9/2008 and 5/10.2008 in the Clear Creek Watershed located in east-central Iowa. IOWATER volunteers sampled at eight locations in the main channel of Clear Creek (●), including at the SAC and Coralville sensing stations on 5/10/2008. Data from high-frequency sensors and IOWATER were used to calibrate the QUAL2K model in the main channel of Clear Creek from the SAC sensing station to the Coralville sensing station. 131

Figure 7.2 Clear Creek discharge measurements (○) from 5/9/2008 versus distance upstream from the Coralville sensing station used to calibrate the QUAL2K water quality model (—). 132

Figure 7.3 QUAL2K Temperature results calibrated to Hydrolab DS5X sensor data (box plot with errors bars equal to 10th and 90th percentiles; outliers, (●) collected on 5/9/2008 and 5/10/2008 compared to IOWATER measurements (Δ) collected on 5/10/2008 versus distance upstream from the Coralville sensing station. 133

Figure 7.4 QUAL2K DO results calibrated to Hydrolab DS5X sensor data (box plot with error bars equal to 10th and 90th percentiles; outliers, (●) collected on 5/9/2008 and 5/10/2008 compared to IOWATER measurements (Δ) collected on 5/10/2008 versus distance upstream from the Coralville sensing station. 134

Figure 7.5 QUAL2K TSS results calibrated using TSS estimations from Hydrolab DS5X turbidity data (A, box plot with error bars equal to 10^{th} and 90^{th} percentiles; outliers, (●) from 5/9/2008 and 5/10/2008 and IOWATER transparency measurements (B) used in tandem versus distance upstream from the Coralville sensing station. 135

Figure 7.6 QUAL2K pH results calibrated to Hydrolab DS5X sensor data (box plot with error bars equal to 10^{th} and 90^{th} percentiles and outliers, (●) collected on 5/9/2008 and 5/10/2008 compared to IOWATER measurements (Δ) collected on 5/10/2008 versus distance upstream from the Coralville sensing station. 136

Figure 7.7 QUAL2K total dissolved solids results (A) calibrated to Hydrolab DS5X sensor data (box plots with error bars equal to 10th and 90th percentiles and outliers, (●) collected on 5/9/2008 and 5/10/2008 and QUAL2K orthophosphate results calibrated to IOWATER (□) collected 5/10/2008 versus distance upstream from the Coralville sensing station. 137

Figure 7.8 QUAL2K nitrate results calibrated to grab samples collected by IOWATER and analyzed by the University of Iowa Hygienic Laboratory (○) on 5/10/2008 compared to IOWATER measurements (Δ) collected on 5/10/2008 versus distance upstream from the Coralville sensing station. 138

Figure 7.9 TDS, nitrate, and orthophosphate loading rates versus distance upstream from the Coralville sensing station and drainage area (log_{10} – log_{10} scale) in the Clear Creek Watershed on 5/10/2008 calculated using results from QUAL2K. 139

Figure 7.10 TDS, nitrate and, orthophosphate areal loading rates (A) and water yield (B) versus distance upstream from the Coralville sensing station in the Clear Creek Watershed on 5/10/2008. 140

Figure A.1 Temperature measurements from water quality sensors deployed at the SAC sensing station during 2006. 151

Figure A.2 pH measurements from water quality sensors deployed at the SAC sensing station during 2006. 152

Figure A.3 Specific conductivity measurements from water quality sensors deployed at the SAC sensing station during 2006. 153

Figure A.4 Turbidity measurements from water quality sensors deployed at the SAC sensing station during 2006. 154

Figure A.5 Dissolved oxygen measurements from water quality sensors deployed at the SAC sensing station during 2006. 155

Figure A.6 Battery voltage from at the SAC sensing station during 2006. 156

Figure A.7 Temperature measurements from water quality sensors deployed at the SAC sensing station during 2007. 160

Figure A.8 pH measurements from water quality sensors deployed at the SAC sensing station during 2007. 161

Figure A.9 Specific conductivity measurements from water quality sensors deployed at the SAC sensing station during 2007. 162

Figure A.10 Turbidity measurements from water quality sensors deployed at the SAC sensing station during 2007. 163

Figure A.11 Dissolved oxygen measurements from water quality sensors deployed at the SAC sensing station during 2007. 164

Figure A.12 Battery voltage from at the SAC sensing station during 2007. 165

Figure A.13 Temperature measurements collected at the SAC, Oxford and Coralville sensing stations from 5/9/2008 to 5/12/2008. 171

Figure A.14 pH measurements collected at the SAC, Oxford and Coralville sensing stations from 5/9/2008 to 5/12/2008. 172

Figure A.15 Specific conductivity measurements collected at the SAC, Oxford and Coralville sensing stations from 5/9/2008 to 5/12/2008. 173

Figure A.16 Turbidity measurements collected at the SAC, Oxford and Coralville sensing stations from 5/9/2008 to 5/12/2008. 174

Figure A.17 Chlorophyll a measurements collected at the SAC, Oxford and Coralville sensing stations from 5/9/2008 to 5/12/2008. 175

CHAPTER 1:

INTRODUCTION

Perspective

Swimmable and fishable: that is the goal of our nation's Clean Water Act, but we are still far short of reaching it. About 40% of the nation's water bodies are polluted, mostly from diffuse-source runoff (US EPA 2000). Pollutants leading to poor water quality in our waters include suspended solids, pathogens, and nutrients such as nitrogen and phosphorus. In Iowa, almost 150 lakes and rivers were listed as "impaired" by the Iowa Department of Natural Resources (Iowa DNR) during a 2004 assessment (Iowa DNR 2007a). This includes Clear Creek in the Iowa River Basin, which is located directly west of Iowa City.

Recent advances in sensor technology make possible the high-frequency determination of water quality measurements as well as an increased variety of parameters (Tränkler and Kanoun 2001; Chong and Kumar 2003; Alcock 2004; Martinez-Manez et al. 2005; Rogers 2006). These technologies, when coupled with telemetry hardware, such as modems and data loggers, may be used to relay water quality measurements in near real-time (minutes to hours) to decision-making agencies. Measurements could also be input directly into models creating near real-time predictions of downstream water quality. Decision makers may then use these forecasts to make timely decisions on how to best utilize their resources. The high-frequency nature of the data may also reveal unexpected biogeochemical phenomena. In a manner analogous to monthly carbon dioxide measurements at the Mauna Loa Observatory revealing atmospheric processes occurring on a seasonal and decadal time scale (Thoning et al. 1989), high-frequency data from *in situ* water quality sensors could reveal processes occurring on hourly and daily time scales.

Once constructed, the WATERS Network will provide the framework to help researchers make these new discoveries with using high-frequency environmental data and use this data to warn resources managers of future environmental events via water quality forecasts (Montgomery et al. 2007). This network will be comprised of environmental sensors, cyberinfrastructure, databases, and environmental models that will "transform the understanding of the earth's water and related biogeochemical cycles across multiple spatial and temporal scales" (Montgomery et al. 2007). However, before the network can be constructed, research is required on how to best utilize the recent advances in sensor and cyberinfrastructure technologies, and how to glean new understanding from the high-frequency data promised by the network.

The goal of this research was to construct and operate a system with these capabilities in the Clear Creek Watershed in Iowa. This system, a sensing station within an environmental observatory, was comprised of sensors, data loggers, and water quality models. This sensing station enables the discovery of fundamental biogeochemical processes that dictate Clear Creek water quality, and provides insight on the factors affecting the design and operation of the WATERS Network. What follows are research objectives, review of significant literature, and results and findings in the investigation of high-frequency water quality data collected in Clear Creek, Iowa.

Research Objectives

The **overall objective** of this research is to understand the mechanistic processes of dissolved oxygen (DO), turbidity, and nutrients (nitrogen and phosphorus) from the 1st and 2nd order stream (fine scale) to the larger watershed area in an intensive agricultural setting. In doing this, a Clear Creek sensing station was constructed and new phenomena were uncovered by collection of high-frequency water quality data. To complete the main objective, the following **sub-objectives** and associated hypotheses were tested.

Sub-Objective #1 (SO1). Previously undiscovered biogeochemical phenomena can be detected in the Clear Creek Watershed using high-frequency data (20 minute period) collected by an environmental observatory. Preliminary data allowed the following specific hypotheses to be posed:

Hypothesis #1 (SO1/H1): Nighttime increases in DO concentrations are due to an increased reaeration flux driven by decreases in water temperature at the small scale of a low order stream which can be modeled mathematically.

Hypothesis #2 (SO1/H2): Diel turbidity cycles are due to aluminosilicate clay particles suspended via bioturbation by nocturnal fishes.

Sub-Objective #2 (SO2). High-frequency data from a sensing station in an environmental observatory can be used to determine water quality impairments that may be missed using traditional sampling methods.

Hypothesis #1 (SO2/H1): Critical periods for DO occur during nighttime due to the respiration of photosynthetic organisms.

Hypothesis #2 (SO2/H2): The magnitude of suspended solids daily loads determined by grab sampling is inaccurate due to the high temporal variation in suspended solids loadings during storm events and diel cycles.

Thesis Organization

This thesis contains eight chapters to address the sub-objectives described above. Chapter 2 contains a review of the literature regarding environmental observatories, nutrient discharge, and water quality models including the QUAL2K Water Quality Model (QUAL2K). Chapter 2 also contains a site description of the Clear Creek Watershed, the location where sub-objectives 1 and 2 were tested.

Chapter 3 describes and investigates the design, construction, and performance of the sensing stations in Clear Creek. This includes factors such as power, transmission of environmental data, and performance of *in situ* sensors. Specific information on the

construction and configuration of the environmental sensing station located at the South Amana Catchment (SAC) is also provided in this chapter.

Chapter 4 investigates the DO dynamics at sensing stations in the Clear Creek Watershed (SO1/H1, SO2/H1). Nighttime increases in DO concentrations were investigated using a mass balance model. Modeling results also revealed how DO modeling parameters scaled throughout the watershed. Results from this research have been accepted for publication in the *Journal of Environmental Engineering* (Loperfido et al. 2009). DO data from 2006 and 2007 were analyzed for the presence of water quality criterion excursions.

Chapter 5 investigates the biogeochemical phenomenon of diel turbidity cycles observed at sensing stations in Clear Creek. Specifically, this chapter characterizes the particles responsible for the diel turbidity cycles, investigates the cause of the cycles (SO1/H2), and the implications of diel turbidity cycles on the export of suspended solids and nutrients from the SAC (SO2/H2). A manuscript of this research has been submitted for review to *Water Resources Research*.

Chapter 6 and Chapter 7 address the scaling of water quality data throughout the Clear Creek Watershed. In Chapter 6, environmental data sets containing channel width, discharge, and chloride concentrations were modeled using GIS software to understand the spatial scaling of these parameters. In Chapter 7, water quality data collected by sensors and a volunteer monitoring organization, IOWATER, were used to calibrate QUAL2K. A manuscript of this research is currently in preparation. Input data and parameters used for the QUAL2K model are presented in Appendix B.

Chapter 8 summarizes the findings from this research and the implications to environmental observatories. Future research areas suggested by this research are also presented in Chapter 8. Water quality data collected during this research is located in Appendix A.

CHAPTER 2:
LITERATURE REVIEW AND SITE DESCRIPTION

Environmental Observatories for the Advancement of Water Science

As the effects of climate change are fully realized, current hydrological models based on assumptions of an unchanging envelope of climatological variability will become obsolete (Milly 2008). Climate change will alter both the magnitude and frequency of precipitation events (Christensen et al. 2007), leading to changes in discharge and pollutant loading in streams and rivers. In the agricultural Midwest, an increase in extreme precipitation events will lead to increases in discharge (Miller and Russell 1992; Christensen et al. 2007) and nutrient export to the Gulf of Mexico worsening the already problematic hypoxic zone (Justić et al. 1996). In addition to climate change, global stressors such as human population growth, water use, and the need for biofuels will further strain the supply of freshwater for agricultural and consumptive use (Zimmerman et al. 2008).

Advances in water science must be made to fully comprehend how climate change and other water stressors will affect freshwater supply and to mitigate the effects of climate change. Environmental observatories offer a paradigm shift in how natural and anthropogenic fluxes of water and pollutants are studied and predicted. The high-frequency nature of environmental data from these observatories will allow researchers to understand fine-scale processes occurring in the water cycle including nonlinear pollutant transport during extreme precipitation events. Transmission of real-time water quantity and water quality measurements during these extreme events can be used as input to updated hydrological models.

The WATERS Network is an environmental observatory that aims to "transform the understanding of the earth's water and related biogeochemical cycles across multiple

spatial and temporal scales." (Montgomery 2007), and it was formed by the joining of two national initiatives, CLEANER (Collaborative Large-Scale Engineering Analysis Network for Environmental Research) and CUAHSI (Consortium of Universities for the Advancement of Hydrologic Science) (Montgomery et al. 2007). Currently, there are several WATERS Test Bed projects to investigate aspects of constructing a nation-wide observatory, such as development of sensors, real-time transmission of data, and data storage (WATERS 2009). These Test Beds are located in vastly different environments to gain experience on operating sensing stations exposed to different climatic elements, as well as to gain understanding of different biogeochemical processes that occur in these environments. The first group of WATERS Test Beds that were originally funded exemplifies this range of environments and is listed in Table 2.1.

Nutrient Discharge from the Agricultural Midwest and Associated Water Quality Issues

In coastal waters, widespread episodes of depressed DO levels have made a significant impact on those ecosystems' abilities to maintain an abundant, healthy, and diverse population of local fauna (Breitburg 2002; Gray et al. 2002). Episodes of DO concentrations below 2 mg L^{-1} are known as hypoxia (Rabalais et al. 1999). Hypoxia has been documented off the coasts of several countries worldwide including Japan, Namibia, Sweden and the United States (Hamukuaya et al. 1998; Nordberg et al. 2001; Rabalais et al. 1996; Suzuki 2001). The largest hypoxic zones in the world are in the Baltic Sea which reaches up to 84,000 km^2 (Rosenberg 1985; Rabalais et al. 2002) and in the Black Sea which reaches up to 40,000 km^2 (Mee 2001; Rabalais et al. 2002). In the United States, a significant hypoxic zone exists on the northwestern continental shelf of the Gulf of Mexico. This zone was estimated to cover approximately 16,000 km^2 to 20,000 km^2 during the time span from 1993 to 2000 (Rabalais et al. 2001). Hypoxic waters in the Gulf of Mexico mainly prevail near the bottom of the water column, in the benthic zone.

They can include up to 80% of the total column in more shallow waters (Rabalais et al. 2001) with the most extreme events seen during June, July, and August (Rabalais et al. 1999). The predominant ecological effects of hypoxia seen in the Gulf of Mexico include mortality, elimination of larger species, elimination of longer lived species, and a shifting of productivity to non-hypoxic periods (Diaz and Solow 1999). The US EPA currently has a goal to reduce the five-year average areal extent of the hypoxic zone to 5000 km^2 (US EPA 2007a) by 2015.

Two factors contribute to gulf hypoxia: stratification of the water column and the input of nutrients to the gulf coast (Rabalais et al. 2002). Nutrients input into the Gulf of Mexico are incorporated into the phytoplankton community. Phytoplankton not consumed by higher organisms sink to the gulf bed, where bacteria aerobically decompose the biomass, creating an oxygen demand. Stratification of the colder and more saline ocean water below the less dense fresh water from the Mississippi River isolates it from reaeration processes occurring at the water surface-air interface. The presence of an oxygen demand and lack of reaeration processes can create hypoxic conditions that last months at a time. In the Gulf of Mexico, approximately a two month lag period has been observed for the input of nutrients to create an oxygen deficit (Justic et al. 1993).

Nutrients that increase primary production rates in the Gulf of Mexico include nitrate-nitrogen and to some extent, phosphorus and silica (Lohrenz et al. 1997; Rabalais et al. 1999). Nutrient concentrations in coastal waters have been positively correlated with the percentage of agricultural land existing in the drainage basin of that coastal water (Handler et al. 2006). This is exemplified in the Mississippi River basin as approximately 35% of the nitrogen discharged into the Gulf of Mexico originates from the agriculturally intensive states of Iowa and Illinois (Goolsby et al. 2001). Annual discharges of nitrogen, phosphorus and silica into the Gulf of Mexico are 1.6 x 10^6 t yr^{-1},

0.1×10^6 t yr^{-1} and 2.1×10^6 t yr^{-1} respectively, and are increasing (Goolsby et al. 2001; Rabalais et al. 1999).

Discharge of these nutrients from agricultural lands does not occur continuously and is largely associated with the most extreme precipitation events. A study analyzed the loading of nitrate, orthophosphate, and organic phosphorus from three agricultural watersheds in Illinois and found that extreme discharges ($\geq 90^{th}$ percentile) accounted for >50% of the nitrate export and >80% of the total phosphorus discharge (Royer et al. 2006). While nitrate export was due to drain tile discharge, total phosphorus discharge occurred both through drain tile discharge and overland flow. These nonlinear nutrient releases largely dictate the annual amount of nutrients and suspended solids discharged from an agricultural field into nearby waterbodies.

Spatial heterogeneities in the release of nutrients and soil in a watershed can occur due to variations in the application of fertilizer and the degree to which agricultural soils erode. Two sub-watersheds in the Cottonwood River watershed in Minnesota were found to differ considerably in the amount of nitrogen and phosphorus applied to agricultural lands despite similarities in landscape and crop production (Strock et al. 2005). A study of an Iowa watershed and two of its subbasins found that the concentration of nitrate was higher in the outlet of the subbasins than in the watershed outlet (Tomer et al. 2003). This highlights the spatial variation of nutrient discharge that can occur inside a single watershed. The presence of drain tile also plays a key role in the discharge of nutrients into surface waters. A positive log-log relation between drain tile installation and effluent nitrate concentration has been observed (Hofmann et al. 2004). This is an extremely important factor to consider in the highly tiled Midwest.

The literature stresses the issue of heterogeneity that is involved in the release of nutrients. Along with the nonlinear of nutrient release, “hot spots” of nutrient release must be identified and understood in order to curb the flow of nutrients into the Gulf of Mexico. An environmental observatory with sensors collecting instream measurements

could allow for the detection and further understanding of nutrient fluxes from the agricultural Midwest. As climate change increases nutrient export during extreme events (Miller and Russell 1992; Justić et al. 1996; Christensen et al. 2007), the high-frequency nature of data from an environmental observatory will be critical for the implementation of nutrient pollution mitigation strategies necessary to protect the Gulf of Mexico.

Water Quality Modeling

Review of Water Quality Models

Water quality models will be an integral part of the advancement of water science when integrated with an environmental observatory and high-frequency data. These models will use data from multiple sources including sensors deployed *in situ*, data from monitoring agencies such as the US Geological Survey (USGS), and data in historical databases such as that from volunteer water quality monitoring organizations. Modeling using data transferred from sensing stations in real-time could aid hydrological predictions and management decisions. The high-frequency nature of the data can be used in modeling processes to discover and understand previously unknown biogeochemical processes. For this research, several models, including those supported by the US EPA, were considered for use in modeling the Clear Creek Watershed and are summarized below.

Water Analysis Simulation Program version 7 (WASP7) is a three-dimensional box model that simulates fate and transport in surface waters (Wool et al. 2008). With chemical and biological constituents modeled in WASP7 including carbonaceous biochemical oxygen demand (CBOD), DO, nutrients, phytoplankton, and benthic algae, this model has been used to assess eutrophication and volatile organic compounds in estuaries and rivers (US EPA 2007b). Hydraulics can be simulated as steady or unsteady flow and processes modeled include advection and dispersion. The model can operate on several different timescales including, hourly, daily, and monthly.

AQUATOX is a process-based instream ecological model that simulates nutrients, DO, organic and inorganic sediments, toxic inorganic sediments, phytoplankton, invertebrates, and fishes (US EPA 2007b). This model can be applied to rivers and vertically stratified lakes and simulates the nutrient cycle, DO dynamics, partitioning of organic toxicants, and toxic organic chemical transformations. AQUATOX is primarily used as a water quality criteria, Total Maximum Daily Load (TMDL), and ecological risk assessment model. Hydraulic inputs required for the model are minimal and include volume, inflow, outflow, and velocity.

The Soil Water Assessment Tool (SWAT) is a GIS-based basin-scale watershed model that simulates hydrology, sediment, nutrient, and pesticide yields from ungaged drainage areas (Pullar and Springer 2000; Borah et al. 2006; Gassman et al. 2007). SWAT can also simulate the effect of agricultural management changes on water quality and water quantity. A SWAT study area is divided into subwatersheds and further divided into hydrological response units (HRUs), where a water balance on a daily time step is simulated (Gassman et al. 2007). Spatial data required to perform the water balance includes climate data, land use data, topology map, and management practices maps. Runoff volume is simulated using the SCS curve number method (Borah et al. 2006). Sediment yields are calculated using the Modified Universal Soil Loss Equation (MUSLE) and instream kinetics are simulated based on the QUAL2E model (Gassman et al. 2007). This model has been widely used for the assessment of non-point source loading throughout the United States (Cheng et al. 2007).

Hydrological Simulation Program--Fortran (HSPF) is a watershed model that simulates surface runoff processes and instream hydraulic and water quality processes (Borah et al. 2006). Constituents modeled include conventional pollutants like CBOD, nutrients, and sediments, as well as toxic organic pollutants. HSPF has been used to assess land use change, point and non-point source pollution, and reservoir operations.

Instream hydraulics are simulated in one dimension and are modeled with time steps ranging from one minute to one day.

The SPARROW (SPAtially Referenced Regressions On Watershed attributes) model supported by the USGS is a statistical model that relates watershed characteristics such as land use and soil type to instream water quality concentrations and loads in receiving streams (Schwarz et al. 2006). Although statistical in nature, the SPARROW model does include some physically based processes like mass balance requirements. Constituent loads from watersheds determined in the model are calculated on an annual basis and the SPARROW model has been used to calculate annual loads of nitrogen, phosphorus, suspended solids, pathogens, and organic contaminants (Preston et al. 2009).

After careful consideration of the models described above and others, the instream water quality model chosen for this research was the US EPA (US EPA 2007b) supported QUAL2K River and Stream Water Quality Model (QUAL2K). QUAL2K is a modernized version of the QUAL2E developed by Brown and Barnwell (1987) that employs Microsoft Excel as the graphical user interface. There are currently two versions of QUAL2K available: version 2.11b8 of QUAL2K an updated version based on QUAL2K 2.04 developed by Chapra et al. (2006) and the QUAL2Kw model supported by the Washington State Department of Ecology (Washington State Department of Ecology 2007). Although these models have significant differences, they were both developed from QUAL2K version 1.4 created in 2004 (Greg Pelletier, personal communication, Apr. 17, 2007). There are two key differences between the current versions of the QUAL2K model. First, QUAL2Kw contains a genetic algorithm for the automatic calibration of kinetic rate parameters while QUAL2K does not (Pelletier et al. 2006). Second, QUAL2K has the ability to model a main channel with several tributaries whereas QUAL2Kw may only be used to model a main channel without a branching stream network.

Both versions of the QUAL2K model have been used to assess the fate and transport of pollutants in the literature. QUAL2K has been used to perform TMDL analyses (e.g. Boyacioglu and Alpaslan 2008; Chen and Ma 2008) and to estimate riverine pollution loading for input into a lake model (Capodaglio et al. 2005). The QUAL2Kw model has been used to evaluate the potential effectiveness of pollution reductions strategies in the Bagmati River in Nepal (Kannel et al. 2007). Results from the implementation of CBOD and total nitrogen (TN) point source restrictions investigated in that study are shown in Figure 2.1. A point of confusion in the literature is a report from Park and Lee (2002) that like Chapra et al. (2006) developed a model titled QUAL2K; however, this model is not supported by the US EPA (2007b).

QUAL2K is a time-variable, steady flow model with constant coefficients in each designated reach of the stream. It accounts for nutrient, temperature, suspended solids, and DO dynamics. The principal advantage of the QUAL2K model is its ability to incorporate hourly data like that obtained from sensing stations in the Clear Creek Watershed. Although WASP7 can model on an hourly time scale, the ease of incorporating and viewing hourly water quality data in QUAL2K made QUAL2K more ideal for this study. The other instream model, AQUATOX, contained ecological modeling elements that were outside of the scope of this study and would have required additional data collection. The SPARROW model was not suitable for this research due to its inability to simulate water quality on an hourly timescale and detailed physically based processes. HSPF was not selected due to the requirement of detailed spatial data. A significant strength of QUAL2K in the application to near real-time modeling is its relatively short run-times, which are on the order of seconds to minutes (Borah et al. 2006). The SWAT model has longer run-times on the order of minutes to hours which would reduce its utility as a near real-time water quality forecasting model in some applications.

QUAL2K Description

As stated above, QUAL2K has the ability to simulate a system comprised of a main branch and several tributaries. This model is one-dimensional with the assumption that the channel is well mixed in the vertical and lateral directions. All hydraulics are simulated as steady state with non-uniform flow (i.e. water depth and velocity may vary depending on location in the channel). The model captures diel variations as water quality kinetics and the heat budget are determined on a diel time scale. The following description of QUAL2K is modified from the QUAL2K documentation manual (Chapra et al. 2006).

QUAL2K divides a study river into segments called reaches, which are further divided into elements. Elements are the basic computational unit (spatial step, Δx) from which all calculations are performed. Reaches are assigned based on the physiographic characteristics and hydraulics present in the study river; sections of river with similar slope, Manning roughness coefficient, bottom width, and side slope will be defined as a reach. Other factors also defining reaches include constant longitudinal dispersion, bottom algae coverage, bottom sediment oxygen demand (SOD) coverage, and the rate constants for mass transfer (to the air and sediment) of oxygen, methane, ammonium, and inorganic phosphorus. A QUAL2K model representation of a study river is created by sequentially numbering the reaches starting at the headwaters of the main channel. Tributaries are incorporated by continuing the reach numbering from the reach just upstream of the junction on the main channel and the tributary to the headwaters of the tributary. The numbering scheme continues down the tributary, through the junction reach, and continues along the main channel. Figure 2.2 illustrates this number scheme applied to the QUAL2K representation of a hypothetical river.

Hydraulic Modeling

Once the boundaries of each reach are defined, QUAL2K will determine the water depth and velocity using Manning's equation.

Equation 2.1 $$Q = \frac{S_0^{1/2} A_c^{5/3}}{nP^{2/3}}$$

where, Q is the discharge in $m^3\ s^{-1}$, S_0 is the bottom slope, A_c is the cross-sectional area in m^2, n is Manning's roughness coefficient, and P is the wetted perimeter in meters. QUAL2K can also determine water depth and velocity based on weir heights and rating curves.

Heat Balance

Temperature is modeled in QUAL2K, by performing a heat balance on each element in the study area. Transfer of heat in the model includes the input and output of heat from water flowing into and out of the element. The model also takes into account the water flowing into and out of each element from point and non-point inputs and withdrawals. Dispersion of heat, heat transfer to and from the atmosphere, and heat transfer to and from sediments are also included in the heat balance for each element.

Constituents Modeled

QUAL2K uses a mass balance approach to model all water quality parameters including DO, nutrients, phytoplankton, and bottom sediment. Constituents simulated in QUAL2K are listed in Table 2.2 and are defined by Equation 2.2 through Equation 2.8 below.

Equation 2.2 m_i = Total Suspended Solids – Volatile Suspended Solids

Equation 2.3 n_o = Total Kjehdahl Nitrogen – NH_4^+ – r_{na}Chorophyll *a*

Equation 2.4 $$n_n = NO_2^- + NO_3^-$$

Equation 2.5 p_o = Total Phosphorus – Soluble Reactive Phosphorus –…

$\ldots r_{pa}$Chlorophyll *a*

Equation 2.6 m_o = Volatile Suspended Solids – r_{da}Chlorophyll *a*

Equation 2.7 $$ALK = 2[CO_3^{2-}] + [HCO_3^-] + [OH^-] - [H^+]$$

Equation 2.8 $$c_T = [H_2CO_3^*] + [HCO_3^-] + [CO_3^{2-}]$$

Fundamental processes included in the mass balance include advection, dispersion, mass loading and abstraction, sedimentation, resuspension, biogeochemical reactions, algal growth and decay, and atmospheric transfer (Figure 2.3).

The general mass balance for the model constituents in element *i* (except bottom algae and sediments) is written as follows:

Equation 2.9 $$\frac{dc_i}{dt} = \frac{Q_{i-1}}{V_i}c_{i-1} - \frac{Q_i}{V_i}c_i - \frac{Q_{out,i}}{V_i}c_i + \frac{E'_{i-1}}{V_i}(c_{i-1} - c_i) + \ldots$$

$$\ldots\frac{E'_i}{V_i}(c_i - c_{i+1}) + \frac{W_i}{V_i} + S_i$$

where Q_{i-1} is flowrate from the *i* - 1th element, $L^3\ T^{-1}$, Q_i is flowrate from the *i*th element, $L^3\ T^{-1}$, $Q_{out,i}$ is total out flow from the *i*th element due to point and non-point withdrawals, $L^3\ T^{-1}$, V_i is the volume of the *i*th element, L^3, E'_{i-1} is the bulk dispersion coefficient between elements *i* - 1 and *i*, $L^3\ T^{-1}$, E'_i is the bulk dispersion coefficient between elements *i* and *i* + 1, $L^3\ T^{-1}$, c_{i-1} is the constituent concentration in the *i* – 1th element, $M\ T^{-1}$, c_i is the constituent concentration in the *i*th element, $M\ T^{-1}$, c_{i+1} is the constituent concentration in the *i* + 1th element, $M\ T^{-1}$, W_i is the external point and non-point source loading of the constituent to the *i*th element, $M\ T^{-1}$, and S_i is sources and sinks of the constituent due to reactions and mass transfer mechanisms in the *i*th element, $M\ L^{-3}\ T^{-1}$. The S_i term in the mass balance is the generic term for a variety of different biological, chemical, and physical reactions which may occur in each model element (Table 2.3).

First-order reaction equations that dictate the transformation water quality parameters like nitrate, orthophosphate, DO and, TSS are shown below. In these reaction equations, the effect of temperature on the first-order reaction is shown in Equation 2.10 below:

Equation 2.10 $$k(T) = k(20)\theta^{T-20}$$

where $k(T)$ is the reaction rate at temperature T (°C) and θ is the temperature coefficient for the reaction. The inhibitory effect of oxygen on a reaction rate, F_{ox} (dimensionless), is described in Equation 2.11 below:

Equation 2.11 $$F_{ox} = \left(1 - e^{-K_{so}o}\right)$$

where K_{so} is the exponential coefficient for the effect of oxygen (L mgO_2^{-1}).

The reaction term in the mass balance on nitrate, S_{nn}, includes nitrification of ammonia as a source and denitrification and uptake by phytoplankton (PhytoPhoto) and bottom algae (BotAlgUptakeN) as sinks:

Equation 2.12 $$S_{n_n} = F_{oxna}k_n(T)n_a - (1 - F_{oxdn})k_{dn}(T)n_n - \ldots$$
$$\ldots r_{na}(1 - P_{ap})\text{PhytoPhoto} - (1 - P_{ab})\text{BotAlgUptakeN}$$

where k_n is the temperature dependant nitrification rate (day^{-1}), k_{dn} is the temperature dependant denitrification rate (day^{-1}), r_{na} is the mass ratio of nitrogen to chlorophyll *a* in organic matter (i.e. phytoplankton and detritus) and P_{ap}, P_{ab}, PhytoPhoto, and BotAlgUptake N are described in Equation 2.13 through Equation 2.16:

Equation 2.13 $$P_{ap} = \frac{n_a n_n}{(k_{hnxp} + n_a)(k_{hnxp} + n_n)} \frac{n_a k_{hnxp}}{(n_a + n_n)(k_{hnxp} + n_n)}$$

Equation 2.14 $$P_{ab} = \frac{n_a n_n}{(k_{hnxb} + n_a)(k_{hnxb} + n_n)} \frac{n_a k_{hnxb}}{(n_a + n_n)(k_{hnxb} + n_n)}$$

where k_{hnxp} is the preference coefficient of phytoplankton for ammonium (µgN L^{-1}) and k_{hnxb} is the preference coefficient of bottom algae for ammonium (µgN L^{-1}),

Equation 2.15 $$\text{PhytoPhoto} = k_{gp}(T)\phi_{Np}\phi_{Lp}a_p$$

where k_{gp} is the maximum photosynthesis rate at temperature T, φ_{Np} is the phytoplankton nutrient attenuation factor (dimensionless number between 0 and 1), and φ_{Lp} is the phytoplankton light attenuation coefficient (dimensionless number between 0 and 1), and

Equation 2.16 $$\text{BotAlgUptake N} = \rho_{mN}\frac{n_a + n_n}{k_{sNb} + n_a + n_n}\frac{K_{qN}}{K_{qN} + (q_N - q_{0N})}\frac{a_b}{H}$$

where ρ_{mN} is the maximum uptake rate for nitrogen (mgN mgA^{-1} day^{-1}), k_{sNb} is the half-saturation constant for external nitrogen (µgN L^{-1}), K_{qN} is the half-saturation constant for intracellular nitrogen (mgN mgA^{-1}), q_N is the cell quota of nitrogen (i.e. the ratio of intracellular nitrogen concentration to bottom algae biomass, in units of mgN mgA^{-1}), q_{0N} is the minimum cell quota of nitrogen (mgN mgA^{-1}), and H is the water depth (m).

The reaction term in the mass balance on orthophosphate, S_{pi}, includes hydrolysis of organic phosphorus and phytoplankton respiration as sources and uptake from phytoplankton and bottom algae, and settling as sinks:

Equation 2.17 $$S_{pi} = k_{hp}(T)p_o + r_{pa}\text{PhytoResp} - r_{pa}\text{PhytoPhoto} - \ldots$$

$$\ldots\text{BotAlgUptakeP} - \frac{v_{ip}}{H}p_i$$

where k_{hp} is the temperature dependant organic phosphorus hydrolysis rate (day^{-1}), r_{pa} is the mass ratio of phosphorus to chlorophyll *a* in organic matter, v_{ip} is the settling velocity of orthophosphate (m day^{-1}), and PhytoResp and BotAlgUptakeP are defined below:

Equation 2.18 $$\text{BotAlgUptake P} = \rho_{mP}\frac{p_i}{k_{sPb} + p_i}\frac{K_{qP}}{K_{qP} + (q_P - q_{0P})}\frac{a_b}{H}$$

where ρ_{mP} is the maximum uptake rate for phosphorus (mgP mgA^{-1} day^{-1}), k_{sPb} is the half-saturation constant for external phosphorus (µgP L^{-1}), K_{qP} is the half-saturation constant for intracellular phosphorus (mgP mgA^{-1}), q_P is the cell quota of phosphorus (i.e. the ratio

of intracellular phosphorus concentration to bottom algae biomass, mgP mgA^{-1}), and q_{0P} is the minimum cell quota of phosphorus (mgP mgA^{-1}), and

Equation 2.19 $$\text{PhytoResp} = F_{oxp} k_{rp}(T) a_p$$

where k_{rp} is the temperature dependant phytoplankton respiration rate (day^{-1}).

The reaction term in the mass balance on DO, S_o, includes production from photosynthetic activity from phytoplankton and benthic algae and losses from fast reacting CBOD oxidation, nitrification, and respiration activity from phytoplankton and benthic algae. DO is also gained or lost via reaeration depending whether the water is supersaturated or undersaturated with oxygen (Equation 2.20).

Equation 2.20 $$S_o = r_{oa}\text{PhytoPhoto} + r_{od}\text{BotAlgPhoto} - r_{oc} F_{oxc} k_{dc}(T) c_f - \ldots$$

$$\ldots r_{on} F_{oxna} k_n(T) n_a - r_{oa}\text{PhytoResp} - r_{od}\text{BotAlgResp} + \text{k}_\text{a}(o_s - o)$$

where r_{oa} is the mass ratio of oxygen to chlorophyll *a* in organic matter, r_{od} is the mass ratio of oxygen to bottom algae biomass, r_{oc} is the mass ratio of oxygen to carbon in fast reacting CBOD, k_{dc} is the temperature dependant fast reacting CBOD oxidation rate (day^{-1}), r_{on} is the ratio of oxygen to nitrogen consumed during nitrification (4.57 mgO_2 mgN^{-1}), k_a is the reaeration rate (day^{-1}), o_s is the DO saturation concentration (mgO_2 L^{-1}), and BotAlgPhoto and BotAlgResp are described in Equation 2.21 and Equation 2.22 below:

Equation 2.21 $$\text{BotAlgPhoto} = \frac{C_{gb}}{H}(T)\phi_{Nb}\phi_{Lb}$$

where C_{gp} is the zero-order maximum photosynthesis rate of bottom algae ($mgA\ m^{-2}\ day^{-1}$) at temperature T, φ_{Nb} is the bottom algae nutrient attenuation factor (dimensionless number between 0 and 1), and φ_{Lb} is the bottom algae light attenuation coefficient (dimensionless number between 0 and 1).

Equation 2.22 $$\text{BotAlgResp} = F_{oxb} k_{rb}(T)\frac{a_b}{H}$$

where k_{rb} is the temperature dependant bottom algae respiration rate (day^{-1}).

The reaction term in the mass balance on TSS, S_{tss}, includes phytoplankton growth and settling, bottom algae death, detritus dissolution and settling, and inorganic suspended solids settling:

Equation 2.23 $$S_{tss} = r_{da}\text{PhytoPhoto} - r_{da}\frac{v_a}{H}a_p + r_{da}k_{db}(T)\frac{a_b}{H} - \ldots$$

$$\ldots k_{dt}(T)m_o - \frac{v_{dt}}{H}m_o - \frac{v_i}{H}m_i$$

where r_{da} is the mass ratio of detritus to chlorophyll *a*, v_a is the phytoplankton settling velocity, k_{db} is the temperature dependant bottom algae death rate (day^{-1}), k_{dt} is the temperature dependant detritus dissolution rate (day^{-1}), v_{dt} is the detritus settling velocity (m day^{-1}), and v_i is the inorganic suspended solids settling velocity (m day^{-1}).

Operation of the QUAL2K Model

Setup of QUAL2K requires several steps that are described below.

1. Characterization of the creek features in the physical study area: First, any inputs or withdrawals from the system are noted. This includes tributaries, drain tiles, storm sewers, etc. Second, the length of the entire stream and the location of any important hydraulic features (i.e. dams, weirs, or waterfalls) are determined. Finally, the elevation of the creek bed at several points (ideally, the beginning and end of each reach) is determined.

2. Division of the physical water body into hypothetical modeling reaches: In this step the study river is divided into sections with similar physiographic features (i.e. slope, channel width, creek bed composition, etc). Once these reaches are determined, information about each reach is entered into QUAL2K on the "reach" tab. Additional information that is input into the model includes length of each reach, upstream and downstream locations of the reach in the stream, and the number of elements it will be

divided into. These elements serve as the fundamental computational unit from which all calculations are based on.

3. Characterization of water quality parameters in the headwaters of the creek: This includes all of the constituents listed in Table 2.2. Hourly estimation of constituents over a one day span are input into the headwaters tab of QUAL2K. These measurements serve as initial conditions which the model will use to make diel predictions of water quality throughout the creek.

4. Addition of all other model parameters and running of the model: Other data required to run the model includes air temperature, wind speed, the amount of shade covering the creek, and any point sources and non-point inputs into the study river. Before running the model, all of the values on the "rates" tab are calibrated. These rates include various chemical reaction rates, growth rates, settling velocities, and temperature correction coefficients.

Site Description

The Clear Creek watershed is a 267 km^2 HUC (Hydrologic Unit Code) 10 unit located in east-central Iowa (Figure 2.4). It is part of the Lower Iowa HUC 8 unit and discharges into the Iowa River. Approximately 85% of the land cover in the watershed is agricultural or grassland, 8% is forest, 6% is roads or urban, and the remaining area is water or barren (Iowa DNR 2008). Drain tiles are installed in the agricultural lands and anhydrous ammonia is commonly applied as a fertilizer. Best management practices such as grassed waterways and buffer strips are used in the watershed. Soils in the watershed are mainly silty loams of the Fayette-Downs complex and the Colo-Ely complex (NRCS 2007).

Discharge is measured at two US Geological Survey (USGS) gaging stations located in the middle of the watershed at Oxford, and near the outlet of the watershed at Coralville. The average annual discharge at the Coralville gaging station near the outlet

of the Clear Creek Watershed ranged from 0.18 $m^3 s^{-1}$ to 9.3 $m^3 s^{-1}$ from 1953 to 2008 with the mean average annual discharge calculated as 2.0. $m^3 s^{-1}$(USGS 2008a) during that period. The mean average annual discharge at the Oxford gaging station was 1.2 $m^3 s^{-1}$ from 1995 to 2008. The main channel of Clear Creek is approximately 47 km long.

Current Research Efforts in the Clear Creek Watershed

Since becoming the site of a WATERS Network Testbed (Montgomery et al. 2007), the Clear Creek Watershed has become the focus of studies conducted by several researchers in the Environmental Engineering and Science (EES) and IIHR Hydroscience and Engineering programs at the University of Iowa. These studies have focused on processes occurring in both the water and land environment. Dr. Athanasios N. Papanicolaou has focused on erosion processes in the South Amana Catchment (SAC) (Abaci and Papanicolaou 2009). Dr. Marian V. I. Muste has focused efforts in the development of the digital watershed, a GIS-based digital representation of the Clear Creek Watershed including data such as tipping bucket precipitation measurements, water quality measurements, and real-time discharge data (IIHR Hydroscience and Engineering 2009). Research directed by Dr. Jerald L. Schnoor and Dr. Craig L. Just, including this research has focused on instream water quality processes and the deployment of water quality sensors and cyberinfrastructure throughout the watershed (Loperfido et al. 2009a; Loperfido et al. 2009b). Research in this thesis focuses on fundamental processes affecting DO, turbidity and nutrients.

Summary

Increased pressures from climate change, nutrient pollution, and the need for biofuels will affect water quality and water quantity will require a more detailed understanding of water processes to meet designated use requirements. Together, high-frequency data provided by an environmental observatory like the WATERS Network and water quality models can help to reveal nonlinear processes and improve our

understanding of the water environment. In this research, a sensing station within the WATERS Network was designed, constructed and operated in the Clear Creek Watershed to advance the science and engineering of the water environment.

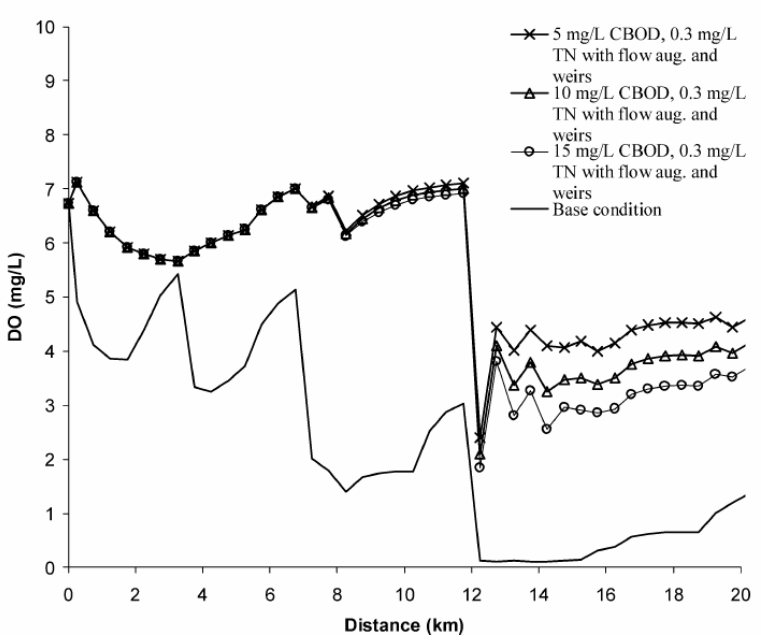

Figure 2.1 QUAL2K DO simulated profiles for various CBOD point loads with restrictions of 0.3 mg L^{-1} TN from point sources, 1 m^3 s^{-1} flow augmentation and weirs at 12.5 km, 13.5 km and 14.5 km (Source: Kannel et al. 2007).

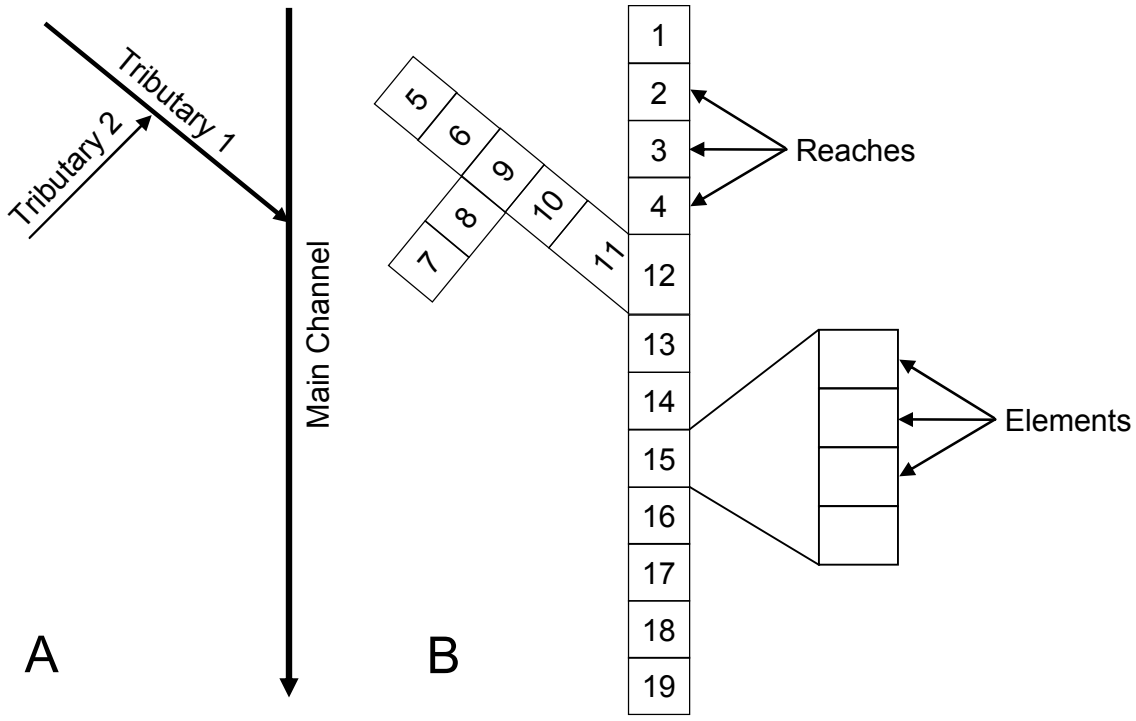

Figure 2.2 Transformation of a hypothetical river (A) into the QUAL2K representation of that river (B) (Adapted from Chapra et al. 2006).

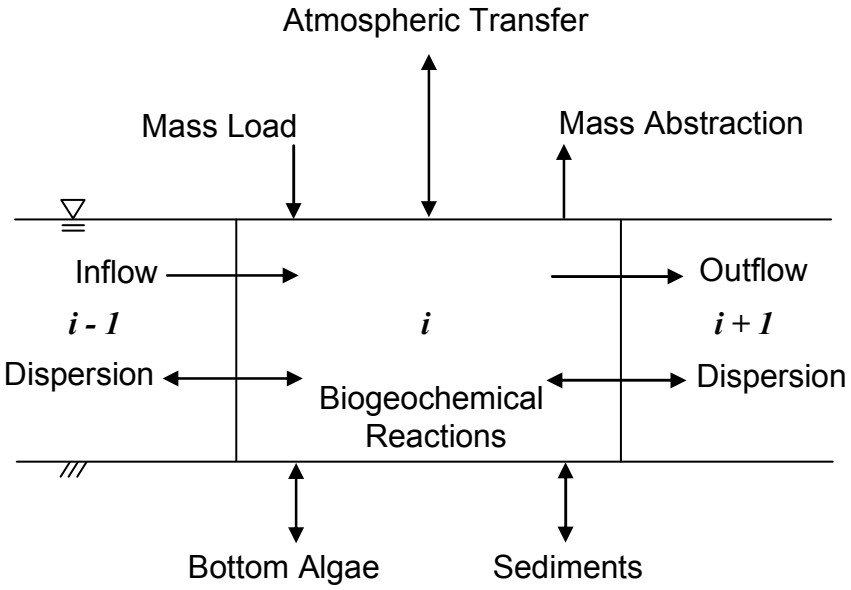

Figure 2.3 Processes included in the general mass balance in the modeling of QUAL2K water quality parameters for a segment without a tributary (Adapted from Chapra et al. 2006).

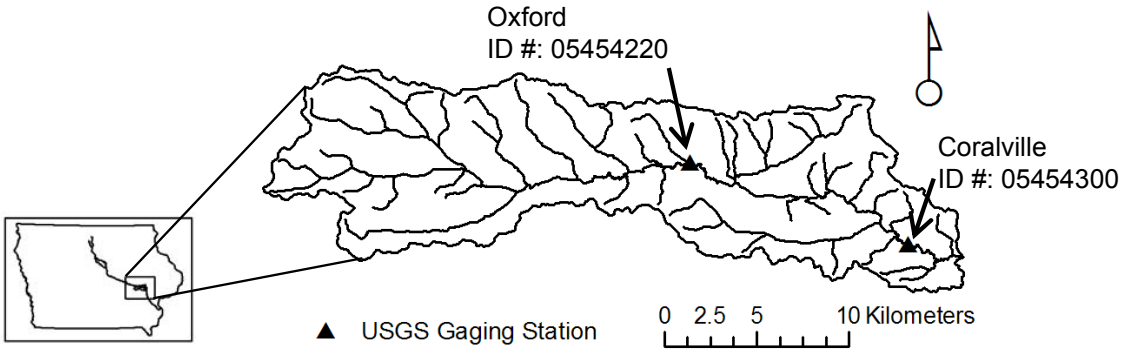

Figure 2.4 The Clear Creek Watershed located in east-central Iowa. USGS Gaging stations are present in the middle of the watershed and at the outlet which drains to the Iowa River.

Table 2.1 Location of the first group of WATERS Network Test Beds and the participating universities.

Test Bed Location	Primary Participant(s)
San Joaquin Valley and Sierra Nevada	University of California - Merced
Flathead River Basin	University of Montana
Little Bear River	Utah State University
Corpus Christi Bay	University of Texas
Minnehaha Creek Watershed	University of Minnesota
Clear Creek Environmental Hydrologic Observatory	University of Iowa
Santa Fe Basin	University of Florida
Susquehanna River Basin and Chesapeake Bay	Penn State University, Drexel University
Baltimore	University of Maryland, Baltimore County
Pamlico Sound and the FerryMon	University of North Carolina – Chapel Hill

Source: WATERS 2009

Table 2.2 Water quality parameters simulated in the QUAL2K model.

Variable	Symbol	Units
Specific conductivity	s	μmhos/cm
Inorganic suspended solids	m_i	mgD L^{-1}
Dissolved oxygen	o	mgO_2 L^{-1}
Slowly reacting CBOD	c_s	mgO_2 L^{-1}
Fast reacting CBOD	c_f	mgO_2 L^{-1}
Organic nitrogen	n_o	μgN L^{-1}
Ammonia nitrogen	n_a	μgN L^{-1}
Nitrate nitrogen	n_n	μgN L^{-1}
Organic phosphorus	p_o	μgP L^{-1}
Inorganic phosphorus (orthophosphate or soluble reactive phosphorus)	p_i	μgP L^{-1}
Phytoplankton biomass	a_p	μgA L^{-1}
Detritus	m_o	mgD L^{-1}
Pathogen	X	cfu 100 mL^{-1}
Alkalinity	Alk	$mgCaCO_3$ L^{-1}
Total inorganic carbon	c_T	mole L^{-1}
Bottom algae biomass	a_b	mgA m^{-2}
Bottom algae nitrogen	IN_b	mgN m^{-2}
Bottom algae phosphorus	IP_b	mgP m^{-2}

Source: Chapra et al. 2006

Table 2.3 Kinetic processes and mass transfer processes incorporated in the QUAL2K model.

Kinetic Processes	Mass Transfer Processes
Dissolution	Reaeration
Hydrolysis	Settling
Oxidation	Sediment Oxygen Demand
Nitrification	Sediment Exchange
Denitrification	Sediment Inorganic Flux
Photosynthesis	
Death	
Respiration/Excretion	

CHAPTER 3:
DESIGN, CONSTRUCTION, AND PERFORMANCE OF THE SENSING STATIONS IN THE CLEAR CREEK WATERSHED*

Abstract

Environmental observatories containing sensing stations will drive future advances in water science. In this study, the design, construction, and performance of sensing stations in the Clear Creek Watershed were analyzed to make recommendations for the deployment of next-generation sensing stations. Sensing stations in the Clear Creek Watershed were constructed using commercially available hardware and software and configured to relay high-frequency environmental data in near-real time from remote locations in Clear Creek to a central data server. Key performance factors of these stations deployed in Clear Creek were analyzed including the ability to sustain power at a sensing station and successfully connect and transmit data successfully from the station to the data server. Water quality sensors that acquired instream measurements were analyzed for their ability to meet demands of extended deployment in an environmental observatory. Environmental data from several sensing stations were analyzed to illustrate the ability of an observatory to advance the fundamental understanding of water science on a temporal and spatial scale, and inform regulatory issues.

Introduction

Sensing stations in an environmental observatory are essential to advance water science and allow new biogeochemical processes in aquatic systems to be discovered (e.g. Chapter 4; Chapter 5), inform resource managers of critical environmental events (e.g. Chapter 4; Chapter 5), and reveal watershed processes occurring over spatial scales

*Modified from Loperfido, J.V., Schnoor, J.L., and Just, C.L. (2007). "Near Real-Time Sensing of Clear Creek Water Quality.", Proc. World Environmental & Water Resources Congress 2007, American Society of Civil Engineers, Tampa, FL., 243, pg 291.

(e.g. Chapter 7). Thus, the sensors, hardware, and software in an environmental observatory that measure, collect, and relay environmental data to researcher and resource manager databases are essential for advancing water science. The components in a sensing station and the cyberinfrastructure required to transmit data must be reliable, durable, and easy to operate. Ideally, an environmental sensing station should be able to operate for an extended period of time without daily maintenance.

The goal of this study was to identify key factors regarding the design, construction, and performance of environmental sensing stations that will provide insight on how to built and operate an environmental observatory. The SAC sensing station, operated during 2006, 2007, and 2008, provided an example to help inform the creation next generation of sensing stations. Specifically, insight was gained on which water quality sensors were durable and reliable, which components of the data storage and transfer system were effective, and how power at the sensing station was adequately maintained. High-frequency water quality data collected at the SAC, Oxford, and Coralville sensing stations were analyzed to illustrate the advances in water science that an environmental observatory can achieve.

Materials and Methods

Deployment History of Water Quality Sensors in the Clear Creek Watershed

Water quality data sondes were deployed at the SAC, Oxford, and Coralville sensing stations for this research (Figure 3.1). Due to land access restrictions, operation at the SAC sensing station in 2006 (termed SAC-2006 sensing station) could not be continued and the sensing station was moved downstream for operation during 2007 and 2008 (termed SAC sensing station). Since land use in the riparian zone of Clear Creek at the 2006 site and the 2007/2008 site were similar and mainly consisted of tall grasses, the construction, operation, and maintenance activities at each site were similar (Figure 3.2).

A description of the deployment history at each sensing station including dates and data sondes deployed is provided in Table 3.1. The location of data collected at the Clear Creek sensing stations in this thesis is also listed in Table 3.1.

Construction of the SAC Sensing Station

Two data sondes were deployed at the SAC sensing station. The primary data sonde was the Hydrolab DS5X Water Quality Multiprobe (Hach, Loveland, Colorado) which measured chlorophyll *a*, DO, pH, specific conductivity, temperature and turbidity and contained a sweeper arm to wipe debris from the sensors prior to taking measurements (Figure 3.3). The Hydrolab DS5X data sonde relayed measurements to the data logger via a Hydrolab SDI-12 Adapter (Hach, Loveland, Colorado) and a Hydrolab Calibration Cable (Hach, Loveland Colorado). The secondary data sonde deployed at the SAC sensing station, during 2007 only, was the DTS-12 Turbidity Sensor (FTS Forest Technology Systems, Ltd, Victoria, BC, Canada). This sensor measured turbidity and temperature, and was also equipped with a sweeper arm to remove debris and biological buildup on the sensor. Measurements collected by this data sonde were transferred to the data logger using the cable supplied with the data sonde.

Measurements from data sondes were collected, stored and transmitted through a remote data collection platform purchased from Campbell Scientific, Inc. The data logger installed in the SAC sensing station, a CR1000 Measurement and Control System (Campbell Scientific Inc., Logan, Utah), was programmed to receive and store measurements taken by the data sondes until these data were transmitted to the data server at the Environmental Engineering and Sciences (EES) Laboratory at the University of Iowa. Environmental data collected at the SAC sensing station were transmitted from the telemetry hardware in the remote collection platform, a Redwing 100 CMDA Modem (Campbell Scientific Inc., Logan, Utah) and a YA Series Yagi Directional Antenna (Radiall/Larsen Antenna Technologies, Vancouver, Washington), through the Verizon

Cellular Network (Verizon, Elgin, Illinois). The wireless cellular plan purchased for this system was an America's Choice II for Business 450 Plan which included 450 minutes per month and was sufficient to meet data transmission needs at the SAC sensing station.

The SAC sensing station was powered by a NP12 Rechargeable 12-Volt Lead Battery (Campbell Scientific Inc., Logan, Utah) and a BP SX20U Solar Cell (British Petroleum, London, United Kingdom) via a CH100 12 Volt Charger/Regulator (Campbell Scientific Inc., Logan, Utah). These components, the data logger, and cellular modem were enclosed in a Stahlin non-metallic enclosure (Stahlin, Belding, Michigan) (Figure 3.2) with desiccant bags that helped protect the sensing station components from excess moisture. Locks were placed on the enclosure latches to discourage vandalism and demonic intrusions (Hurlbert 1984). Holes in the bottom of the enclosure for the data sonde and antenna cables were filled with clay to minimize air and moisture exchange between the ambient air and the inside of the enclosure. However, an air tight seal could not be consistently maintained, subjecting hardware components inside the enclosure to moisture during humid conditions.

Configuration of Hardware and Cyberinfrastructure for Data Transmission from the SAC Sensing Station

Transmission of water quality data from the SAC sensing station to the data server in the EES Laboratory required the configuration of the data sondes and the data logger. Hydras3 LT software (Hach, Loveland, Colorado) was used to configure the Hydrolab DS5X data sonde. Basic functions and operations of this software described below are summarized from the Hydrolab DS5X User Manual (Hach Environmental 2005). The Hydras 3LT software enabled sensor calibration, configuration of the data sonde clock, and configuration of the instrument ID number. Hydras3LT was also used to create measurement schedules, termed log files, which the sensor used to collect water quality measurements when it was deployed without a data logger and other sensing

station components. Log files were used when the Hydrolab DS5X data sondes were not connected to the data logger at the SAC sensing station, or deployed at the Oxford and Coralville sensing stations. Measurements could not be received in near real-time when using log files and were manually downloaded from the data sonde in the EES Laboratory. Options in the "settings" tab in Hydras3 LT were configured to set the SDI-12 address of the Hydrolab DS5X data sondes to "1" in order to program the Hydrolab DS5X data sondes with a different SDI-12 address than the default "0" address of the DTS-12 Turbidity Sensor that was not programmable.

Loggernet 3.1.5 software was used to configure the CR1000 data logger to create monitoring programs used by the data logger, communicate with the data logger to download water quality measurements, update drivers on the data logger, and set the clock in the data logger. The "Short Cut" function in the Loggernet software was used to create a data logger program, which dictated when sensors connected to the data logger performed measurements. The "Short Cut" feature required the input of sensor measurement frequency (20 minutes), the type of sensor connected to the CR1000, and the specific measurements that were stored by the data logger. Following the creation of the monitoring program, it was compiled into a format that is usable by the data logger and uploaded onto the data logger.

To relay water quality data to the EES Laboratory in near real-time, the cellular modem was programmed to be compatible with Verizon Network. The system ID (SID) number was programmed into the cellular modem and the baud rate was set to 9600 using the Cellset.exe program available from Campbell Scientific, Inc (2009). The EZSetup function in Loggernet 3.1.5 software was configured to retrieve water quality data from the SAC sensing station and download them to the data server in the EES Laboratory. The EZSetup wizard was used to specify the type of data logger deployed, the type of connection used to communicate with the data logger, and the data logger program used at the SAC sensing station. To configure the connection to the SAC sensing station, the

cellular phone number associated with the cellular modem at the sensing station was entering using the EZSetup wizard. The Loggernet 3.1.5 software was programmed to download water quality measurements once an hour. This download frequency was selected to avoid overages on the cellular plan.

While deployed in the field, the data logger was monitored and maintained using the status and connection screens in Loggernet 3.1.5. The status screen was used to record the communication history, including successful and unsuccessful connection attempts, between the Loggernet software and the data logger deployed at the SAC sensing station. The status screen was also used to collect data from the data logger manually and suspend the automatic collection of data. The connect screen was used to set the clock on the data logger when daylight savings was in effect, and update the data logger monitoring program when the DTS-12 Turbidity Sensor was connected to the data logger in September, 2007.

Results and Discussion

Powering an Environmental Sensing Station

Adequate power was maintained at the SAC sensing station as the voltage in the NP12 Rechargeable 12-Volt lead battery remained above 12 volts during deployments in 2006 and 2007 (Figure 3.4). A diel cycle in voltage was observed in both years with the voltage above 13.0 during the daytime and near 12.5 during the nighttime. Throughout 2006 and up until 9/11/2007, this diel cycle remained relatively constant. During this period the BP SX20U Solar Cell provided adequate power to support a Hach Hydrolab DS5X data sonde, the CR1000 Data logger, the Redwing 100 CMDA Cellular Modem, and the CH100 12 Volt Charger/Regulator. However, after the DTS-12 Turbidity Sensor was added to the SAC sensing station on 9/11/2007, the battery voltage decreased until the components of the sensing station were removed for the season. It remains to be seen if there would have been sufficient power to sustainedly collect water quality

measurements using the Hydrolab DS5X data sonde and the DTS-12 Turbidity Sensor while transmitting high-frequency data via the cellular modem.

Transmission of Water Quality Data in Near-Real Time

Transmission of environmental data from the SAC sensing station to the data server located in the EES Laboratory was successful; however, achieving a connection between the data server and the modem in the field was somewhat problematic. The average successful connection rate from 4/21/2007 to 10/15/2007 was 73% (Table 3.2). Both the average monthly (Figure 3.5A) and average daily (Figure 3.5B) successful connection rates decreased from April to October. It is unknown what factors contributed to decreased connection rates at the SAC sensing station. On 6/22 the successful connection rate was zero percent with rainfall on that day totaling 153 mm (NCDC 2008) near the Clear Creek Watershed. However, on 4/22, 6/28, and 8/12 successful connection rates of 0.0%, 29.2%, and 20.8% were observed with no rainfall occurring those days (NCDC 2008). Despite the fact that failed connections persisted during the entire field campaign, no data was actually lost. When a connection between the data server and cellular modem was not achieved, sensor measurements remained on the data logger at the SAC sensing station until the next successful connection was achieved.

Failed connections between a sensing station and the data server can have important implications to an environmental observatory. If real-time environmental data are required to create hydrologic predictions of potential public health threats, a delay in the transmission of this data, as observed in Clear Creek, may result in either exposure to health risks, or the a priori closing of facilities that do not wish to risk a potential public health episode.

Water Quality Sensor Performance

The water quality data sondes and associated sensors used to make environmental measurements are critical components to environmental observatories. At the SAC

sensing station, the Hydrolab DS5X data sonde and the DTS-12 Turbidity Sensor were successfully deployed and operated during portions of 2006, 2007, and 2008. The DTS-12 Turbidity Sensor was easy to deploy; once the data sonde was wired into the CR1000 data logger, measurements could be collected from the sensor with minor configuration of the monitoring program on the data logger. One disadvantage to the DTS-12 Turbidity Sensor was that the SDI-12 address number could not be reprogrammed from the default value of zero which, meant that the SDI-12 address on the Hydrolab DS5X was required to be reprogrammed from the default value of zero. This was not difficult as the parameters that were returned to the data logger during a measurement had to be programmed as well and could be done simultaneously.

Water quality sensors deployed at the SAC sensing station performed reasonably well. Table 3.3 lists the water quality sensors deployed at the SAC sensing station and comments related to their performance and maintenance. Both temperature sensors on the Hydrolab DS5X data sondes and the DTS-12 Turbidity Sensor performed very well with little interference from fouling, and good agreement between measurements. The specific conductivity sensor experienced virtually no fouling issues but, the calibration of the sensors did introduce some measurement differences between Hydrolab DS5X data sondes deployed simultaneously. The pH sensor on the Hydrolab DS5X data sondes performed relatively well; the wiper arm on the self cleaning turbidity sensor did an adequate job removing fouling from the sensor meaning that biofouling of this sensor was minimal. The sensor did loose calibration after roughly two weeks, which was expected for a pH probe deployed *in situ*. Measurements taken using the DO sensor indicated relatively good performance. The sensor cap was serviceable through one full season of deployment which, met manufacturer expectations for this replaceable part. Like the pH probe, the DO sensor did lose calibration after roughly two weeks.

Turbidity measurements collected using the Hydrolab DS5X data sonde revealed several issues not experienced using the DTS-12 Turbidity Sensor. The primary issue with the DS5X turbidity sensor was fouling; grasses and soil would become attached to the sweeper arm, designed to clean the sensor, and cover the turbidity sensor during measurements. This resulted in turbidity measurements that could vary one to three orders of magnitude. Calibration of the Hydrolab DS5X sensor was problematic as measurements from sensors calibrated using the same stock solution varied significantly. The self-cleaning mechanism on one turbidity sensor did fail due to an unknown reason. Contrary to the turbidity measurements collected using the Hydrolab DS5X, sensor measurements collected using the DTS-12 Turbidity Sensor indicated virtually no fouling issues. The sweeper arm on the DTS-12 Turbidity Sensor was effective in removing fouling from the sensor, and grass and soil did not accumulate on the sweeper arm. Calibration of this sensor was not a concern since the calibration curve in the sensor is held for one year and recalibrated by the manufacturer.

Applying experiences with the Hydrolab DS5X data sondes and the DTS-12 Turbidity Sensor to an environmental observatory, both data sondes could be deployed with one exception, the DS5X turbidity sensor. The DTS-12 Turbidity Sensor is an ideal data sonde for an environmental observatory as it was essentially maintenance free and did not suffer from fouling issues, in contrast to the Hydrolab DS5X turbidity sensor. The temperature, specific conductivity, pH, and DO sensors on the Hydrolab DS5X data sondes performed well and required only a moderate amount of maintenance. Calibration of the specific conductivity, pH, and DO sensors could likely be performed in the field, reducing the time required to maintain a sensing station deploying a Hydrolab DS5X data sonde.

Water Science Advances from High-frequency Clear Creek Water Quality Data

DO data from 2006 (Figure 3.6) exemplifies how a high-frequency data series collected at just one sensing station at the SAC enabled to understanding of biogeochemical processes and revealed water quality criterion excursions. Analyzed closer, a 30-hour portion of the DO data set collected from April to September (Figure 3.6A) revealed a temperature driven nonlinear reaeration process (Figure 3.6B) that was investigated in Chapter 4. DO measurements at nighttime in late summer (Figure 3.6C) revealed water quality criterion excursions also investigated in Chapter 4. Though outside of the scope of this study, the complete set of time series data set from 2006 (Figure 3.6A) could be analyzed to understand seasonal trends.

Deployment of water quality sensors at the SAC, Oxford, and Coralville sensing stations revealed spatial scaling of water quality parameters such as DO throughout the Clear Creek Watershed (Figure 3.7). Baseflow conditions occurred prior to a 54.6 mm precipitation period from 19:52 on 5/10/2009 to 7:52 on 5/11/2009 measured at the Iowa City Municipal Airport (NCDC 2009). Scaling of DO during this baseflow period was analyzed in Chapter 4 and revealed decreasing primary production rates and respiration rates as drainage area increased. During the rain event, decreases in DO concentrations were similar at all three sensing stations and were dominated by the intense rain event. Following the rain event, the diel DO cycles began to reappear at the SAC to the greatest extent, and lesser so at the Oxford and Coralville sensing stations and was likely due to the phytoplankton community reestablishing at the SAC. Since the travel time from the SAC to Coralville was 1.3 days during the baseflow period prior to the rain event, the rain event was likely still influencing DO cycling at the Oxford and Coralville sensing stations during the first photoperiod after the rain event. Thus, the reestablishment of DO cycling at the Oxford and Coralville stations was minimal the first day, but noticeably increased during the second photoperiod after the rain event. This quicker return to

baseflow values at the SAC than at Oxford and Coralville was also seen in pH (Figure A.14) and specific conductivity (Figure A.15) data collected during the same period.

Conclusions

Sensing stations in the Clear Creek Watershed were constructed to collect, store and transfer high-frequency water quality data from instream sensors. The commercially available hardware and software used to construct these stations were adequate to withstand environmental elements such as rain and moisture and successfully transfer data during spring through fall in 2006 and 2007. Connectivity to the SAC sensing station in 2007 did become limited at times and this system could have limitations if sensor measurements were required constantly for near real time (minutes to hours) water quality forecasts. A combination of a Hydrolab DS5X data sonde and a DTS-12 Turbidity Sensor provided a wide array of water quality measurements with minimal maintenance time required. These measurements were sufficient to understand biogeochemical phenomenon, detect water quality impairments, and reveal spatial scaling of water quality parameters in the Clear Creek Watershed.

Since the water quality data sondes were deployed between the months of March and November during 2006-2008, no experience was gained during the months when ice was present in Clear Creek. However, inferences can be made regarding the potential issues of deploying during the winter months. First, due to the shallow water depth at the SAC sensing station, the potential for freezing the data sondes in ice exists. This would likely lead to sensor damage and inaccurate water quality measurements. Second, because calibration of the DO, pH, and turbidity sensors is required every two weeks, the presence of ice at all three locations may inhibit regular maintenance activities, leading to data with significant errors. Third, lower temperatures and shorter days could lead to decreases in the average daily potential difference in the battery at the SAC sensing station causing power failures to become problematic. Due to these and unforeseen

potential issues, the success of operating a sensing station in the Clear Creek Watershed during winter months may be difficult and impractical.

Results and experience from the operation of the SAC sensing station during 2006, 2007, and 2008 can help inform the planning and final design of environmental observatories such as the WATERS Network, scheduled for construction in 2016-2017 (WATERS 2009). The data sondes used in this study, including the Hydrolab DS5X and the DTS-12 Turbidity Sensor, would be recommended for deployment in the WATERS Network. Sensors to measure nutrients like nitrate and orthophosphate, were not deployed in this study, but should be investigated by the WATERS Network. The remote data collection platform containing a Campbell Scientific CR1000 data logger collected and stored water quality data without losing a single measurement during two field seasons in the Clear Creek Watershed and can be used by the WATERS Network. However, alternative ways to transmit data from a sensing station to data servers such as radio telemetry should be investigated and selected based on site location.

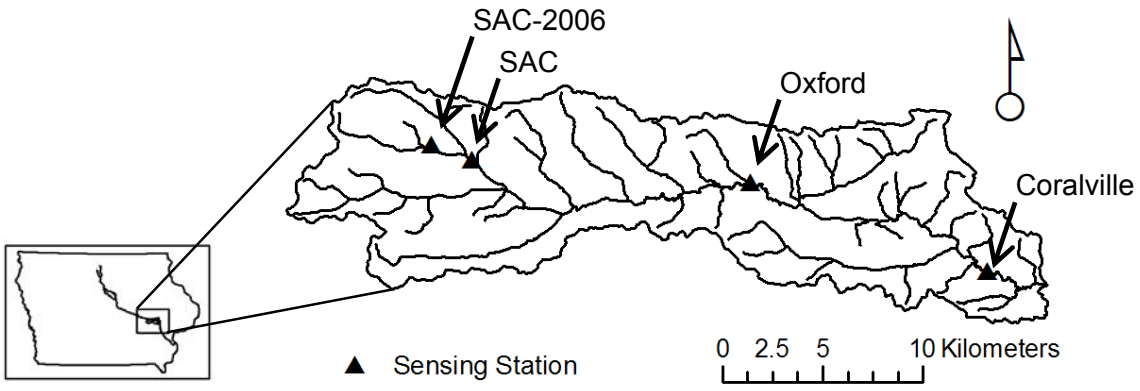

Figure 3.1 Locations of sensing stations used for deployment of high-frequency water quality sensors in the Clear Creek Watershed for this research.

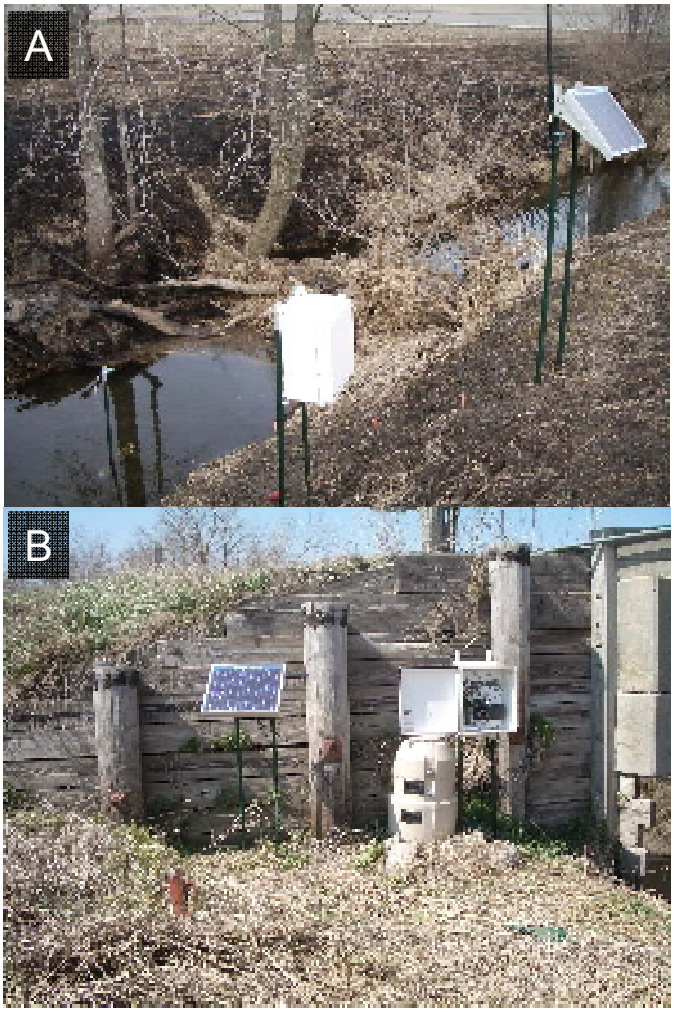

Figure 3.2 The SAC Sensing Station located in the headwaters of the Clear Creek Watershed during 2006 (A) and 2007/2008 (B).

Figure 3.3 Hydrolab DS5X data sonde deployed at the SAC sensing station.

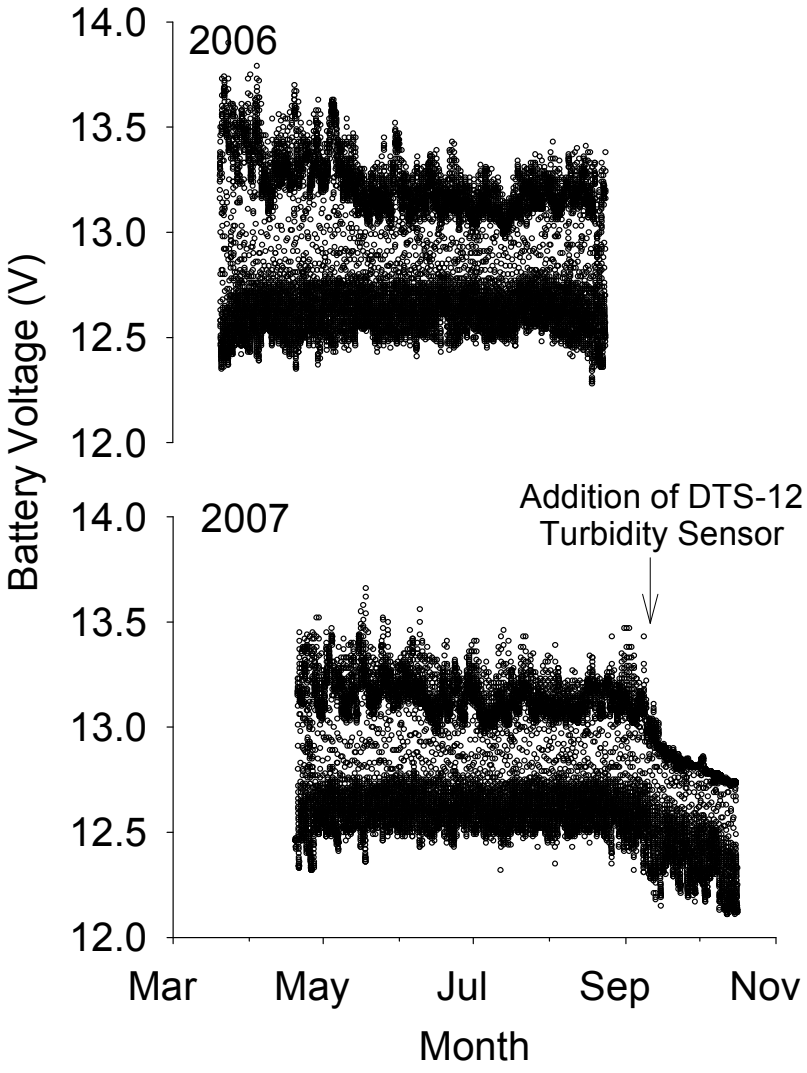

Figure 3.4 Battery voltage at the SAC sensing station during 2006 and 2007 when powering a Hydrolab DS5X data sonde, CR1000 Data logger, Redwing 100 CMDA Cellular Modem, and a CH100 12 Volt Charger/Regulator. The addition of the DTS-12 Turbidity Sensor in September 2007 resulted in a decreasing trend in battery voltage.

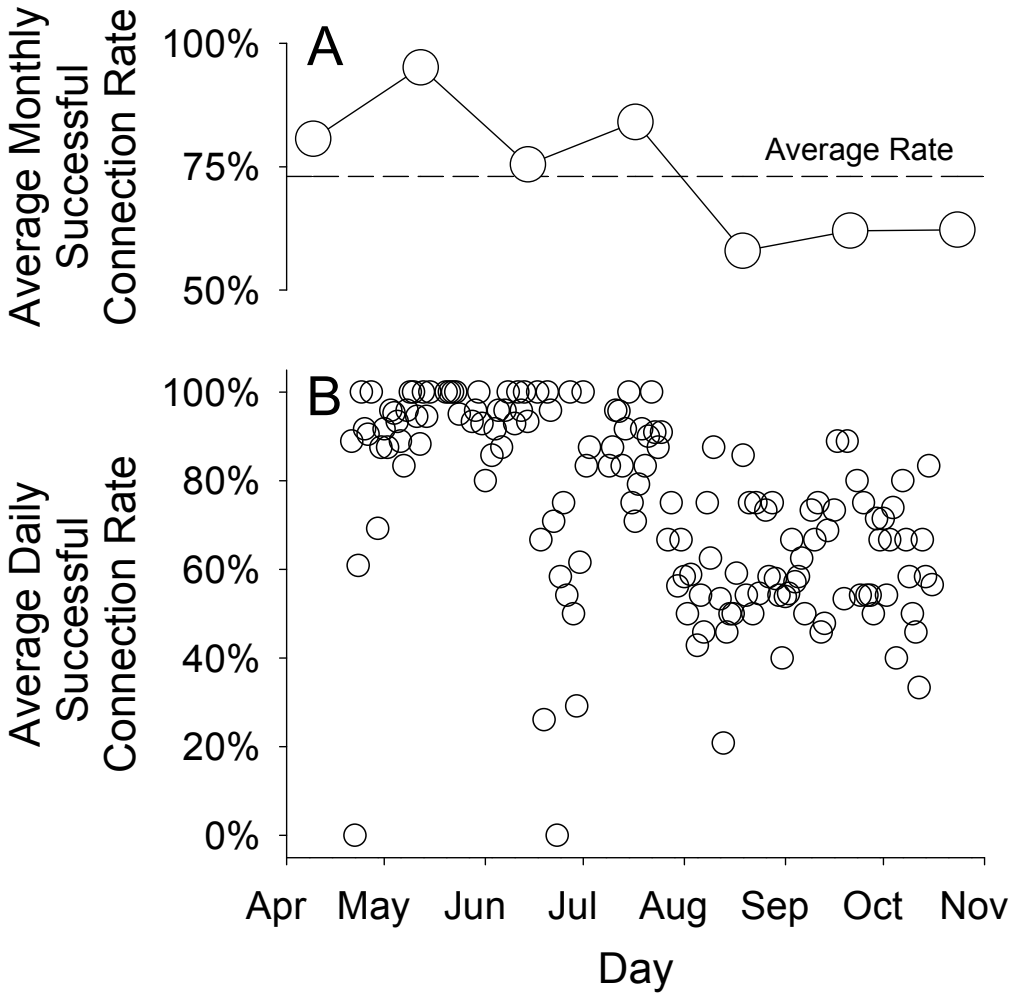

Figure 3.5 Average monthly (A) and daily (B) successful connection rates between the data server in the EES Laboratory and the SAC sensing station from 4/21/2007 to 10/15/2007.

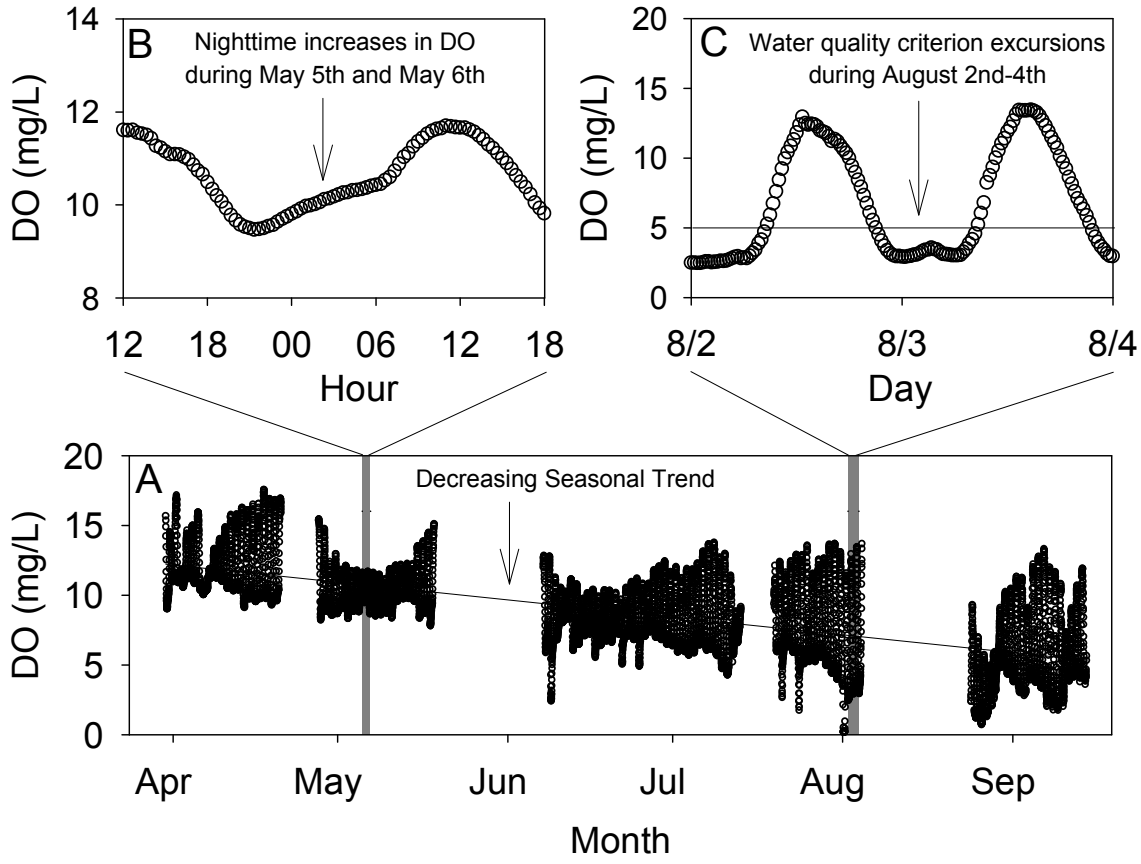

Figure 3.6 High-frequency DO measurements collected at the SAC sensing station during 2006 (A) exemplify the ability of an environmental observatory to transform the understanding of fundamental hydrologic processes (B) and inform water resources management decisions (C).

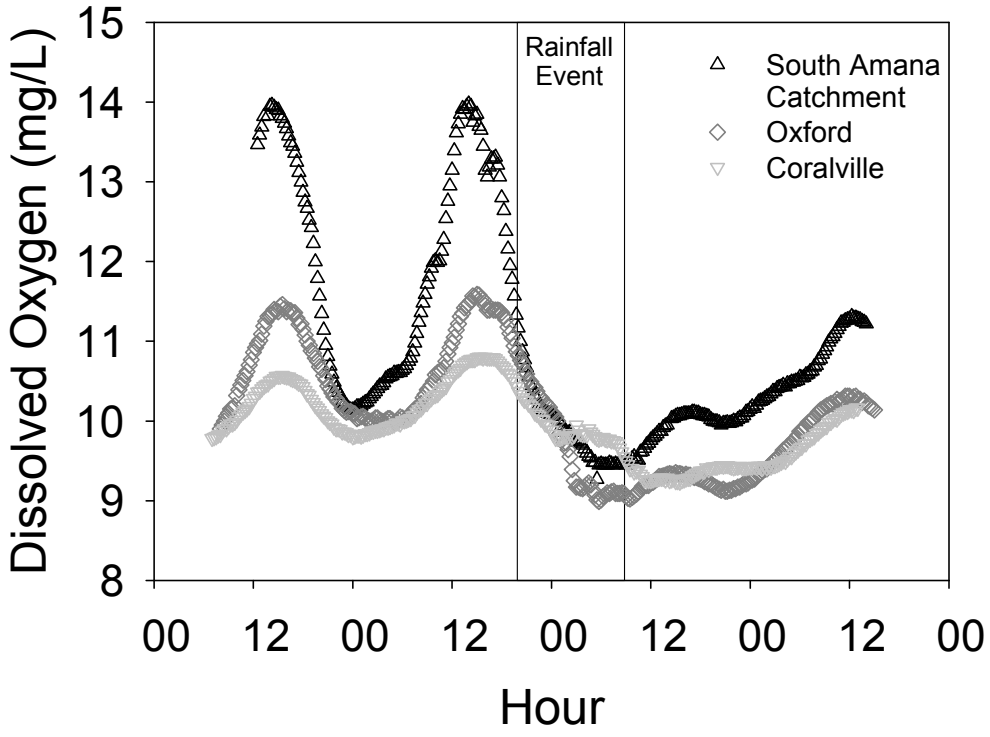

Figure 3.7 Dissolved oxygen measurements collected at the SAC, Oxford and Coralville sensing stations from 5/9/2008 to 5/12/2008.

Table 3.1 Deployment history of data sondes deployed in the Clear Creek Watershed.

Location	Deployment Dates	Data Sonde(s) Deployed	Thesis Chapter(s) Where Data Appears
SAC-2006	3/22/2006 - 9/12/2006	Hydrolab DS5X	3, 4, Appendix A
SAC	4/19/2007 - 11/16/2007, 5/9/2008 - 5/12/2008	Hydrolab DS5X, DTS-12 Turbidity Sensor[a]	3, 4, 5 (2007 data), 6 (2008 data), Appendix A
Oxford	5/9/2008 - 5/12/2008	Hydrolab DS5X	3, 6, Appendix A
Coralville	5/9/2008 - 5/12/2008	Hydrolab DS5X	3, 6, Appendix A

[a]DTS-12 Turbidity Sensor was deployed from 9/11/2007 – 10/16/2007.

Table 3.2 Number of successful hourly connections between the data server in the EES Laboratory and the SAC sensing station per month from 4/20/2007 to 10/15/2007.

Month	Number of Observations	Number of Successful Connections	Successful Connection Rate (%)
April	181	146	81%
May	449	427	95%
June	541	408	75%
July	426	358	84%
August	547	317	58%
September	458	284	62%
October	291	181	62%
Total Monitoring Period	2893	2121	73%

Table 3.3 Performance and maintenance attributes of water quality sensors deployed at the SAC sensing station.

Sensor	Required Calibration	Prone to Calibration Errors by User	Loss of Calibration During Deployment	Prone to Fouling	Other Issues / Comments	Recommend for use in an Environmental Observatory?
Temperature (DS5X)	Not required	No	No	No	-	Yes
Temperature (DTS-12)	Not required	No	No	No	-	Yes
Specific Conductivity (DS5X)	2 weeks, probably longer	Slightly	No	No	-	Yes
pH (DS5X)	2 weeks	No	Yes	Possibly	-	Yes, but requires regular field visits
Dissolved Oxygen (DS5X)	2 weeks	No	Yes	Possibly	Sweeper arm did not clean the entire sensor	Yes, but requires regular field visits
Turbidity (DS5X)	2 weeks	Yes	No	Yes	Fouling very problematic	No
Turbidity (DTS-12)	Yearly by manu-facturer	No	No	No	SDI-12 address not programm-able	Yes

CHAPTER 4:
HIGH-FREQUENCY DISSOLVED OXYGEN STREAM DATA TO INVESTIGATE DIEL PROCESSES AND WATER QUALITY CRITERION EXCURSIONS*

Abstract

Diel DO concentrations and temperature were sensed at high frequency and modeled in an eastern Iowan stream, Clear Creek, in an agricultural setting. The magnitude of the diel changes in DO and temperature were largest at the upstream (headwater) station. Inclusion of temperature change factors increased the accuracy of modeling results and yielded estimates of the reaeration rate constant, primary production rate, and respiration rate. DO modeling of the high-frequency measurements (15 min intervals) revealed a temperature-driven nonlinear reaeration process that led to increases in nighttime DO concentrations. DO modeling results from three sensing stations in the watershed revealed decreasing trends in primary productivity, respiration, and the reaeration rate constant with increasing drainage area. Light extinction from suspended solids was the main factor limiting net primary production. As a result, the ratio of primary production to respiration (P/R) also decreased with increasing drainage area. Water quality criterion excursions were observed using seasonal data sets of DO captured by *in situ* sensors. High-frequency sensor data and DO modeling revealed the effects of temperature and watershed scale on the primary factors that dictate diel DO dynamics in a stream setting.

*Modified from Loperfido, J.V., Just, C.L., and Schnoor, J.L. (2009). "High-frequency Diel Dissolved Oxygen Stream Data Modeled for Variable Temperature and Scale." *J. Environ Eng.*, Accepted.

Introduction

DO is a benchmark for measuring the ecological health of riverine systems. Minimum DO standards are used by environmental agencies to regulate the harmful effects to organisms in aquatic environments. For example, the Iowa Department of Natural Resources (DNR) sets water quality criteria to maintain a minimum value of 5 mg L^{-1} (Iowa DNR 2007b). DO mass-balance dynamics have also been used to elucidate instream processes. Models using the classical equations of Streeter and Phelps (1925) can simulate changes in DO concentrations over distance due to the mechanisms of deoxygenation and reaeration following a point source loading of organic material. For streams not significantly affected by such point sources but which receive nonpoint source nutrient inputs, diel variations of DO may occur due to primary production and respiration. Primary production refers to the addition of DO to a water body as a product of photosynthetic activity by aquatic plants such as phytoplankton, periphyton, and macrophytes during sunlight hours (Cox 2003). Respiration by these plants will occur continuously over the diel cycle and consumes DO. Reaeration is the transfer of oxygen between the atmosphere and the stream when it is undersaturated with DO. Gas transfer can also provide a sink for oxygen if the water is supersaturated with DO. Several different techniques have been developed to simulate DO and estimate the magnitude of the parameters that control it (e.g., Odum 1956; O'Connor and Di Toro 1970; Hornberger and Kelly 1975; Chapra and Di Toro 1991). These models, however, are affected by diel changes in temperature (Kosinski 1984) or built on the assumption of constant temperature. Small streams are subject to greater cooling during the night and warming during the day which changes the shape of the DO diel curve and involves nonlinear dynamics. As the scale of the problem increases (larger streams and drainage areas), the diel swing in temperature is dampened due to greater heat capacities of larger volumes of water.

Temperature changes in the water column can have several effects on the processes which affect DO. Temperature decreases cause an increase in the saturation concentration of DO (Colt 1984). Changes in the saturation concentration affect the DO deficit and ultimately the reaeration driving force. In addition, the reaeration rate constant increases with increasing temperature (Elmore and West 1961), as does the rate of respiration (DeNicola 1996). Although temperature does not affect primary production at lower levels of irradiance, it does dictate the rate of primary production in phytoplankton at irradiance levels near saturation and above saturation (DeNicola 1996; Rae and Vincent 1998). To account for temperature change, Butcher and Covington (1995) added temperature change factors to the primary production, reaeration, and respiration terms on the DO mass balance, allowing their model to account for the effects described above. The model has subsequently been used in a study by Wang et al. (2003).

Reports regarding the scaling of primary production and respiration rates as a function of drainage area have been made. Wiley et al. (1990) found that in an agricultural setting, both rates decreased with increasing drainage area and that channel shading and turbidity are the primary factors driving the relationship. This is contrary to the increasing rates of gross primary production and community respiration with increasing drainage area observed in forest and desert areas (Bott et al. 1985; McTammany et al. 2003). Wang et al. (2003) reported on primary production and respiration rates at stations located 2.16 km apart in an urban setting and 0.32 km apart in an agricultural setting; however, no inference on the scalability of these rates was made.

Decreased nighttime DO levels can occur in an aquatic environment due to the respiration by large phytoplankton communities (Chapra and Di Toro 1991). Grab sampling conducted by regulatory agencies during the daytime may miss frequent, reoccurring DO excursions allowing the persistence of hypoxic conditions in an aquatic environment that may lead to mortality of aquatic species (e.g. Moore 1942; Sparks and

Strayer 1998). The use of high-frequency sensors could aid regulators when the collection of grab samples is impractical or not feasible. Knowledge of DO excursions could lead to the implementation of strategies designed to mitigate persistent hypoxic conditions.

The objective of this study was to understand and model the observed nonlinear DO dynamics of the diel cycle and monitor for DO water quality criterion excursions at Clear Creek, a small upland watershed (270 km^2) in eastern Iowa influenced by intensive agricultural activities. High-frequency sensing and data capture allows one to calibrate and verify modeling processes with greater fidelity than ever before. The diel DO model described by Butcher and Covington (1995) was selected to estimate primary production, reaeration, and respiration parameters at three sensing stations in the Clear Creek Watershed. From the observations and modeling results, inferences about temperature effects and modeling errors were achieved. Primary production, reaeration, and respiration rates were also estimated and compared throughout the watershed to understand the scaling of these processes on DO dynamics. Deployment of high-frequency DO sensors during the spring, summer, and fall during 2006 and 2007 yielded data sets used to analyze the presence of DO water quality criterion excursions.

Materials and Methods

Site Description

The Clear Creek Watershed located in eastern Iowa is a Hydrologic Unit Code (HUC) 10 that drains into the Iowa River and eventually into the Mississippi River (Figure 4.1). Approximately 85% of the land cover in the watershed is agricultural or grassland, 8% is forest, 6% is roads or urban, and the remaining area is water or barren (Iowa DNR 2008). DO and temperature measurements were taken at three high-frequency sensing stations (Hach Hydrolab DS5X data sondes) located within the watershed at the SAC, Oxford, and Coralville. Drainage areas, distance from headwaters,

channel width, water depth, mean discharge, and calculated mean velocity at the three sensing stations are shown in Table 4.1. The average slope of the main channel from SAC to Coralville is 0.001.

The presence of DO sinks in the Clear Creek Watershed such as CBOD, nitrogenous biochemical oxygen demand (NBOD), and sediment oxygen demand (SOD) are not believed to be significant. Regulated point source discharges in the watershed are located above the Oxford and Coralville sensing stations but are a relatively small volumetric addition (< 1% of flow). Samples of creek bed material at the SAC indicate that it largely consists of quartz with a relatively low percentage of organic material that would not act as a sediment oxygen demand (SOD). The background concentration of CBOD in the watershed can be estimated as 0.5–2 mg L^{-1}, based on typical values cited in the literature (Schnoor 1996). Assuming a typical deoxygenation rate constant of 0.2 day^{-1} (Schnoor 1996), the deoxygenation rate in Clear Creek would be 0.1-0.4 mg L^{-1} day^{-1}.

Primary production at the SAC sensing station is largely due to the extensive community of benthic algae and rooted plants with a relatively smaller contribution from free-floating algae (phytoplankton). Quantitative data for the benthic community were not available; however, during spring, summer, and fall, gas bubbles commonly cover the benthic algae in the late afternoon that were not present during the morning or nighttime. Lack of a phytoplankton community is supported by sensor data and observations; the average chlorophyll *a* measurements collected by a Hydrolab DS5X data sonde during the deployment period in this study was only 0.1 μg L^{-1}, and filter papers from water samples collected at the SAC have consistently been light brown as opposed to green indicating a lack of phytoplankton. At the Oxford and Coralville sensing stations, the combination of increased water depth and suspended solids concentrations did not allow for visual observation of the creek bed suggesting that the role of benthic algae was diminished at these sensing stations.

DO, temperature, turbidity, and chlorophyll *a* were measured every fifteen minutes beginning at 12:30 on 5/9/2008 and continued through 20:30 on 5/10/2008 using three Hach Hydrolab DS5X data sondes (Hach, Loveland, Colorado). Prior to deployment of the data sondes, the sensors were calibrated as per the manufacturer's instructions.

Dissolved Oxygen Modeling

DO concentrations were simulated using methods described in Butcher and Covington (1995). Briefly, this method is based on a mass balance of DO in a stream as described by O'Connor and Di Toro (1970) and later modified by Chapra and Di Toro (1991):

Equation 4.1
$$\frac{dD}{dt} + k_a D = R - P(t)$$

where D = DO deficit (mg L^{-1}); t = time (days); k_a = reaeration rate constant (day^{-1}); R = respiration rate (mg L^{-1} day^{-1}); and $P(t)$ = primary production rate (mg L^{-1} day^{-1}). Sensing stations selected in the Clear Creek Watershed satisfy the assumptions of this model which include constant coefficients, such as uniform plant distribution for a sufficiently long distance ($>3u/k_a$ where u = mean stream velocity), and the DO deficit does not vary spatially ($\delta D/\delta x \approx 0$). Although believed not to exist in the Clear Creek Watershed, a DO sink such as CBOD, NBOD, or SOD would be modeled in Equation 4.1 and lumped into the respiration term. Equation 4.1 is a linear, first order, ordinary differential equation that admits a periodic solution for diel DO dynamics at a point location. The primary production rate is approximated by a half sine wave:

Equation 4.2
$$P(t) = P_{av} \frac{\pi \tau}{2f} \sin\left(\frac{\pi t}{f}\right), \; 0 \le t \le f$$

Equation 4.3
$$P(t) = 0, \; f \le t \le \tau$$

where P_{av} = the average primary production rate (mg L^{-1} day^{-1}), f = the photoperiod (days), and τ = the diel period (= 1 day). Butcher and Covington (1995) modified Equation 4.1 to incorporate temperature, including its affect on rate constants in a modified van't Hoff-Arrhenius form:

Equation 4.4
$$\frac{dD}{dt} + \bar{k}_a g(T) D = \bar{R} h(T) - \bar{P}(t) i(T) + \frac{dC_s}{dt}$$

where $g(T) = 1.02^{(T-20)}$, $h(T) = 1.08^{(T-20)}$, $i(T) = 1.066^{(T-20)}$, T = water temperature (°Celsius), C_s = DO saturation concentration (mg L^{-1}) and $\bar{k}_a$, $\bar{R}$, and $\bar{P}(t) = k_a$, R, and $P(t)$, respectively, at a reference temperature of 20°C. Unlike Equation 4.1, Equation 4.4 is a nonlinear differential equation due to the product between the temperature-dependent reaeration rate and the DO deficit. In Equation 4.4, T can be considered as another dependent variable to be determined from an energy balance or, alternatively, measured frequently through time (as in this study). Equation 4.4 was then approximated in finite difference form between times t and $t + 1$ (Butcher and Covington 1995):

Equation 4.5
$$\frac{D_{t+1} - D_t}{\Delta t} + \bar{k}_a g(T) D_t = \bar{R} h(T) - \bar{P}(t) i(T) + \frac{C_{s,t+1} - C_{s,t-1}}{\Delta t}$$

where Δt = the time increment. Butcher and Covington (1995) propagated the DO deficit differential as a forward difference from time t, and the differential on the DO saturation concentration as a central difference at time t. Substituting Equation 4.2 and Equation 4.3 into Equation 4.5 and solving for D_{t+1} as in Butcher and Covington (1995), the DO deficit at time $t + 1$ can be predicted as shown:

Equation 4.6
$$D_{t+1} = D_t - \bar{k}_a g(T) D_t \Delta t + \bar{R} h(T) \Delta t - \ldots$$
$$\ldots \bar{P}_{av} \frac{\pi \tau}{2f} \sin\left(\frac{\pi t}{f}\right) i(T) \Delta t + C_{s,t+1} - C_{s,t-1}, \; 0 \le t \le f$$

Equation 4.7
$$D_{t+1} = D_t - \bar{k}_a g(T) D_t \Delta t + \bar{R} h(T) \Delta t + C_{s,t+1} - C_{s,t-1}, \; f \le t \le \tau$$

where $\overline{P}_{av}$ = the average primary production rate at a reference temperature of 20°C (mg L^{-1} day^{-1}). The DO deficit in the water column was modeled using Equation 4.6 and Equation 4.7 with temperature data used at every time step and the DO deficit from the second measurement collected at each sensing station. Estimations of the saturation concentration of DO in freshwater were calculated and corrected for elevation as described in APHA (1998). Predictions of DO concentrations were calculated using Equation 4.8.

Equation 4.8 $$\hat{C}_{t+1} = C_{s,t+1} - D_{t+1}$$

The parameters $\overline{k}_a$, $\overline{R}$, and $\overline{P}_{av}$ were optimized by minimizing the sum of squared errors (SSE) between predicted DO concentrations, $\hat{C}$, and actual DO concentrations, C, for the n observations (126) during the monitoring period using the solver tool in Microsoft Excel (Equation 4.9).

Equation 4.9 $$\text{SSE} = \sum_{i=1}^{n} \left(\hat{C}_t - C_t\right)^2$$

Two model runs were performed using DO and temperature data from each sensing station. Model M1 optimized the parameters $\overline{k}_a$, $\overline{R}$, and $\overline{P}_{av}$ as described above to calculate the DO deficit. Model M2 used values of $\overline{k}_a$, $\overline{R}$, and $\overline{P}_{av}$ that were determined from Model M1 to simulate the DO deficit. However for Model M2, the temperature change factors were set equal to 1 (i.e. $g(T) = h(T) = i(T) = 1$) in Equation 4.6 and Equation 4.7. In both model runs, M1 and M2, a different $\overline{P}_{av}$ was used for each day due to slight differences in cloud cover. DO concentration predictions for both Models M1 and M2 were calculated using Equation 4.8.

High-frequency Sensing of DO Water Quality Criteria

High-frequency DO data were used to assess the occurrence of water quality criterion excursions in Clear Creek during 2006 and 2007. DO sensors on Hydrolab DS5X data sondes were used to collect high-frequency data at two SAC sensing stations,

SAC-2006 and SAC (Figure 4.1), during the spring, summer, and fall of 2006 and 2007. Gaps exist in the data set due to fouling issues and sensor maintenance.

Results and Discussion

Temperature and Dissolved Oxygen Data

Water temperature measurements were lowest at the upstream location, the SAC, and highest at the downstream location, Coralville (Figure 4.2A). It is common for such streams to warm during the spring as they flow downstream. The average water temperatures at the SAC, Oxford, and Coralville sensing stations were 10.3°C, 11.6°C, and 13.0°C respectively. The average air temperature recorded during the modeling period at the Iowa City Municipal Airport, located 6 km southeast of the Coralville sensing station, was 13.6°C (NCDC 2008). The change in diel temperature was greatest at the headwaters, the SAC, due to a reduced thermal buffering capacity to solar radiation during the day and increased relative contribution of source groundwater which, led to larger temperature decreases during the nighttime. Decreasing water temperature trends and magnitudes of temperature change in agricultural watersheds have been noted in the literature (Hynes 1970). A constant temperature trend with decreasing magnitudes of change as drainage area increased has also been observed by Wiley et al. (1990) in a stream fed by shallow subsurface (tile drain) runoff and not spring water.

DO concentrations during the daytime were much higher at the SAC and slightly higher at Oxford as compared to those at Coralville (Figure 4.2B). Nighttime DO concentrations were similar at all three sights. The magnitude of the diel DO swing was highest at the SAC, next highest at Oxford, and lowest in Coralville. Based on the observations and modeling results, this is due to the increased primary production in the upstream reaches of the creek. At all three sites the water was supersaturated with oxygen during the day and was below the saturation level during the nighttime. DO concentrations at all three sensing stations were well above the Iowa state standard of 5

mg L^{-1}. However, diel sensing of DO in locations upstream of the SAC during the summer months revealed that concentrations as low as 2 mg L^{-1} are common at midnight due to lower DO saturation concentrations and greater net primary production.

Temperature Effect on Modeling Results

Optimization of the average primary production rate, reaeration rate constant, and respiration rate parameters provided excellent fits between Model M1 results and actual DO data (Figure 4.3). Optimized parameters (Table 4.2) from Model M1 resulted in a less accurate fit when used with Model M2. This is because the modeling rates are normalized for 20°C and Model M2 does not account for temperature changes throughout the diel cycle. The highest root mean squared error (RMSE), determined as per Judd et al. (2009), in Model M1 was calculated at the SAC sensing station and the lowest at the Coralville sensing station (Table 4.2). The RMSE exceeded the accuracy of the DO sensor, ± 0.2 mg L^{-1}, at the SAC sensing station for Model M2 suggesting that factors other than sensor accuracy contributed to modeling error. For instance, cloud cover may have temporarily reduced the primary production rate. A halving in primary production would have a greater influence on DO concentrations at the SAC because the magnitude of the primary production rate is larger at this sensing station.

Diel temperature swings at the SAC (Figure 4.3A) caused error in Model M2 at the times of minimum and maximum DO, but these errors were dampened as the diel temperature fluctuations decreased downstream (Figure 4.3B & C). The RMSE values reflect this phenomenon in Table 4.2. Increased modeling errors with smaller drainage area would also be seen in other streams that are fed by cooler groundwater, or those fed by snowmelt that have lower water temperatures near the source and higher temperature near the mouth of the watershed.

The mass rates of DO in the water column at each site by the processes of primary production, reaeration, and respiration are shown in Figure 4.4. These indicate that the

variability of the rates were much higher in the SAC as compared to downstream sensing stations at Oxford and Coralville. Respiration varies by 47% from 4.7 mg L^{-1} day^{-1} to 6.9 mg L^{-1} day^{-1} at the SAC sensing station due to the 5°C change in water temperature which occurred during the monitoring period. Respiration rate variations observed at Oxford and Coralville were smaller and varied by 0.6 mg L^{-1} day^{-1} and 0.1 mg L^{-1} day^{-1} respectively. This is reflective of the smaller changes in temperature that occurred at the Oxford (2.7°C) and Coralville (3.4°C) sites.

Nighttime nonlinear increases in DO concentrations were measured in Clear Creek and caused the curves to appear non-sinusoidal. This agrees with data in the literature (e.g. Butcher and Covington 1995; Wang et al. 2003), however, the mechanism has not been previously addressed. Model results in Figure 4.3 successfully simulated the increases in DO concentration during nighttime observed at the SAC sensing station. Figure 4.4 indicates that at this location, DO production from reaeration was greater than consumption due to respiration. Although slight increases in DO concentrations at nighttime were observed at the Oxford and Coralville sensing stations, they were smaller than the accuracy of the sensor of ± 0.2 mg L^{-1}.

Several factors contributed to large increases of DO concentration at the SAC and not at Oxford or Coralville. First, the reaeration rate constant was two times larger at the SAC than at Coralville, and 1.5 times greater than at Oxford. This is largely due to a more shallow water depth seen at the SAC (0.5 m), versus Oxford (1.3 m) and Coralville (1.0 m). Second, larger changes in the DO deficit at the SAC, due to a rapid decrease in temperature, created a larger change in the DO flux into the water column due to reaeration. Third, the large temperature change at the SAC affected the rates of reaeration and respiration by different magnitudes. The 4°C temperature change during nighttime at the SAC decreased $g(T)$ by only 8% (0.85 to 0.79), but decreased $h(T)$ by 26% (0.54 to 0.40). Taken together, these factors created a highly nonlinear process that resulted in nighttime increases in DO concentration and marked deviation from the

typical sinusoidal pattern usually reported in the literature. The fundamental mass balance describing DO concentration changes at night, Equation 4.4, illustrates this nonlinear relationship if Equation 4.8 and the equation for the DO saturation concentration are substituted into it:

Equation 4.10 $$\frac{dD}{dt} = \overline{R} \cdot 1.08^{(T-20)} + \frac{dC_s}{dt} - \overline{k}_a \cdot 1.02^{(T-20)}\left(C_s - C\right)$$

where (APHA 1998) $\ln C_s = -139.34411 + (1.575701\text{x}10^5 / T_k) - (6.642308\text{x}10^7 / T_k{}^2) + (1.243800\text{x}10^{10} / T_k{}^3) - (8.621949\text{x}10^{11} / T_k{}^4)$, assuming zero chlorinity, and T_k = water temperature (Kelvin).

Watershed Scaling of Model Parameters

Results from Model M1, using temperature change factors, indicate that average primary productions rates in the Clear Creek Watershed decreased by 76% from the SAC to Oxford and by 96% from the SAC to Coralville (Figure 4.5). These large decreases in average primary production are likely due to light extinction in the downstream portions of the watershed and resulted in a dampening of the diel DO swing at Oxford and Coralville. The equations for light energy in the water column as a function of depth, $I(z)$, and the light extinction coefficient, k_e, presented in Chapra (1997), show light energy as a function of nonvolatile suspended solids, detritus, and water depth:

Equation 4.11 $$I(z) = I_0 e^{-k_e z}$$

Equation 4.12 $$k_e = 0.052N + 0.174D$$

where $I(z)$ = light energy at depth z (ly hr^{-1}); I_0 = surface light energy (ly hr^{-1}); z = water depth (m); k_e = light extinction coefficient (m^{-1}); N = nonvolatile suspended solids (mg L^{-1}); and D = detritus (mg L^{-1}).

In the Clear Creek Watershed, turbidity, a surrogate parameter for suspended solids measurements (e.g. Finlayson 1985; Gippel 1995), increased nearly ten-fold from the SAC sensing station to the Oxford and Coralville sensing stations while water depth

increased two to three-fold during the photoperiod for this study (Table 4.3). Increases in both turbidity and stream depth lead to significant decreases in the percentage of surface light energy that reached the bottom sediments, $I(z)/I_0$, from the SAC sensing station to the Oxford and Coralville sensing stations (Table 4.3). Increased suspended solids were the primary factor in reducing light energy to the creek bed as drainage area increased, an observation made by Wiley et al. (1990) as well. Increased shading has also been found to correlate with decreased primary production rates in the literature (Wiley et al. 1990). In Clear Creek however, sampling was conducted in early May, so trees in the riparian zone had not fully canopied yet, reducing the importance of this factor. Since light extinction led to reduced populations of primary producers, the respiration rate that plants exhibited was reduced in a similar manner leading to the decrease in the respiration rate with increasing drainage area shown in Figure 4.5.

High-frequency sensor data at the Oxford and Coralville stations indicated diel DO swings due to primary production and respiration despite low light penetration to bottom sediments (Table 4.3). It is possible that shallow tributaries feeding into Clear Creek above the Oxford and Coralville stations may have contributed to the diel DO swings in the main channel. If this was the case, then the actual rates of primary production and respiration in the main channel of Clear Creek would be lower than estimated in this study. Other reaeration models (e.g. Covar/Zison Method as presented in Chapra 1997) indicate somewhat lower reaeration rate constants than estimated in this study, which could be offset by DO inputs from tributaries. Decreased reaeration rate constants could lead to uncertainty whether there is station independence ($3u/k_a > x$), meaning that rates derived in this study are not statistically independent from one another. Even if tributaries did significantly influence the DO swings at Oxford and Coralville, the general trend of decreasing rates versus drainage area depicted in Figure 4.5 would still be valid.

Watershed Scaling of P/R Ratio

The ratio of P/R has been used to determine whether a stream is primarily autotrophic (P/R >1) or heterotrophic (P/R <1) in several studies (e.g. Wilcock et al. 1998; Williams et al. 2000; Wang et al. 2003). In the Clear Creek Watershed, the $\overline{P}_{av} / \overline{R}$ ratio was highest in the headwaters and decreased in downstream locations (Figure 4.6) as observed in Wiley et al. (1990). Increased suspended solids concentrations in the downstream sites caused the decrease in $\overline{P}_{av} / \overline{R}$ ratio. Light extinction caused by greater suspended solids decreased the primary production rate. Small streams in agricultural settings like Clear Creek, Iowa, receive large amounts of nutrients from runoff and tile drainage. Thus, their primary production is largely limited to the greatest extent by a lack of light for photosynthesis as turbidity from soil erosion increases downstream as was the case in Wiley et al. (1990). Background CBOD may have also played a role in decreasing the downstream ratio. The background CBOD deoxygenation rate of 0.1-0.4 mg L^{-1} day^{-1} is relatively small compared to respiration at the SAC sensing station, however, becomes increasingly important at the Coralville sensing station.

The decrease in primary production rates and the $\overline{P}_{av} / \overline{R}$ ratio through the Clear Creek Watershed is due to light extinction as described above and may have had the most profound effect on the benthic community of primary producers. Contributions to diel DO swings from free-floating algae are likely to be minimal as chlorophyll *a* measurements in the water column at the SAC were only 0.1 µg L^{-1} on average. Benthic primary production and respiration was not explicitly included in Equation 4.4, but it easily could be included as an additional term on the right hand side of the equation as $(R_b\text{-}P_b)/H$, where H is the mean depth of the water column, and $(R_b\text{-}P_b)$ is the net primary production of the benthic algae expressed as g day^{-1} m^{-2} of bottom area. Since $\overline{R}$ and R_b are both zero order terms, and $\overline{P}_{av}$ and P_b are zero order terms multiplied by the same sinusoidal term to take solar radiation into account, the primary production and respiration terms can be lumped together. Thus, the model used in this study essentially

lumps benthic organisms into the phytoplankton net primary production term, and their effect on diel DO measurements is included in the DO data. Assuming the contribution to the diel DO swing by free-floating algae is zero, the net primary production rate by the benthic algae community at the SAC averaged over the two-day monitoring period would be $1.1x10^{1}$ g day^{-1} m^{-2}

Excursions of DO Water Quality Criteria

Frequent excursions of the Iowa DNR DO water quality criterion occurred during the late summer and early fall of 2006 but only during one event in 2007 (Figure 4.7). Of the 8,282 total measurements collected from 3/30/2006 to 8/14/2006, DO excursions were recorded 13% of the time. The first excursion was measured on 6/8/2006 from 19:40 to 1:00 on 6/9/2006 while most excursions occurred during late July, August, and September. A majority (79%) of the DO excursions occurred between 17:00 and 8:00. Additional DO excursions are likely to have occurred during unmonitored periods in 2006 from 7/13 to 7/19 and from 8/4 to 8/24.

Contrary to the frequent DO excursions in 2006, only one DO criterion excursion occurred in 2007. On 6/22/2007, from 10:20 AM to 1:00 PM, DO excursions were measured several hours after a 66.2 mm rainfall event, measured at the Iowa City Airport from 1:00 to 5:00 (IEM 2008a). Since the DO sensor was tethered to the bottom of the channel, excessive amounts of organic carbon that runoff from farm fields in agricultural areas during extreme rain events (Dalzell et al. 2007) could have provided an oxygen demand, creating the severely depleted DO concentrations. Alternately, the large bed load of sediment that is delivered during extreme rain events (Coats et al. 1985) could have led to sensor fouling, creating "false positive" DO excursion measurements.

High-frequency sensor data in Figure 4.7 (black circles) were statistically sampled to simulate daily noon grab samples (Figure 4.7, white circles). In 2006, simulated daily noon grab samples resulted in DO excursions on three of the 115 days sampled, meaning

that DO water quality criterion excursions would have been reported 2.6% of the time. Compared to the 13% of sensor measurements that would have been reported as DO water quality criterion excursions, daily noon grab samples would have severely underestimated the presence and severity of these excursions. In 2007 however, daily noon grab samples would have reported the one water quality criterion excursion captured with high-frequency data on 6/22/2007.

Lower annual average discharge was likely the cause of frequent DO excursions in 2006 that were not present in 2007. Matthews (1998) describes how drought and low discharge in a stream can lead to depressed DO concentrations. In the first stages of drought when surface flow still exists, but the stage is lower than base flow, decreased water velocities can promote the growth of floating and benthic algae mats as was observed in Clear Creek. Algae mats in shallow pools can create supersaturated DO conditions during the daytime and partially anoxic conditions in the nighttime as seen in DO data captured at the SAC sensing station (Figure 4.8). Lower discharge and higher algae and light per unit volume results in a greater affect on diel DO swings and larger magnitude of the diel DO swing as observed in July, August and September in Figure 4.7.

Two key factors contributed to lower discharge at the SAC sensing station in 2006 as compared to 2007 which led to the DO excursions observed in 2006. First, site location; even though the 2007 SAC sensing station was only 2.2 km downstream of the 2006 site, the drainage area to that station was more than two times the size of that to the 2006 site, 26.1 km^2 versus 12.6 km^2. Second, higher rainfall rates presided in 2007. While the average annual rainfall for Iowa City is approximately 863.6 mm (NWS 2009), in 2006 the Iowa City airport recorded 825.5 mm of rain, with 340.4 mm occurring during the months of May through August, termed MJJA rainfall (IEM 2008b). In 2007, 988.9 mm of rainfall was recorded with MJJA rainfall accounting for 515.6 (IEM 2008b). The lower total rainfall and MJJA rainfall may have resulted in lower groundwater levels and less subsurface infiltration into the creek resulting in lower discharges. Box plots of

the average annual discharge at the Coralville USGS gaging station, based on data from 1953 to 2008, and at the Oxford USGS gaging station, based on data from 1995 to 2008 illustrate the effect of decreased rainfall in 2006 on average annual discharge during that year (Figure 4.9). The difference in average annual discharge during 2006 and 2007 is evident as the 2006 discharge was near the tenth percentile and 2007 discharge was above the 75th percentile at both USGS gaging stations. The flood in June 2008 resulted in average annual discharges much greater than the 95th percentile discharge (Figure 4.9).

Conclusions

Deployment of water quality sensors and subsequent high-frequency measurements of DO and temperature have revealed nonlinear changes in the diel DO curve at three stream locations in the Clear Creek Watershed. Modeling with and without diel temperature change factors indicated that temperature plays a major role in DO production and consumption rates at the benthic-algal dominated headwater location. Nighttime reaeration was triggered by cooling stream temperatures, especially at the upstream station of the watershed. This results in a nonlinear mass balance for DO, and causes a lack of sinuosity in the diel DO response. Analysis of the high-frequency data and inclusion of the role of temperature yielded an excellent fit between model and observations for average primary production rate, the reaeration rate constant, and the respiration rate.

In addition to temperature, drainage area was shown to be an important scaling factor affecting primary production, respiration and, reaeration. Magnitudes of the diel swing in DO concentrations were also shown to decrease as drainage area increased. This was due to increased suspended solids concentrations leading to greater light extinction in the downstream portions of the creek. Modeling results including high-frequency measurements of temperature change and DO dynamics allowed for a more accurate prediction of the diel DO throughout the watershed.

High-frequency DO data also revealed the persistence of repeated water quality criterion excursions at the SAC-2006 sensing station during 2006. These excursions were largely due to lower discharges which increased the influence of phytoplankton on the diel DO curve. The extent and severity of these DO excursions were easily captured by sensors deployed *in situ* and could greatly assist regulators in the identification of DO excursions in other watersheds.

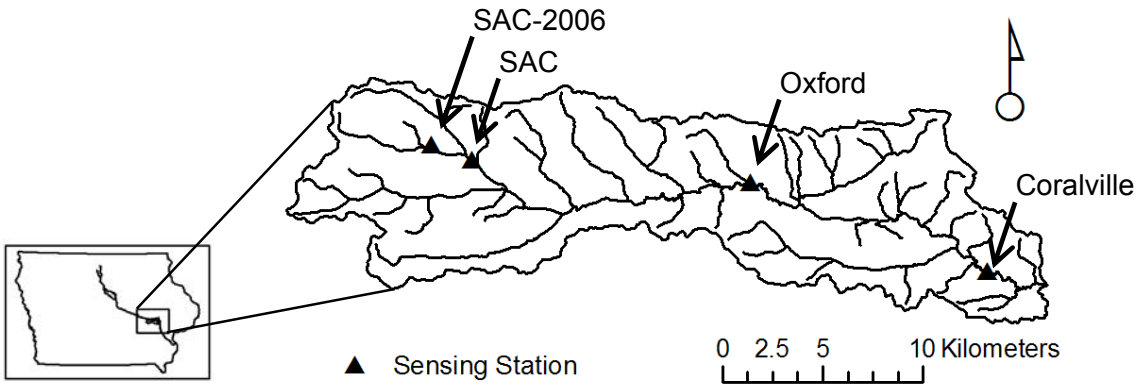

Figure 4.1 Location of the South Amana Catchment sensing stations during 2006 (SAC-2006) and 2007/2008 (SAC), and the Oxford, and Coralville sensing stations in the Clear Creek Watershed.

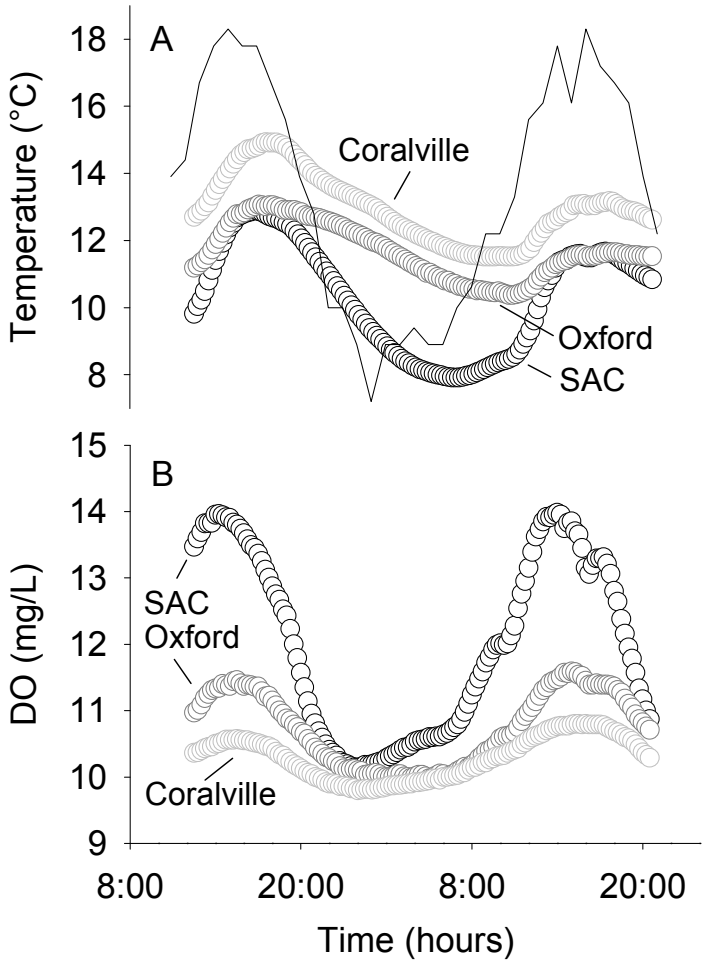

Figure 4.2 High-frequency air temperature ——, water temperature (A), and DO (B) data collected at the SAC, Oxford and Coralville sensing stations every 15 minutes.

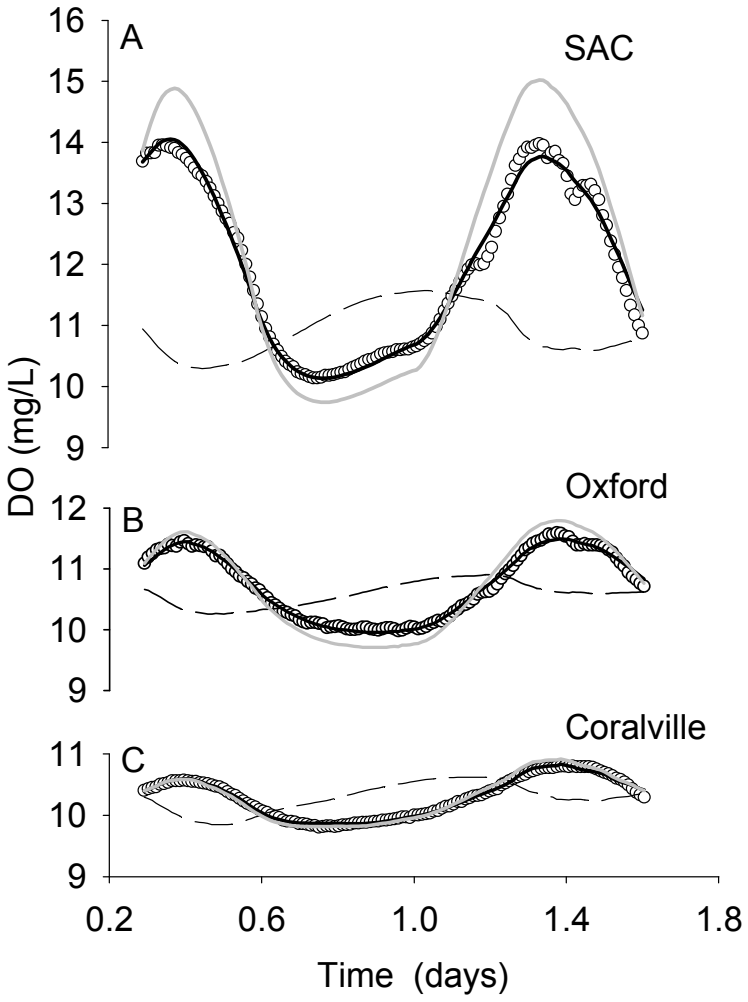

Figure 4.3 DO modeling results from Model M1 ——— and Model M2 ——— compared to high-frequency DO measurements ○ and DO saturation concentrations – – – at the SAC (A), Oxford (B), and Coralville (C) sensing stations in the Clear Creek Watershed.

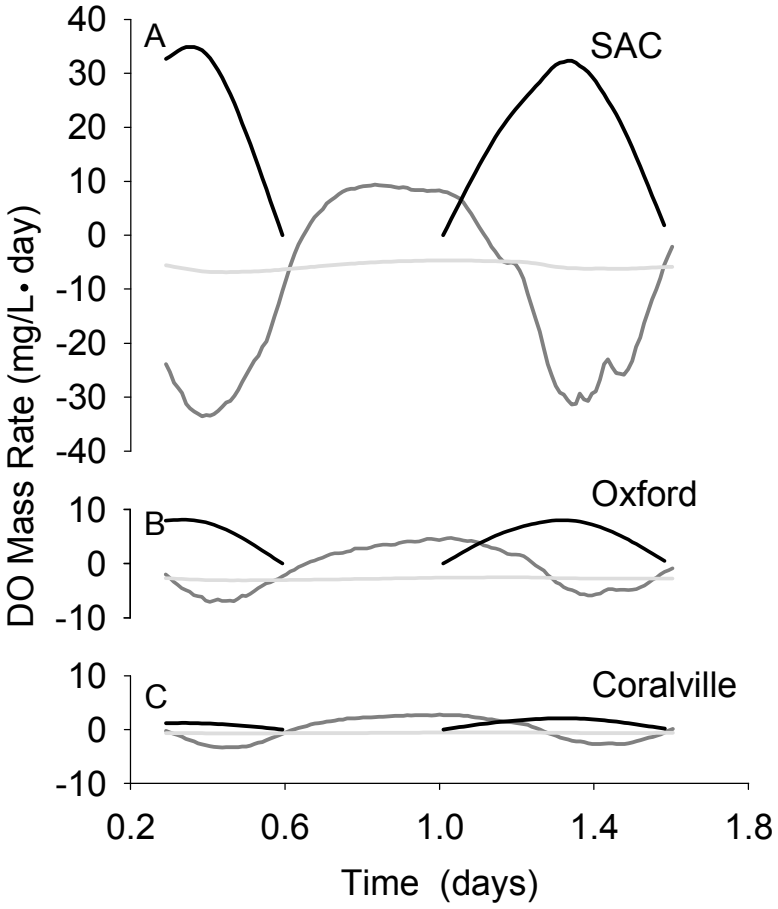

Figure 4.4 DO mass rates into the Clear Creek water column due to primary production ——, reaeration ——, and respiration —— rates determined from high-frequency measurements and optimized with Model M1 using temperature change factors for sensing stations at the SAC (A), Oxford (B), and Coralville (C) in the Clear Creek Watershed.

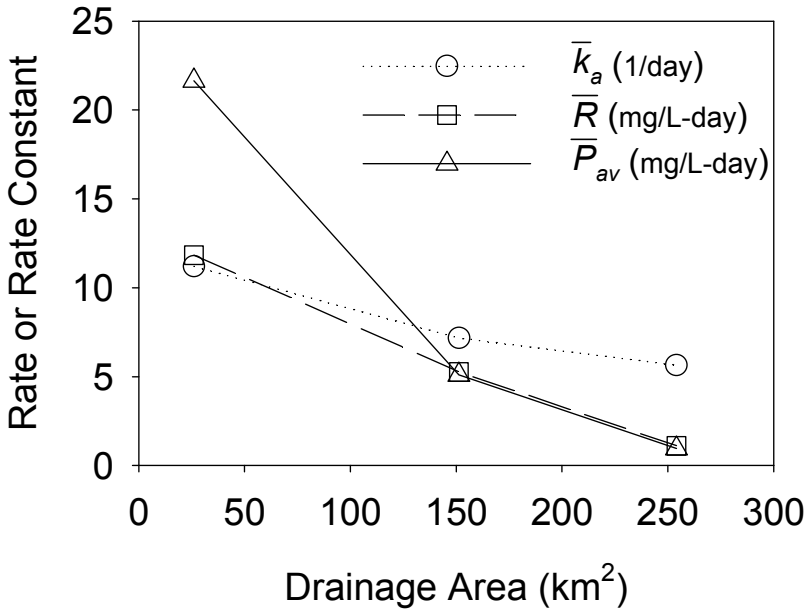

Figure 4.5 Scaling of reaeration rate constant, average primary production and respiration rates at a reference temperature of 20°C from Model M1 versus drainage area in the Clear Creek Watershed. Average primary production values are averages of values for day 1 and day 2 of the model simulation.

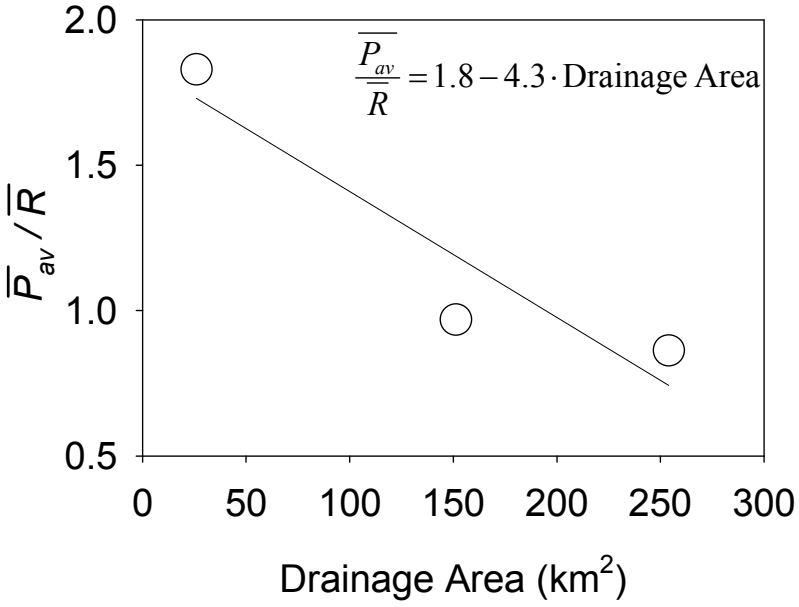

Figure 4.6 Scaling of $\overline{P}_{av} / \overline{R}$ ratio (average primary production rate to respiration rate) at a reference temperature of 20°C versus drainage area in the Clear Creek Watershed. Average primary production values are averages of values for day 1 and day 2 of the model simulation.

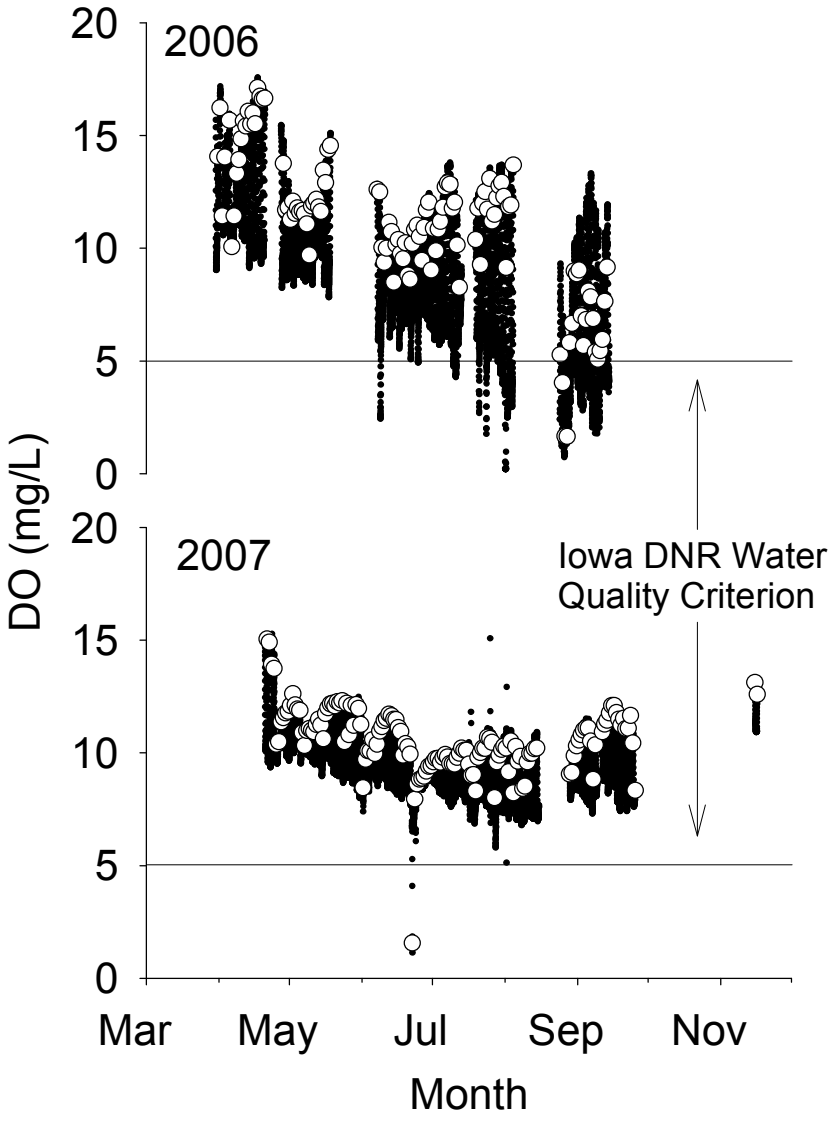

Figure 4.7 DO data collected during 2006 and 2007 (●) statistically sampled to simulate daily noon grab samples (○). Iowa DNR water quality criterion excursions were frequently observed in 2006 whereas, DO excursions were only observed during one event in 2007.

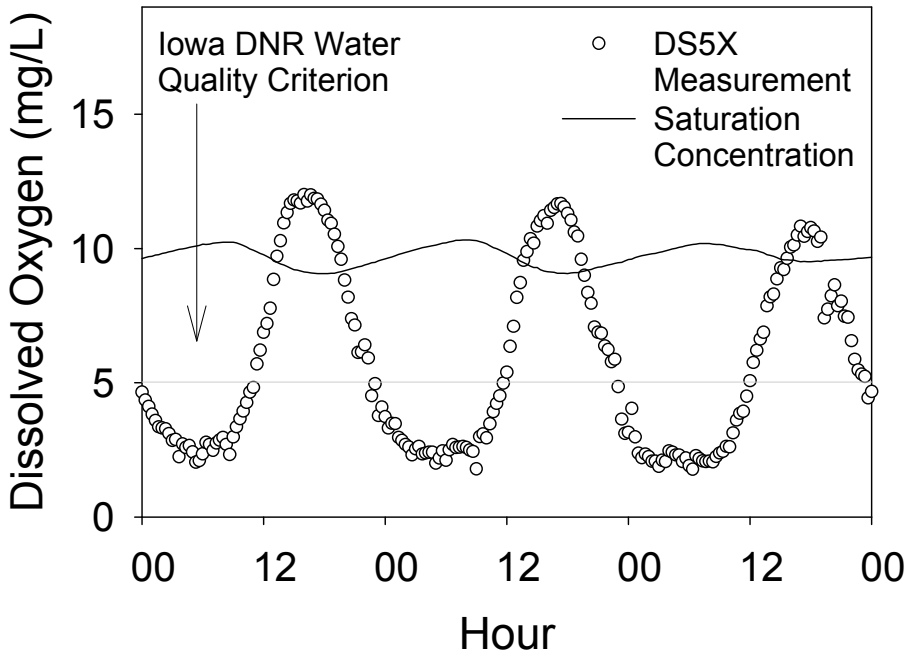

Figure 4.8 Dissolved oxygen measurements from 9/7/06 to 9/10/06 in Clear Creek show periods of super-saturation and violations of Iowa DNR water quality criteria.

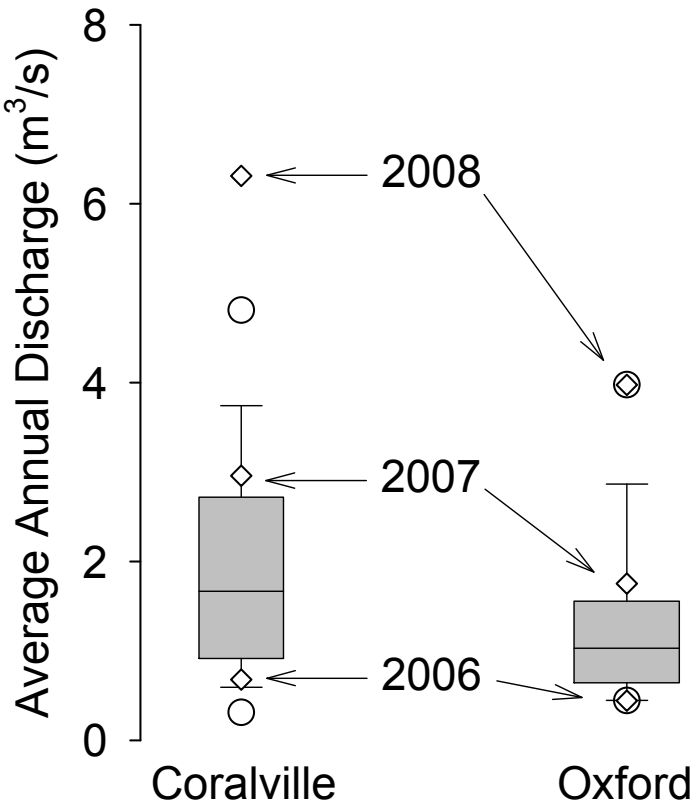

Figure 4.9 Box plot showing the average annual discharges at the Coralville and Oxford USGS gaging stations in the Clear Creek Watershed with 10th and 90th percentiles (whiskers), 5th and 95th percentiles (○), and average annual discharge values from 2006, 2007, and 2008 (◊). Data source: USGS (2008a).

Table 4.1 Drainage area, distance from headwaters, channel width, water depth, mean discharge, and calculated mean velocity at the SAC, Oxford, and Coralville sensing stations in the Clear Creek Watershed.

Sensing Station	Drainage Area (km^2)	Distance From Headwaters (km)	Channel Width (m)	Water Depth (m)	Mean Discharge[a] ($m^3\ s^{-1}$)	Calculated Mean Velocity ($m\ s^{-1}$)
SAC	26.1	7.9	3.0	0.5	0.4	0.26
Oxford	151.3	25.9	9.5	1.3	2.4	0.20
Coralville	254.1	42.1	14.0	1.0	3.3	0.23

[a]Mean discharge and water depth data at Oxford and Coralville were from approved USGS data.

Table 4.2 Reaeration rate constants, respiration rates, and average primary production rates at a reference temperature of 20° Celsius determined from optimization of Model M1.

Sensing Station	$\overline{k}_a$ (day^{-1})	$\overline{R}$ ($mg\ L^{-1}\ day^{-1}$)	$\overline{P}_{av}$ ($mg\ L^{-1}\ day^{-1}$)		RMSE Model M1[a] ($mg\ L^{-1}$)	RMSE Model M2[a] ($mg\ L^{-1}$)
			Day 1	Day 2		
SAC	11.2	11.8	22.4	20.9	0.15	0.69
Oxford	7.2	5.3	5.1	5.1	0.05	0.20
Coralville	5.6	1.1	0.7	1.2	0.03	0.06

[a]RMSE values determined from optimization of Model M1 to high-frequency DO data and comparison of Model M2 to high-frequency DO data collected in the Clear Creek Watershed.

Table 4.3 Fraction of surface light energy available at the creek bed in the Clear Creek Watershed.

Sensing Station	Average Turbidity (NTU)[a]	Estimated N ($mg\ L^{-1}$)	Estimated D ($mg\ L^{-1}$)	z (m)	k_e (m^{-1})	$I(z)/I_0$ (%)
SAC	2.7	2.8	0.7	0.5	0.3	87%
Oxford	27	49	12	1.3	4.7	0.2%
Coralville	20	33	8.3	1.0	3.2	4.2%

[a]87 turbidity measurements, in units of nephelometric turbidity units (NTU), collected during the modeling photoperiod were averaged at each station and converted to N and D concentrations using available field data.

CHAPTER 5:
HIGH FREQUENCY SENSING TO UNDERSTAND DIEL TURBIDITY CYCLES, SUSPENDED SOLIDS AND NUTRIENT TRANSPORT IN CLEAR CREEK, IOWA*

Abstract

Recent advances in sensor technology have made high-frequency environmental data readily available. In this study, high-frequency monitoring of turbidity revealed diel turbidity cycles with peak values during the nighttime and lower values occurring during daytime. Particles responsible for these cycles were fixed suspended solids consisting mostly of aluminosilicates (clay particles) emanating from bed sediments. High-frequency data were used to investigate the transport of total suspended solids (TSS) during base flow. A majority of the baseflow TSS loading occurred during the nighttime in a small agricultural catchment in Iowa. Elevated nighttime turbidity also resulted in increased total suspended phosphorus loading during nighttime. Bioturbation, as a result of nocturnal feeding of fishes, is the suspected cause of the diel turbidity cycles. High-frequency monitoring was also used to detect TSS loading during storm events. Results from this study highlight the importance of high-frequency environmental measurements to reveal and understand biogeochemical transport phenomena.

Introduction

The transport of pollutants and pathogens associated with solids suspended in the water column can lead to the degradation of water quality and designated use impairments in a water body. Excessive suspended solids alter fish community composition and reduce the population of benthic algae and invertebrates (Ryan 1991;

*Loperfido, J.V., Just, C.L., Papanicolaou, A.N., and Schnoor, J.L. (2009). "High-frequency sensing to understand diel turbidity cycles, suspended solids and nutrient transport in Clear Creek, Iowa." *Water Resour. Res.*, In review.

Davies-Colley et al. 1992; Quinn et al. 1992). Suspended solids transport organic nitrogen and organic phosphorus to the Gulf of Mexico, contributing key nutrients that create hypoxic conditions in coastal waters (House et al. 1997; Mayer et al. 1998; Goolsby et al. 1999).

Total suspended solids (TSS) concentrations vary dramatically depending on the time scale. Seasonal variations in TSS are often caused by changes in rainfall patterns (Meybeck et al. 1999). Storm events can trigger changes in TSS on an hourly time scale (Lewis 1996). Variations of TSS occurring on a daily basis have been documented in coastal areas where tidal action dictates resuspension (Schoellhamer 2002). Daily variations of turbidity, a measurement of light scattering in the water and a surrogate parameter for TSS, have been previously reported in freshwater. Turbidity peaked near sunrise and reached a minimum at sunset at eleven monitoring stations in Gwinnett County, Georgia (Gillain 2005), where biological activity was suspected to be the source of the turbidity. Diel turbidity measurements were observed to be three to four times higher at nighttime than at daytime in a small rural stream in Michigan (Morse et al. 2002).

In Clear Creek, Iowa, diel turbidity cycles have been consistently observed from spring to fall during 2006 and 2007, and are reported here for the first time. The goal of this study was to identify the mechanism/s causing this phenomenon and to characterize the particles causing the diel turbidity cycles. The impact of the diel cycles on the export of TSS from the catchment was analyzed using high-frequency data collected by *in situ* sensors.

Materials and Methods

Site Description

The Clear Creek Watershed (267 km^2), located in east-central Iowa, is a Hydrologic Unit Code (HUC) 10 watershed which discharges into the Iowa River (Figure

5.1). Land cover is dominated by agricultural activities including corn, soybeans and pasture (≈ 85%). An environmental sensing station was installed near the headwaters of the Clear Creek Watershed at the outlet of the highly erodable South Amana Catchment (SAC) which has a drainage area of 26.1 km^2.

Field Study Methods

Turbidity in Clear Creek was measured every twenty-minutes using a Forest Technology Systems Ltd. DTS-12 Turbidity Sensor deployed *in situ* from 9/11/2007 to 10/16/2007. Data from this sensor were recorded on a Campbell Scientific CR1000 data logger. Stage was measured using a Global WL16 Water Level Data Logger, and flow data were obtained from a stage-discharge curve (Abaci and Papanicolaou 2009). Grab samples were collected during the spring, summer, and fall of 2007 and analyzed for turbidity, TSS, fixed suspended solids, and volatile suspended solids as described in APHA (1989). The same samples were also analyzed for total suspended phosphorus by modifying the method described in APHA (1989) with the assumption that total dissolved phosphorus was quantifiable through direct colorimetry of the filtrate (i.e. total dissolved phosphorus was approximately equal to dissolved reactive phosphorus). Rainfall measurements from the Cedar Rapids Municipal Airport, located 23.3 km northeast of the SAC sensing station, was obtained from the National Climatic Data Center (NCDC 2009).

Laboratory Methods

Suspended solids from 100 ml Clear Creek samples collected at 13:03 and 19:59 on 9/18/2007 were filtered onto Millipore 0.22 micrometer nitrocellulose filters, dried in an oven at 105° C, mounted on aluminum SEM stubs, sputter coated in carbon, and visualized on a Hitachi S-4800 Scanning Electron Microscope (SEM). Elemental maps of these filtered samples were generated using a Hitachi S-3400N variable-pressure SEM equipped with a Bruker AXS energy dispersive spectroscopy (EDX) x-ray microanalysis

system using an acceleration voltage of 15 kV. An x-ray diffraction (XRD) pattern of Clear Creek bed material was obtained using a Rigaku MiniFlex II benchtop X-ray diffraction system. Sample pretreatment for the XRD analysis included soaking in H_2O_2 to remove organic material, and rinsing in deionized water, centrifuging, and decanting to remove excess ions. The particles were then dried in an oven at 105° C for two days prior to performing the XRD.

Statistical analyses of time series data from the sensor and grab samples were performed using SAS 9.1 statistical software. Linear regressions, as described in Piegorsch and Bailer (2005), were performed to describe the associations among grab sample variables.

Results and Discussion

Characterization of the Diel Turbidity Cycle

High-frequency turbidity measurements revealed diel cycles in Clear Creek with maximum values occurring during nighttime and minimum values during daytime (Figure 5.2A). These cycles were observed consistently from spring to fall in 2006 and 2007 in the Clear Creek Watershed and occurred during base flow periods of relatively constant discharge. Minimum turbidity values were typically observed between 12:00 and 18:00, and maximum turbidity occurred between 22:00 and 8:00 (Figure 5.2 Inset). Turbidity measured during precipitation events on 10/2/2007 and 10/14/2007 was larger than measurements during base flow. Discharge data from the SAC revealed that base flow conditions existed during most of the monitoring period except during 29.5 mm and 31.8 mm storm events (NCDC 2009) occurring on 10/2/2007 and 10/14/2007, respectively (Figure 5.2B).

Data from grab samples collected during a field study performed from 11:00 on 9/18/2007 to 14:00 on 9/19/2007 revealed a similar diel cycle in fixed and volatile suspended solids concentrations as seen in the turbidity data of Figure 5.3. A

precipitation event totaling 14.5 mm (NCDC 2009), highlighted in gray in Figure 5.3, led to elevated measurements of turbidity during the rain event; however, the typical diel cycle resumed shortly thereafter and was largely unaffected. The precipitation event was responsible for the peak fixed suspended solids and volatile suspended solids measurements sampled at 0:10. Turbidity measurements from grab samples were on average, 22% lower (n=27) than *in situ* sensor measurements perhaps due to particle flocculation (Gippel 1989) during the 36 hour sample storage time. Fixed suspended solids concentrations were consistently higher than volatile suspended solids during daytime (2.4 times greater) and nighttime (6.5 times greater), not including the sample collected at 0:10 during the precipitation event.

Linear regression modeling of logarithm transformed turbidity measurements versus logarithm transformed TSS, fixed suspended solids, and volatile suspended solids concentrations from Figure 5.3 yielded statistically significant relationships (p-value < 0.05) shown in Table 5.1. The R^2 value was highest for the turbidity–TSS regression, second highest for the turbidity–fixed suspended solids regression, and lowest for the turbidity–volatile suspended solids regression. R^2 values suggest that fixed suspended solids concentrations account for more variability in turbidity measurements than volatile suspended solids (0.94 versus 0.85).

As expected, SEM images of filtered Clear Creek particles showed an increased concentration of suspended solids from daytime to nighttime (Figure 5.4), confirming measurements shown in Figure 5.3. The SEM images also revealed that large particles (> 20 micrometers), small amorphous particles (< 5 micrometers), and phytoplankton were all more abundant at nighttime. The number of filter pores (black areas on Figure 5.4) appeared to decrease from daytime to nighttime due to an increased presence of small particles clogging the filter pores. Previous research indicated that nephelometric turbidity (light scattering) is maximized by a mean particle diameter of 1.2 – 1.4 micrometers for a given suspended solids concentration (Gippel 1995). The small

particles which clogged the pores in Figure 5.4B are believed to have played an important role in the diel turbidity observed in Clear Creek.

An EDX analysis of TSS during periods of both low and high turbidity revealed solids largely comprised of silicon, aluminum, iron, and oxygen (Figure 5.5). The elemental composition of the particles together with their amorphous appearance suggests that the suspended solids are primarily aluminosilicate clay, similar to particles collected from bed sediments in simulated agitation experiments. Silicon, aluminum, iron, and oxygen which, were present at mass percentages of 20%, 8%, 5%, and 48%, respectively, based on an average of two point analyses on the large particles. This would be consistent with the stoichiometry of aluminosilicate clays (Schaetzl and Anderson 2005). Sodium, potassium, magnesium, calcium, and titanium were also detected but at lower levels, perhaps indicative of feldspar minerals. Turbidity levels had little or no influence on diel elemental particle composition, suggesting that the particles suspended at nighttime and daytime were of the same origin.

Mechanism for Diel Turbidity Cycles

Bioturbation is the likely cause of the diel cycling of turbidity. The stream biota is known to include nocturnal bottom-feeding fishes, and the particles analyzed from samples at night were consistent with resuspended bed material (inorganic clays). Sampling conducted by the Iowa Department of Natural Resources and Iowa State University has recorded the presence of the black bullhead (*Ameiurus melas*), channel catfish (*Ictalurus punctatus*), common carp (*Cyprinus carpio*), white sucker (*Catostomus commersoni*) and yellow bullhead (*Ameiurus natalis*) in the Clear Creek Watershed (IRIS 2008). These species are known to feed on plankton, detritus, and insects on the creek bed from dusk to dawn (Reynolds and Casterlin 1978a; Reynolds and Casterlin 1978b; Becker 1983; Pflieger 1997). Averaged turbidity data from 9/11/2007 to 10/2/2007 for each measurement during the daily cycle indicates that initial increases in turbidity

occurred immediately after sunset (Figure 5.6). Turbidity values increased to a maximum just before sunrise and declined sharply with the onset of daytime, correlating well with the dusk to dawn activity of the fishes listed above and the time required for particles to settle-out from the water column. Exclusion of fishes from the water column enclosures successfully eliminated the diel turbidity cycle and resulted in constant or slightly decreasing turbidity trends (explained in more detail below).

Behavior of fishes described in the literature provides evidence that bioturbation was the source of diel turbidity cycling in Clear Creek. The black bullhead and common carp have been positively correlated to increased turbidity measurements in pond and wetland settings (Zambrano and Hinojosa 1999; Braig and Johnson 2003). Furthermore, elevated suspended solids concentrations measured in ponds stocked with common carp were predominantly inorganic in nature (Parkos III et al. 2003), similar to Clear Creek (Figure 5.3). The geographic range of common carp includes Georgia, the range of the black bullhead includes Michigan, and the range of the yellow bullhead includes both states (Becker 1983; Pflieger 1997). It is believed their presence explains the diel turbidity cycles observed in Clear Creek and those of Morse et al. (2002) and Gillain (2005). It is striking how reproducible the diel turbidity cycle is from day to day in Clear Creek (Figure 5.2A and Figure 5.6), suggesting the consistent behavior of nocturnal bioturbation by fishes dominates the particle dynamics of the water column in this small, upland stream during base flow.

Analysis of the settling velocity explains the decline in elevated suspended solids concentrations after sunrise due to sedimentation. The settling velocity of the particles was estimated using Stokes' law (as presented in Chapra (1997)):

Equation 5.1
$$v_s = \alpha \frac{g}{18}\left(\frac{\rho_s - \rho_w}{\mu}\right)d^2$$

where α = a dimensionless form factor reflecting the effect of the particle's shape on settling velocity (for a sphere it is 1.0), g = acceleration due to gravity, ρ_s = density of

the particle, ρ_w = density of the water, μ = dynamic viscosity, and d = effective particle diameter. If a density of 2500 kg m^{-3} is assumed for a typical clay particle (Das 2000), and ρ_w and μ are estimated from tables in (Crowe et al. 2001) based on a mean water temperature of 15 °C, measured from 7:00 to 10:00 during 9/11/2007 to 10/2/2007, then the average settling velocity of a 5 micron particle observed in Figure 5.4 and Figure 5.5 would be 1.8×10^{-5} m s^{-1}. Turbidity measurements in Clear Creek required three hours from sunrise to fall below 10 NTU (Figure 5.6). This is approximately equal to the 4.6 hours required for a 5 micron clay particle to settle from the 0.3 m water column at the study site. Thus, the slow settling velocity of clay particles, calculated by Stokes Law, explains the persistence of elevated turbidity due to bioturbation at nighttime as well as the decline in turbidity during the morning (daytime) hours.

Diel turbidity measurements of Clear Creek water contained in plexiglass boxes deployed *in situ* provides additional evidence that bioturbation is the driving force of diel turbidity cycles (Figure 5.7). Three 0.3 m x 0.3 m x 0.6 m tall plexiglass boxes were filled with water from Clear Creek and secured in the creek on 11/15/2007 to 11/16/2007. Two plexiglass boxes with open bottoms, one clear and one covered in tinfoil on the sides and top, were hand-driven into the creek bed to exclude fishes and upstream water influx. An additional box with a plexiglass bottom was filled with creek water, placed in the creek, and secured to the bed. Turbidity in the boxes was measured using Hydrolab DS5X data sondes (Hach Company, Loveland, CO) and turbidity in Clear Creek was measured using a DTS-12 Turbidity Sensor. High-frequency turbidity data from the sensor deployed *in situ* recorded the diel turbidity cycle of the entire creek while the three sensors in the plexiglass boxes measured constant or declining turbidity trends. Since fishes were not present in the plexiglass boxes, the absence of a diel turbidity cycle measured provides additional evidence supporting bioturbation as the diel turbidity driving force.

Alternative hypotheses, dissolution/precipitation reaction and stabilization/destabilization of creek bed particles, were posed and rejected as possible sources of the diel turbidity cycles in Clear Creek. The inorganic nature of the particles responsible for the diel turbidity trend suggested that a nighttime precipitation/daytime dissolution reaction may have occurred; however, there are several lines of evidence that indicate this is not the case. High frequency pH data collected during 2006 and 2007 consistently showed a decrease in pH at nighttime as a result of CO_2 (a weak acid) addition from algal respiration. During the daytime, the pH in Clear Creek increased as CO_2 was taken up by algae during photosynthesis. Generally, it would be expected that the concentration of precipitated solids would decrease with a lower pH such as the in the case of calcium carbonate (Jensen 2003). Thus, if a dissolution/precipitation reaction were responsible for the diel turbidity cycles, it would cause larger turbidity values at higher pH values, an observation that is contrary to what is observed in Clear Creek. In addition, a linear regression analysis relating turbidity data from 2007 to specific conductivity data yielded an R^2 of 0.01 (n = 1186, P-value = 0.004). If a dissolution/precipitation reaction were occurring, a diel trend in specific conductivity would be expected and variability in specific conductivity data would explain the variability in turbidity data but this was not observed. Given these lines of evidence, a dissolution/precipitation reaction as the driving force for the diel turbidity trends was rejected.

Diel changes in pH could have led to the colloidal destabilization of Clear Creek bed particles, leaving them susceptible to suspension into the water column; however, physical properties of Clear Creek bed particles discount this hypothesis. The SEM-EDX analysis of particles suspended in Clear Creek indicated that the particles responsible for the diel turbidity cycles were aluminosilicate clay particles. Clay particles such as kaolinite have been observed to erode at higher rates at a pH range from 5.5 – 7.0 (Ravisangar et al. 2001) with typical point of zero charge values ranging from 3.0 – 5.0

(Schroth and Sposito 1997), however these ranges are well below the pH values typically observed in Clear Creek during 2007 (Figure A.8). XRD patterns of washed bed material from Clear Creek indicated that a large portion of the bed material is silicon dioxide, quartz sand (Figure 5.8). The presence of elements comprising quartz, silicon and oxygen, were also observed in filtered Clear Creek suspended solids during both the daytime and nighttime (Figure 5.5). If quartz has a point of zero charge, it is likely in a pH range from 2 to 4 (Kosmulski 2006). Thus, destabilization of Clear Creek bed particles is not likely to have contributed to the diel turbidity swing.

Influence of Diel Turbidity on Suspended Solids and Nutrient Transport

Statistical relationships linking TSS concentrations to turbidity measurements are frequently reported in the literature (e.g. Grayson et al. 1996; Christensen et al. 2000; Harter and Mitsch 2003). Logarithm transformed TSS and turbidity data from the Clear Creek Watershed and the Iowa River were used to construct a statistically significant (p-value < 0.05) regression model for the prediction of TSS (Figure 5.9). The R^2 value indicates that the logarithm of turbidity data accounts for 87% of the variability of the logarithm of TSS concentrations.

TSS concentrations calculated using the regression in Figure 5.9 were multiplied by interpolated discharge data from Figure 5.2B to estimate the TSS loading rate from the SAC (Figure 5.10). During the base flow period prior to the 10/2/2007 storm event, 77% of the TSS exported from the SAC occurred during the nighttime (Table 5.2). The TSS load that occurred during the two storm periods from 9/12/2007 to 10/15/2007 accounted for 70% of the total TSS loading during the period despite the presence of storm flow for only 4% of the time (Table 5.2).

Knowledge of this TSS transport would be difficult to obtain using grab samples because sampling typically does not occur during the nighttime, and sampling campaigns

often fail to capture storm events in remote locations like the SAC in the Clear Creek Watershed. Furthermore, water quality sensors can perform high-frequency measurements compared to a grab sampling campaign, which should result in more accurate estimation of TSS loads. For example, by statistically re-sampling TSS loadings in Figure 5.10 to simulate a daily grab sample campaign occurring at noon each day (12:00 from 9/12/2007 to 10/15/2007), the total TSS load estimated from the SAC would be three times smaller than that obtained from high-frequency sensors (Table 5.2). The standard deviation of the daily mean load was also smaller using daily grab samples as compared to high-frequency sensors. This implies that grab sampling substantially underestimates both the total load and the magnitude of peak TSS loading rates.

In addition to TSS, diel turbidity cycling has implications for the transport of nutrients. Total suspended phosphorus measurements from Clear Creek exhibited a diel cycle similar to turbidity and TSS (Figure 5.11). Seventy-one percent of the total suspended phosphorus load occurred during the nighttime (Table 5.3). If daytime grab sampling was used to monitor this nutrient, the total load would be severely underestimated and possibly lead to pollution mitigation strategies that are ineffective in achieving desired environmental goals.

Conclusions

High-frequency measurements from water quality sensors aided the understanding of particle dynamics in the Clear Creek watershed. The high-frequency nature of the data revealed the unexpected biogeochemical phenomenon of diel turbidity cycles. Bioturbation is the likely cause of the diel turbidity cycles as nocturnal feeding activity of fishes suspend amorphous clay particles that settle following sunrise. In Clear Creek, Iowa, high-frequency turbidity data (twenty-minute periods) were used to estimate high-frequency loading rates of TSS and revealed that the diel turbidity cycles had a significant impact on the transport of TSS. Increased nighttime transport of TSS were

associated with nighttime increases in total suspended phosphorus transport and imply transport of other pollutants often sorbed to suspended solids such as organic nitrogen, metals, and pathogens. Episodes of TSS loading during storm events were also monitored using high-frequency sensor data despite their occurrence during only 4% of the total monitoring period. High-frequency measurements can help resource managers gain a better understanding of pollutant transport and dynamics, and they can help inform better pollution reduction strategies.

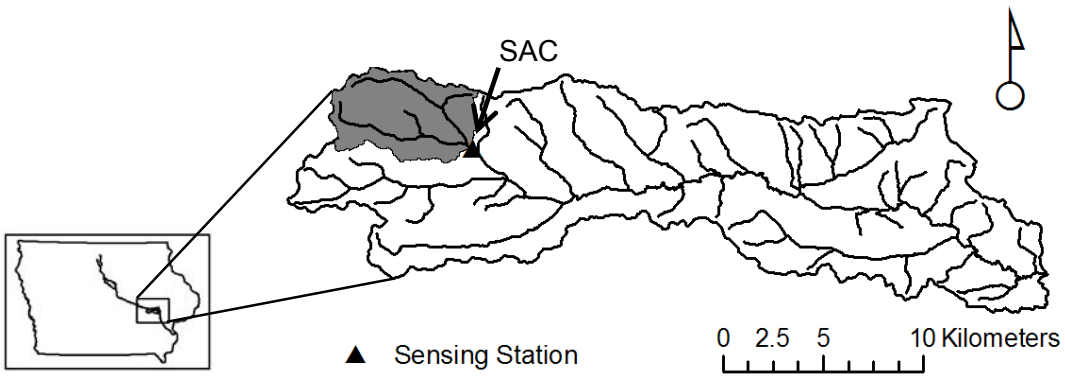

Figure 5.1 Location of the Clear Creek HUC 10 study area with respect to Iowa and the Iowa River. Experiments in this study were performed at the environmental sensing station (▲) at the outlet of the SAC (shaded area).

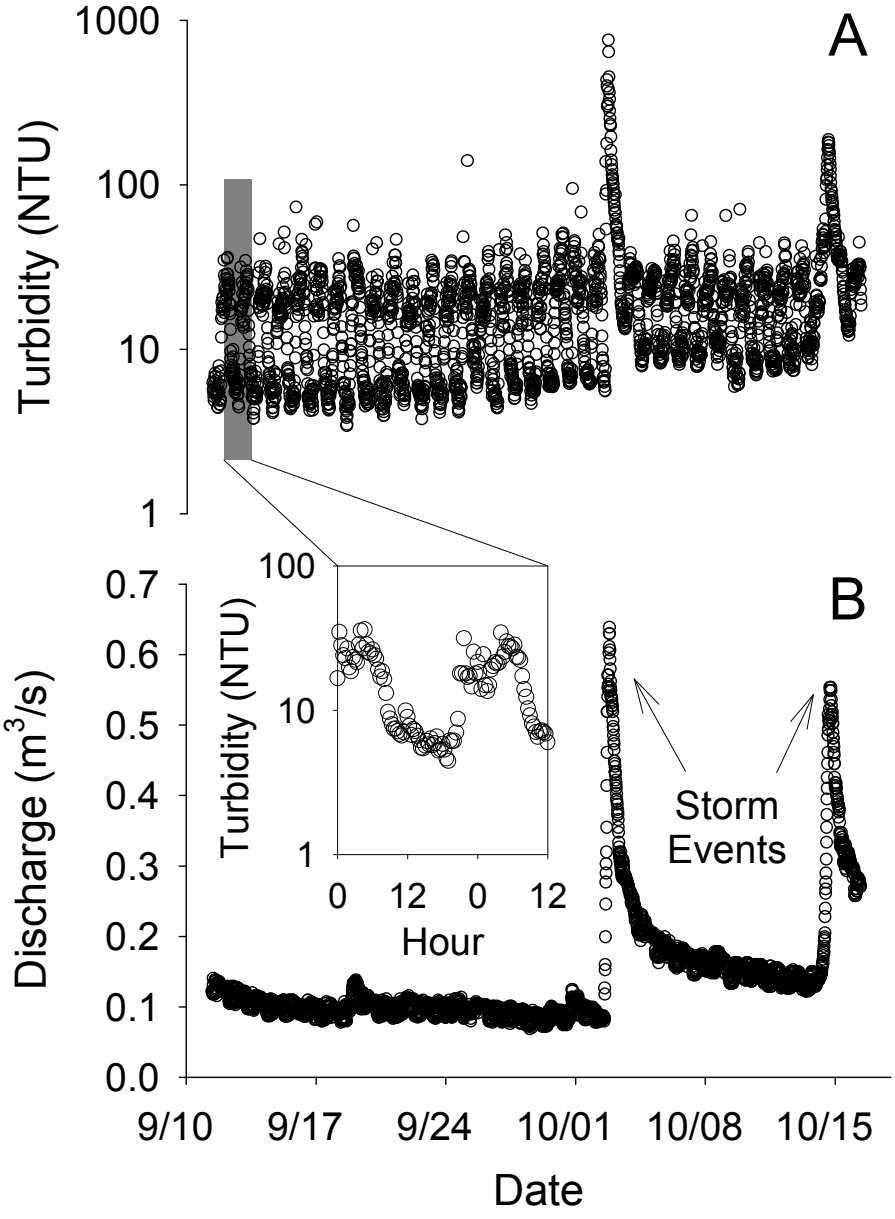

Figure 5.2 High-frequency turbidity (A) and discharge (B) data from the SAC sensing station observed from 9/11/2007 to 10/16/2007 by *in situ* water quality sensors. The diel cycling in turbidity during base flow periods is shown by the inset with high turbidity at night and low turbidity values during the day. Storm events on 10/2/2007 and 10/14/2007 led to the highest turbidity and discharge measurements during the monitoring period.

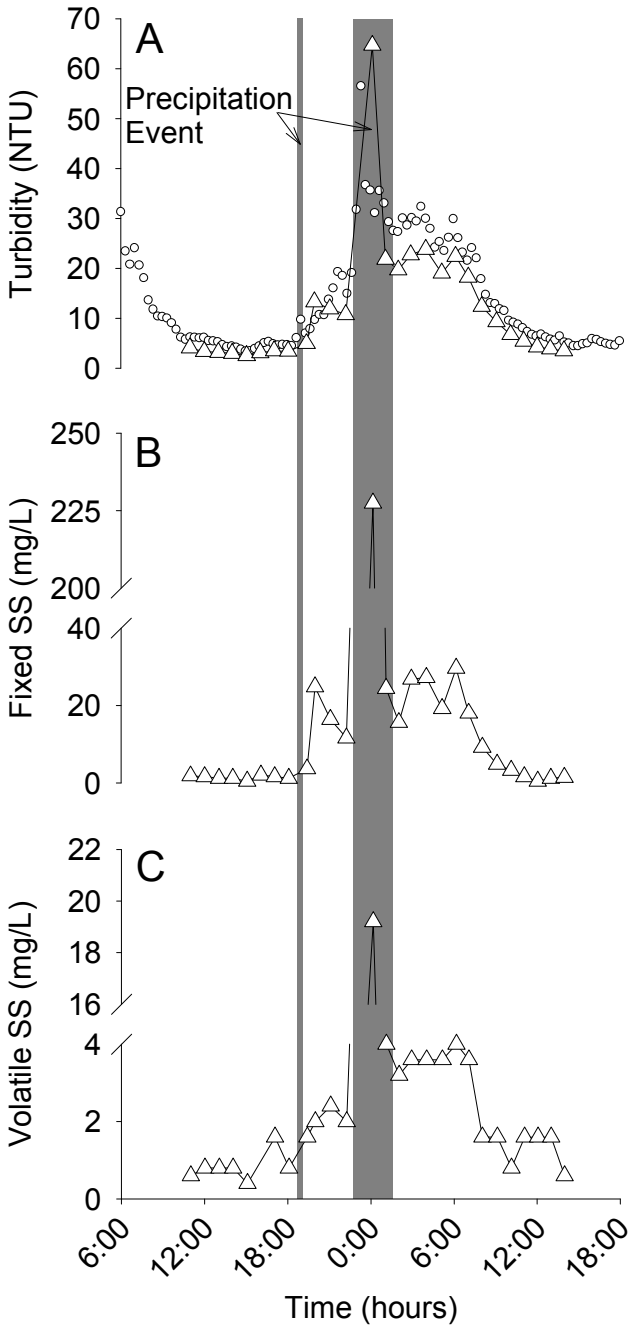

Figure 5.3 Sensor (○) and grab sample (Δ) measurements of turbidity (A), fixed suspended solids (B), and volatile suspended solids (C) from 11:00 on 9/18/2007 to 14:00 on 9/19/2007. Averages of duplicate suspended solids samples are shown for data points at 11:00 on 9/18 and 00:10, 6:10, and 13:59 on 9/19.

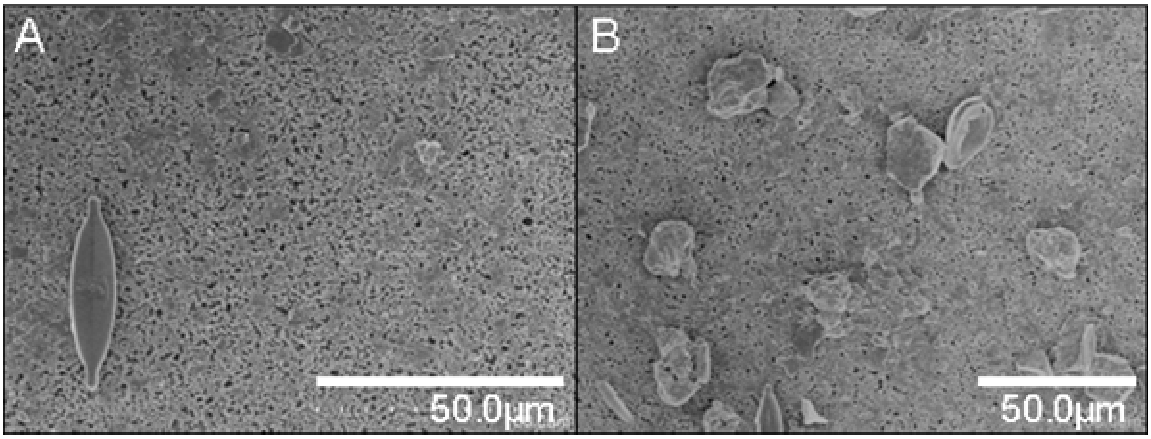

Figure 5.4 SEM images of Clear Creek TSS filtered from grab samples during periods of low (A) and high (B) turbidity collected at 13:03 and 19:59 on 9/18/2007, respectively.

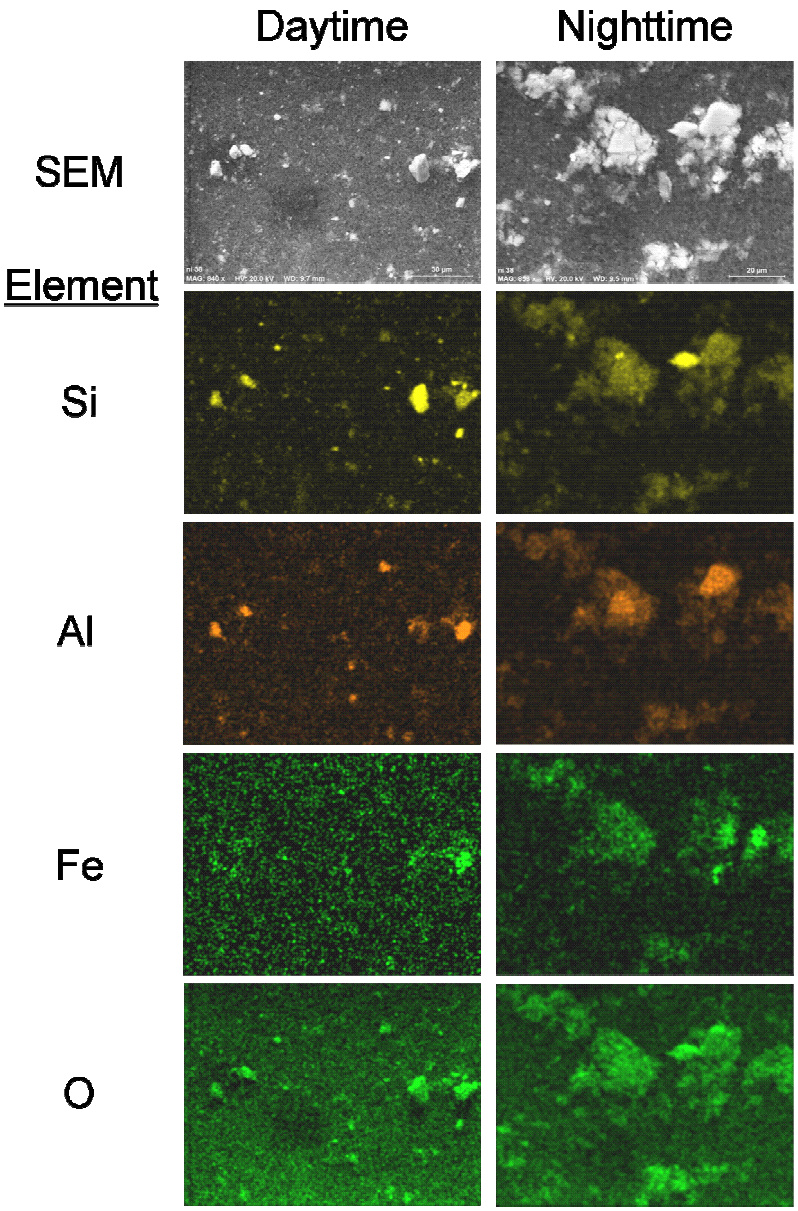

Figure 5.5 EDX images of TSS filtered from Clear Creek during daytime and nighttime on 9/18/2007 indicated the particles are largely comprised of silicon, aluminum, iron, and oxygen.

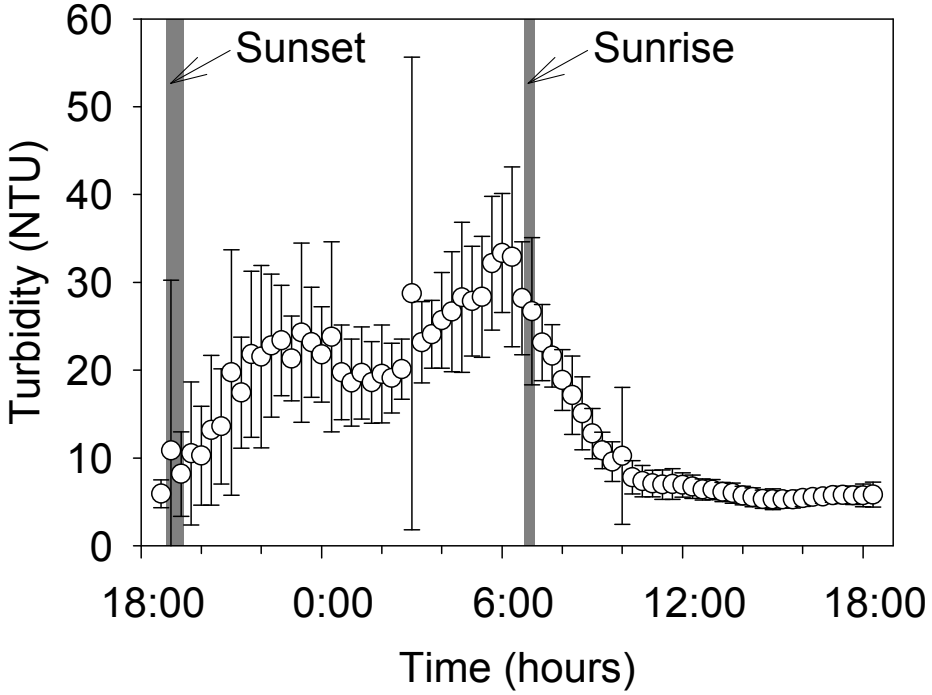

Figure 5.6 Turbidity measurements from 9/11/2007 to 10/2/2007 averaged for each measurement in the daily cycle. Error bars indicate one standard deviation for each set of measurements. The vertical gray bars indicate the range of sunrise and sunset times during the data period (sunrise/sunset data source: AAD (2008)).

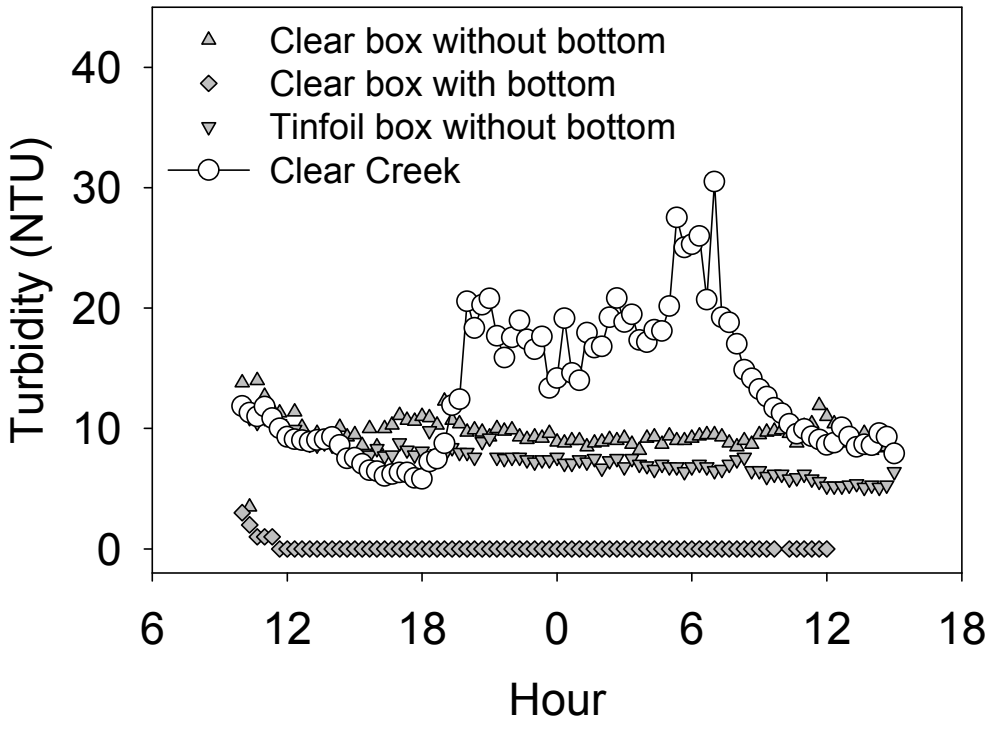

Figure 5.7. Turbidity measured in Clear Creek (○) and in plexiglass boxes deployed in Clear Creek on 11/15/2007 and 11/16/2007.

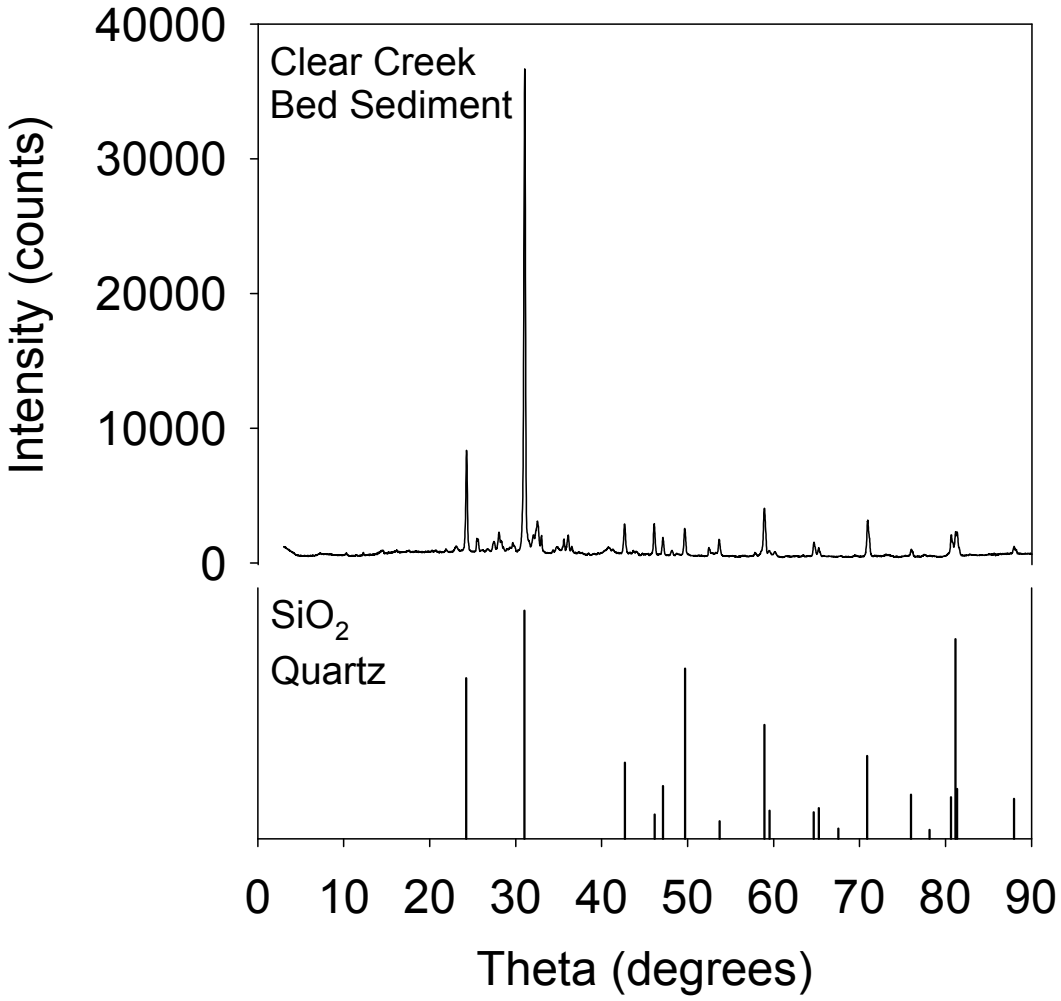

Figure 5.8 XRD analysis of Clear Creek bed sediment indicated a large presence of quartz (SiO_2).

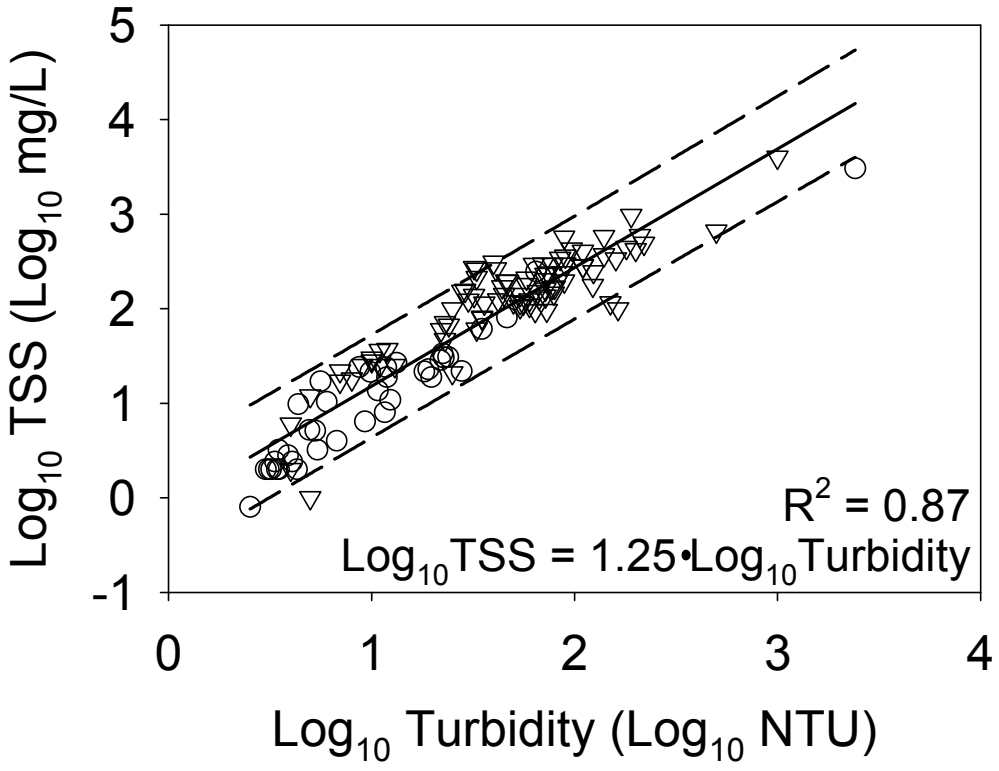

Figure 5.9 Linear regression (—) and 95% prediction intervals (— — —) of log transformed TSS and turbidity data from the Clear Creek Watershed (○) and the Iowa River (▽).

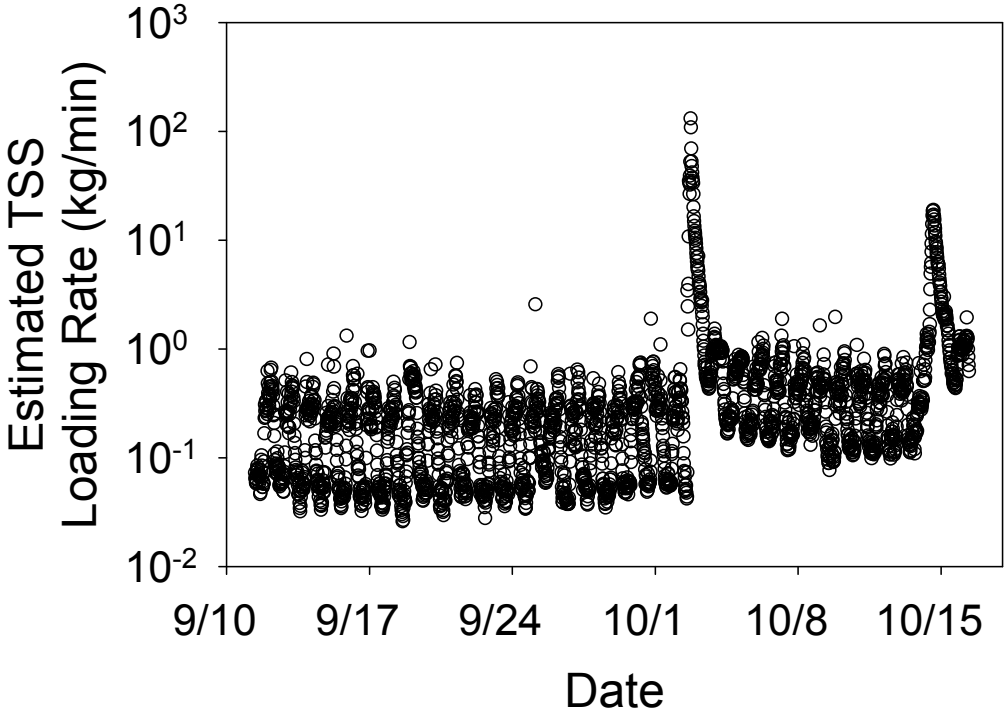

Figure 5.10 Estimated TSS loading rates from the SAC from 9/11/2007 to 10/16/2007.

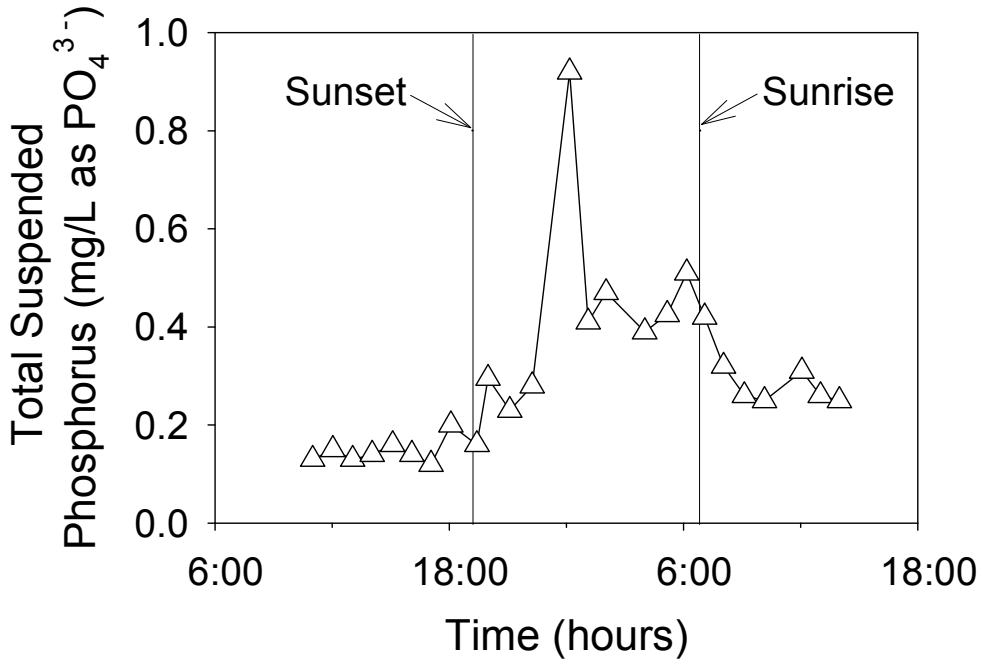

Figure 5.11 Total suspended phosphorus concentrations in Clear Creek on 9/18/2007 and 9/19/2007.

Table 5.1 Coefficient of determination (R^2) values from linear regression analyses between log_{10} turbidity and log_{10} TSS, log_{10} fixed suspended solids, and log_{10} volatile suspended solids from grab samples in Figure 5.3 collected on 9/18/2007 and 9/19/2007.

Model	n[a]	R^2	p-value
Log_{10} TSS = 1.53*Log_{10} Turbidity – 0.52	31	0.96	< 0.0001
Log_{10} Fixed SS = 1.72*Log_{10} Turbidity – 0.85	31	0.94	< 0.0001
Log_{10} Volatile SS = 0.94* Log_{10} Turbidity – 0.64	30	0.85	< 0.0001

[a]n = number of measurements

Table 5.2 Comparison of estimated TSS loading from the SAC under different conditions: daytime versus nighttime loading during base flow (9/12/2007 - 10/2/2007), storm event versus base flow loading (9/12/2007 – 10/15/2007), and sampling strategy using high-frequency sensors versus daily noon grab samples (9/12/2007 – 10/15/2007).

Comparison	Total Load kg	Mean Daily Load kg (std dev)	% of Total Load	% of Time
Base Flow Day/Night				
Daytime	1.3×10^3	6.6×10^1 (1.0×10^1)	23%	51%
Nighttime	4.3×10^3	2.1×10^2 (5.0×10^1)	77%	49%
High/Low Flow				
Storm Events	3.0×10^4	-	70%	4%
Base Flow	1.3×10^4	-	30%	96%
Sampling Strategy				
High-frequency Sensors	4.3×10^4	1.3×10^3 (3.4×10^3)	-	-
Daily Noon Grab Samples	1.4×10^4	4.1×10^2 (1.4×10^3)	-	-

Table 5.3 Total suspended phosphorus (as PO_4^{3-}) concentrations and loading from the SAC during daytime and nighttime from 10:34 on 9/18/2007 to 10:34 on 9/19/2007.

Period	Mean Concentration mg L^{-1} (std dev)	Total Load kg	% of Total Load	% of Time
Daytime	0.20 (0.09)	0.91	29%	51%
Nighttime	0.41 (0.21)	2.27	71%	49%

CHAPTER 6:
GEOSPATIAL INTERPRETATION OF PHYSICOCHEMICAL DATA FOR THE CLEAR CREEK WATERSHED

Abstract

Geospatial and environmental data from the Clear Creek Watershed were modeled using GIS software to uncover spatial relationships of channel width, average annual discharge, and water quality parameters in Iowan Watersheds. Results from this research revealed a positive linear relationship between channel width and drainage area ($R^2 = 0.95$) in the Clear Creek Watershed. A positive linear relationship was also revealed between the logarithm of drainage area and the logarithm of average annual discharge ($R^2 = 0.99$) measured at 83 USGS gaging stations in Iowa. Statistically significant relationships (p-value < 0.05) between water quality parameters and stream location were uncovered for several water quality parameters in the Clear Creek Watershed. Chloride concentrations decreased downstream from the known septic tank inputs into the creek likely due to the dilution of the sewage. Nitrate concentrations decreased downstream of the SAC and the Conroy branches likely due to the dilution of fertilizer runoff and sewage discharge from the SAC and Conroy tributaries, respectively. Higher orthophosphate concentrations were discovered near the mouth of the Clear Creek Watershed and may be due to either urban fertilizer application or the hydrolysis of organic matter in the downstream portion of the watershed. DO and pH measurements were relatively uniform throughout the Clear Creek Watershed.

Introduction

Water quality models are frequently used to assess the ecological health of a watershed. Using a mass balance approach, they apply fundamental laws of biology, chemistry and physics to simulate the fate and transport of nutrients and suspended solids. The shortfall to these models often is that they do not readily incorporate detailed

geospatial data. Relationships created using spatial data in a GIS platform could be used to describe watershed characteristics such as discharge or land cover and facilitate their input into a non-spatial water quality model. The goal of this research is to develop models which can be used to input geospatial data from the Clear Creek watershed into the QUAL2K water quality model.

Material and Methods

Channel Width/Drainage Area Relationship

A linear regression model relating channel width based on drainage area was constructed using the digital elevation model (DEM) and field measurements in the Clear Creek Watershed. The Clear Creek drainage network was determined by using the Arc Hydro Data Model (Maidment 2002) in ArcMap 9.1 (ESRI, Redlands, CA) to delineate the DEM. Locations used to measure channel width in the Clear Creek Watershed were selected to encompass the range of drainage areas contributing to channelized flow and where public access was available (i.e. where Clear Creek intersected with public roads). Drainage area contributing to the channel width sample points in the creek was determined by using the batch watershed delineation function in Arc Hydro. A database containing creek width and drainage area was then analyzed in SAS 9.1 using a regression analysis and visualized in Sigmaplot 8.0. All GIS data used in this analysis were downloaded from the Iowa DNR (2008).

Average Annual Discharge/Drainage Area Relationship

A linear regression model relating average annual discharge based on drainage area was developed using data from the USGS. USGS gaging stations included in this analysis were selected based on spatial proximity to the centroid of the Clear Creek Watershed (<175 km) and were determined using the USGS gaging station data layer downloaded from the Iowa DNR (2008). The gaging stations located inside the Clear

Creek Watershed, Coralville and Oxford, were not included in this analysis so they could be used to validate the model. Average annual discharge and drainage area to the gaging stations were downloaded from USGS Water Resources webpage (USGS, 2008b), and the mean of all available average annual discharge values for each station was calculated and input into a database containing the ID numbers and drainage areas of the selected USGS stations. A regression analysis was performed on average annual discharge and drainage area data in SAS 9.1 statistical software (SAS Institute Inc., 2003). Model results were visualized using SigmaPlot 8.0 (SPSS Inc., 2001).

Watershed Scaling of Chloride

The influence of location in the main channel of Clear Creek scale on chloride concentrations was investigated using data downloaded from the IOWATER Online Database (IOWATER, 2008) and ArcMap 9.1. Chloride measurements collected during IOWATER "Snapshot Sampling Events" in May from 2004 to 2007 in the Clear Creek Watershed were averaged for each sampling site. The distance upstream to IOWATER sampling sites from the Coralville USGS station was determined using the cost distance tool in ArcMap 9.1. IOWATER chloride measurements and upstream distance measurements were input into a Microsoft Access database. Two regression analyses relating distance upstream from the Coralville USGS gaging station and chloride concentration were performed using SAS 9.1; one for the main channel continuing up the SAC branch in the Clear Creek headwaters, and a second for the main channel and continuing up the Conroy branch in the Clear Creek headwaters (Figure 6.1). Mean May concentrations were imported into ArcMap 9.1 and linked with an IOWATER sampling site data layer (Iowa DNR, 2008) for visualization of the measurements throughout the Clear Creek Watershed.

Results and Discussion

Channel Width/Drainage Area Relationship

Channel width measurements throughout the Clear Creek Watershed are shown in Figure 6.2. Many of the channel width measurements taken in the headwaters of Clear Creek were less than three meters with channelized flow nonexistent at some sampling locations. Based on field observations, the minimum drainage area required for channelized flow in the Clear Creek Watershed is approximately 0.9 km^2. For the sampling locations with drainage areas smaller than 0.9 km^2, water flow was either intermittently in channelized flow, or entirely overland flow. Near the confluence of the SAC and Conroy branches in the headwaters, the channel width began to steadily increase towards the outlet of the watershed. The channel width measured at the outlet of Clear Creek, 27 m, was significantly larger than the channel width measured three km upstream at the Coralville USGS gaging station, 14 m). Heavy modifications to the channel existed at the outlet that were not present at the Coralville USGS gaging station such as constructed trapezoidal shape and placement of rip-rap.

Linear regression analysis of channel width measurements and drainage area to the sampling sites yielded a statistically significant (p-value < 0.05) relationship and is shown in Figure 6.3. Drainage area measurements predicted 95% of the variation in channel width measurements with a steady positive relationship throughout the entire watershed. Channel width measurements were not included in the channel width/drainage area regression analysis including the measurement near the outlet of the watershed and those collected at locations that drained less than 0.9 km^2. The 9.1 $m^3 s^{-1}$ discharge that was measured at the Coralville USGS gaging station on the sampling day was higher than average annual discharge typically measured at the site (Figure 4.9), thus some caution should be exhibited when using this model during low flow conditions.

Average Annual Discharge/Drainage Area Relationship

A statistically significant relationship (p-value < 0.05) between the logarithm of average annual discharge and the logarithm of drainage area was reveled based on data from 83 Iowan USGS gaging stations (Figure 6.4). An R^2 value of 0.99 indicates that log drainage area can account for nearly all (99%) of the variation in log average annual discharge measurements. The regression model in Figure 6.4 predicted the average annual discharge at gaging stations in the Clear Creek Watershed with percent differences of -10.1% and 4.4% for the Oxford and Coralville gaging stations, respectively (Table 6.1). Given the high R^2 value, and the low percent differences between predicted and measured discharges, this model can be successfully used to predict average annual discharge at locations without gaging stations in the Clear Creek Watershed and other Iowan watersheds. Results from Figure 6.4 suggest that discharge processes from Iowa Watersheds surrounding and including the Clear Creek Watershed are relatively homogenous. This is due to the agricultural land use that dominates much of the landscape meaning that drain tiles and groundwater supply much of the water to local streams.

Watershed Scaling of Chloride Concentrations

Chloride concentrations throughout the Clear Creek Watershed were between 13 mg L^{-1} and 52 mg L^{-1} with the exception of three high measurements, 65 mg L^{-1}, 87 mg L^{-1} and 123 mg L^{-1}, on the western edge of the watershed (Figure 6.5). These three measurements averaged 92 mg L^{-1}, which was over three times greater than the average of the remaining sites in watershed, 29 mg L^{-1}. Chloride is commonly used as a tracer of human activity (Herlihy et al. 1998) and in the Clear Creek Watershed, raw sewage discharged from the city of Conroy (Pulliam, 2005) is the likely source of the peak chloride concentrations on the western edge of the watershed. In Conroy, septic tanks in the city are tied to a tile line that drains directly into the creek. Because chloride is

relatively unreactive in the environment, dilution is primary factor contributing in chloride concentration reductions in the environment (Feth 1981). Figure 6.6 shows the dilution of chloride in the Clear Creek as it travels from the tile line source to the USGS gaging station in Coralville. Chloride concentrations from the Conroy branch are diluted to background concentrations at the confluence of the Conroy and SAC branches. There does appear to be a slight increase in chloride concentration towards the mouth of the creek as it flows though the city of Coralville. Low chloride concentrations in the SAC and other tributaries of the main channel suggest that waste discharges do not exist in these portions of the watershed.

Conclusions

Results from the investigation of physicochemical data from the Clear Creek Watershed indicated spatial scaling of several parameters such as channel width, average annual discharge, and chloride concentrations. Field measurements of channel width combined with geospatial data analyzed using GIS software provided a model to predict channel width in unmeasured portions of the watershed. This relationship can be used to provide model inputs for detailed, physically based instream models. The relationship between average annual discharge and drainage area can be used in a similar manner to predict average annual discharge for unmonitored locations and provide input into water quality models. Volunteer water quality data proved to be valuable in revealing spatial scaling of chloride concentrations and could have implications on management decisions regarding the sewage discharge from Conroy.

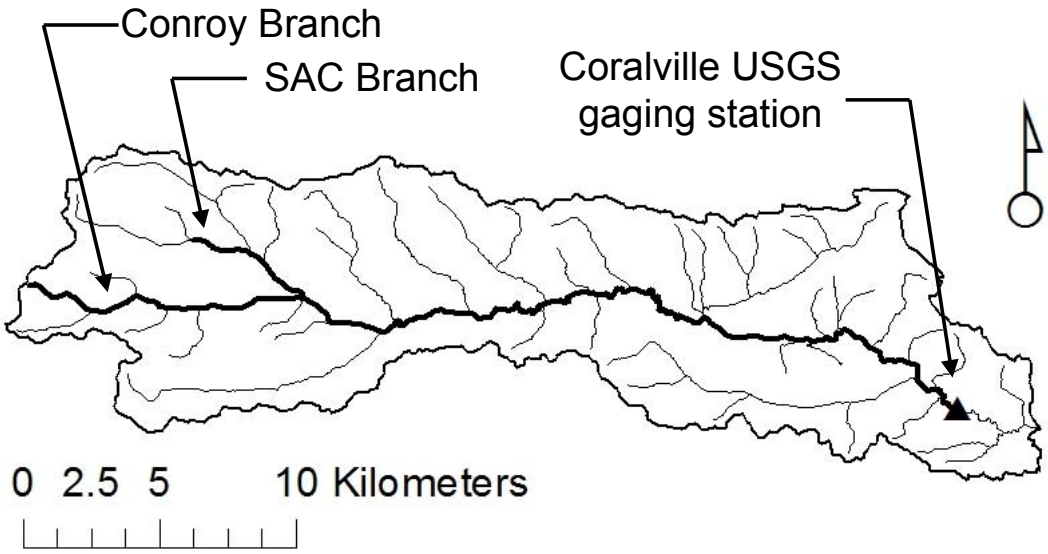

Figure 6.1 SAC and Conroy branches of Clear Creek included in regression models relating distance upstream from the Coralville USGS gaging station to mean May IOWATER measurements from 2004 to 2007.

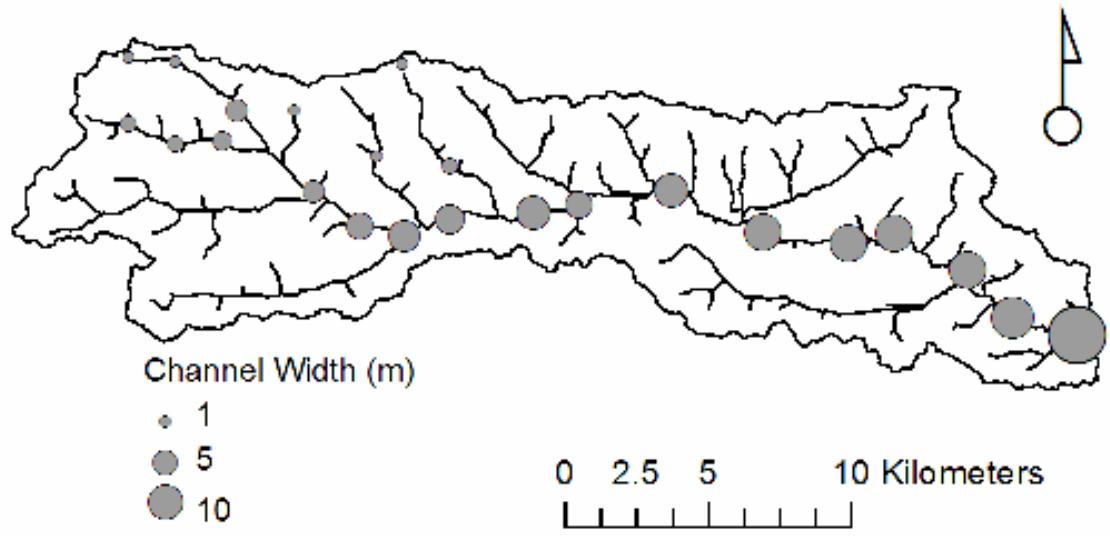

Figure 6.2 Channel width measurements in the Clear Creek Watershed on 4/28/2008 when the average daily discharge at the USGS gaging station in Coralville near the mouth of the watershed was 9.1 $m^3 s^{-1}$.

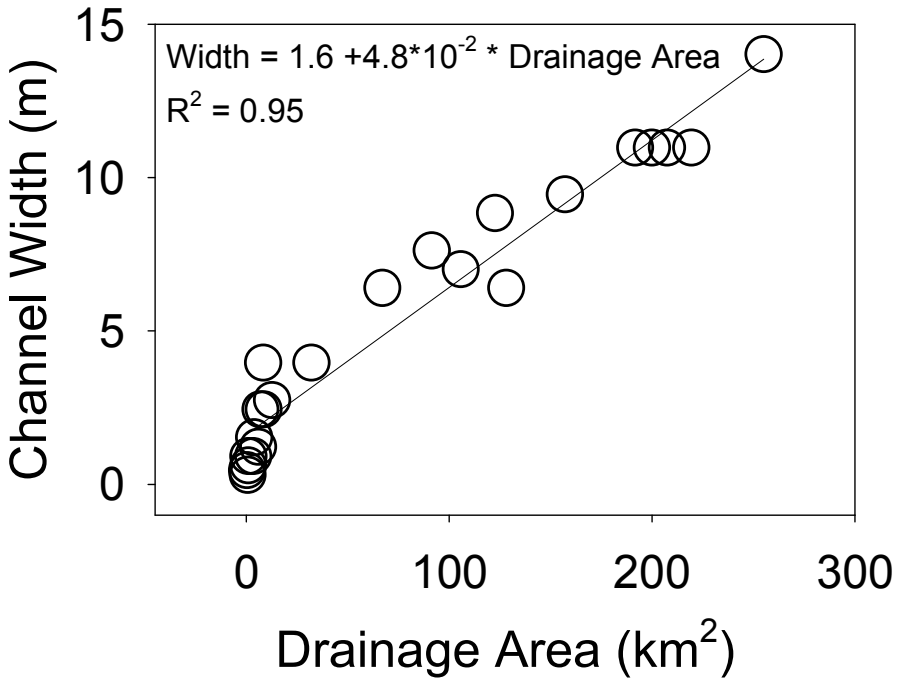

Figure 6.3 Linear regression model predicting channel width in the Clear Creek Watershed on 4/28/2008 based on drainage area to that point (n = 23). The average daily discharge measured at the USGS gaging station in Coralville was 9.1 $m^3 s^{-1}$.

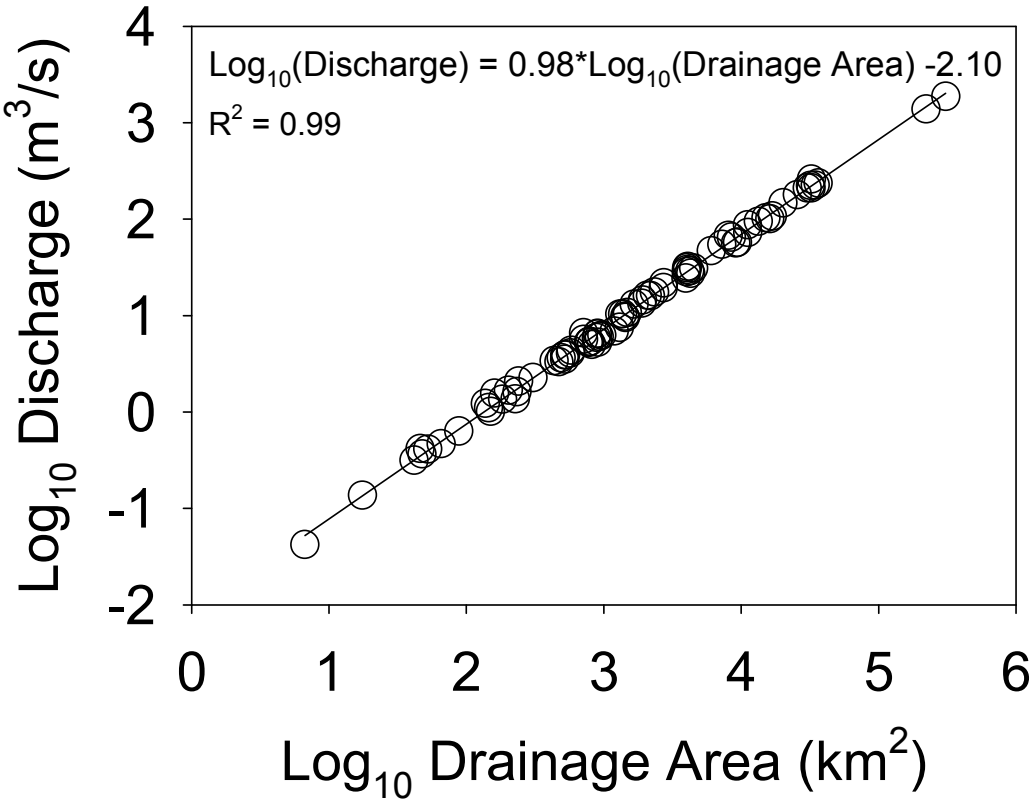

Figure 6.4 Linear regression of $\log_{10}$ drainage area versus $\log_{10}$ average annual discharge at 83 USGS gaging stations in eastern Iowa.

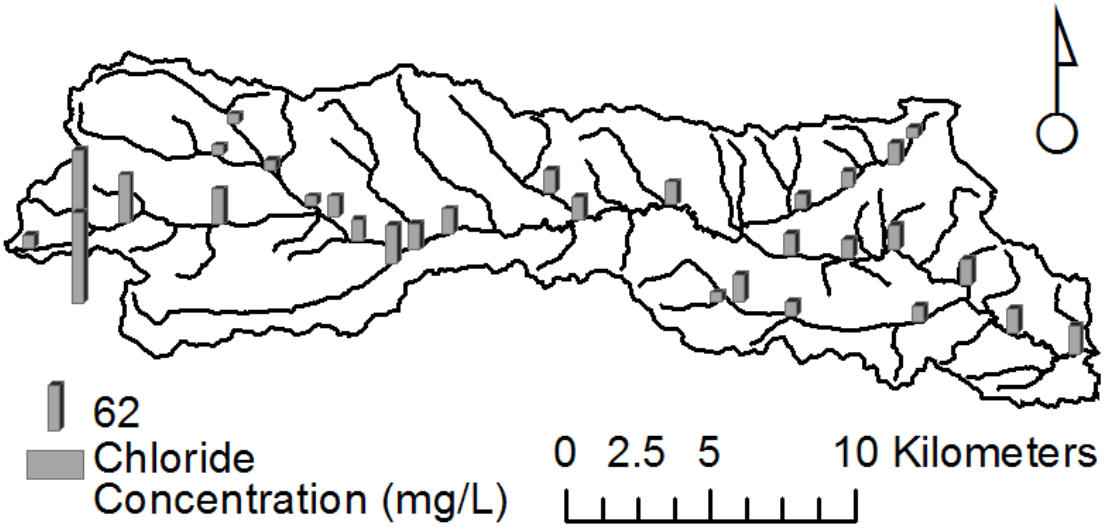

Figure 6.5 Average chloride concentrations (mg L^{-1}) from available May IOWATER Snapshot sampling events during 2004 to 2007 in the Clear Creek Watershed during May.

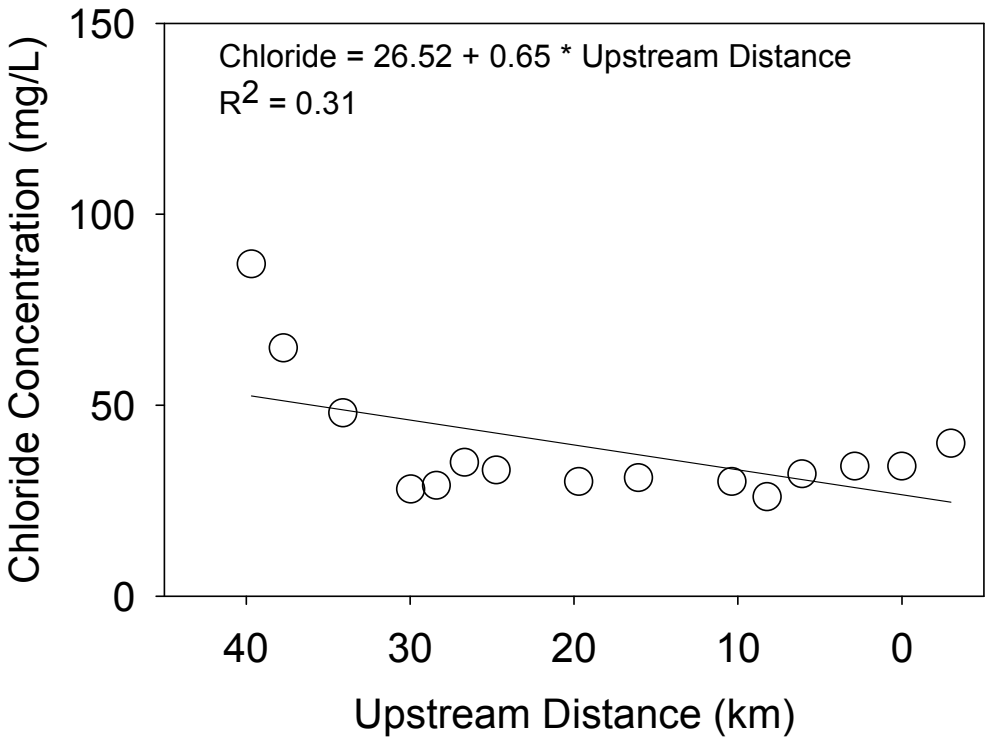

Figure 6.6 Average chloride concentration (mg L^{-1}) from available May IOWATER Snapshot sampling events during 2004 to 2007 versus distance upstream from the Coralville sensing station in the main channel of Clear Creek and the Conroy tributary.

Table 6.1 Predicted values of average annual discharge at the two Clear Creek gaging stations compared to the measured average annual discharges.

USGS Station	Predicted Discharge ($m^3 s^{-1}$)	Measured Discharge ($m^3 s^{-1}$)	Percent Difference
Oxford	1.13	1.01	-10.1%
Coralville	1.88	2.00	4.4%

CHAPTER 7:
WATER QUALITY MODELING OF HIGH-FREQUENCY SENSOR DATA AND VOLUNTEER DATA USING QUAL2K*

Abstract

Knowledge of spatial scaling of water quality parameters in a watershed is imperative for the management of ecological health of the watershed. Data from high-frequency sensors coupled with instream models in an environmental observatory promises to advance the fundamental knowledge of these spatial relationships and trends. The high cost and lack of parameters however may limit modeling processes. Water quality data from volunteer monitoring organizations could be used to fill data gaps that may exist in a sensor network. In this study high-frequency sensor data and water quality models were used to understand the error and bias in volunteer data and spatial scaling of water quality parameters in an agricultural watershed. QUAL2K model results for temperature, DO, and pH calibrated to high-frequency sensor data revealed consistent low bias of IOWATER measurements of DO and pH, and a bias in a subset of the IOWATER temperature measurements. IOWATER nitrate samples analyzed using standard methods were used to calibrate the QUAL2K model and revealed a bias to underestimate the nitrate concentration using the test strip method standard for the IOWATER program. TSS estimations from high-frequency sensors and IOWATER transparency data were used in tandem to calibrate QUAL2K TSS results. The logarithm of total dissolved solids (TDS) and nutrient (nitrate and orthophosphate) loading rates scaled linearly with logarithm of drainage area indicating that the magnitude of discharge largely controlled the transport of these water quality parameters throughout the Clear Creek Watershed.

*Loperfido, J.V., Beyer, P., Just, C.L., and Schnoor, J.L. "Water Quality Modeling of High-frequency Sensor Data and Volunteer Data Using QUAL2K." In Preparation.

Introduction

The export of pollutants from watersheds can have deleterious effects on downstream waterbodies. For example, nutrient pollutants like nitrogen and phosphorus from agricultural watersheds in the Mississippi River basin leads to events of hypoxia, DO concentrations less than 2 mg L^{-1}, in the Gulf of Mexico (Rabalais et al. 2002). Pollutants associated with suspended solids, such as polychlorinated biphenyls (PCBs), pesticides, and metals (Lick 2009) can also lead to designated use impairments and water quality standard violations. Knowledge of the fate and transport of these pollutants throughout the watershed is essential to mitigating their negative impacts on water quality.

High-frequency water quality sensors, when coupled with hydrologic models and cyberinfrastructure in an environmental observatory, can simultaneously give warning of water quality events that may impact human health, such as HABs, and advance our understanding of the fate and transport of pollutants in aqueous systems. Recent advances in sensor technology have allowed the high-frequency detection of multitude of water quality parameters (Tränkler and Kanoun 2001; Chong and Kumar 2003; Alcock 2004; Martinez-Manez et al. 2005; Rogers 2006). However, due to the high capitol and operation and maintenance cost of high-frequency water quality sensors, their widespread deployment in an environmental observatory can be difficult. As a solution, water quality data collected by volunteer monitoring organizations may be used supplement sensor data and fill the spatial gaps in an environmental observatory.

Use of water quality data collected by volunteer organizations must be handled with care. Beyer (2008) presents a review of the literature analyzing the bias and accuracy of water quality measurements collected by volunteer organizations. This review found conflicting results as a portion of the studies suggested that bias and accuracy errors existed, while other studies found no evidence of the same issues. Beyer (2008) also conducted a study to test for bias and variance in the IOWATER (Iowa)

volunteer water quality monitoring program, and found statistically significant bias and error in pH and nitrate samples, and a tendency to overestimate lower concentrations of orthophosphate and underestimate higher concentrations of orthophosphate.

In Iowa, the IOWATER volunteer water quality monitoring program (IOWATER) is a citizen-based program that is supported in the Iowa Geological Survey, Water Monitoring and assessment section of the Department of Natural Resources (IOWATER 2007). Since 1999, IOWATER has been training Iowa citizens to assess chemical (e.g. nutrients, DO, pH, etc.), physical (e.g. temperature and transparency), and biological parameters in the state's waterbodies. Water quality measurements collected by IOWATER are stored in a publicly available online database (IOWATER 2008). Snapshot sampling events conducted by IOWATER are of particular interest to environmental observatories. During these events grab samples are collected within a short period of time on spatial scales ranging from watersheds (≈100 km^2) to statewide (≈150,000 km^2).

The objective of this study is to utilize water quality data from high-frequency sensors in an environmental observatory and grab samples from a volunteer water quality monitoring organization, IOWATER, to understand bias and error associated with volunteer water quality measurements. Water quality data from sensors and volunteer sampling were used to calibrate the QUAL2K water quality model. Temperature, DO, and pH model results calibrated using sensor measurements were used to examine the bias and error associated with volunteer data. Transparency data collected by IOWATER and high-frequency turbidity measurements were used in conjunction to help inform the calibration of TSS in QUAL2K. Water samples collected by IOWATER and measured by a professional laboratory were used to calibrate QUAL2K and compared to IOWATER nitrate data. Finally, results from QUAL2K were used to understand the flux and spatial scaling of total dissolved solids and nutrients in the main channel of the agriculturally dominated Clear Creek.

Materials and Methods

Water Quality Data Collection

Hydrolab DS5X data sondes, measuring for specific conductivity, chlorophyll *a*, DO, pH, temperature, and turbidity every fifteen minutes, were deployed at three sensing stations, SAC, Oxford, and Coralville, in the Clear Creek Watershed on 5/9/2008 and 5/10/2008 (Figure 7.1). Water quality measurements from the Clear Creek Watershed collected by IOWATER volunteers during a 5/10/2008 "Snapshot Sampling Event" were downloaded from the IOWATER on-line Database (IOWATER 2008). These data included DO, nitrate, orthophosphate, pH, temperature, and transparency measured by IOWATER and water samples collected by IOWATER that were measured for nitrate + nitrite by the University Hygienic Laboratory (UHL) at the University of Iowa according to EPA method 353.2. In this study UHL nitrate + nitrite measurements were assumed to equal the instream nitrate concentration (i.e. nitrite was assumed to equal zero).

Instream Modeling

Water quality in the main channel of Clear Creek was simulated by calibrating the QUAL2K water quality model (Chapra et al. 2006) from the SAC sensing station to the Coralville sensing station. Originally, sensor data collected entirely on 5/10/2008 were to be modeled and the modeling period would coincide with the IOWATER Snapshot Sampling event. However, a large precipitation event occurring after IOWATER sampling was completed during the evening of 5/10/2008 eliminated steady flow conditions. Thus, DO, pH, specific conductivity, temperature, and turbidity data from instream sensors collected on the previous day when steady flow conditions existed were used to replace measurements collected in the afternoon and evening on 5/10/2008.

Physical Model Inputs

Physical features of reaches in the main channel and tributaries of Clear Creek were determined using geospatial databases, measurements, and observations from the Clear Creek Watershed (Table 7.1). The Clear Creek drainage network was determined by using the Arc Hydro Data Model (Maidment 2002) in ArcMap 9.1 (ESRI, Redlands, CA) to delineate the DEM of Iowa, available from the Iowa DNR (2008).

Hydraulic Model Inputs

Tributary inputs to the main channel of Clear Creek were modeled for 100 meters and entered the main channel as point sources with no hydraulic inputs being modeled as non-point sources. Daily mean discharge measurements from 5/9/2008 to 5/12/2008 at the SAC sensing station (0.4 $m^3 s^{-1}$), the Oxford USGS gaging station (2.4 $m^3 s^{-1}$), and the Coralville USGS gaging station (3.3 $m^3 s^{-1}$) were used to calibrate discharge from the tributaries entering the main channel of Clear Creek. The difference in discharge at the SAC and Oxford sensing stations was distributed to the tributaries that entered the main stem of Clear Creek between these stations based on tributary drainage area (Table 7.2). This process was repeated for tributaries entering the main channel of Clear Creek between Oxford and Coralville sensing stations (Table 7.3). A majority of the 2.9 $m^3 s^{-1}$ (69.6%) increase in discharge from the SAC sensing station to the Coralville sensing station entered Clear Creek above the Oxford sensing station (Figure 7.2).

Chemical and Biological Model Inputs

Chemical and biological data were used to prescribe upstream boundary conditions at the SAC sensing station and tributary point source inputs into the main channel of Clear Creek (Table 7.4). Data used includes high-frequency sensor data, IOWATER volunteer and laboratory measurements, and values from the literature. Since bottom algae were assumed to cover 100% of the creek bed based on field observations, sediment oxygen demand, particulate organic matter flux, methane flux, and nutrient

fluxes were assumed to equal zero. Chemical and biological modeling rates were based on values in the literature and model defaults and are presented in Table B.5, Table B.6, and Table B.7. TDS concentrations were calculated using specific conductivity data as described in Snoeyink and Jenkins (1980):

Equation 7.1 $$TDS\ (\text{mg L}^{-1}) = 0.64 * specific\ conductivity\ \left(\mu\text{mhos cm}^{-1}\right)$$

Atmospheric, Light, and Heat Inputs

Atmospheric, light, and heat inputs into QUAL2K were prescribed based on published data, values cited in the literature, and model calibration. Air temperature, dew point temperature, and wind speed data measured at the Iowa City Municipal Airport on 5/9/2008 and 5/10/2008 (Table B.8) were downloaded from the National Climatic Data Center (NCDC 2008). These parameters were measured every 52 minutes after the hour and were assume to equal the measurement at the top of the following hour (eight minutes later) for input into QUAL2K. Cloud cover was estimated as 30% based on sky condition observations (NCDC 2008) at the Iowa City Municipal Airport during the model period. QUAL2K model settings for light parameters and surface heat transfer models are presented in Table B.9. The reaeration rate constants in the main channel and tributaries (Table B.1) were prescribed using results from Chapter 4. The reaeration rate was scaled linearly between estimates made at the SAC, Oxford, and Coralville sensing stations. The reaeration rate prescribed to tributaries was 11.2 day^{-1} as calculated at the SAC sensing station based on diel DO data (Table 4.2). Creek shading was determined by calibration of the QUAL2K model to high-frequency temperature sensor data collected at the SAC, Oxford, and Coralville sensing stations. Shade percentages are presented in Table B.10.

Results and Discussion

Comparison of IOWATER Volunteer Data to QUAL2K Modeling Results

Results from the calibrated QUAL2K model revealed increasing water temperature as water flowed downstream to the Coralville sensing station on 5/9/2008 and 5/10/2008 (Figure 7.3). This is due to the colder source groundwater absorbing energy from solar radiation and the warmer air. The magnitude of the daily temperature swing measured by *in situ* sensors decreased from five degrees Celsius at the SAC sensing station to three degrees Celsius the Coralville sensing station (box plots in Figure 7.3) likely due to increased thermal buffering capacity in the larger volumes of water downstream. The two upstream and three downstream IOWATER measurements fall within the daily temperature envelope predicted by the calibrated QUAL2K model. The average difference between sensor measurements and IOWATER data collected at the SAC and Coralville was 1.2% indicating good agreement between the two methods. Three measurements collected in between the SAC and Oxford sensing stations however, were higher than the daily maximum predicted by the QUAL2K model, all sensor measurements, and the five other IOWATER measurements.

The three higher IOWATER measurements are believed to be collected by a different volunteer from the remaining five measurements in Clear Creek; differences in the measurements between samplers may have been a result of differences in sample handling. For example, a small volume of creek water held in a jar could have been allowed to heat to the ambient air temperature before a measurement was taken or measured immediately resulting in different temperature values. Alternatively, other the sampler could have misunderstood sampling protocol and measured air temperature or simply entered the measurements into the IOWATER database incorrectly.

Significant differences existed between DO concentrations measured simulated by QUAL2K and the IOWATER measurements from 5/10/2008 (Figure 7.4). Mean DO concentrations and magnitude of the diel swing determined from the calibrated QUAL2K model indicated a decreasing trend downstream, due to increased light extinction as discussed in Chapter 4. While the mean DO concentration predicted by QUAL2K ranged from 10.4 mg L^{-1} to 12.4 mg L^{-1}, seven of the eight IOWATER measurements in Clear Creek were 8 mg L^{-1} with the remaining measurement being 10 mg L^{-1}. Since the measurement interval of the method used by IOWATER to measure DO is 2 mg L^{-1}, the range of error in the 10 mg L^{-1} measurement is within the diel DO range predicted by the QUAL2K model. However, the measurement interval of the seven DO measurements of 8 mg L^{-1} was outside the diel DO range predicted by the QUAL2K model, suggesting that the method used by IOWATER is biased to underestimate DO concentrations. IOWATER measurements at the SAC and Coralville sensing stations were on average 29% lower than measurements collected by *in situ* sensors.

Two possible factors, water temperature and turbidity do not explain the systematic lower bias in the IOWATER measurements. Poor sample handling could have caused the temperature of the sample to increase to the ambient air temperature and lead to decreases in the DO saturation concentration of the sample and mass transfer of oxygen from the sample to the air. This however, does not explain the IOWATER DO measurements of 8 mg L^{-1} since the DO saturation concentration at the peak air temperature during the monitoring period, 18 °C, was 9.5 mg L^{-1} assuming zero chlorinity (Schnoor 1996). The presence of excessive turbidity would explain a positive interference as higher particle concentrations may make the sample appear darker, indicating a higher DO concentration. However, this effect was not captured in IOWATER measurements taken in the turbid waters that exist near the Oxford and Coralville sensing stations.

Transparency measurements collected by IOWATER and TSS estimations created using turbidity sensor measurements from 5/9/2008 and 5/10/2008 were used in tandem to calibrate the QUAL2K model (Figure 7.5). Use of the sensor TSS estimations alone informed the magnitude of TSS concentrations throughout the watershed. Transparency measurements from IOWATER provided additional qualitative information regarding the relative magnitude of TSS concentrations at different points in Clear Creek. Specifically, IOWATER transparency data suggested that the peak TSS concentrations occurred at an upstream distance range of 2.9 km to 19.7 km. In this study, sensor data alone could not have been used to narrow the longitudinal range of peak TSS concentrations since two of the three data sondes were deployed at the headwaters and terminus of the study area. Transparency could eventually be used to quantitatively inform modeling processes if TSS grab samples were collected and statistically significant regression models were constructed to estimate TSS based on transparency measurements.

TSS modeling results indicated relatively low concentrations near the SAC headwaters ($x > 26$ km), a sudden increase in TSS in the middle portion of the main channel ($26 \text{ km} > x > 16$ km), and a relatively high constant TSS concentration in the downstream half of the main channel ($x < 16$ km). This suggests that different processes may dictate TSS concentrations at different points in the Clear Creek Watershed. In the headwaters ($x > 26$ km), low TSS concentrations are likely due to the settling of particles through the shallow water column as calculated in Chapter 5. In the middle of the watershed ($26 \text{ km} > x > 16$ km), increasing discharge led to increases in water depth which may have allowed fine particles to stay suspended longer resulting in an accumulation of TSS. In the downstream portion ($x < 16$ km), increases in discharge were modest as 30% of the discharge measured at the Coralville sensing station entered the main channel in this section. Coupled with a 23% decrease in water depth, based on data in Table 4.1, these factors together may have created a situation where TSS losses due to settling were equal to TSS gains due to resuspension. In the Clear Creek

Watershed, processes occurring in the middle portion of the main channel appear to dictate the downstream TSS concentration, a phenomenon that may translate to larger watershed as well, and should be the focus of future research.

TSS results from the calibrated QUAL2K model also captured the scaling of the diel turbidity cycles from the SAC sensing station to the Coralville sensing station. Bioturbation was not modeled in the main channel, but was accounted for in the tributaries as upstream boundary conditions, inputs from tributaries, reflected the diel turbidity cycles observed at the SAC. The translation of this phenomenon from the tributaries to the downstream sensing stations was captured by the QUAL2K model. However, it remains to be seen whether bioturbation is an important process in the main channel or not. The source of TSS in the middle and downstream portions of the main channel are also unclear since in this study, calibration of TSS model results to concentrations estimated at the Oxford and Coralville sensing stations was performed by increasing the TSS concentrations in the downstream tributaries. Other sources of TSS such as the creek bed, channel walls, or drain tiles are more likely sources of TSS, but can not be confirmed based on this study and requires further research.

Significant differences existed between QUAL2K pH results calibrated to sensor measurements and IOWATER measurements (Figure 7.6) collected on 5/9/2008 and 5/10/2008. Modeling results reveled that the pH in Clear Creek remained relatively constant near 8. The magnitude of the diel swing in pH appeared to decrease from the headwaters (0.4) to the mouth of the creek (0.2) which was likely due to light extinction inhibiting primary production rates and the uptake rate of carbon dioxide by photosynthetic organisms as shown in Chapter 4. Six of the eight pH measurements taken by IOWATER volunteers had measurement intervals that were below the mean pH predicted by QUAL2K. This bias to underestimate the pH of prepared samples was also observed by Beyer (2008).

Dissolved Solids

Results from calibration of QUAL2K indicate that the concentration of total dissolved solids (TDS) (Figure 7.7A), and orthophosphate (Figure 7.7B) were relatively constant throughout the main channel of Clear Creek on 5/9/2008 and 5/10/2008. TDS and orthophosphate concentrations increased by 0.0% and 13%, respectively. Sensor and grab sample measurements fit the calibrated model results very well, with two exceptions. First, the mean TDS concentration at the Oxford sensing station, estimated using specific conductivity measurements, were 3.1% lower than the mean TDS concentration predicted by the calibrated QUAL2K model. These differences were likely due to errors during the calibration of the specific conductivity sensors on the Hydrolab DS5X data sondes. Second, the orthophosphate measurement collected at x = 32.48 km was 281% higher than the mean of all other IOWATER measurements and outside three standard deviations from the mean of these measurements. Thus, the peak orthophosphate measurement at x = 32.48 km was considered an outlier and not used to calibrate orthophosphate in the QUAL2K water quality model. Downstream increases in the concentration of orthophosphate were due to the hydrolysis of organic phosphorus during the 1.3 day travel time from the SAC sensing station to the Coralville sensing station.

QUAL2K modeling results revealed higher nitrate concentrations in the headwaters and decreasing concentrations downstream on 5/10/2008 (Figure 7.8). This was largely due to dilution as land use in the upstream tributaries is more agriculturally intensive than land use of the downstream tributaries. Thus, nutrient runoff from the widespread tile lines in the upstream tributaries gets diluted from the downstream tributaries with lower intensity of agricultural activity. Wider riparian zones in the lower portion of the watershed may also have contributed to lower nitrate concentrations in the downstream tributaries. Nitrate concentrations measured by IOWATER volunteers were on average 61.1% lower than those measured by the UHL via standard methods. These

results were similarly observed by Beyer (2008) when comparing nitrate concentrations in deionized water measured by IOWATER volunteers to standard method analyses.

The bias of underreporting nitrate concentrations has implications to an environmental observatory. First, since nitrate measurements by IOWATER essentially serve as a presence-absence test, in an agricultural setting like Clear Creek where high nutrient concentrations are expected, nitrate measurements using the Hach Test Strips (method # 2745425) are unnecessary and not cost effective. Second, if the goal of nitrate monitoring is to locate and report high nutrient concentrations which may have implications to Gulf Hypoxia or drinking water treatment, underreported nitrate concentrations using the Hach Test Strips could allow tributaries with significant pollution issues to be bypassed. Despite issues with nitrate concentrations measured using the Hach Test Strips, data generated by IOWATER samples analyzed by the UHL via standard methods were essential for modeling and understanding the fate and transport of nitrate through Clear Creek in this study (Figure 7.8).

The loading rate of TDS, nitrate and orthophosphate increased from the SAC sensing station to the Coralville sensing station by 757%, 535%, and 884%, respectively (Figure 7.9A). Since the concentration of TDS was constant, an increase in the TDS loading rate was due to the increase in discharge downstream of the SAC sensing station. A larger increase in the orthophosphate loading rate was due to a combination of discharge increases and hydrolysis of organic phosphorus. Nitrate loading rates also increased due to discharge increases however, they were offset slightly by the decreases in nitrate concentration due to dilution as shown in Figure 7.8. A linear relationship was revealed between TDS, nitrate and orthophosphate loading rates and drainage area when plotted on a $\log_{10}$-$\log_{10}$ scale (Figure 7.9B). This is due to the linear relationship between $\log_{10}$ discharge and $\log_{10}$ drainage area that exists in most agricultural watersheds (e.g. Figure 6.4).

Normalizing the loading rate to drainage area revealed that the areal loading rates of TDS, nitrate and orthophosphate were relatively constant throughout the Clear Creek Watershed (Figure 7.10A). Since loading of these solids is dictated by discharge, the general trend of the aerial discharge rate, termed water yield (Figure 7.10B), is reflected in the areal loading rates. The water yield calculated in Clear Creek at Coralville was slightly higher, but on the same order of magnitude as values calculated in May, 2008 (Table 7.5) in other Iowa Watersheds. The Clear Creek water yield was again slightly higher, but on the same order of magnitude as average daily water yields in other Iowa Watersheds calculated from 1980 to 1996 (Table 7.6). The nitrate areal loading rate in Clear Creek and other Iowa Watershed followed a similar pattern to the water yield indicating that the processes which dictate nitrate transport in Clear Creek, largely dilution of headwater inputs, are similar to those in the other Iowa Watersheds (Table 7.5 and Table 7.6). Orthophosphate areal loading rates from Clear Creek were again on the same order of magnitude and rates calculated in other Iowan Watersheds, however, they were near the mean of the rates (Table 7.5 and Table 7.6). This indicates that nitrate pollution may be more problematic than orthophosphate pollution in the Clear Creek Watershed. The result of increasing TDS, orthophosphate, and nitrate loading rates was expected and is a consequence of the mass balance equations for water and nutrients in the QUAL2K model. Since the areal loading rates of TDS, orthophosphate, and nitrate were relatively constant, increases in discharge with increasing drainage area observed in agricultural areas (e.g. Figure 6.4) and modeled in QUAL2K implies that loading rates of dissolved solids and nutrients will increase as discharge increases with downstream distance.

Conclusions

Calibration of the QUAL2K model revealed scaling processes of water quality parameters in the Clear Creek Watershed. Modeling of TSS indicated different processes

that occurred over three distinct sections of the main channel. Understanding of processes that led to large TSS increases in the middle section of the main channel could aid efforts in reducing TSS pollution, and pollution due contaminants sorbed to suspended solids. The fate and transport of dissolved solids and nutrients was largely dictated by dilution with little transformation occurring in the main channel of Clear Creek. This result would likely be true for larger systems in the Mississippi River Basin meaning that once nutrients reach a system the size of the SAC, that they will likely be transported to coastal zones contributing to gulf hypoxia.

The utility of volunteer water quality data collected by IOWATER for modeling activities in an environmental observatory was mixed. Parameters such as DO, and pH, and nitrate, measured using test strips, were consistently lower than measurements using sensors or standard methods. Thus, these data served more as a qualitative descriptor of relative values in a watershed, but could be used in the absence of sensor data if the bias in these data were better understood. Temperature, transparency, orthophosphate, and nitrate data, measured using standard methods, collected by IOWATER proved very valuable in calibrating the QUAL2K model and helped reveal processes dictating water quality in the watershed. Validation of IOWATER measurements to standard methods would be recommended for orthophosphate since sensor measurements of this parameter are difficult to obtain and this parameter plays an important role in the eutrophication of the water environment.

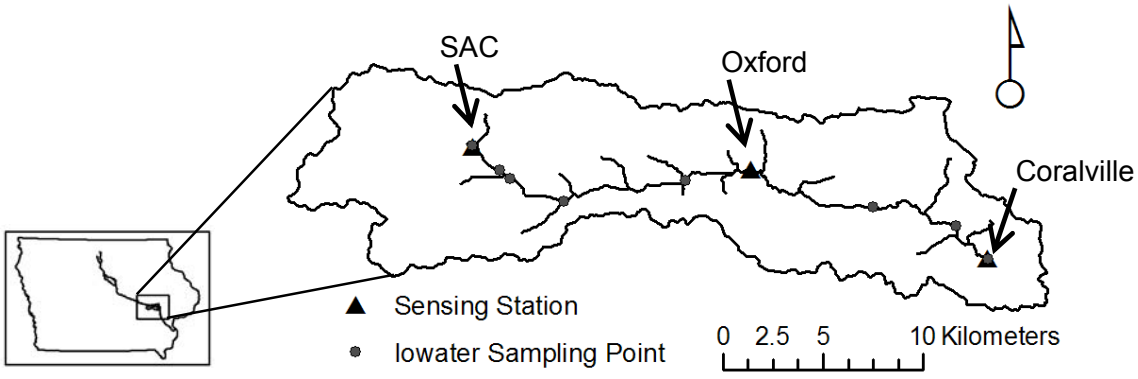

Figure 7.1 High-frequency sensors were deployed at three sensing stations (▲) on 5/9/2008 and 5/10.2008 in the Clear Creek Watershed located in east-central Iowa. IOWATER volunteers sampled at eight locations in the main channel of Clear Creek (●), including at the SAC and Coralville sensing stations on 5/10/2008. Data from high-frequency sensors and IOWATER were used to calibrate the QUAL2K model in the main channel of Clear Creek from the SAC sensing station to the Coralville sensing station.

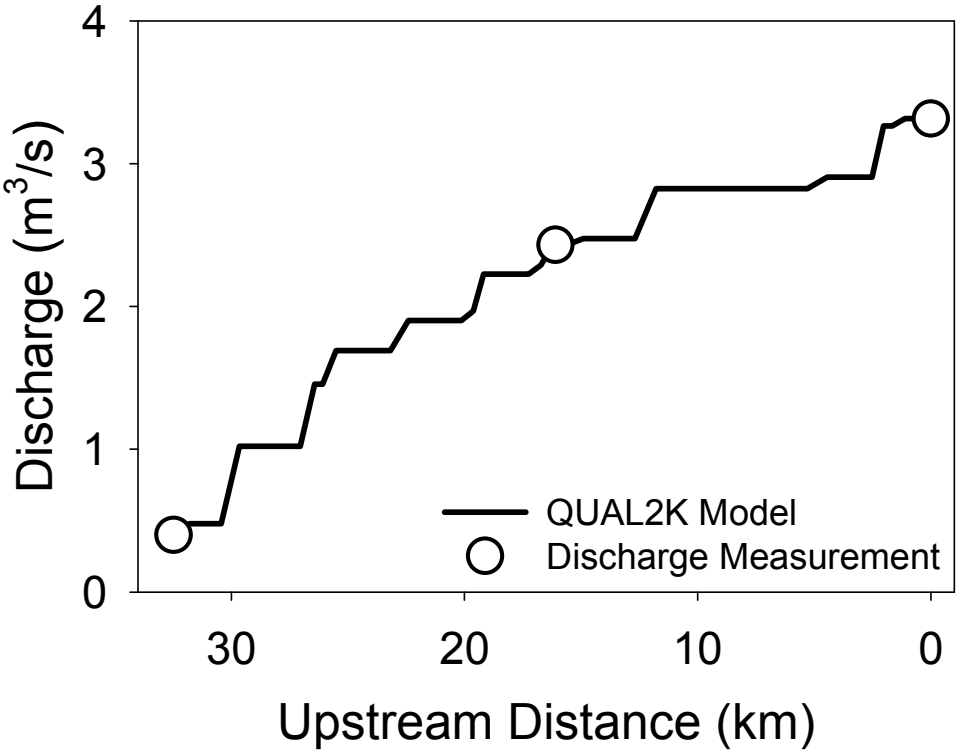

Figure 7.2 Clear Creek discharge measurements (○) from 5/9/2008 versus distance upstream from the Coralville sensing station used to calibrate the QUAL2K water quality model (—).

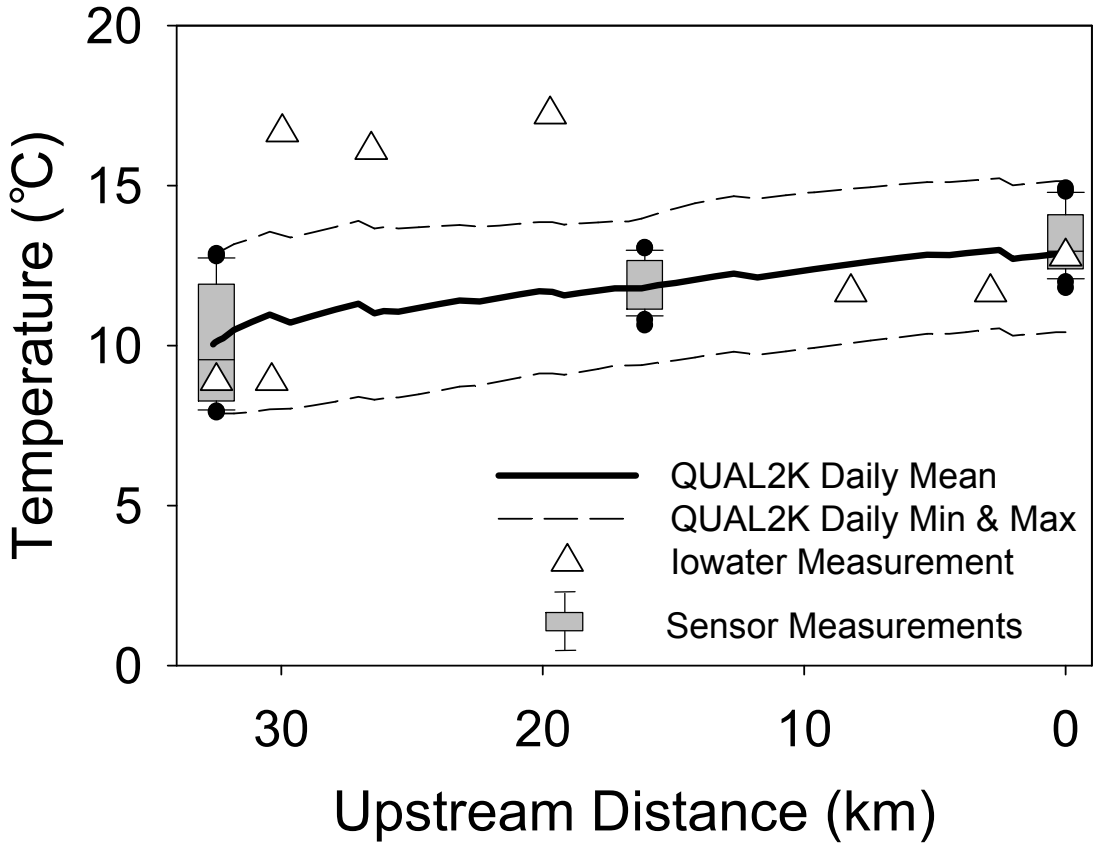

Figure 7.3 QUAL2K Temperature results calibrated to Hydrolab DS5X sensor data (box plot with errors bars equal to 10th and 90th percentiles; outliers, (●) collected on 5/9/2008 and 5/10/2008 compared to IOWATER measurements (Δ) collected on 5/10/2008 versus distance upstream from the Coralville sensing station.

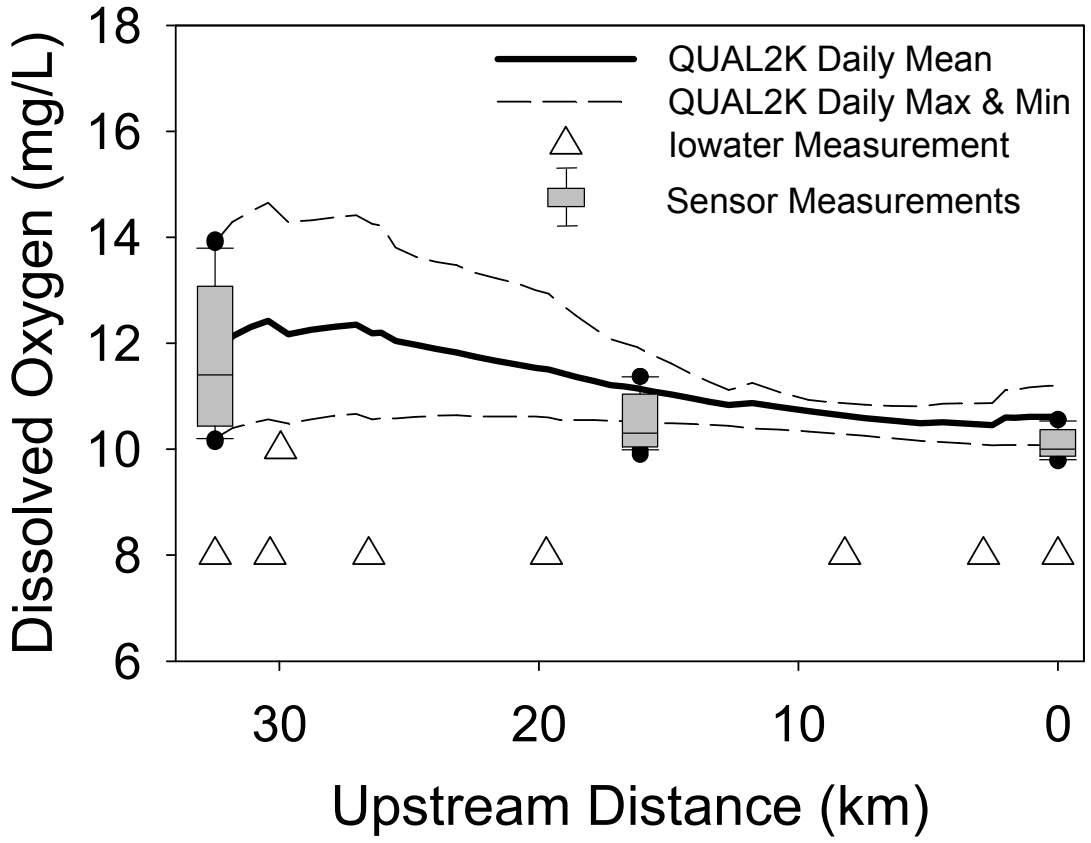

Figure 7.4 QUAL2K DO results calibrated to Hydrolab DS5X sensor data (box plot with error bars equal to 10th and 90th percentiles; outliers, (●) collected on 5/9/2008 and 5/10/2008 compared to IOWATER measurements (Δ) collected on 5/10/2008 versus distance upstream from the Coralville sensing station.

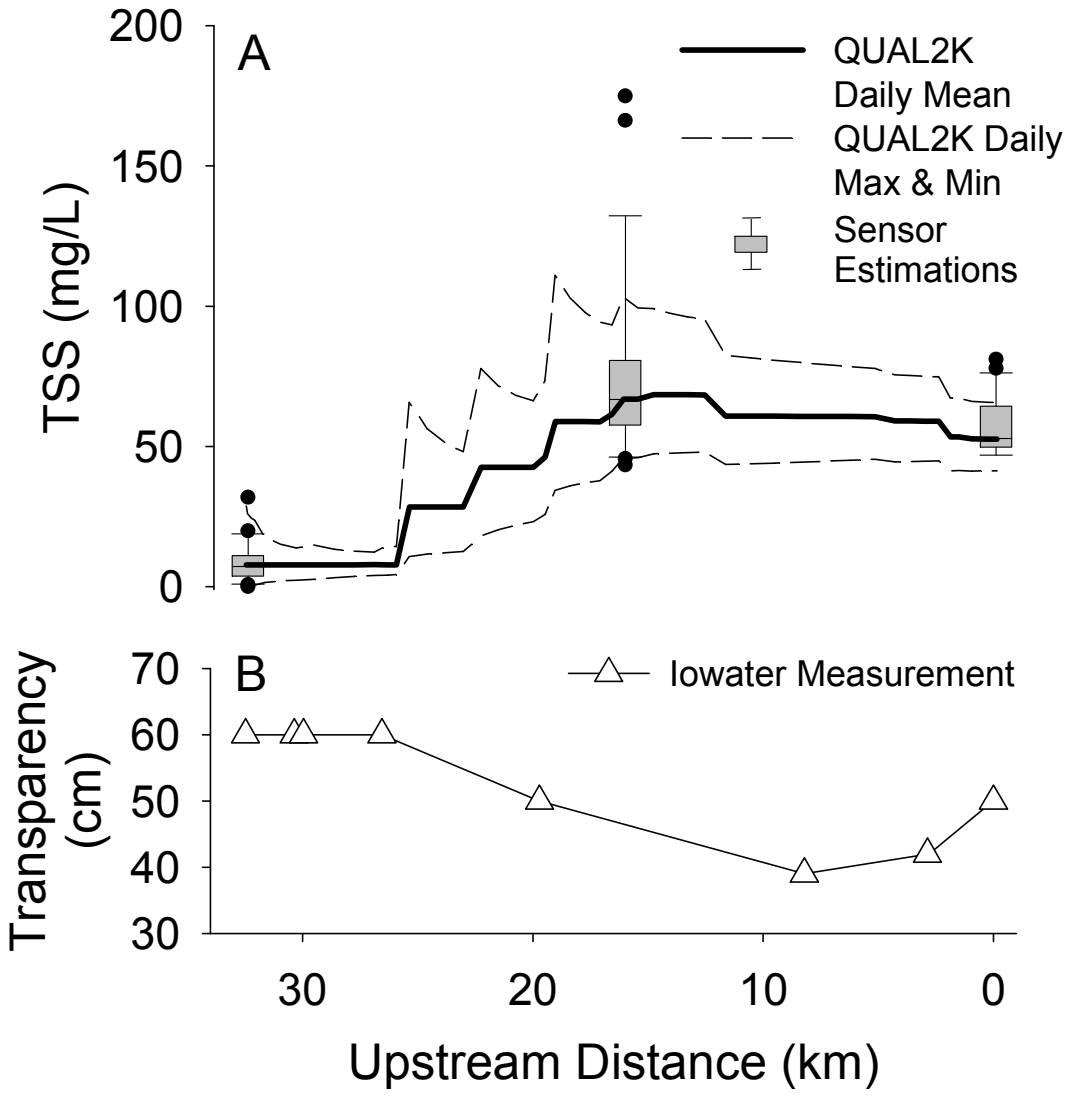

Figure 7.5 QUAL2K TSS results calibrated using TSS estimations from Hydrolab DS5X turbidity data (A, box plot with error bars equal to 10th and 90th percentiles; outliers, (●) from 5/9/2008 and 5/10/2008 and IOWATER transparency measurements (B) used in tandem versus distance upstream from the Coralville sensing station.

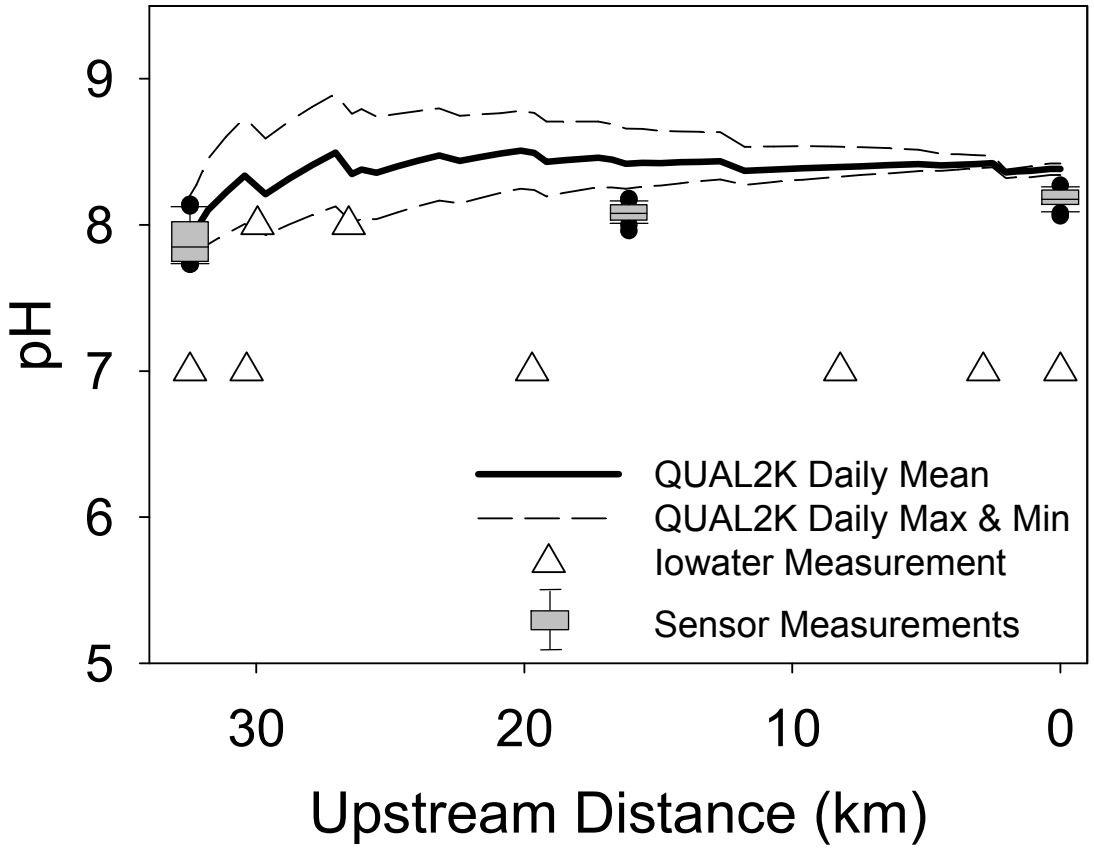

Figure 7.6 QUAL2K pH results calibrated to Hydrolab DS5X sensor data (box plot with error bars equal to 10th and 90th percentiles and outliers, (●) collected on 5/9/2008 and 5/10/2008 compared to IOWATER measurements (Δ) collected on 5/10/2008 versus distance upstream from the Coralville sensing station.

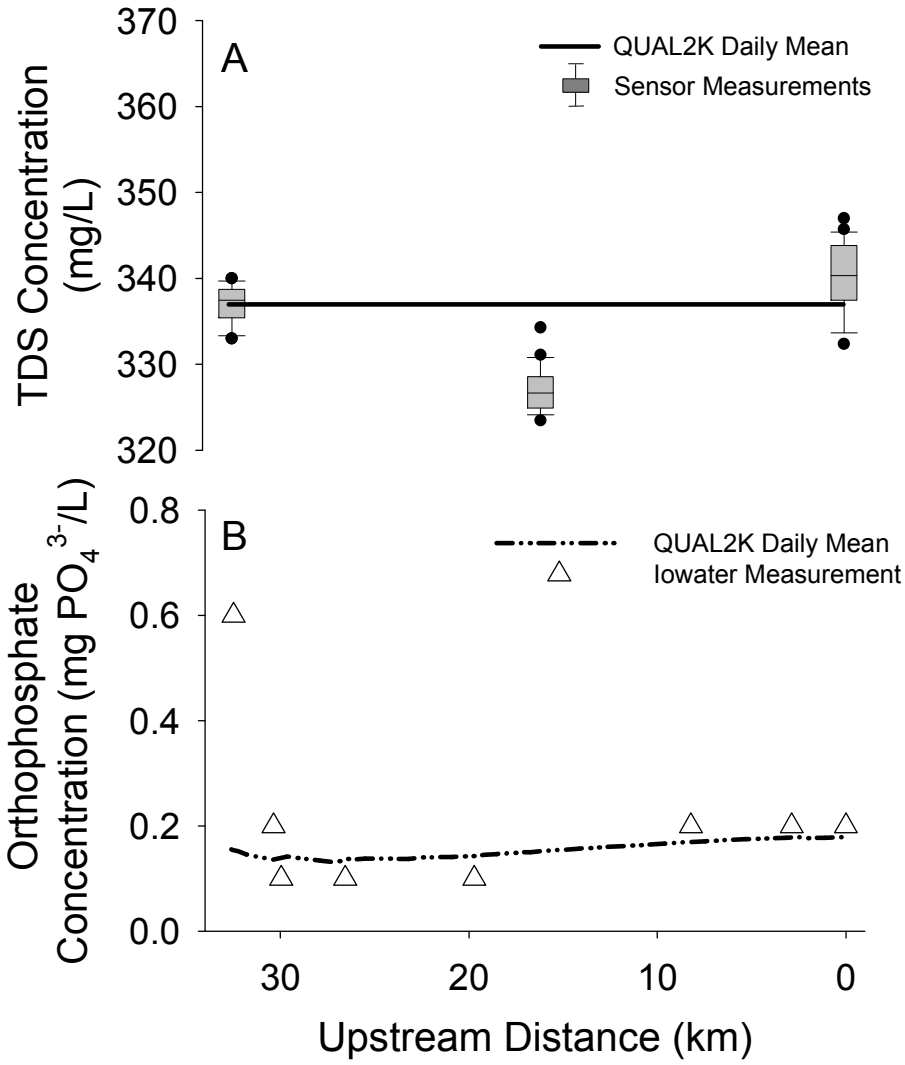

Figure 7.7 QUAL2K total dissolved solids results (A) calibrated to Hydrolab DS5X sensor data (box plots with error bars equal to 10th and 90th percentiles and outliers, (●) collected on 5/9/2008 and 5/10/2008 and QUAL2K orthophosphate results calibrated to IOWATER (□) collected 5/10/2008 versus distance upstream from the Coralville sensing station.

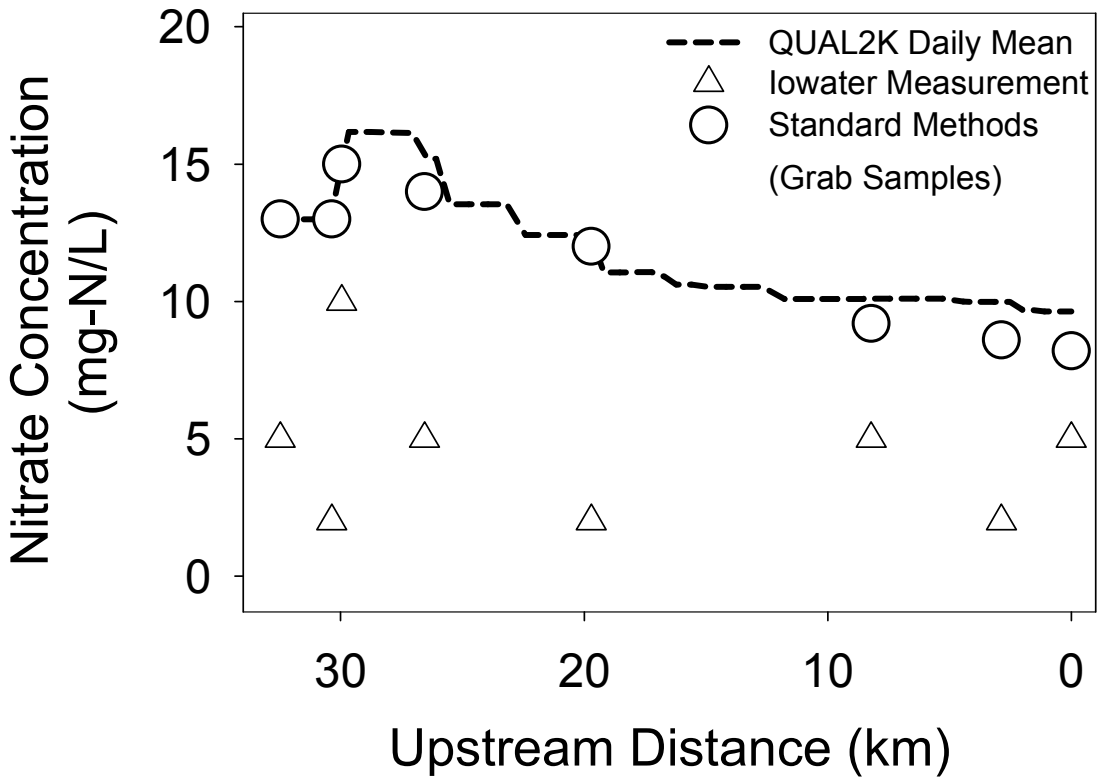

Figure 7.8 QUAL2K nitrate results calibrated to grab samples collected by IOWATER and analyzed by the University of Iowa Hygienic Laboratory (○) on 5/10/2008 compared to IOWATER measurements (Δ) collected on 5/10/2008 versus distance upstream from the Coralville sensing station.

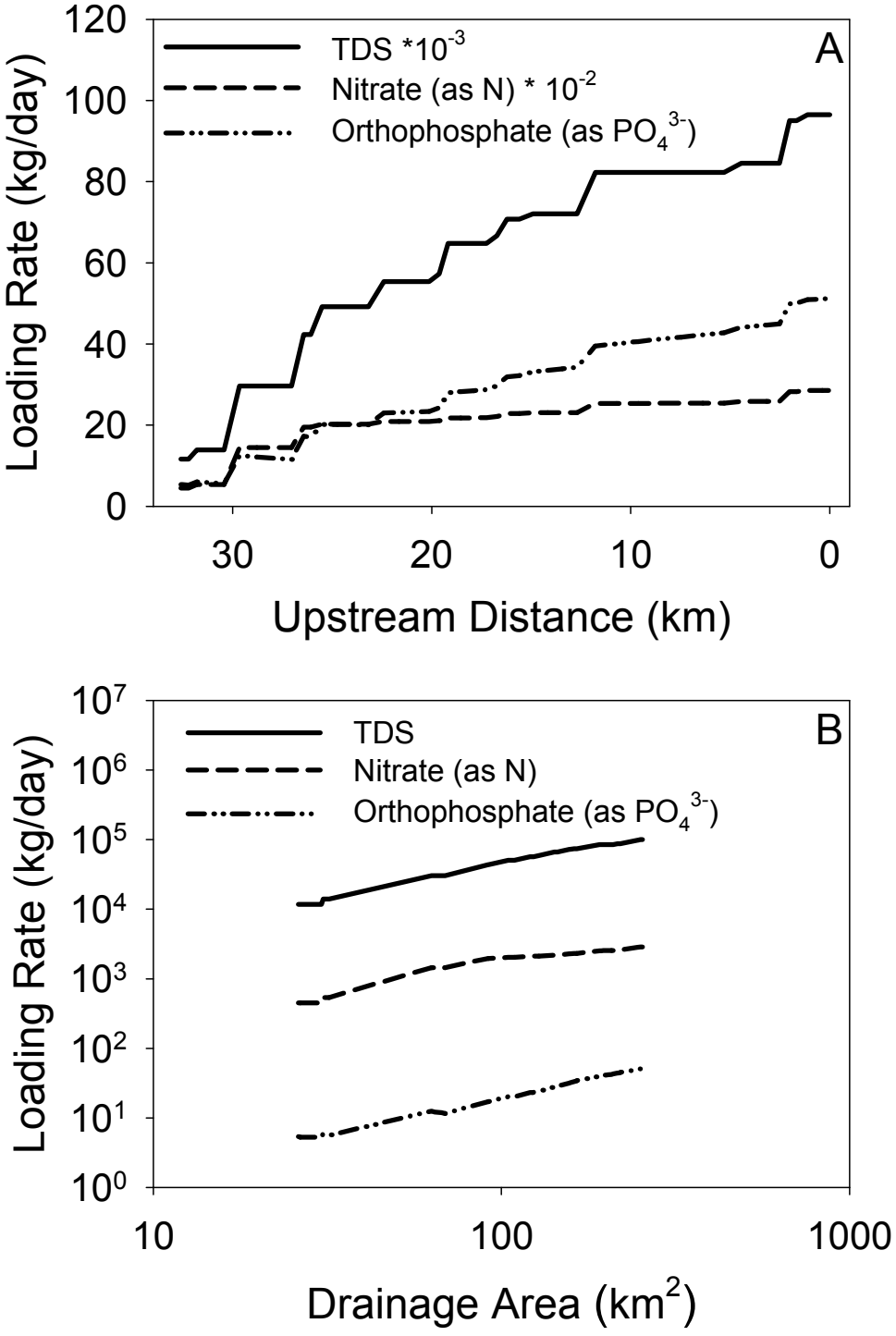

Figure 7.9 TDS, nitrate, and orthophosphate loading rates versus distance upstream from the Coralville sensing station and drainage area ($\log_{10}$ – $\log_{10}$ scale) in the Clear Creek Watershed on 5/10/2008 calculated using results from QUAL2K.

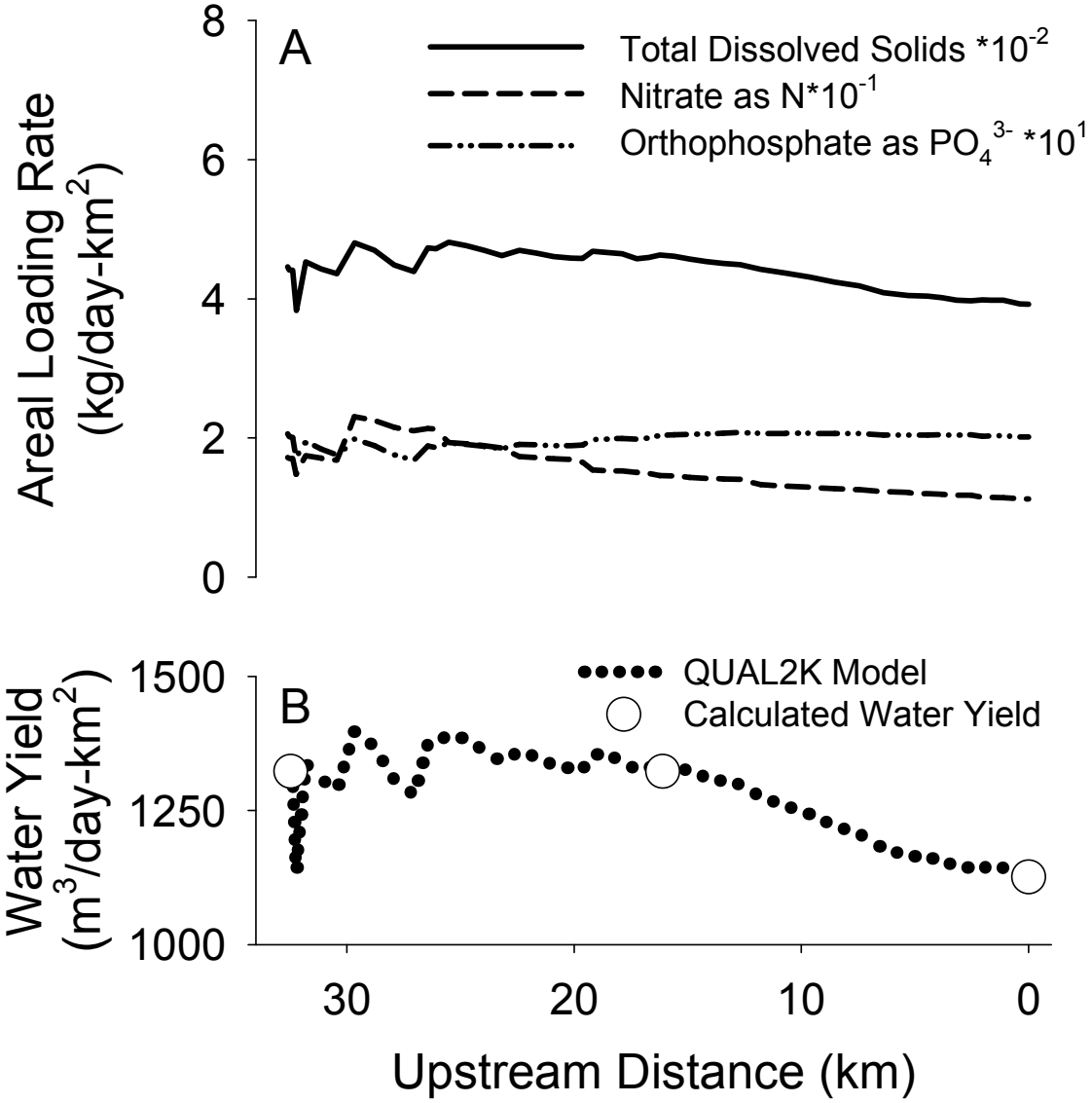

Figure 7.10 TDS, nitrate and, orthophosphate areal loading rates (A) and water yield (B) versus distance upstream from the Coralville sensing station in the Clear Creek Watershed on 5/10/2008.

Table 7.1 Data sources used to describe physical feature model inputs to model Clear Creek using QUAL2K.

Feature	Data Source	Model Input
Reach Length	Arc Hydro delineation of Iowa DEM	Table B.1
Reach Elevation	Iowa DEM	Table B.1
Channel Width	Drainage area-channel width regression (Figure 6.3), field measurements	Table B.1
Channel Slope	Iowa DEM	0.001
Manning's Roughness Coefficient	Model calibration to depth data and velocity estimations (Table 4.1)	0.08
Side Slope	Field observation	1.0

Table 7.2 Discharge values prescribed to tributaries entering Clear Creek between the SAC and Oxford sensing stations based on tributary drainage area.

Contributing Tributary	Drainage Area (km^2)	% of Total Tributary Drainage Area	Tributary Discharge ($m^3\ s^{-1}$)
T1	3.93	4%	0.08
T2	27.66	27%	0.54
T3	22.14	21%	0.43
T4	12.03	12%	0.24
T5	10.81	10%	0.21
T6	3.32	3%	0.07
T7	13.17	13%	0.26
T8	3.26	3%	0.06
T9	7.16	7%	0.14
Total	103.5	100%	2.03

Table 7.3 Discharge values prescribed to tributaries entering Clear Creek between the Oxford and Coralville sensing stations based on tributary drainage area.

Contributing Tributary	Drainage Area (km^2)	% of Total Tributary Drainage Area	Tributary Discharge ($m^3\ s^{-1}$)
T10	3.29	5%	0.05
T11	25.56	39%	0.35
T12	5.9	9%	0.08
T13	26.29	41%	0.36
T14	3.67	6%	0.05
Total	64.71	100%	0.89

Table 7.4 Chemical and biological upstream boundary conditions at the SAC sensing station and tributaries along the main channel used for QUAL2K modeling of Clear Creek.

Parameter	Value/Data Source
Temperature	High-frequency sensor data (Table B.2)
Specific Conductivity	High-frequency sensor data (Table B.2)
Inorganic Solids*	High-frequency sensor data (Table B.3) and turbidity/TSS regression model (Figure 5.9)
Dissolved Oxygen	High-frequency sensor data (Table B.2)
CBODSlow	Assumed to be 0 mg L^{-1} (Chapra et al. 2006)
CBODFast	Assumed to be 2 mg L^{-1} (Schnoor 1996)
Organic Nitrogen (as N)	Assumed to be 1.5 mg L^{-1} based on Coralville Reservoir data
NH_4 (as N)	Assumed to be 0.22 mg L^{-1} based on Clear Creek 2007 15 grab samples (Table A.4)
NO_3 (as N)[a]	Assumed to be 13.0 mg L^{-1} based on IOWATER grab samples measured for nitrate + nitrite using standard methods (Table B.4)
Organic Phosphorus (as PO_4^{3-})	Assumed to be 0.310 mg L^{-1} based on calibration of orthophosphate to IOWATER orthophosphate measurements in the main channel of Clear Creek
Orthophosphate (SRP as PO_4^{3-})	Assumed to be 0.157 mg L^{-1} based on seven IOWATER orthophosphate measurements in the main channel of Clear Creek
Phytoplankton	Assumed to be 0.1 µg L^{-1} based on high-frequency sensor data (Figure A.17)
Detritus (POM)*	High-frequency sensor data (Table B.3) and turbidity/TSS regression model (Figure 5.9)
Pathogen	Not modeled
Alkalinity (as $CaCO_3$)	Assumed to be 196 mg L^{-1} based on Clear Creek grab sample data (n=7)
pH	High-frequency sensor data (Table B.2)

[a]Input values in this table were only prescribed at the SAC sensing station with tributary input values of these parameters being prescribed based on the calibration of QUAL2K to measurements in the main channel of Clear Creek.

Table 7.5 Water yield, areal nitrate loading rate, and areal orthophosphate loading rate during May, 2008 calculated for Clear Creek (this study) and for other Iowan Watersheds.

Name and Sampling Location	USGS Gaging Station Number	Drainage Area (km^2)[a]	Measurement Date	Water Yield ($m^3\ day^{-1}\ km^{-2}$)[a]	Nitrate Areal Loading Rate[b] ($kgN\ day^{-1}\ km^{-2}$)	Orthophosphate Areal Loading Rate[b] ($kgPO_4^{3-}\ day^{-1}\ km^{-2}$)
Clear Creek at Coralville, IA	05454300	254	5/10/2008	1,126	11	0.20
Rapid Creek near Iowa City, IA	05454000	66	5/10/2008	971	7.3	0.10
Duck Creek at Davenport, IA[c]	05422600	148	5/13/2008	2,572	25.7	2.57
Fourmile Creek at Des Moines, IA	05485640	240	5/21/2008	560	6.1	1.12
Old Mans Creek near Iowa City, IA	05455100	521	5/10/2008	916	8.9	-
Beaver Creek near Grimes, IA	05481950	927	5/21/2008	686	6.6	-
Raccoon River at Van Meter/Des Moines, IA	05484500	8,912	5/21/2008	763	7.4	0.15
Des Moines River near Saylorville, IA	05481650	15,128	5/21/2008	1,260	11.7	0.38

[a]Drainage area and water yield were determined using data from USGS (2008a).

[b]Areal loading rates calculated based on data from Iowater 2009.

[c]Discharge at Duck Creek on 5/13/2008 was above baseflow conditions due to a rain event on 5/11/2008.

Table 7.6 Average daily water yield, nitrate areal loading rate, and orthophosphate areal loading rate for Iowan Watersheds from 1980 to 1996.

Name and Sampling Location	USGS Gaging Station Number	Drainage Area (km^2)	Average Daily Water Yield ($m^3\ day^{-1}\ km^{-2}$)	Average Daily Nitrate Areal Loading Rate ($kgN\ day^{-1}\ km^{-2}$)	Average Daily Orthophosphate Areal Loading Rate ($kgPO_4^{3-}\ day^{-1}\ km^{-2}$)
Raccoon River at Van Meter/Des Moines, IA	05484500	8,912	1260	11.7	0.38
Cedar River at Cedar Falls, IA	05463050	12,260	862	6.8	0.24
Iowa River at Wapello, IA	05465500	32,400	770	4.8	0.17
Skunk River at Augusta, IA	05474000	11,100	721	4.3	0.11

Source: Goolsby et al 1999

CHAPTER 8:
ENGINEERING AND SCIENTIFC SIGNIFCANCE

Summary of Findings

Results from this research illustrate how sensing stations in environmental observatories like the WATERS Network can transform water science. The WATERS Network will change the way environmental data is collected, transferred, stored, and analyzed using high-frequency sensors and cyberinfrastructure. Spatially and temporally diverse data will be used to observe and understand previously unknown biogeochemical processes. High-frequency data modeled in near real-time will offer predictions of water quality and quantity that can inform management decisions.

High-frequency data allowed for the detection and understanding of the unexpected biogeochemical phenomena of nighttime increases in DO concentrations and diel turbidity cycles in the Clear Creek Watershed. Nighttime increases in DO were modeled to reveal that large decreases in water temperature led to a nonlinear mass transfer of oxygen from the atmosphere to the water column at the SAC sensing station. Diel turbidity data were analyzed to suggest that nocturnal feeding activity of fishes led to elevated concentrations of suspended aluminosilicate clay particles at nighttime which was reflected in higher nighttime turbidity measurements. Observation of these phenomena at coarser temporal resolution (e.g. daily sampling) would not allow for insight into the nature of these processes which illustrates the need for environmental observatories to advance fundamental understanding in water science.

High-frequency data informed water quality impairments that would be missed by traditional grab sampling methods in the Clear Creek Watershed. Low DO water quality criterion excursions were repeatedly detected at the SAC during 2006. High-frequency data were used to estimate the loading of suspended solids and nutrients from the SAC that was significantly higher than estimations based on a traditional grab sampling

campaign. At the fine temporal scale, collection of grab samples becomes impractical; however, sampling with water quality sensors is easy, highlighting the importance of an environmental observatory on a regulatory and resource management basis.

Water quality data from sensing stations in Clear Creek and volunteer monitoring organizations were used to scale-up phenomenon from the catchment scale (26 km^2) to the watershed scale (254 km^2). The hydrological data from both sources allowed for the calibration of a physically-based instream model used to gain insight on the longitudinal scaling of water quality parameters in the main channel of Clear Creek. For example, dissolved solids and nutrient loading was linearly related to drainage area when plotted on a $\log_{10}$-$\log_{10}$ scale, a relationship driven by the magnitude of discharge throughout the watershed. High-frequency DO data were modeled to reveal spatial scaling of parameters affecting the diel DO cycle including primary production, respiration, and the reaeration rate constant due to light extinction from downstream increases in TSS. The diversity of data sources used in this study (e.g. sensors, volunteer monitoring organizations, government agencies, etc.) highlights the significance and convenience of an environmental observatory's ability to store data from a wide breadth of sources.

The SAC sensing station can provide a blueprint from which to construct sensing stations in an environmental observatory. Water quality sensors deployed in Clear Creek performed well with regular bi-monthly maintenance. Power supplied to the SAC sensing station using a solar panel was adequate to support one data sonde and the cyberinfrastructure necessary to relay measurements to a data server for two field seasons. Connecting to the remote SAC sensing station using cellular technology was somewhat problematic; however, no data collected by water quality sensors were lost. The sensing station constructed at the SAC can essentially be replicated for use throughout an entire environmental observatory with modifications being made as specific sites dictate.

Future Research

Data and results from this research revealed processes that can drive future research questions. Like findings in this research, these questions exist on several different levels including fundamental science, and resource management. Key fundamental science topics include, but are not limited to understanding the scaling of TSS throughout the watershed, determining shifts in phytoplankton communities with increased TSS in downstream portions of the main channel, and identifying primary sources of nitrate and orthophosphate in the watershed. Understanding these processes could help realize resource management goals such as making Clear Creek near Coralville safe for primary contact and reducing nutrient export from agricultural and urban areas in the Clear Creek Watershed to the Gulf of Mexico. Other research areas to investigate that were outside of the scope of this work include water quality sensing of groundwater and modeling and monitoring for pathogens. Detection of water quality parameters at a higher frequency (e.g. thirty second intervals) in new locations such as groundwater wells and drain tiles, or in the main channel of Clear Creek could reveal new processes missed by the sample frequency used in the this research (15 minutes and 20 minutes).

Experience from this research can be incorporated into the design of the WATERS Network and future research can address issues not in the scope of this work. For example, in this research data sondes were only deployed during the months of March through November. To deploy throughout the entire year, sensing stations in the WATERS Network must be robust enough to operate through the winter months and withstand freezing water in environments like Clear Creek. Sustaining power to a sensing station during cold weather or with additional data sondes is also a key issue that should be investigated more closely. With new sensing equipment continually being introduced, the WATERS Network should strive to field test new data sondes such as nutrient sensors. These data sondes could be deployed in alternative locations in a

watershed such as groundwater wells, agricultural drain tiles, or storm sewers to further understand processes occurring within a watershed.

Conclusions

Operation of the SAC sensing station led to advances in the understanding of fundamental water processes and had implications in the management of water resources. The creation and operation of sensing stations in Clear Creek Watershed yielded data that when coupled with data from volunteer organizations and government agencies, enabled for research that could not have been conducted using sensor data alone. This research provides a proof of concept for the larger WATERS Network to be successful in transforming the science and engineering of the water environment. This transformation will lead to a marked improvement in the quality of the nation's water environment, making it swimmable and fishable.

APPENDIX A:

CLEAR CREEK WATER QUALITY DATA 2006-2008

2006 Water Quality Data

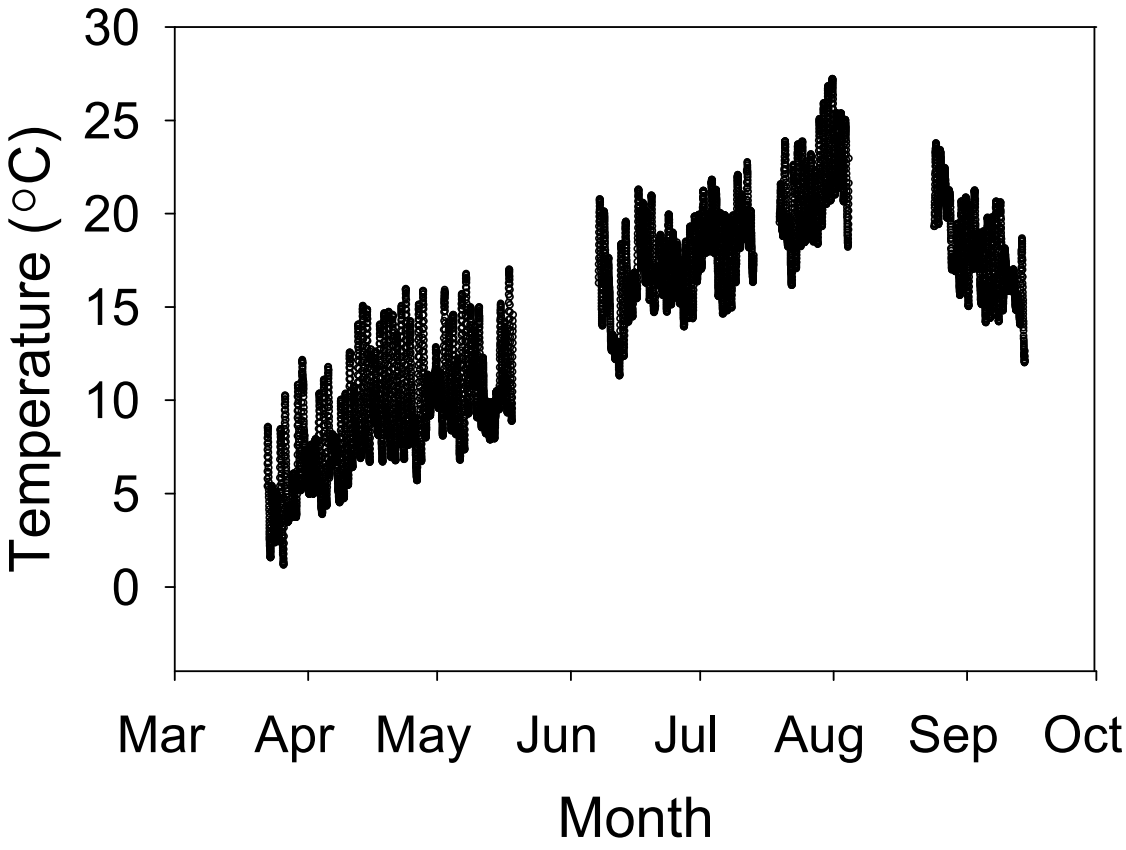

Figure A.1 Temperature measurements from water quality sensors deployed at the SAC sensing station during 2006.

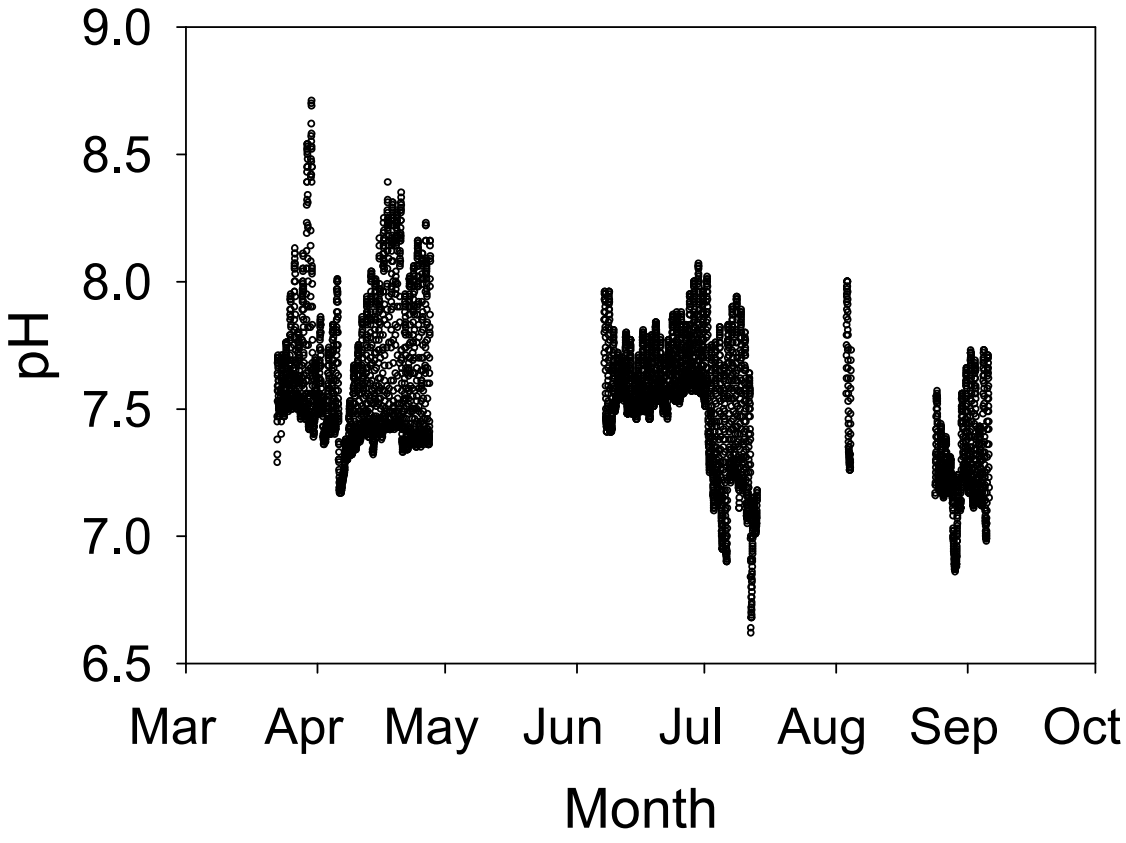

Figure A.2 pH measurements from water quality sensors deployed at the SAC sensing station during 2006.

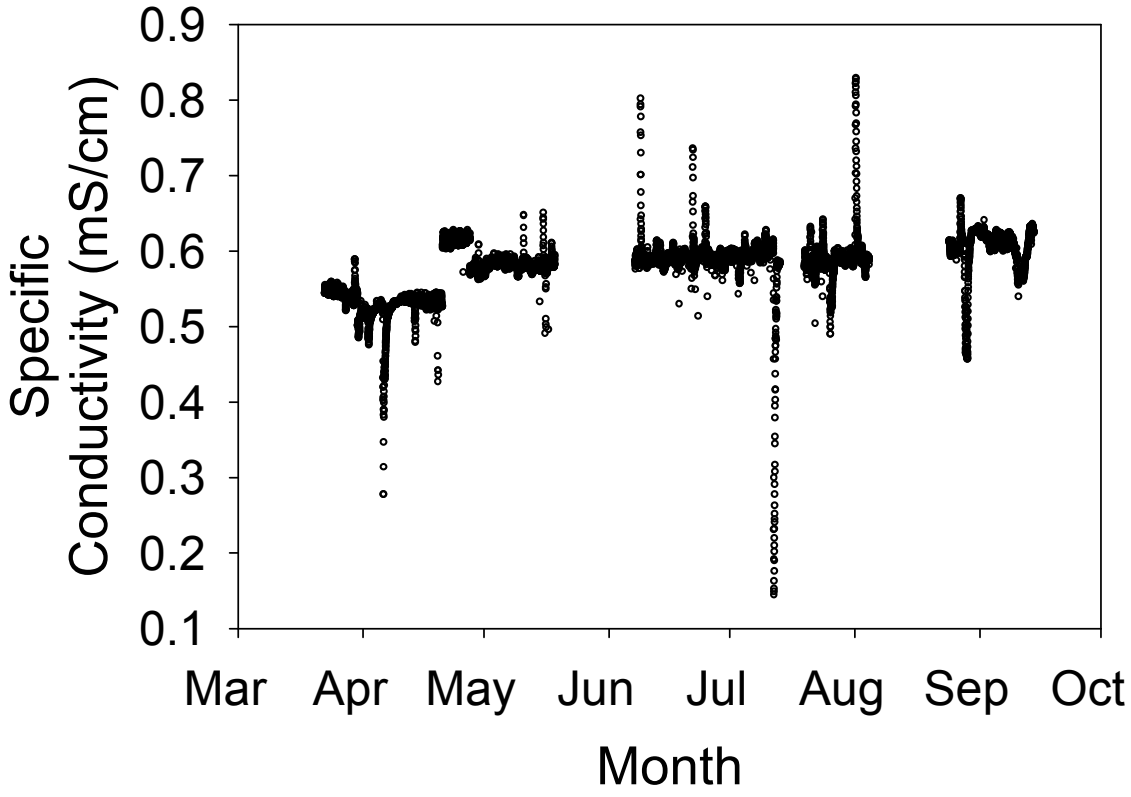

Figure A.3 Specific conductivity measurements from water quality sensors deployed at the SAC sensing station during 2006.

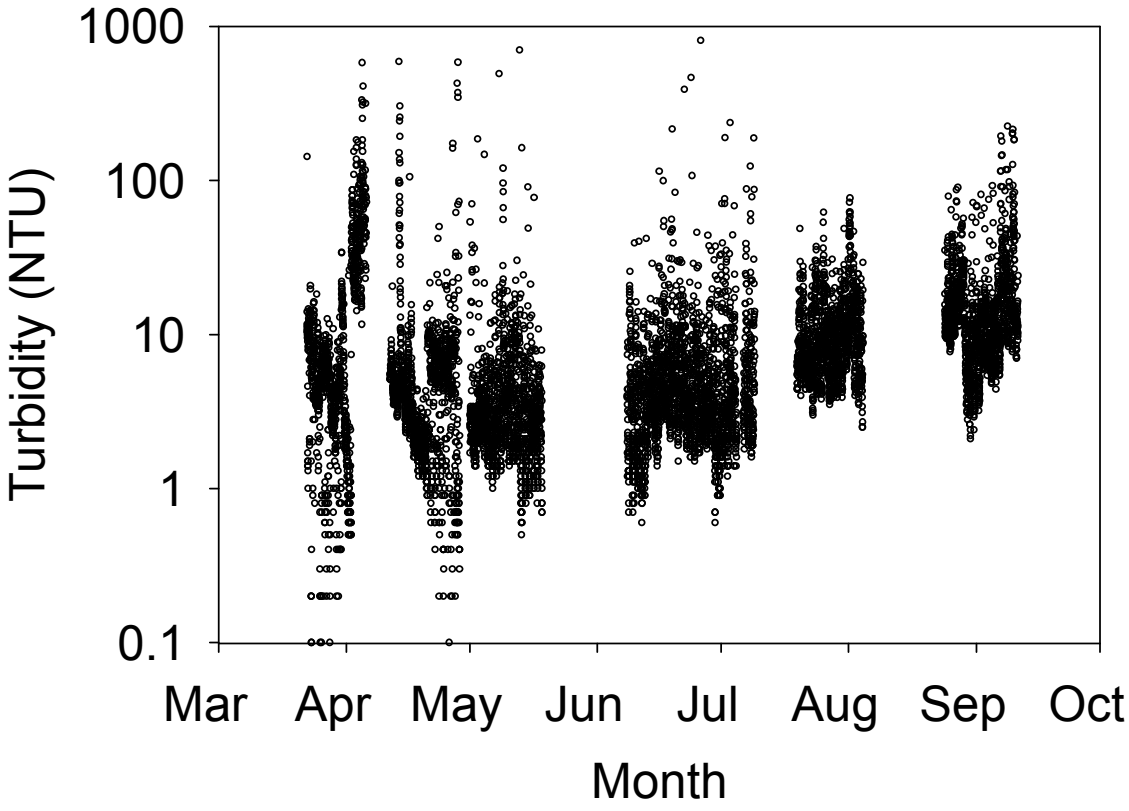

Figure A.4 Turbidity measurements from water quality sensors deployed at the SAC sensing station during 2006.

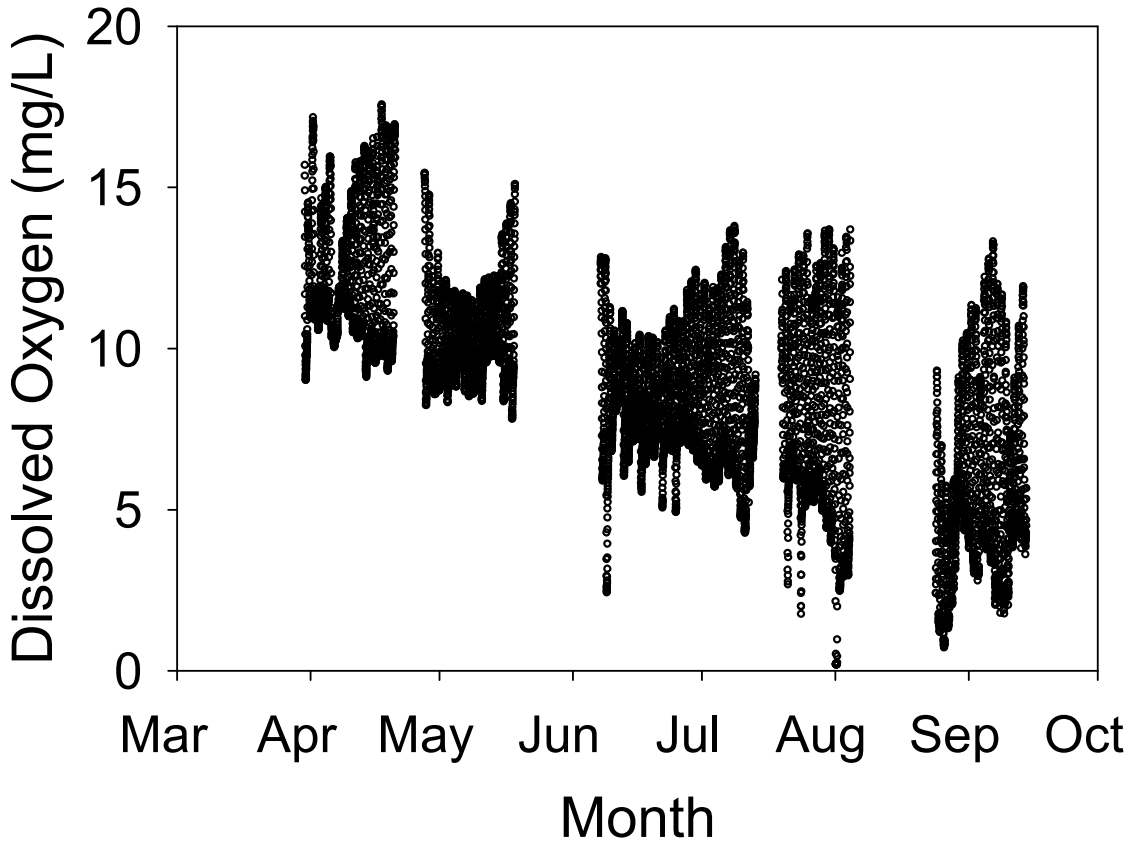

Figure A.5 Dissolved oxygen measurements from water quality sensors deployed at the SAC sensing station during 2006.

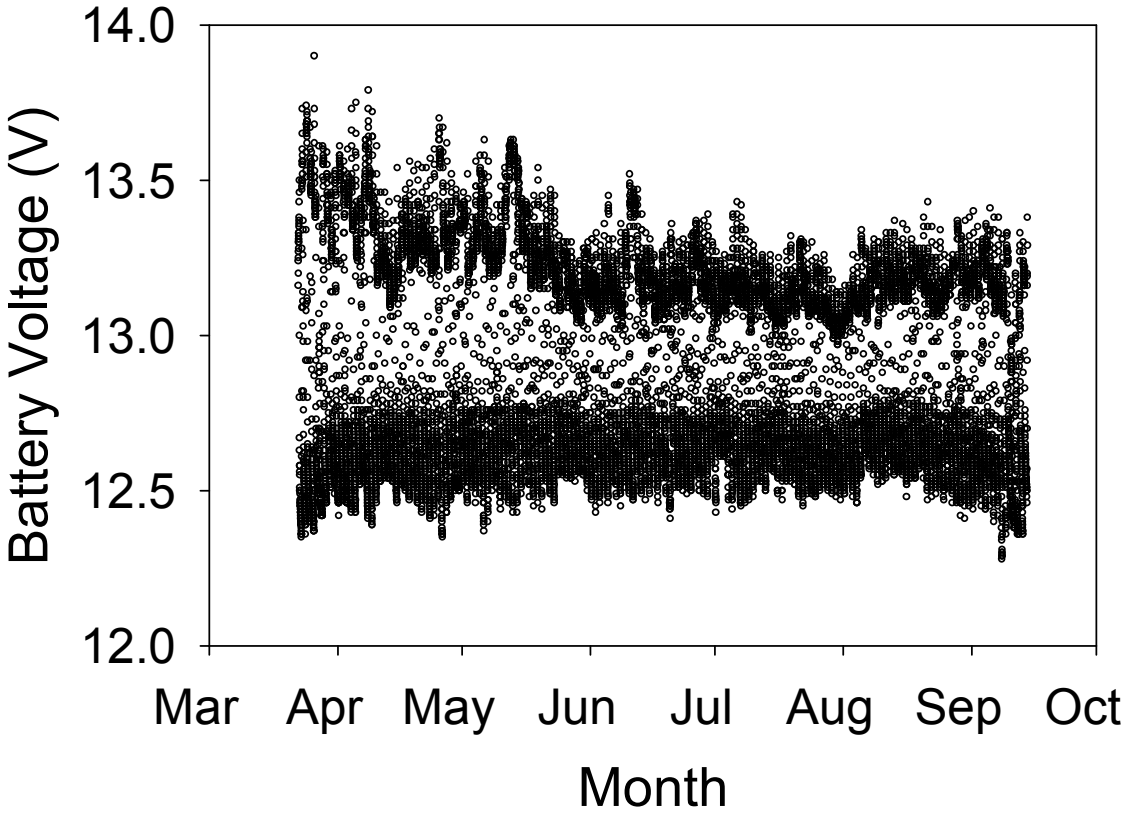

Figure A.6 Battery voltage from at the SAC sensing station during 2006.

Table A.1 Water quality samples collected at the SAC sensing station during 2006.

Date	Dissolved Oxygen (mg L^{-1})[a]	Turbidity 1 (NTU)	Turbidity 2 (NTU)	Turbidity 3 (NTU)	Turbidity 4 (NTU)	Turbidity 5 (NTU)	Turbidity 6 (NTU)	Turbidity 7 (NTU)	Turbidity 8 (NTU)	Turbidity 9 (NTU)	Turbidity 10 (NTU)	pH	TDS - 1 (mg L^{-1})	TDS - 2 (mg L^{-1})	TDS - 3 (mg L^{-1})	TDS - 4 (mg L^{-1})	TS - 1 (mg L^{-1})	TS - 2 (mg L^{-1})
3/30/2006 16:10	11.9	1.86	1.54	2.20	3.14	1.97	2.39	1.93				8.13						
4/11/2006 15:40	11.1	4.75	4.66	4.10	3.79	4.96	3.53	3.50	3.52	4.00	5.77	7.58						
4/20/2006 16:20	12.2	1.56	1.71	1.62	1.44	1.41	1.31	1.50	1.94	1.56	1.52	7.88						
4/27/2006 12:40	12.0	4.20	10.60	4.44	5.43	4.87	4.14	4.73	5.71	4.37	4.59	7.88						
5/4/2006 13:30	9.7	1.60	2.42	2.26	2.40	2.14	2.67	3.66	1.83	1.78	2.33	7.52						
5/18/2006 13:15	11.4	3.68	2.04	4.28	1.77	2.93	2.57	2.95	3.03	2.79	4.73	7.84						
6/7/06 10:00	8.7	4.71	2.66	7.21	5.42	4.22	3.55	4.15	3.41	6.16	3.33	7.60						
6/29/2006 11:30		3.46	3.27									7.55						
7/6/2006 10:40		5.20	4.46	4.17								7.76	408	420	460	408	412	428
7/6/2006 10:45																		
7/13/2006 11:02		4.21	5.33	7.08								7.36						
7/13/2006 10:45																		
7/19/2006 11:10		4.82	3.93	4.16								7.41	456	316	464	460	404	460
8/24/2006 9:00	3.6	20.70										7.02						
9/14/2006 10:00	3.6	55.30										7.34						
8/3/2006 9:45		3.09										7.56						
8/3/2006 11:12		2.37										7.78						
8/3/2006 12:11		2.69										7.94						
8/3/2006 13:04		3.29										8.00						
8/3/2006 14:03		2.11										8.08						
8/3/2006 15:04		2.48										8.11						
8/3/2006 16:03		3.49										8.13						
8/3/2006 17:00		3.95										8.05						
8/3/2006 18:03		4.24										7.94						
8/3/2006 19:00		7.71										7.85						
8/3/2006 20:01		5.25										7.66						
8/3/2006 21:00		6.55										7.63						
8/3/2006 21:55		10.30										7.55						
8/3/2006 23:00		9.43										7.51						
8/3/2006 23:58		8.17										7.38						
8/4/2006 1:05		7.51										7.43						
8/4/2006 2:05		2.82										7.36						
8/4/2006 4:08		4.50										7.30						
8/4/2006 6:08		3.95										7.41						
8/4/2006 7:00		2.83										7.40						
8/4/2006 8:00		2.13										7.39						
8/4/2006 8:55		1.16										7.59						
8/4/2006 9:55		4.72										7.61						
8/4/2006 11:00		7.86										7.84						
8/4/2006 12:00		5.03										7.72						

[a]Dissolved oxygen concentrations were measured *in situ* using a Hach HQ-10 dissolved oxygen sensor.

Table A.2 Water quality measurements taken at the SAC sensing station during 2006 using a Hach Quanta G data sonde.

Date	Temperature (°C)	Specific Conductivity (µmhos cm^{-1})	Dissolved Oxygen (mg L^{-1})[a]	pH	ORP (mV)
3/30/2006 16:10	12.33	0.541	14.89	7.70	292
4/11/2006 15:40	10.76	0.572	13.46	7.72	323
4/20/2006 16:20	14.81	0.484	13.19	8.05	254
5/4/2006 13:30	13.25	0.596	11.09	7.81	268
6/7/06 10:00	15.59	0.583	11.05	7.66	292
6/29/2006 11:30	16.51	0.482	10.65	7.86	272
7/6/2006 10:45	16.08	0.599	10.65	7.81	274
7/13/2006 10:45	17.68	0.588	7.84	7.44	289
9/14/2006 10:00	13.47	0.373	4.17	7.73	203
8/3/06 9:50	21.21	0.605	7.01	7.62	272
8/3/06 11:12	22.08	0.600	8.14	7.79	239
8/3/06 12:01	22.68	0.598	9.03	7.89	237
8/3/06 13:07	23.62	0.591	10.08	7.99	241
8/3/06 14:03	23.84	0.587	10.48	8.05	237
8/3/06 15:07	24.68	0.584	9.56	8.07	237
8/3/06 16:05	24.90	0.585	9.42	8.07	233
8/3/06 17:05	24.91	0.594	8.26	8.00	237
8/3/06 18:06	24.86	0.598	7.76	7.93	232
8/3/06 19:04	24.67	0.601	6.36	7.81	242
8/3/06 20:01	24.44	0.604	5.20	7.72	243
8/3/06 21:02	24.04	0.609	4.20	7.62	245
8/3/06 21:55	23.50	0.612	3.28	7.53	240
8/3/06 23:00	22.70	0.614	2.46	7.47	240
8/3/06 23:58	21.94	0.615	2.10	7.42	241
8/4/06 1:05	21.17	0.615	2.20	7.41	242
8/4/06 2:05	20.54	0.614	2.49	7.42	249
8/4/06 4:08	19.10	0.614	2.88	7.43	253
8/4/06 6:08	18.53	0.617	3.11	7.44	251
8/4/06 7:02	18.24	0.618	3.47	7.46	255
8/4/06 8:03	18.25	0.618	4.49	7.50	258
8/4/06 8:59	18.54	0.618	5.74	7.55	264
8/4/06 10:00	19.24	0.616	7.63	7.68	258
8/4/06 11:03	20.37	0.611	9.28	7.80	268
8/4/06 12:03	21.33	0.608	9.57	7.90	262

[a]DO sensor on the Quanta G was the Clark Cell/membrane style sensor.

Table A.3 Water quality measurements from sensors placed at the SAC sensing station from 8/03/2006 to 8/04/2006.

Date	Hydrolab DS5X data sonde #1					Hydrolab DS5X data sonde #2				
	Temperature (°C)	pH	Turbidity (NTU)	Dissolved Oxygen (mg/L)	Battery Voltage (V)	Temperature (°C)	pH	Turbidity (NTU)	Dissolved Oxygen (mg/L)	Battery Voltage (V)
8/3/06 10:00	21.32	7.56	2.6	8.16	11.6	21.27	7.55	11	7.98	11.9
8/3/06 10:20	21.55	7.62	0.8	8.87	11.6	21.51	7.62	3	8.82	11.9
8/3/06 10:40	21.82	7.66	0.7	9.53	11.6	21.77	7.67	2	9.49	11.9
8/3/06 11:00	22.04	7.71	0.9	10	11.6	21.99	7.7	2	10.07	11.8
8/3/06 11:20	22.29	7.75	1.4	10.56	11.5	22.19	7.74	2	10.3	11.8
8/3/06 11:40	22.5	7.79	2.3	11.02	11.5	22.4	7.77	3	10.76	11.8
8/3/06 12:00	22.77	7.83	2.3	11.51	11.5	22.64	7.81	3	11.19	11.8
8/3/06 12:20	23.01	7.86	2.6	11.91	11.5	22.88	7.85	3	11.58	11.8
8/3/06 12:40	23.29	7.89	3.6	12.27	11.5	23.16	7.87	5	11.94	11.8
8/3/06 13:00	23.59	7.92	3.5	12.56	11.5	23.44	7.9	5	12.24	11.8
8/3/06 13:20	23.82	7.94	2.3	12.72	11.5	23.66	7.93	3	12.43	11.8
8/3/06 13:40	23.99	7.95	1.9	12.75	11.5	23.83	7.95	3	12.47	11.8
8/3/06 14:00	24.18	7.97	1.2	12.82	11.5	24.03	7.96	2	12.54	11.8
8/3/06 14:20	24.36	7.98	1.4	12.86	11.5	24.2	7.98	2	12.6	11.7
8/3/06 14:40	24.53	8	1.5	12.81	11.5	24.39	7.99	2	12.57	11.7
8/3/06 15:00	24.66	8	1.5	12.73	11.4	24.52	8	3	12.51	11.7
8/3/06 15:20	24.77	8	1.9	12.58	11.4	24.64	8	2	12.34	11.7
8/3/06 15:40	24.85	8	2.4	12.34	11.4	24.72	8	3	12.15	11.7
8/3/06 16:00	24.9	8	4.6	12.09	11.4	24.79	8	4	11.93	11.6
8/3/06 16:20	24.93	7.98	7.4	11.76	11.4	24.83	7.98	7	11.62	11.6
8/3/06 16:40	24.94	7.96	4.7	11.38	11.4	24.84	7.96	6	11.25	11.6
8/3/06 17:00	24.93	7.93	5.9	10.94	11.4	24.84	7.94	6	10.87	11.6
8/3/06 17:20	24.93	7.91	4.5	10.56	11.4	24.85	7.92	5	10.52	11.6
8/3/06 17:40	24.91	7.88	6	10.22	11.4	24.84	7.9	6	10.21	11.6
8/3/06 18:00	24.92	7.85	7.4	9.8	11.4	24.86	7.87	8	9.89	11.6
8/3/06 18:20	24.88	7.81	9.1	9.39	11.4	24.83	7.84	9	9.53	11.5
8/3/06 18:40	24.83	7.79	5.8	9	11.4	24.79	7.82	6	9.11	11.5
8/3/06 19:00	24.74	7.74	12.2	8.41	11.4	24.71	7.77	14	8.6	11.5
8/3/06 19:20	24.68	7.73	6.5	7.97	11.4	24.65	7.76	7	8.15	11.5
8/3/06 19:40	24.6	7.69	5.6	7.45	11.4	24.57	7.72	7	7.6	11.5
8/3/06 20:00	24.5	7.66	6.4	6.96	11.4	24.48	7.7	8	7.16	11.5
8/3/06 20:20	24.41	7.62	6.4	6.59	11.4	24.38	7.67	7	6.78	11.4
8/3/06 20:40	24.29	7.59	8	6.21	11.4	24.26	7.64	9	6.44	11.4
8/3/06 21:00	24.12	7.56	7.6	5.75	11.4	24.11	7.61	9	5.98	11.4
8/3/06 21:20	23.95	7.53	12.2	5.21	11.4	23.93	7.58	13	5.47	11.4
8/3/06 21:40	23.75	7.49	14.4	4.69	11.4	23.74	7.54	16	4.96	11.4
8/3/06 22:00	23.52	7.46	14	4.19	11.4	23.52	7.51	18	4.46	11.4
8/3/06 22:20	23.26	7.44	15.7	3.81	11.4	23.29	7.49	18	4.05	11.4
8/3/06 22:40	23.02	7.41	13.3	3.5	11.4	23.03	7.47	14	3.73	11.4
8/3/06 23:00	22.78	7.39	14.7	3.24	11.4	22.79	7.45	16	3.47	11.4
8/3/06 23:20	22.52	7.37	19.5	2.97	11.3	22.54	7.43	21	3.23	11.4
8/3/06 23:40	22.28	7.35	17.9	2.8	11.3	22.29	7.41	24	3.01	11.4
8/4/06 0:00	22.03	7.35	10.1	2.77	11.3	22.05	7.41	14	2.94	11.4
8/4/06 0:20	21.8	7.34	5.4	2.76	11.3	21.81	7.4	8	2.94	11.4
8/4/06 0:40	21.57	7.33	7.8	2.76	11.3	21.59	7.4	9	2.94	11.4
8/4/06 1:00	21.33	7.33	8.7	2.86	11.3	21.35	7.4	11	3	11.4
8/4/06 1:20	21.1	7.33	5.2	2.98	11.3	21.13	7.4	8	3.13	11.4
8/4/06 1:40	20.89	7.33	3.3	3.08	11.3	20.91	7.41	4	3.22	11.4
8/4/06 2:00	20.68	7.32	2.1	3.17	11.2	20.69	7.41	4	3.3	11.3
8/4/06 2:20	20.47	7.32	1.9	3.25	11.2	20.5	7.41	3	3.39	11.3
8/4/06 2:40	20.29	7.31	11.1	3.34	11.2	20.31	7.41	3	3.47	11.3
8/4/06 3:00	20.11	7.31	1.8	3.38	11.2	20.13	7.41	3	3.55	11.3
8/4/06 3:20	19.94	7.3	2.1	3.46	11.2	19.96	7.41	3	3.6	11.3
8/4/06 3:40	19.76	7.3	2.9	3.51	11.2	19.78	7.41	4	3.69	11.3
8/4/06 4:00	19.59	7.29	4.3	3.6	11.2	19.62	7.41	5	3.76	11.3
8/4/06 4:20	19.43	7.29	7.4	3.62	11.2	19.46	7.41	9	3.79	11.3
8/4/06 4:40	19.27	7.28	6.1	3.64	11.2	19.3	7.41	9	3.82	11.2
8/4/06 5:00	19.12	7.28	3.3	3.72	11.2	19.15	7.41	6	3.87	11.2
8/4/06 5:20	18.97	7.27	2.6	3.79	11.2	19	7.41	5	3.95	11.2
8/4/06 5:40	18.82	7.26	2.8	3.85	11.2	18.86	7.41	4	4.01	11.2
8/4/06 6:00	18.67	7.26	3.4	3.92	11.2	18.72	7.41	5	4.06	11.2
8/4/06 6:20	18.54	7.26	3.2	4.04	11.1	18.6	7.42	5	4.18	11.2
8/4/06 6:40	18.44	7.26	3.6	4.18	11.1	18.49	7.42	5	4.33	11.2
8/4/06 7:00	18.35	7.27	1.7	4.38	11.1	18.39	7.43	4	4.53	11.2
8/4/06 7:20	18.31	7.27	1.1	4.6	11.1	18.35	7.44	3	4.77	11.2
8/4/06 7:40	18.35	7.29	1.1	5.2	11.1	18.39	7.46	2	5.32	11.1
8/4/06 8:00	18.36	7.29	0	5.5	11.1	18.36	7.46	2	5.41	11.1
8/4/06 8:20	18.41	7.3	0	5.65	11.1	18.41	7.48	2	5.71	11.1
8/4/06 8:40	18.49	7.32	0	6.16	11.1	18.5	7.5	1	6.2	11.1
8/4/06 9:00	18.68	7.36	0	6.92	11.1	18.68	7.54	2	6.93	11.1
8/4/06 9:20	18.91	7.4	3.3	7.65	11.1	18.89	7.57	4	7.69	11.1
8/4/06 9:40	19.13	7.44	5.3	8.49	11.1	19.1	7.6	7	8.37	11.1
8/4/06 10:00	19.4	7.48	5.6	9.3	11.1	19.35	7.65	8	9.17	11.1
8/4/06 10:20	19.76	7.54	13.2	10.08	11.1	19.7	7.71	13	10.1	11.1
8/4/06 10:40	20.16	7.58	16.4	10.69	11.1	20.1	7.75	20	10.87	11.1
8/4/06 11:00	20.5	7.62	8.8	11.26	11.1	20.42	7.78	12	11.3	11.1
8/4/06 11:20	20.8	7.65	6.1	11.72	11.1	20.69	7.8	9	11.55	11.1
8/4/06 11:40	21.08	7.69	5.9	12.23	11.1	20.99	7.83	8	11.92	11.1
8/4/06 12:00	21.44	7.73	6.6	12.63	11.1	21.33	7.87	8	12.36	11.1

2007 Water Quality Data

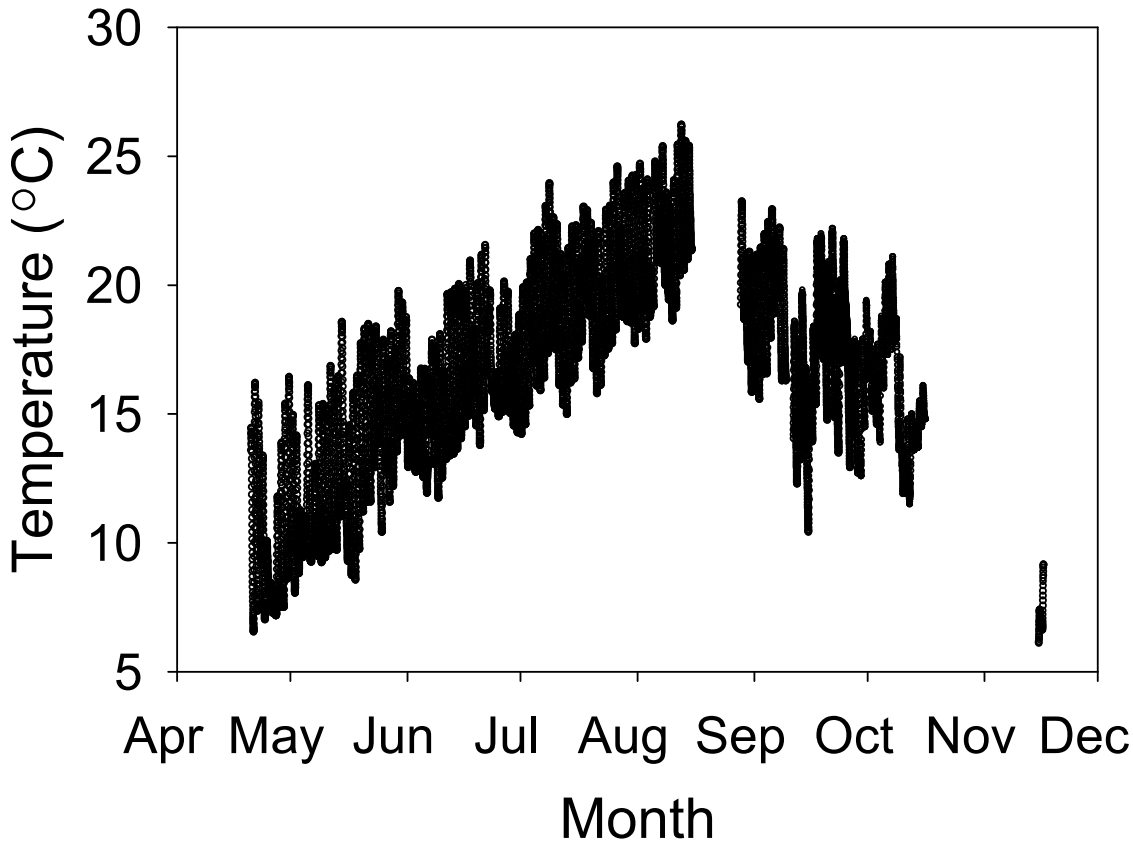

Figure A.7 Temperature measurements from water quality sensors deployed at the SAC sensing station during 2007.

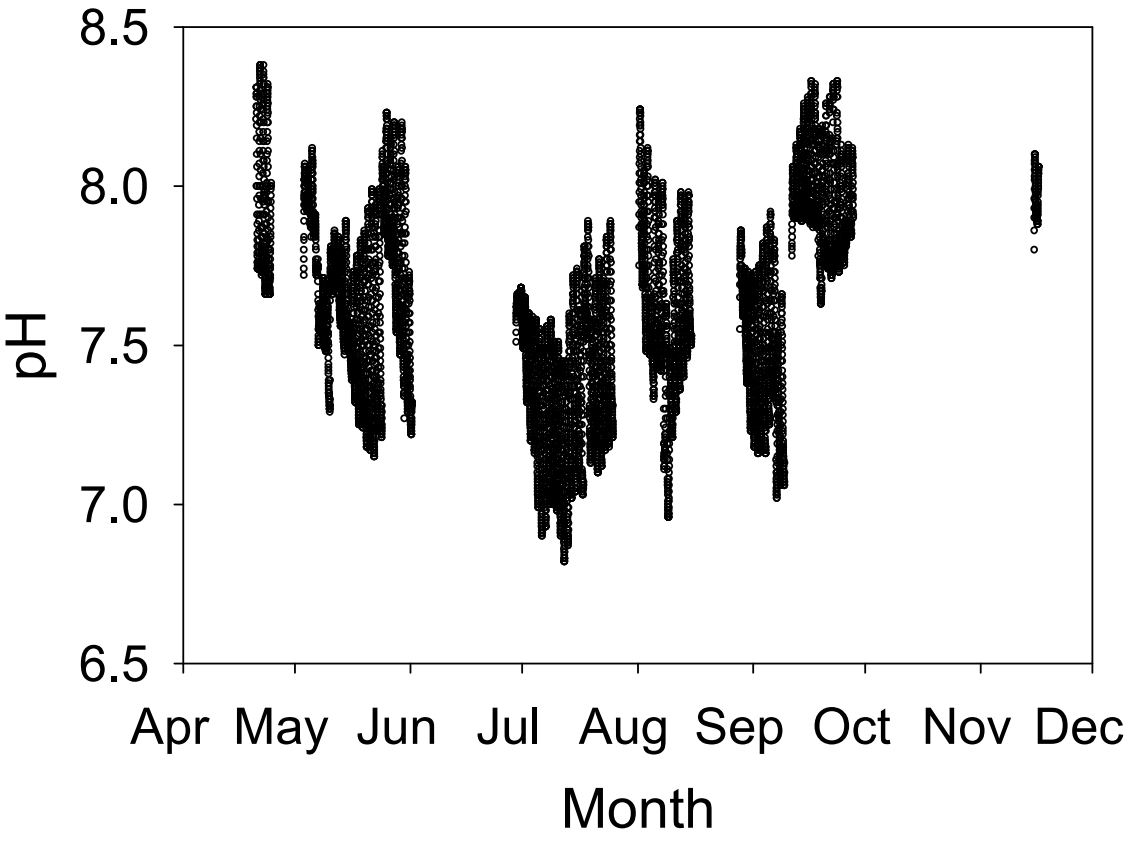

Figure A.8 pH measurements from water quality sensors deployed at the SAC sensing station during 2007.

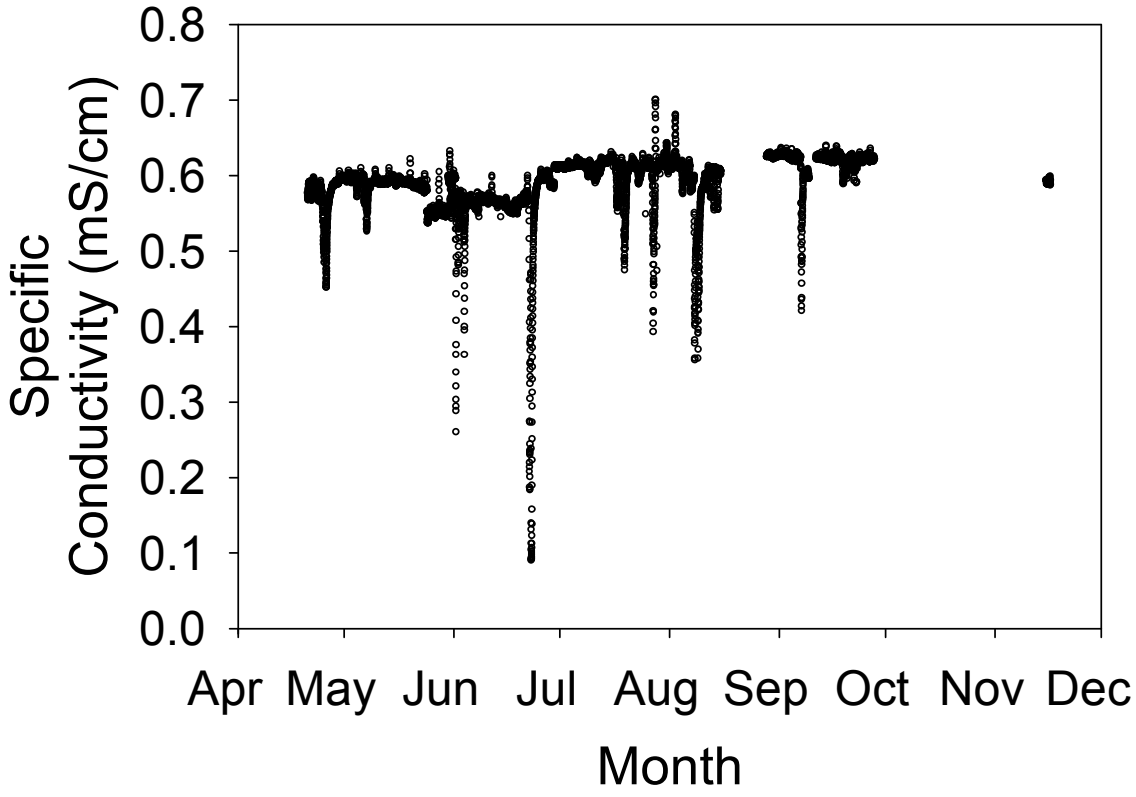

Figure A.9 Specific conductivity measurements from water quality sensors deployed at the SAC sensing station during 2007.

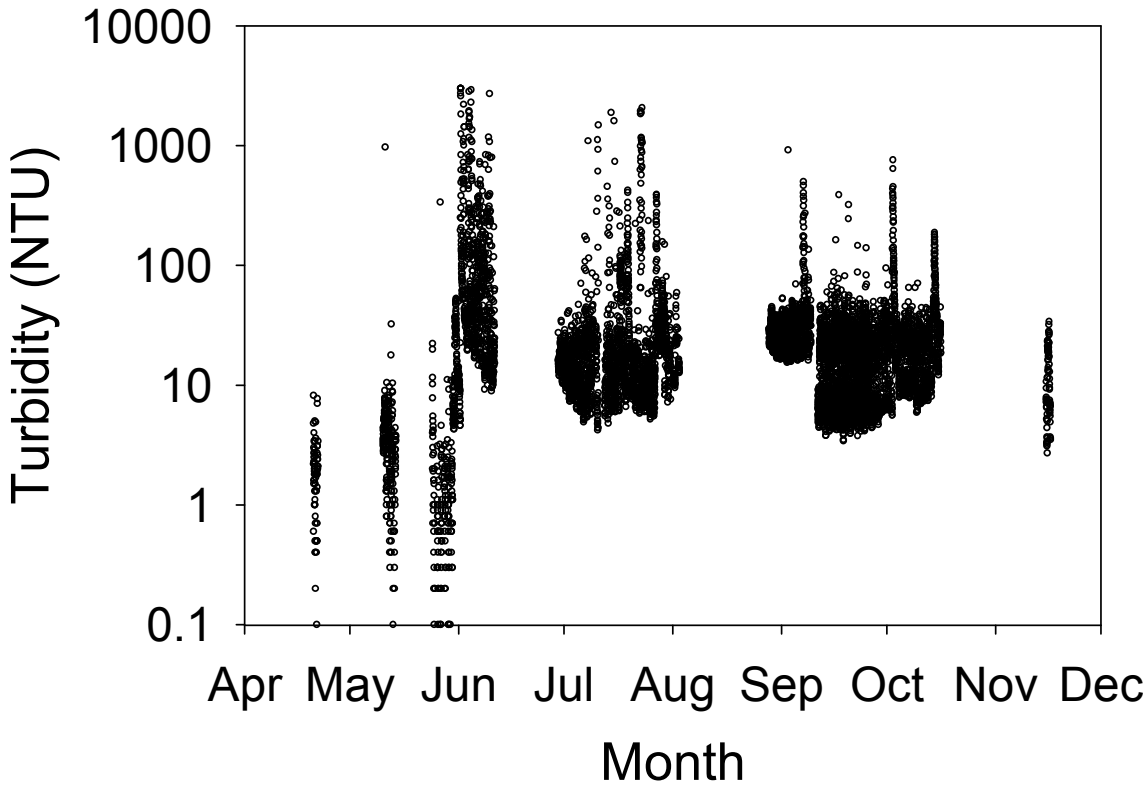

Figure A.10 Turbidity measurements from water quality sensors deployed at the SAC sensing station during 2007.

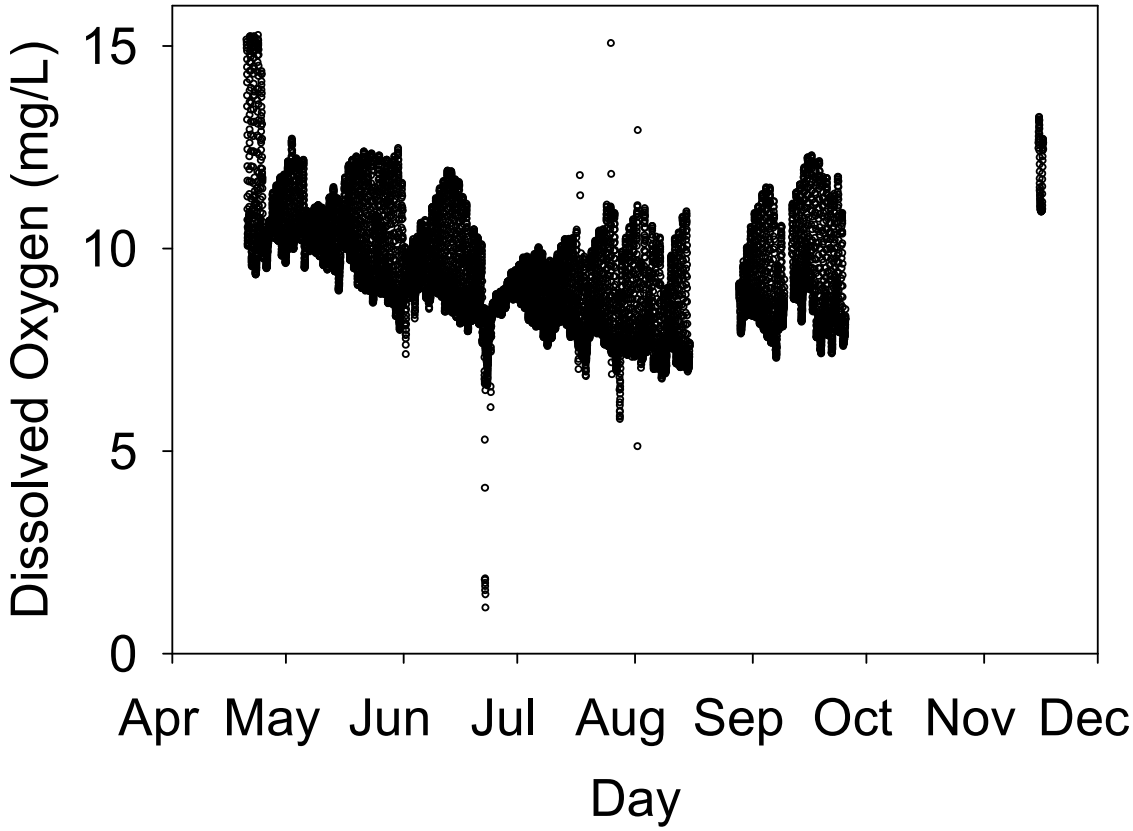

Figure A.11 Dissolved oxygen measurements from water quality sensors deployed at the SAC sensing station during 2007.

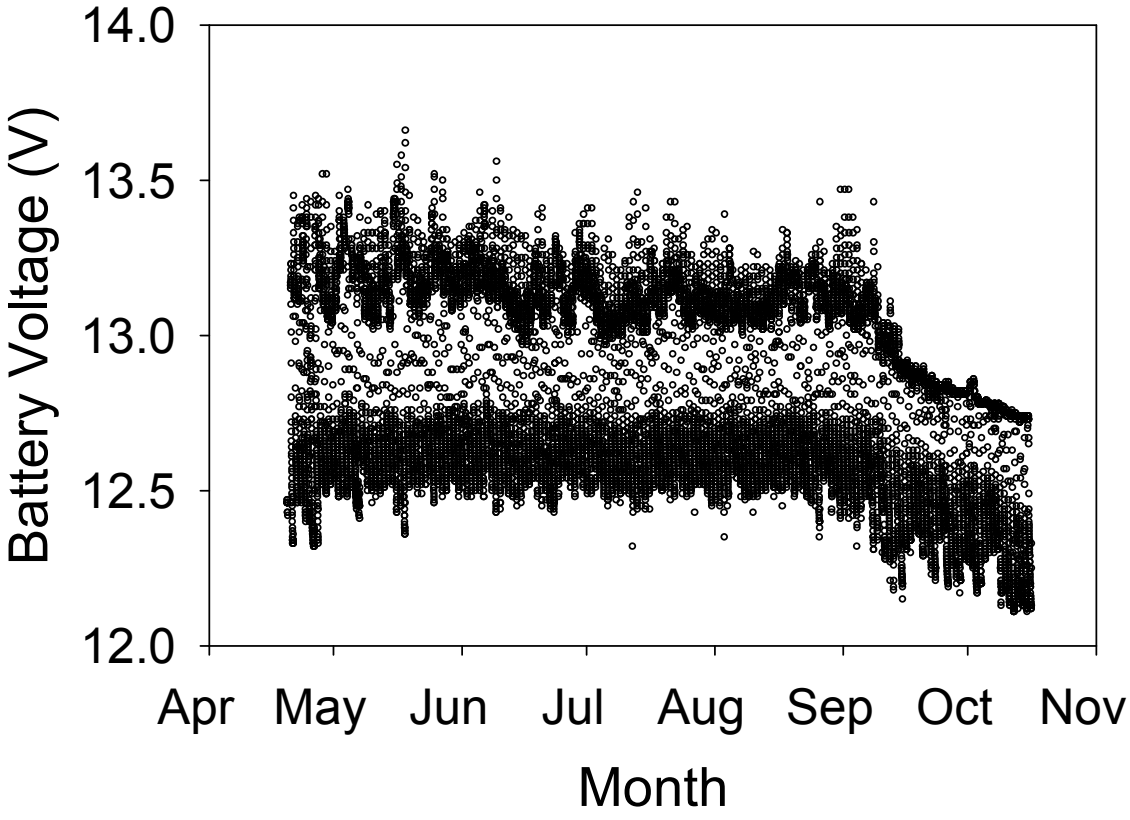

Figure A.12 Battery voltage from at the SAC sensing station during 2007

Table A.4 Water quality samples collected at the SAC sensing station during 2007[a].

Date	pH	TSS[b] 1 (mg L^{-1})	TSS 2 (mg L^{-1})	TSS 3 (mg L^{-1})	Average TSS (mg L^{-1})	Stdev TSS (mg L^{-1})	TDS[c] 1 (mg L^{-1})	TDS 2 (mg L^{-1})	TDS 3 (mg L^{-1})	Average TDS (mg L^{-1})	Std dev TDS (mg L^{-1})	Turbidity 1 (NTU)	Turbidity 2 (NTU)	Turbidity 3 (NTU)	Turbidity 4 (NTU)	Turbidity 5 (NTU)	Turbidity Average (NTU)	Turbidity Std Dev (NTU)	Orthophosphate (mg L^{-1} PO_4^{3-})	Total Phosphorus (mg L^{-1} PO_4^{3-})	Ammonia (mg L^{-1} NH_3-N)	Nitrate + Nitrite (mg L^{-1} as N) - UI hygenic lab	E.Coli (count 100 ml^{-1}) - UI hygenic lab	Alkalinity (mg/L as $CaCO_3$)	Calcium Hardness (mg L^{-1} $CaCO_3$)	Total Hardness (mg L^{-1} as $CaCO_3$)
5/3/2007 8:15	7.62	16.70	25.00	22.30	21.33	4.23	436	432	448	439	8.33	10.4	9.45	9.38	11.2	8.93	9.87	0.92		1.1	0.23			194		
5/10/2007 10:18	7.64	29.00	21.30	22.00	24.10	4.26	364	268	372	335	57.87	8.58	9.37	7.45	10.3	7.92	8.72	1.14	0.28	0.46	0.17			184		
5/24/2007 8:35	7.90	8.33	11.67	9.33	9.78	1.71	404	412	384	400	14.42	4.16	4.81	4.46	4.48	3.89	4.36	0.35	0.28	0.53	0.14				178	280
5/30/2007 8:40	7.54	10.33			10.33		440			440		5.66	5.29	5.95	6.53	6.73	6.03	0.60	0.29	0.38	0.09				180	294.4
6/22/2007 8:07	7.81	2900	3204	3020	3041.3	153.1	230	210	230	223	11.55	2410	2392	2373	2518	2378	2414	59.8	0.50	10.4	1.15					
6/29/2007 8:35	7.53	24.33	23.67	24.00	24.00	0.33	415	425	415	418	5.77	12.4	12.0	11.6	11.3	11.8	11.8	0.41	0.33	0.51	0.08			194		
7/11/2007 14:35	7.66	5.33	5.33	4.67	5.11	0.38	395	400	395	397	2.89	5.84	4.79	5.14	5.2	5.49	5.29	0.39	0.33	0.44	0.12			208		
7/17/2007 10:35	7.44	21.33	23.38	20.67	21.79	1.42	390	400	380	390	10.00	27.2	28.2	28.1	27.8	27.8	27.8	0.39	1.58	2.23	0.57			193		
7/23/2007 8:30	7.73	62.03	60.34	60.66	61.01	0.90	390	415	420	408	16.07	34.7	35.3	33.8	35.6	35.3	34.9	0.72	0.40		0.17	6.4	2600	194		
8/1/07 9:15	7.67											6.25	6.4	6.19	7.06	6.53	6.49	0.35	0.41	0.54	0.09	12	1900			
8/15/07 10:20		9.00	9.00	8.3871	8.7957	0.35	405	325	440	390	58.95								0.44		0.1				193	
8/21/07 0:00		83.00	79.00	79.00	80.33	2.31	420	395	415	410	13.23	47.4	47	46.7	45.2	46.2	46.5	0.85	0.86	1.37	0.18			206	182	273
8/29/07 8:37		8.00			8.00		425			425		11.3	10.8	11.2	12.4	12.5	11.6	0.76	0.43		0.08					
8/29/07 15:35		17.00			17.00		455			455		5.12	5.17	5.65	5.92	6.21	5.61	0.47	0.44		0.09					
9/11/2007 9:34																			0.37		0.1					

[a]The 6/22/2007 and 7/23/2007 samples were collected at the Coralville sensing station.

[b]TSS = Total Suspended Solids

[c]TDS = Total Dissolved Solids

Table A.5 Water quality samples collected at the SAC sensing station during the 28-hour study on 9/18/2007 and 9/19/2007.

Date[a]	pH	Total Suspended Solids (mg L^{-1})	Volatile Suspended Solids (mg L^{-1})	Fixed Suspended Solids (mg L^{-1})	VSS / TSS[b]	Average Total Dissolved Solids (mg L^{-1})	Volatile Dissolved Solids (mg L^{-1})	Fixed Dissolved Solids (mg L^{-1})	VDS / TDS[c]	Turbidity 1 (NTU)	Turbidity 2 (NTU)	Turbidity 3 (NTU)	Turbidity 4 (NTU)	Turbidity 5 (NTU)	Turbidity Average (NTU)	Turbidity Std Dev (NTU)
9/18/07 10:15		91.2	8.40	82.80	0.092	350	120	230	0.343	27.7	26.8	32.5	24.5	15.2	25.34	6.37
9/18/07 10:15																
9/18/07 11:00		2.4	0.40	2.00	0.167	390	150	240	0.385	4.46	3.82	4.12	4.11	3.86	4.074	0.26
9/18/07 11:00		2.4	0.80	1.60	0.333	390	100	290	0.256							
9/18/07 12:02		2.4	0.80	1.60	0.333	400	140	260	0.350	3.13	3.92	3.18	3.36	3.15	3.348	0.33
9/18/07 13:03		2	0.80	1.20	0.400	340	140	200	0.412	3.18	3.04	3.25	3.61	2.96	3.208	0.25
9/18/07 14:03		2	0.80	1.20	0.400	520	200	320	0.385	2.87	2.76	3.01	3.47	2.98	3.018	0.27
9/18/07 15:06	8.32	0.8	0.40	0.40	0.500	400	140	260	0.350	2.4	2.23	2.33	2.75	2.94	2.53	0.30
9/18/07 16:05	8.3	2	0.00	2.00	0.000	410	150	260	0.366	3.51	3.23	3.02	2.95	2.92	3.126	0.25
9/18/07 17:04	8.29	3.2	1.60	1.60	0.500	400	150	250	0.375	3.8	3.7	3.2	3.45	3.29	3.488	0.26
9/18/07 18:05	8.18	2	0.80	1.20	0.400	400	150	250	0.375	3.55	3.34	3.33	3.22	3.69	3.426	0.19
9/18/07 19:25	8.11	5.2	1.60	3.60	0.308	360	120	240	0.333	5.15	5.52	4.42	4.74	4.9	4.946	0.42
9/18/07 19:59	8.04	26.8	2.00	24.80	0.075	340	110	230	0.324	13.2	13.6	13.2	13.3	13.2	13.3	0.17
9/18/07 19:59																
9/18/07 21:06	8.03	18.8	2.40	16.40	0.128	370	110	260	0.297	13.6	11.5	11.5	11.1	11.9	11.92	0.98
9/18/07 22:15	7.98	13.6	2.00	11.60	0.147	370	110	260	0.297	11.9	10.9	10.3	10.6	10.1	10.76	0.71
9/18/07 22:15																
9/19/07 0:10	7.91	230.8	18.00	212.80	0.078	390	120	270	0.308	67.8	64.4	63.9	69.3	58	64.68	4.37
9/19/07 0:10		262.4	20.40	242.00	0.078	360	110	250	0.306							
9/19/07 1:07	7.92	28.4	4.00	24.40	0.141	300	100	200	0.333	23.1	22.1	21.2	21.6	21.3	21.86	0.78
9/19/07 2:02	8.03	18.8	3.20	15.60	0.170	380	130	250	0.342	19.6	20.3	19.6	19.4	19.6	19.7	0.35
9/19/07 2:56	7.92	30.4	3.60	26.80	0.118	270	70	200	0.259	23.8	22.2	22.4	23.8	21.5	22.74	1.02
9/19/07 2:56																
9/19/07 4:01	7.93	30.8	3.60	27.20	0.117	380	120	260	0.316	25	23	24.1	23.2	24	23.86	0.80
9/19/07 5:10	7.82	22.8	3.60	19.20	0.158	350	130	220	0.371	19.4	20.5	18	18.8	18.7	19.08	0.94
9/19/07 5:10																
9/19/07 6:10	7.89	32.8	4.00	28.80	0.122	410	170	240	0.415	24.4	22.3	22.4	21.7	21.4	22.44	1.17
9/19/07 6:10		34.4	4.00	30.40	0.116	410	120	290	0.293							
9/19/07 7:05	7.85	21.6	3.60	18.00	0.167	400	140	260	0.350	19.6	18.5	18	17.7	17.5	18.26	0.84
9/19/07 8:03	7.8	10.8	1.60	9.20	0.148	420	150	270	0.357	13.3	13.1	12.2	12.8	10.6	12.4	1.09
9/19/07 9:07	7.96	6.4	1.60	4.80	0.250	450	140	310	0.311	10.5	9.72	8.96	8.78	8.56	9.304	0.80
9/19/07 10:09	7.93	4	0.80	3.20	0.200	490	140	350	0.286	7.44	7	6.46	6.45	6.4	6.75	0.46
9/19/07 11:05	7.97	3.2	1.60	1.60	0.500	440	140	300	0.318	5.47	5.43	5.25	5.6	5.36	5.422	0.13
9/19/07 12:04	8.04	2	1.60	0.40	0.800	370	110	260	0.297	4.43	4.63	4.24	4.2	4	4.3	0.24
9/19/07 13:01	8.08	2.8	1.60	1.20	0.571	390	140	250	0.359	3.9	3.68	3.82	4.19	3.81	3.88	0.19
9/19/07 13:59	8.14	1.6	0.40	1.20	0.250	410	140	270	0.341	3.55	3.31	3.31	3.78	3.55	3.5	0.20
9/19/07 13:59		2.4	0.80	1.60	0.333	420	110	310	0.262							

[a]Repeated sample times indicate that duplicate samples were measured.

[b]VSS = volatile suspended solids and TSS = total suspended solids

[c]VDS = volatile dissolved solids and TDS = total dissolved solid

Table A.6 Phytoplankton enumeration and identification from grab samples collected on 9/18/2007 and 9/19/2007 at the SAC sensing station.

Date[a]	Cell Count (cells L^{-1})	% Cyanobacteria	% Chlorophyta	% Diatoms	% Dinophyceae	% Protozoa	% Chrysosphyceae	% Euglenophyta	% Cryptophyta
9/18/07 11:00	9.9E+05	0	2	75	0	8	0	0	16
9/18/07 13:03	1.1E+06	0	4	70	0	5	0	0	21
9/18/07 18:04	7.1E+05	0	7	48	0	10	0	0	35
9/18/07 21:06	1.4E+06	<1	4	48	0	14	0	<1	33
9/18/07 22:13	1.4E+06	0	2	31	0	8	0	0	59
9/19/07 6:09	2.1E+06	0	6	36	0	10	0	0	47
9/19/07 7:03	1.7E+06	0	3	38	0	6	0	0	53
9/19/07 9:05	1.8E+06	0	6	39	0	8	0	<1	46
9/19/07 11:03	1.5E+06	0	10	50	0	7	0	<1	33
9/19/07 13:58	1.3E+06	0	5	68	0	5	0	1	21

[a]Species identified in the 13:03 sample include: Navicula sp., Cyclotella sp., Fragilaria sp., Chroomonas sp., Nitzschia sp., Cymbella sp., Chlamydomonas sp., Cymatopleura sp., Synedra sp., Misc. Protozoans, Cryptomonas sp., Hantzschia sp., Achnanthes sp., Gomphonema sp. and species identified in the 22:13 sample include: Cyclotella sp., Chroomonas sp., Gyro/Pleurosigma sp., Nitzschia sp., Achnanthes sp., Chlamydomonas sp., Misc. Protozoan, Gomphonema sp., Cryptomonas sp., Fragilaria sp., Navicula sp., Cymatopleura sp., Cymbella sp., Hantzschia sp., Synedra sp., Surrirella sp.

Table A.7 Zooplankton enumeration and identification from grab samples collected on 9/18/2007 and 9/19/2007 at the SAC sensing station.

Date[a]	Zooplankton Count (number L^{-1})
9/18/2007 11:15	0.687972271
9/18/2007 13:00	1.236355964
9/18/2007 18:01	1.395885766
9/18/2007 21:00	1.898404642
9/18/2007 22:14	1.926322357
9/19/2007 6:20	2.966257253
9/19/2007 7:01	2.128725794
9/19/2007 9:03	1.064362897
9/19/2007 11:01	0.988752418
9/19/2007 13:56	0.791001934

[a]Zooplankton identified in the 13:00 sample includes: Cladocerans (*Daphnia sp*.), Copepods (*Calanoid sp*., *Nauplii sp*.), and Rotifers (*Gastropus sp*., *Monostyla sp*., *Keratella cochlearis sp*., *Testudinella sp*., *Lecane sp*., *Cephalodella sp*., *Euchlanis sp*.). Zooplankton identified in the 22:14 sample includes: Copepods (*Cyclopoid sp*., *Nauplii sp*.), Rotifers (*Monostyla sp*., *Euchlanis sp*., *Cephalodella sp*., *Gastropus sp*.).

Table A.8 Water quality measurements from sensors placed at the SAC sensing station from 9/18/2007 to 9/19/2007.

Date	Hour	Hydrolab DS5X data sonde #1						Hydrolab DS5X data sonde #2						
		Temperature (°C)	pH	Specific Conductivity (mS/cm)	Turbidity (NTU)	Chlorophyll *a* (µg/L)	Battery Voltage (V)	Temperature (°C)	pH	Specific Conductivity (mS/cm)	Turbidity (NTU)	Dissolved Oxygen (mg/L)	Chlorophyll *a* (µg/L)	Battery Voltage (V)
9/18/2007	10:20:00	18.18	7.98	0.606	4.7	0.11	11.6	18.16	7.81	0.627	7	10.22	0.12	11.4
9/18/2007	10:40:00	18.43	8.03	0.606	4.8	0.15	11.5	18.42	7.91	0.627	6.7	10.53	0.12	11.4
9/18/2007	11:00:00	18.71	8.07	0.606	4.5	0.17	11.5	18.71	7.97	0.627	7.2	10.78	0.12	11.4
9/18/2007	11:20:00	19.05	8.11	0.605	4.4	0.18	11.5	19.05	8.03	0.625	6.4	11.06	0.12	11.4
9/18/2007	11:40:00	19.35	8.14	0.603	4.4	0.17	11.5	19.34	8.07	0.625	6.4	11.27	0.13	11.4
9/18/2007	12:00:00	19.72	8.19	0.603	5.1	0.19	11.5	19.72	8.12	0.624	6.7	11.56	0.13	11.4
9/18/2007	12:20:00	19.99	8.22	0.601	3.5	0.16	11.5	19.99	8.16	0.622	5.6	11.75	0.13	11.4
9/18/2007	12:40:00	20.28	8.25	0.602	3.8	0.22	11.4	20.28	8.19	0.622	5.6	11.83	0.13	11.4
9/18/2007	13:00:00	20.46	8.27	0.6	3.9	0.17	11.4	20.46	8.21	0.622	5.4	11.8	0.13	11.4
9/18/2007	13:20:00	20.83	8.3	0.6	3	0.18	11.4	20.84	8.25	0.621	4.5	12.15	0.13	11.4
9/18/2007	13:40:00	21	8.32	0.599	2.3	0.17	11.4	20.99	8.27	0.62	4.2	12.18	0.13	11.4
9/18/2007	14:00:00	21.25	8.34	0.599	1.8	0.17	11.4	21.26	8.3	0.619	3.8	12.25	0.13	11.4
9/18/2007	14:20:00	21.42	8.35	0.598	1.8	0.14	11.4	21.42	8.31	0.619	3.8	12.18	0.13	11.4
9/18/2007	14:40:00	21.52	8.33	0.598	2	0.15	11.4	21.52	8.31	0.619	3.4	11.97	0.13	11.4
9/18/2007	15:00:00	21.69	8.34	0.598	1.3	0.13	11.4	21.69	8.33	0.618	3.1	12.02	0.12	11.4
9/18/2007	15:20:00	21.71	8.34	0.597	1.1	0.12	11.4	21.7	8.32	0.618	3.1	11.73	0.12	11.4
9/18/2007	15:40:00	21.8	8.34	0.598	1.7	0.11	11.4	21.8	8.32	0.618	3.6	11.61	0.12	11.4
9/18/2007	16:00:00	21.84	8.33	0.599	2.7	0.11	11.4	21.84	8.31	0.619	8.5	11.27	0.12	11.4
9/18/2007	16:20:00	21.85	8.31	0.599	3	0.09	11.4	21.86	8.3	0.62	5.4	10.97	0.12	11.4
9/18/2007	16:40:00	21.85	8.3	0.6	3.7	0.09	11.4	21.86	8.28	0.62	5.1	10.67	0.12	11.4
9/18/2007	17:00:00	21.85	8.28	0.602	3.5	0.1	11.4	21.85	8.27	0.621	16.2	10.44	0.12	11.3
9/18/2007	17:20:00	21.8	8.26	0.601	2.4	0.08	11.4	21.81	8.25	0.622	4.6	10.1	0.12	11.3
9/18/2007	17:40:00	21.72	8.23	0.602	3.1	0.09	11.4	21.72	8.22	0.622	4.6	9.64	0.12	11.3
9/18/2007	18:00:00	21.62	8.19	0.603	3	0.09	11.4	21.62	8.19	0.624	24	9.25	0.12	11.3
9/18/2007	18:20:00	21.53	8.17	0.604	2.7	0.08	11.4	21.53	8.15	0.624	5.5	8.94	2000000	11.3
9/18/2007	18:40:00	21.42	8.13	0.606	5.3	0.09	11.4	21.42	8.12	0.626	7.8	8.59	0.01	11.3
9/18/2007	19:00:00	21.17	8.09	0.603	9.8	0.1	11.4	21.17	8.08	0.623	14.6	8.33	0.12	11.3
9/18/2007	19:20:00	21.02	8.06	0.603	6.2	0.09	11.4	21.03	8.05	0.624	35.1	8.12	0.12	11.3
9/18/2007	19:40:00	20.87	8.04	0.6	7.5	0.1	11.4	20.87	8.02	0.621	13.4	7.97	0.12	11.3
9/18/2007	20:00:00	20.72	8.02	0.602	8.9	0.1	11.4	20.72	8	0.621	10.8	7.87	0.12	11.3
9/18/2007	20:20:00	20.57	8	0.601	11	0.11	11.4	20.57	7.97	0.623	13.1	7.79	0.12	11.3
9/18/2007	20:40:00	20.43	7.97	0.6	13.4	0.1	11.4	20.43	7.94	0.619	12.6	7.71	0.12	11.2
9/18/2007	21:00:00	20.28	7.95	0.599	15.1	0.1	11.3	20.27	7.92	0.619	16.6	7.66	0.12	11.2
9/18/2007	21:20:00	20.13	7.94	0.596	19.4	0.18	11.3	20.13	7.9	0.617	19.9	7.61	0.12	11.2
9/18/2007	21:40:00	20.01	7.92	0.597	22.5	0.1	11.3	20.01	7.88	0.617	23.4	7.58	0.12	11.2
9/18/2007	22:00:00	19.9	7.91	0.598	21.4	0.1	11.3	19.9	7.86	0.618	23.1	7.59	0.12	11.2
9/18/2007	22:20:00	19.79	7.9	0.6	16.6	0.09	11.3	19.78	7.85	0.62	18.4	7.62	0.01	11.2
9/18/2007	22:40:00	19.68	7.9	0.6	22.1	0.1	11.3	19.68	7.83	0.619	23	7.62	0.01	11.2
9/18/2007	23:00:00	19.58	7.89	0.595	35	0.1	11.3	19.57	7.82	0.615	30.6	7.68	0.12	11.2
9/18/2007	23:20:00	19.47	7.89	0.588	64.7	0.13	11.3	19.47	7.81	0.609	51.3	7.73	0.12	11.2
9/19/2007	0:00:00	19.23	7.87	0.58	45.6	0.12	11.3	19.23	7.79	0.599	41.2	7.74	0.12	11.2
9/19/2007	0:20:00	19.14	7.86	0.582	37.8	0.11	11.3	19.13	7.77	0.601	37.7	7.71	0.12	11.2
9/19/2007	0:40:00	19.05	7.85	0.577	45	0.12	11.3	19.04	7.76	0.596	38.8	7.71	0.12	11.2
9/19/2007	1:00:00	18.95	7.83	0.575	41.8	0.13	11.2	18.95	7.73	0.595	58.1	7.62	0.12	11.2
9/19/2007	1:20:00	18.85	7.81	0.572	36.7	0.12	11.2	18.85	7.71	0.592	35	7.58	0.12	11.1
9/19/2007	1:40:00	18.75	7.8	0.571	34.1	0.13	11.2	18.75	7.69	0.591	32.9	7.54	0.12	11.1
9/19/2007	2:00:00	18.64	7.79	0.572	34	0.12	11.2	18.63	7.67	0.591	33.4	7.52	0.12	11.1
9/19/2007	2:20:00	18.52	7.78	0.574	35.9	0.12	11.2	18.52	7.65	0.594	36.3	7.54	0.12	11.1
9/19/2007	2:40:00	18.42	7.78	0.573	34.7	0.12	11.2	18.41	7.64	0.592	33.5	7.57	0.12	11.1
9/19/2007	3:00:00	18.31	7.77	0.573	35.8	0.12	11.2	18.31	7.63	0.592	36	7.6	0.12	11.1
9/19/2007	3:20:00	18.21	7.77	0.574	35.4	0.13	11.2	18.2	7.61	0.592	35.5	7.65	0.12	11.1
9/19/2007	3:40:00	18.1	7.77	0.576	40	0.14	11.2	18.09	7.6	0.595	39.3	7.71	0.12	11.1
9/19/2007	4:00:00	17.99	7.78	0.578	36.8	0.12	11.2	17.98	7.6	0.596	37.2	7.78	0.12	11.1
9/19/2007	4:20:00	17.88	7.78	0.58	34.4	0.12	11.2	17.87	7.59	0.599	33.8	7.85	0.12	11.1
9/19/2007	4:40:00	17.78	7.78	0.583	29.4	0.12	11.1	17.77	7.58	0.602	29.2	7.89	0.12	11.1
9/19/2007	5:00:00	17.69	7.78	0.584	31.5	0.12	11.1	17.68	7.57	0.605	31.1	7.91	0.12	11.1
9/19/2007	5:20:00	17.62	7.78	0.584	26.4	0.13	11.1	17.61	7.57	0.604	28.5	7.95	0.12	11.1
9/19/2007	5:40:00	17.55	7.78	0.584	31.9	0.12	11.1	17.55	7.56	0.604	32.4	7.98	0.12	11.1
9/19/2007	6:00:00	17.49	7.79	0.584	35.9	0.14	11.1	17.48	7.56	0.603	36	8.02	0.12	11.1
9/19/2007	6:20:00	17.43	7.79	0.585	31.5	0.13	11.1	17.43	7.55	0.604	31.9	8.06	0.12	11.1
9/19/2007	6:40:00	17.4	7.79	0.585	28.1	0.13	11.1	17.39	7.55	0.603	28.3	8.09	0.12	11.1
9/19/2007	7:00:00	17.35	7.8	0.584	24.4	0.14	11.1	17.34	7.54	0.603	26.2	8.11	0.12	11.1
9/19/2007	7:20:00	17.28	7.8	0.585	29.2	0.12	11.1	17.28	7.54	0.603	29.7	8.14	0.12	11.1
9/19/2007	7:40:00	17.23	7.8	0.584	27	0.13	11.1	17.23	7.53	0.603	26.7	8.2	0.12	11.1
9/19/2007	8:00:00	17.18	7.81	0.583	20.2	0.13	11.1	17.18	7.53	0.603	21.5	8.26	0.12	11.1
9/19/2007	8:20:00	17.16	7.81	0.584	15.8	0.13	11.1	17.15	7.53	0.603	18	8.37	0.12	11.1
9/19/2007	8:40:00	17.18	7.83	0.583	13.7	0.15	11.1	17.18	7.54	0.603	15.5	8.59	0.12	11.1
9/19/2007	9:00:00	17.21	7.83	0.584	13.8	0.17	11.1	17.2	7.53	0.603	15.2	8.73	0.12	11.1
9/19/2007	9:20:00	17.29	7.84	0.585	12.1	0.14	11.1	17.26	7.55	0.605	14.6	9.01	0.12	11.1
9/19/2007	9:40:00	17.41	7.87	0.585	11.7	0.16	11.1	17.39	7.58	0.605	13.6	9.39	0.12	11.1
9/19/2007	10:00:00	17.53	7.9	0.585	9.3	0.16	11.1	17.49	7.61	0.605	11.3	9.68	0.12	11.1
9/19/2007	10:20:00	17.59	7.92	0.586	8.3	0.2	11.1	17.58	7.63	0.605	10.8	9.9	0.13	11.1
9/19/2007	10:40:00	17.69	7.95	0.586	8.2	0.22	11.1	17.68	7.66	0.605	10.1	10.13	0.13	11.1
9/19/2007	11:00:00	17.85	7.98	0.585	7	0.19	11.1	17.84	7.69	0.605	9.3	10.45	0.12	11
9/19/2007	11:20:00	18.06	8.01	0.586	5.8	0.16	11.1	18.02	7.73	0.605	8.3	10.75	0.12	11
9/19/2007	11:40:00	18.22	8.04	0.588	4.8	0.17	11.1	18.21	7.77	0.606	7.4	11.05	0.12	11
9/19/2007	12:00:00	18.44	8.06	0.588	4.5	0.19	11.1	18.43	7.81	0.608	6.9	11.23	0.12	11
9/19/2007	12:20:00	18.68	8.09	0.588	5.5	0.17	11.1	18.66	7.84	0.607	7.8	11.49	0.13	11
9/19/2007	12:40:00	19.03	8.12	0.588	4.8	0.14	11.1	18.94	7.88	0.608	6.9	11.6	0.12	11
9/19/2007	13:00:00	19.32	8.14	0.589	4	0.14	11.1	19.23	7.91	0.609	6.5	11.7	0.12	11
9/19/2007	13:20:00	19.58	8.14	0.59	4.3	0.16	11.1	19.5	7.94	0.611	6	11.68	0.12	11
9/19/2007	13:40:00	19.87	8.15	0.592	5.1	0.17	11.1	19.82	7.96	0.612	7.3	11.66	0.13	11
9/19/2007	14:00:00	20.09	8.16	0.592	3.4	0.18	11.1	20.03	7.98	0.612	5.6	11.59	0.13	11

2008 Water Quality Data

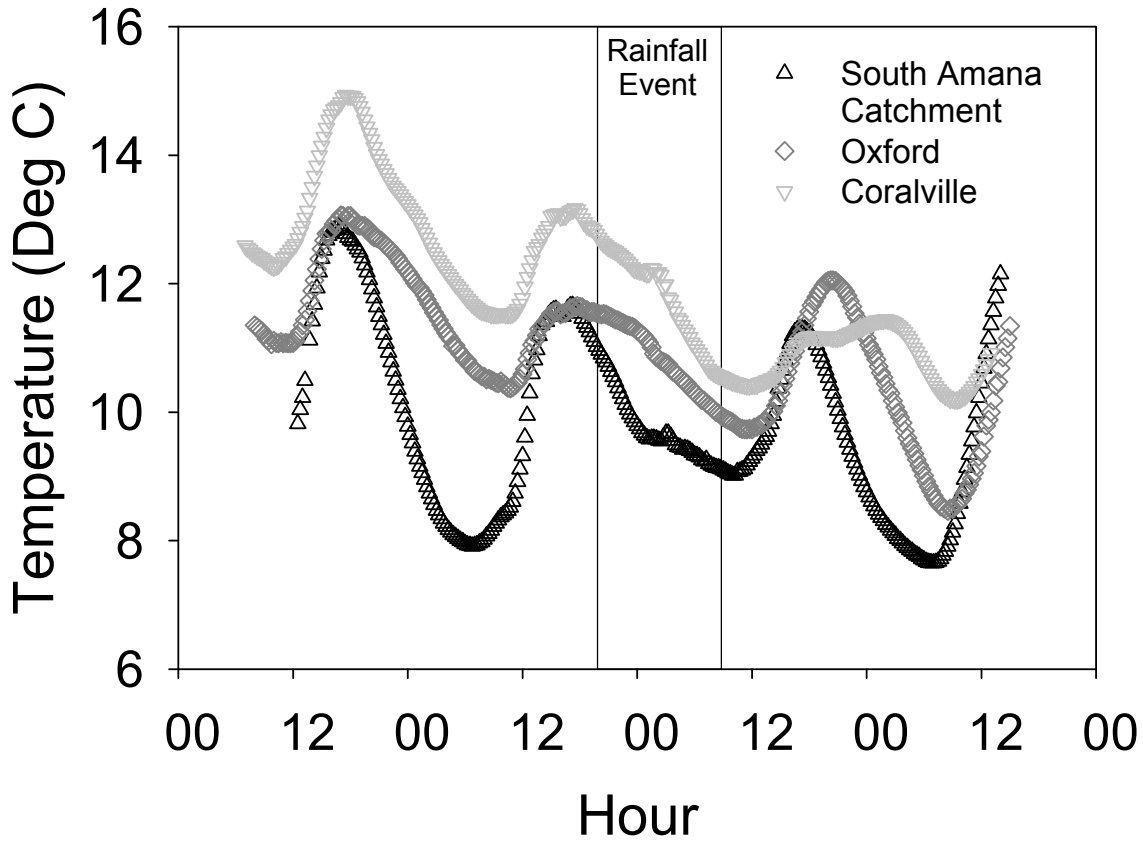

Figure A.13 Temperature measurements collected at the SAC, Oxford and Coralville sensing stations from 5/9/2008 to 5/12/2008.

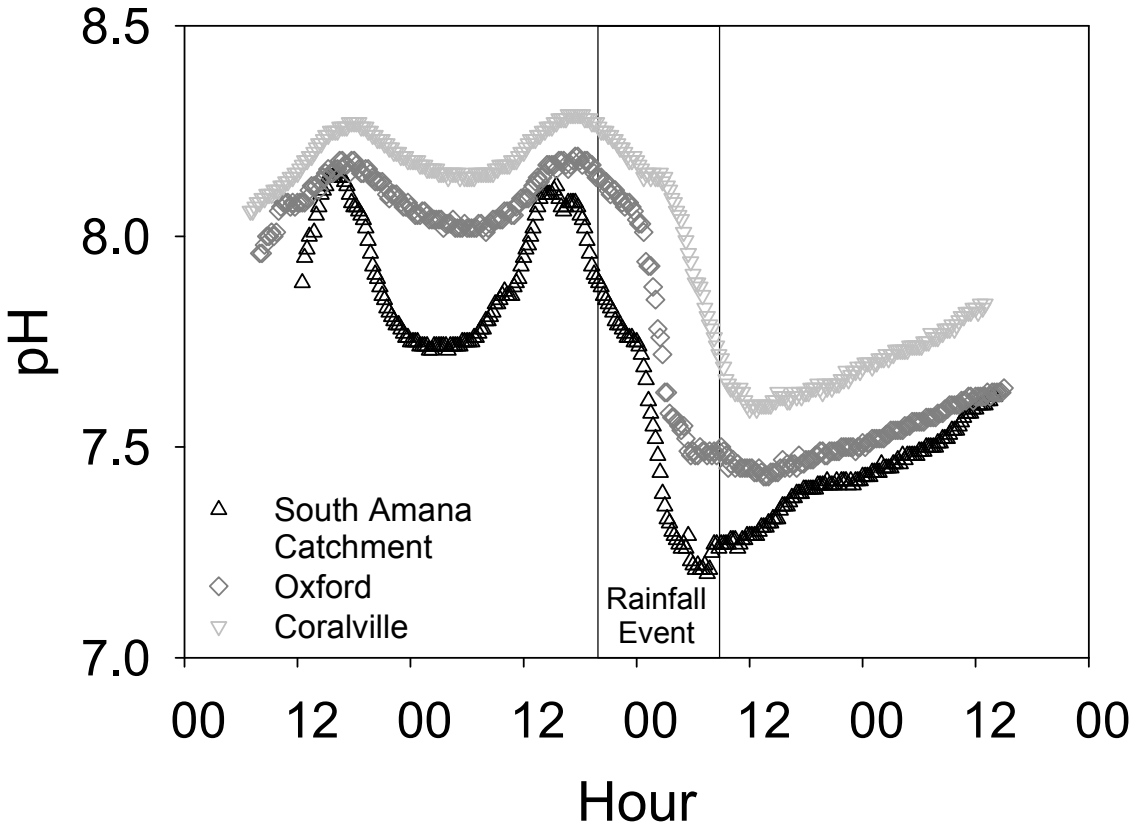

Figure A.14 pH measurements collected at the SAC, Oxford and Coralville sensing stations from 5/9/2008 to 5/12/2008.

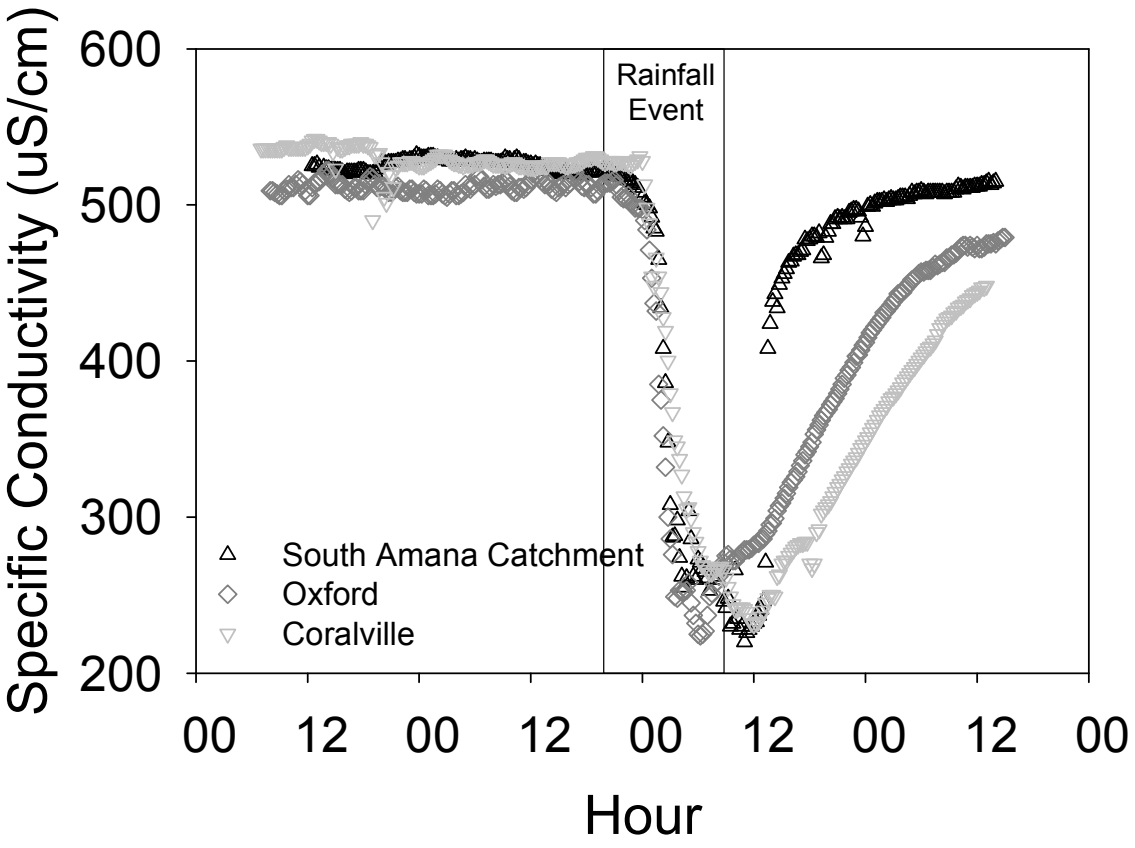

Figure A.15 Specific conductivity measurements collected at the SAC, Oxford and Coralville sensing stations from 5/9/2008 to 5/12/2008.

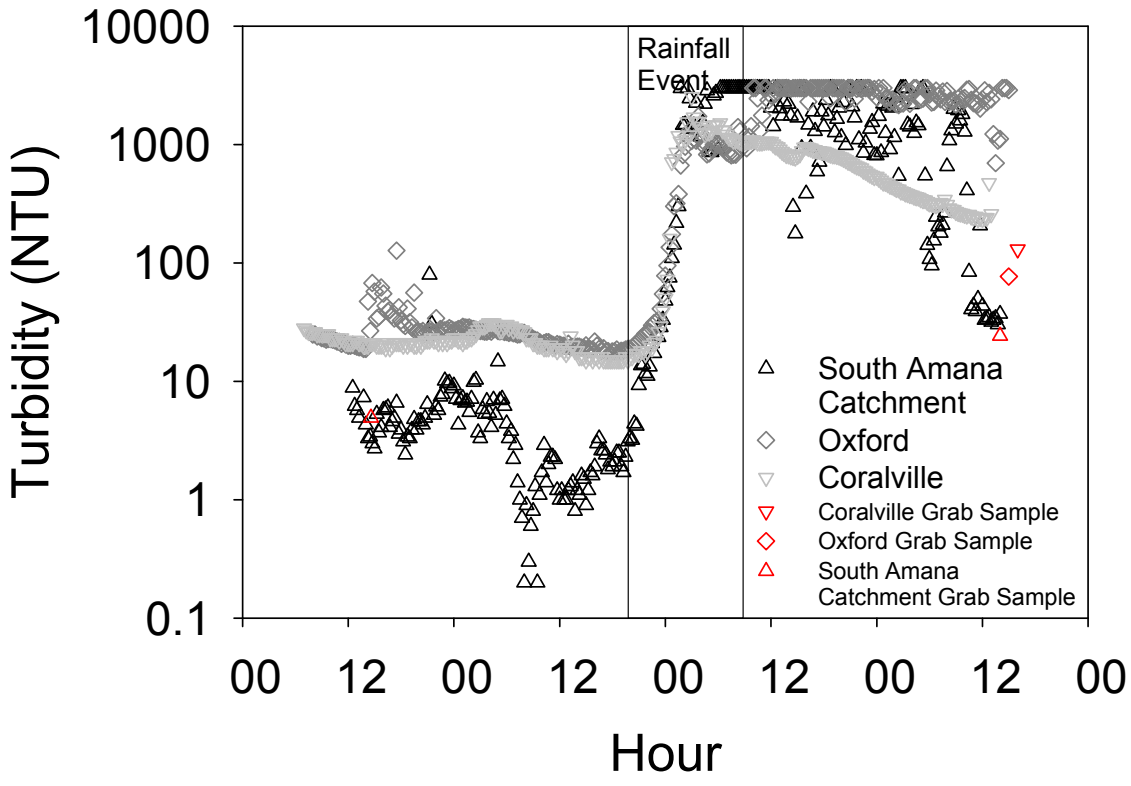

Figure A.16 Turbidity measurements collected at the SAC, Oxford and Coralville sensing stations from 5/9/2008 to 5/12/2008.

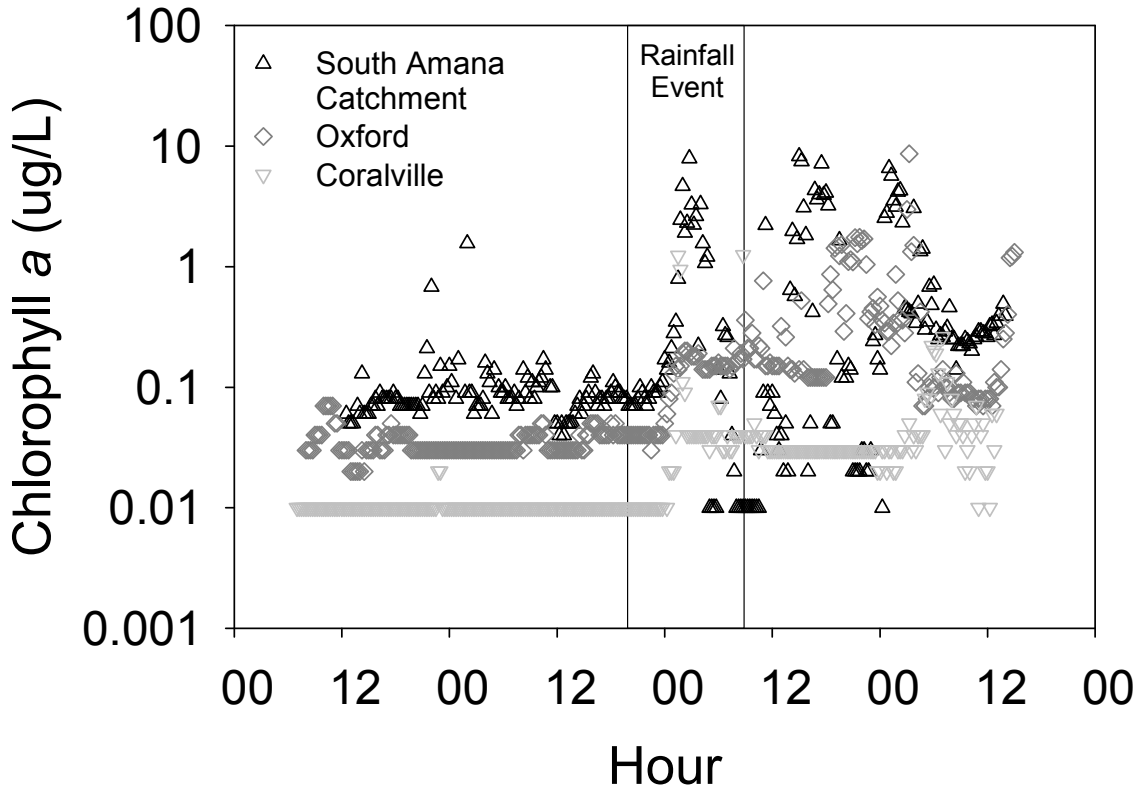

Figure A.17 Chlorophyll *a* measurements collected at the SAC, Oxford and Coralville sensing stations from 5/9/2008 to 5/12/2008.

APPENDIX B:

QUAL2K MODEL INPUT AND PARAMETER SETTINGS

Table B.1 Physical parameters of Clear Creek reaches modeled in QUAL2K.

Reach	Reach Name	Reach Number	Upstream Location (km)	Downstream Location (km)	Element Number	Upstream Elevation (m)	Downstream Elevation (m)	Channel Bottom Width (m)	k_a (day^{-1})
R1	SAC	1	32.61	32.15	3	234.7	230.7	3.0	11.2
R2	T1	2	0.1	0	1	234.7	230.7	2.1	11.2
R3		3	32.15	30.09	3	230.7	228.9	4.0	10.9
R4	T2	4	0.1	0	1	232.0	228.9	3.0	11.2
R5		5	30.09	26.61	4	228.9	221.7	6.4	10.2
R6	T3	6	0.1	0	1	225.6	221.7	2.9	11.2
R7		7	26.61	25.90	2	221.7	220.1	7.6	9.7
R8	T4	8	0.1	0	1	225.5	220.1	2.5	11.2
R9		9	25.90	22.79	4	220.1	219.3	7.0	9.2
R10	T5	10	0.1	0	1	222.5	219.3	2.4	11.2
R11		11	22.79	19.75	4	219.3	218.1	8.8	8.5
R12	T6	12	0.1	0	1	219.5	218.1	2.1	11.2
R13		13	19.75	19.50	1	218.1	218.0	6.4	8.1
R14	T7	14	0.1	0	1	219.8	218.0	2.5	11.2
R15		15	19.50	16.92	4	218.0	216.5	8.6	7.7
R16	T8	16	0.1	0	1	216.8	216.5	2.1	11.2
R17		17	16.92	16.52	1	216.5	215.9	8.9	7.4
R18	T9	18	0.1	0	1	216.2	215.9	2.2	11.2
R19		19	16.52	15.28	2	215.9	213.4	9.4	7.2
R20	T10	20	0.1	0	1	217.9	213.4	2.1	11.2
R21		21	15.28	12.32	4	213.4	210.1	9.5	7.0
R22	T11	22	0.1	0	1	213.7	210.1	3.1	11.2
R23		23	12.32	4.76	7	210.1	203.8	11.0	6.4
R24	T12	24	0.1	0	1	204.9	203.8	2.2	11.2
R25		25	4.76	2.20	4	203.8	201.3	11.0	5.9
R26	T13	26	0.1	0	1	201.4	201.3	3.1	11.2
R27		27	2.20	1.47	2	201.3	201.1	13.5	5.8
R28	T14	28	0.1	0	1	201.1	201.1	2.1	11.2
R29		29	1.47	0	2	201.1	200.8	13.5	5.7

Table B.2 Temperature, specific conductivity, DO, and pH boundary conditions for QUAL2K modeling of Clear Creek at the SAC sensing station and all tributaries (T1-T14) based on instream sensor measurements collected at the SAC sensing station.

Time	Temperature (°C)	Specific Conductivity (μmhos cm^{-1})	DO (mg L^{-1})	pH
0:00	9.78	531	10.14	7.75
1:00	9.27	531	10.19	7.74
2:00	8.84	530	10.28	7.73
3:00	8.47	529	10.41	7.74
4:00	8.22	529	10.53	7.73
5:00	8.06	530	10.60	7.74
6:00	7.95	529	10.64	7.75
7:00	7.92	528	10.79	7.76
8:00	8.02	527	11.24	7.80
9:00	8.22	528	11.72	7.84
10:00	8.40	527	12.01	7.87
11:00	8.61	526	12.28	7.88
12:00	9.32	526	13.15	7.95
13:00	10.23	526	13.69	7.97
14:00	11.42	523	13.95	8.05
15:00	12.39	522	13.90	8.12
16:00	12.80	520	13.67	8.14
17:00	12.87	521	13.36	8.13
18:00	12.68	522	12.87	8.07
19:00	12.49	520	12.43	8.04
20:00	12.06	527	11.57	7.93
21:00	11.49	527	10.81	7.86
22:00	10.93	528	10.41	7.81
23:00	10.35	529	10.21	7.78

Table B.3 Inorganic suspended solids and detritus boundary conditions for QUAL2K modeling of Clear Creek at the SAC sensing station and all tributaries (T1-T14).

Time	SAC, T1-T3, T11-T14		T4-T10	
	Inorganic Suspended Solids (mg L^{-1})	Detritus (mg L^{-1})	Inorganic Suspended Solids (mg L^{-1})	Detritus (mg L^{-1})
0:00	12.82	3.20	256.36	64.86
1:00	9.44	2.36	188.71	47.74
2:00	9.27	2.32	185.44	46.92
3:00	3.56	0.89	71.16	18.00
4:00	6.59	1.65	131.71	33.32
5:00	23.03	5.76	460.54	116.52
6:00	5.10	1.27	101.96	25.80
7:00	3.03	0.76	60.55	15.32
8:00	0.11	0.03	2.14	0.54
9:00	0.61	0.15	12.11	3.06
10:00	1.55	0.39	31.06	7.86
11:00	2.27	0.57	45.32	11.47
12:00	0.80	0.20	16.00	4.05
13:00	7.05	1.76	140.92	35.65
14:00	4.95	1.24	99.07	25.07
15:00	2.77	0.69	55.38	14.01
16:00	7.05	1.76	140.92	35.65
17:00	5.39	1.35	107.79	27.27
18:00	4.38	1.10	87.69	22.19
19:00	3.56	0.89	71.16	18.00
20:00	5.39	1.35	107.79	27.27
21:00	8.14	2.04	162.87	41.21
22:00	7.67	1.92	153.38	38.81
23:00	14.40	3.60	288.09	72.89

Table B.4 Nitrate boundary conditions and assumptions for QUAL2K modeling of Clear Creek at the SAC sensing station and all tributaries (T1-T14).

Boundary	Nitrate as N (mg L^{-1})	Assumption
SAC	13.0	Based on UHL measurement at the SAC sensing station
T1	13.0	Estimated based on UHL measurement at SAC sensing station
T2	19.0	Based on UHL measurement in the tributary
T3	13.0	Based on UHL measurement in the tributary
T4	3.4	Calibration of QUAL2K to UHL measurement at x = 19.7 km
T5	3.4	Calibration of QUAL2K to UHL measurement at x = 19.7 km
T6	3.4	Calibration of QUAL2K to UHL measurement at x = 19.7 km
T7	2.9	Based on UHL measurement in the tributary
T8	5.7	Average of UHL measurements in T7,T11, & T13
T9	5.7	Average of UHL measurements in T7,T11, & T13
T10	5.7	Average of UHL measurements in T7,T11, & T13
T11	6.8	Based on UHL measurement in the tributary
T12	5.7	Average of UHL measurements in T7,T11, & T13
T13	7.3	Based on UHL measurement in the tributary
T14	5.7	Average of UHL measurements in T7,T11, & T13

Table B.5 Stoichiometry, phytoplankton and bottom algae rates prescribed for QUAL2K modeling of Clear Creek.

Parameter	Value	Units	Reference
Stoichiometry			
Carbon	40	gC	Chapra (1997)
Nitrogen	7.2	gN	Chapra (1997)
Phosphorus	1	gP	Chapra (1997)
Dry weight	100	gD	Chapra (1997)
Chlorophyll	1	gA	Chapra (1997)
Phytoplankton			
Max Growth rate	0	d^{-1}	Schnoor (1996) & Chapra (1997)
Temp correction	1.066		Schnoor (1996) & Chapra (1997)
Respiration rate	0.2	d^{-1}	Chapra et al. (2006)
Temp correction	1.08		Bowie et al. (1985)
Death rate	0.2	d^{-1}	Chapra et al. (2006)
Temp correction	1.07		Chapra et al. (2006)
Nitrogen half sat constant	25	ugN L^{-1}	Chapra (1997)
Phosphorus half sat constant	5	ugP L^{-1}	Chapra (1997)
Inorganic carbon half sat constant	0.000013	moles L^{-1}	Chapra (1997)
Light model	Half saturation		
Light constant	250	langleys d^{-1}	Chapra (1997)
Ammonia preference	25	ugN L^{-1}	Chapra et al. (2006)
Settling velocity	0.09	m d^{-1}	Chapra (1997)
Bottom Algae			
Growth model	Zero-order		
Max Growth rate	640	mgA m^{-2} d^{-1}	Briggs (1996)
Temp correction	1.066		Schnoor (1996)
Respiration rate	0.15	d^{-1}	Chapra (1997)
Temp correction	1.08		Bowie et al. (1985)
Excretion rate	0.2	d^{-1}	Chapra (1997)
Temp correction	1.08		Chapra (1997)
Death rate	0.1	d^{-1}	Schnoor (1996)
Temp correction	1.07		Chapra et al. (2006)
External nitrogen half sat constant	300	ugN L^{-1}	Chapra et al. (2006)
External phosphorus half sat constant	100	ugP L^{-1}	Chapra et al. (2006)
Inorganic carbon half sat constant	0.000013	moles L^{-1}	Chapra et al. (2006)
Light model	Half saturation		
Light constant	250	langleys d^{-1}	Chapra (1997)
Ammonia preference	25	ugN L^{-1}	Chapra et al. (2006)
Subsistence quota for nitrogen	0.72	mgN mgA^{-1}	Chapra et al. (2006)
Subsistence quota for phosphorus	0.1	mgP mgA^{-1}	Chapra et al. (2006)
Maximum uptake rate for nitrogen	72	mgN mgA^{-1} d^{-1}	Chapra et al. (2006)
Maximum uptake rate for phosphorus	5	mgP mgA^{-1} d^{-1}	Chapra et al. (2006)
Internal nitrogen half sat constant	0.9	mgN mgA^{-1}	Chapra et al. (2006)
Internal phosphorus half sat constant	0.13	mgP mgA^{-1}	Chapra et al. (2006)

Table B.6 Chemical and suspended solids rates prescribed for QUAL2K modeling of Clear Creek.

Parameter	Value	Units	Reference
Inorganic Suspended Solids			
Settling velocity	1.9	m d^{-1}	Chapter 5
Organic N			
Hydrolysis	0.03	d^{-1}	Schnoor (1996)
Temp correction	1.05		Bowie et al. (1985)
Settling velocity	1.9	m d^{-1}	Chapter 5
Ammonium			
Nitrification	0.75	d^{-1}	Schnoor (1996)
Temp correction	1.08		Schnoor (1996)
Nitrate			
Denitrification	0	d^{-1}	Chapra et al. (2006)
Temp correction	1.07		Chapra et al. (2006)
Sed. denitrification transfer coefficient	0	m d^{-1}	Chapra et al. (2006)
Temp correction	1.07		Chapra et al. (2006)
Organic P			
Hydrolysis	0.2	d^{-1}	Schnoor (1996)
Temp correction	1.05		Bowie et al. (1985)
Settling velocity	1.9	m d^{-1}	Chapter 5
Orthophosphate			
Settling velocity	1.9	m d^{-1}	Chapter 5
Inorganic P sorption coefficient	0	L mgD^{-1}	Chapra et al. (2006)
Sed P oxygen attenuation half sat constant	0.05	mgO_2 L^{-1}	Chapra et al. (2006)
Detritus (POM)			
Dissolution rate	0.1	d^{-1}	Schnoor (1996)
Temp correction	1.03		Bowie et al. (1985)
Fraction of dissolution to fast CBOD	1.0		Chapra et al. (2006)
Settling velocity	1.9	m d^{-1}	Chapter 5
pH			
Partial pressure of carbon dioxide	388.5	ppm	ESRL (2009)

Table B.7 Oxygen and CBOD rates prescribed for QUAL2K modeling of Clear Creek.

Parameter	Value	Units	Reference
Oxygen			
O_2 for carbon oxidation	2.69	$gO_2\,gC^{-1}$	Chapra et al. (2006)
O_2 for NH_4 nitrification	4.57	$gO_2\,gN^{-1}$	Chapra et al. (2006)
Oxygen inhib model CBOD oxidation	Exponential		
Oxygen inhib parameter CBOD oxidation	0.6	$L\,mgO_2^{-1}$	Chapra et al. (2006)
Oxygen inhib model nitrification	Exponential		
Oxygen inhib parameter nitrification	0.6	$L\,mgO_2^{-1}$	Chapra (1997)
Oxygen enhance model denitrification	Exponential		
Oxygen enhance parameter denitrification	0.6	$L\,mgO_2^{-1}$	Chapra (1997)
Oxygen inhib model phyto resp	Exponential		
Oxygen inhib parameter phyto resp	0.6	$L\,mgO_2^{-1}$	Chapra et al. (2006)
Oxygen enhance model bot alg resp	Exponential		
Oxygen enhance parameter bot alg resp	0.6	$L\,mgO_2^{-1}$	Chapra et al. (2006)
Slow CBOD			
Hydrolysis rate	0.1	d^{-1}	Schnoor (1996)
Temp correction	1.03		Bowie et al. (1985)
Oxidation rate	0	d^{-1}	Chapra et al. (2006)
Fast CBOD			
Oxidation rate	0.2	d^{-1}	Schnoor (1996)
Temp correction	1.048		Schnoor (1996)

Table B.8 Air temperature, dew point, and wind speed input for QUAL2K modeling of Clear Creek.

Time	Air Temperature (° C)	Dew Point (° C)	Wind Speed (m s^{-1})
0:00	11.7	1.7	15.7
1:00	11.6	1.7	14.5
2:00	10.8	1.8	5.8
3:00	8.8	2.9	0.0
4:00	8.4	3.4	0.0
5:00	9.4	3.9	1.8
6:00	9.5	3.8	13.1
7:00	10.1	2.9	12.4
8:00	10.7	3.3	17.4
9:00	11.3	3.3	1.8
10:00	12.9	3.3	12.5
11:00	14.0	3.4	7.3
12:00	14.7	4.0	11.8
13:00	16.8	4.5	15.4
14:00	17.9	5.1	13.7
15:00	18.2	5.4	15.4
16:00	17.8	4.3	13.4
17:00	17.7	4.0	13.1
18:00	16.6	5.1	9.7
19:00	15.4	5.7	1.8
20:00	13.8	6.1	11.6
21:00	12.4	6.1	0.0
22:00	10.0	6.1	0.0
23:00	9.9	6.1	0.0

Data Source: NCDC 2008

Table B.9 Light parameters and surface heat transfer models prescribed for QUAL2K modeling of Clear Creek.

Parameter	Value	Unit	Reference
Photosynthetically Available Radiation	0.47		Chapra et al. (2006)
Background light extinction	0.2	m^{-1}	Chapra et al. (2006)
Linear chlorophyll light extinction	0.0088	$L^1\ gA^{-1}\ m^{-1}$	Chapra et al. (2006)
Nonlinear chlorophyll light extinction	0.054	$(L/ugA)^{2/3}\ m^{-1}$	Chapra et al. (2006)
ISS light extinction	0.052	$L^1\ gA^{-1}\ m^{-1}$	Chapra et al. (2006)
Detritus light extinction	0.174	$L^1\ gA^{-1}\ m^{-1}$	Chapra et al. (2006)
Atmospheric attenuation model for solar	Ryan-Stolzenbach		
Atmospheric transmission coefficient (0.70-0.91, default 0.8)	0.91		Calibration of model to temperature data
Atmospheric longwave emissivity model	Brutsaert		Chapra et al. (2006)
Wind speed function for evaporation and air convection/conduction	Adams 2		Chapra et al. (2006)
Sediment thermal thickness	15	cm	Field Measurements
Sediment thermal diffusivity	0.0064	$cm^2\ s^{-1}$	Chapra et al. (2006)
Sediment density	2.6	$g\ cm^{-3}$	Das (2000)
Water density	1	$g\ cm^{-3}$	Chapra et al. (2006)
Sediment heat capacity	0.4	$cal\ g^{-1}\ °C^{-1}$	Chapra et al. (2006)
Water heat capacity	1	$cal\ g^{-1}\ °C^{-1}$	Chapra et al. (2006)
Compute SOD and nutrient fluxes	No		

Table B.10 Creek shading inputs for each hour throughout the modeling period for QUAL2K modeling of Clear Creek. Shading values were determined by calibrating QUAL2K temperature results to instream sensor measurements.

Reach Description	Reach Number(s)	Creek Shading (%)	
		00:00 - 13:00, 20:00 -23:00	14:00 - 19:00
SAC sensing station	1	0%	30%
Clear Creek main channel above Oxford	3,5,7,9,11,13,15,17	0%	30%
Clear Creek main channel below Oxford	19,21,23,25,27,29	0%	0%
All tributaries (T1-T14)	2,4,6,8,10,12,14, 16,18,20,22,24,26,28	0%	30%

REFERENCES

Abaci, O. and Papanicolaou, A. N. (2009). "Long-Term Effects of Management Practices on Water-Driven Soil Erosion in an Intense Agricultural Sub-watershed: Monitoring and Modeling." *Hydrol. Process.*, In Press.

Alcock, S. J. (2004). "New developments in sensor technology for water quality surveillance and early warning." *Water Sci. Technol.*, 50(11), 1-6.

American Public Health Association (APHA) (1989). *Standard Methods for the Examination of Water and Wastewater, 17th Ed.,* L. S. Clesceri, A. E. Greenberg, and R. R. Trussell, eds., Baltimore, Maryland.

American Public Health Association (APHA) (1998). *Standard Methods for the Examination of Water and Wastewater, 20th Ed.*, American Public Health Association, Washington D.C.

Astronomical Applications Department (AAD) (2008). "Sun or Moon Rise/Set Table for One Year", <http://aa.usno.navy.mil/data/docs/RS_OneYear.php> (Feb. 2, 2008).

Becker, G. C. (1983). *Fishes of Wisconsin*, The University of Wisconsin Press, Madison, Wisconsin.

Beyer, P.(2008). "Analysis of Bias and Sources of Variance for Volunteer Water Quality Data" MS thesis, Univ of Iowa, Iowa City, IA.

Borah, D. K., Yagow, G., Saleh, A., Barnes, P. L., Rosenthal, W., Krug, E. C., and Hauck, L. M. (2006). "Sediment and nutrient modeling for TMDL development and implementation." *T. ASABE*, 49(4), 967-986.

Bott, T. L., Brock, J. T., Dunn, C. S., Naiman, R. J., Ovink, R. W., and Petersen, R. C. (1985). "Benthic community metabolism in four temperate stream systems: An inter-biome comparison and evaluation of the river continuum concept." *Hydrobiologia*, 123, 3-45.

Bowie, G.L., Mills, W.B., Porcella D.B, Campbell, C.L., Pagenkopf, J.R., Rupp, G.L., Johnson, K.M., Chan, P.W.H., Gherini, S.A., and Chamberlin, C.E. (1985). *Rates, Constants, and Kinetic Formulations in Surface Water Modeling (2nd Ed.)*, US EPA, EPA/600/3-85/040.

Boyacioglu, H. and Alpaslan, M. N. (2008). "Total maximum daily load (TMDL) based sustainable basin growth and management strategy." *Environ. Monit. Assess.*, 146, 411-421.

Braig, E. C. and Johnson, D. L. (2003). "Impact of black bullhead (*Ameiurus melas*) on turbidity in a diked wetland," *Hydrobiologia*, 490, 11-21.

Breitburg, D. (2002). "Effects of hypoxia, and the balance between hypoxia and enrichment, on coastal fishes and fisheries." *Estuaries*, 25(4B), 767-781.

Briggs, B. J. F. (1996). "Patterns in Benthic Algae of Streams." *Algal Ecology* , R. J. Stevenson, M. L. Bothwell, and R. L. Lowe, eds., Academic Press, San Diego, CA, 31-56.

Brown, L. C., and Barnwell, T. O. (1987). *The Enhanced Stream Water Quality Models QUAL2E and QUAL2E-UNCAS: Documentation and User Manual*, US EPA/600/3-87/007, May 1987, 127 p.

Butcher, J. B., and Covington, S. (1995). "Dissolved-oxygen analysis with temperature dependence." *J. Environ. Eng.*, 121 (10), 756-759.

Campbell Scientific, Inc (2009). "Downloads: Download the Latest Software and Operating System Upgrades", < http://www.campbellsci.com/downloads> (June 17, 2009).

Capodaglio, A. G., Boguniewicz, J., Llorens, E., Salerno, F., Copetti, D., Legnani, E., Buraschi, E., and Tartari, G. (2005). "Integrated lake/cathment approach as a basis for the implementation of the WFD in the Lake Pusiano watershed." *River Basin Management Lawson: progress towards implementation of the European Water Framework Directive*, J. Lawson, ed., Institution of Civil Engineers, London, 77-86.

Chapra S. C. (1997). *Surface water-quality modeling*, McGraw-Hill, New York.

Chapra, S. C., and Di Toro, D. M. (1991). "Delta method for estimating primary production, respiration, and reaeration in streams." *J. Environ. Eng.*, 117 (5), 640-655.

Chapra, S. C., Pelletier, G. J. and Tao, H. (2006). *QUAL2K: A Modeling Framework for Simulating River and Stream Water Quality, Version 2.04: Documentation and Users Manual,* Civil And Environmental Engineering Dept., Tufts University, Medford, MA.

Chen, C. F. and Ma, H. W. (2008). "The uncertainty effects of design flow on water quality management." *Environ*. *Monit*. *Assess*., 144, 81-91.

Cheng, H. G., Ouyang, W., Hao, F. H., Ren, X. Y., and Yang, S. T. (2007). "The non-point source pollution in livestock-breeding areas of the Heihe River basin in Yellow River." *Stoch. Env. Res. Risk A.*, 21(3), 213-221.

Chong, C. Y. and Kumar, S. P. (2003). "Sensor Networks: Evolution, Opportunities, and Challenges." *Proc. of the IEEE,* 91(8), 1247-1256.

Christensen, J. H., Hewitson B., Busuioc, A., Chen, A., Gao, X., Held, I., Jones R., Kolli, R. K., Kwon, W. -T., Laprise, R., Magaña Rueda, V., Mearns, L., Menéndez, C. G., Räisänen, J., Rinke, A., Sarr, A., and Whetton, P., (2007). *Regional Climate Projections. In: Climate Change 2007: The Physical Science Basis. Contribution of Working Group I to the Fourth Assessment Report of the Intergovernmental Panel on Climate Change*, S. Solomon, D. Qin, M. Manning, Z. Chen, M. Marquis, K. B. Averyt, M. Tignor, and H. L. Miller, eds., Cambridge University Press, Cambridge, United Kingdom and New York, NY, USA.

Christensen, V. G., Jian, X., and Ziegler, A. C. (2000). *Regression analysis and real-time water-quality monitoring to estimate constituent concentrations, loads and yields in the Little Arkansas River, South-Central Kansas, 1995-99*, U.S. Geol. Surv. Water-Resour. Invest. Rep. 00-4126, 36 p.

Coats, R., Collins, L., Florsheim, J., and Kaufman, D. (1985) "Channel Change, Sediment Transport, and Fish Habitat in a Coastal Stream: Effects of an Extreme Event." *Environ. Manage.* 9, 35-48.

Colt J. (1984). *Computation of dissolved gas concentrations in water as functions of temperature, salinity, and pressure*, American Fisheries Society, Bethesda, MD.

Cox, B. A. (2003). "A review of dissolved oxygen modelling techniques for lowland rivers." *Sci. Total Environ.*, 314-316, 303-334.

Crowe, C. T., Elger, D. F., and Roberson, J. A. (2001). *Engineering Fluid Mechanics, 7th Ed.,* John Wiley & Sons, Inc., New York.

Dalzell, B. J., Filley, T. R., and Harbor, J. M. (2007). "The role of hydrology in annual organic carbon loads and terrestrial organic matter export from a midwestern agricultural watershed." *Geochim. Cosmochim. Acta* 71, 1448-1462.

Das, B. M. (2000). *Fundamentals of Geotechnical Engineering*, Brooks/Cole, Pacific Grove, CA.

Davies-Colley R. J., Hickey C. W., Quinn, J. M, and Ryan, P. A. (1992). "Effects of clay discharges on streams 1. Optical-properties and epilithon." *Hydrobiologia*, 248, 215-234.

DeNicola, D. M. (1996). "Periphyton responses to temperature at different ecological levels." *Algal Ecology* , R. J. Stevenson, M. L. Bothwell, and R. L. Lowe, eds., Academic Press, San Diego, CA, 149-181.

Diaz, R. J., and Solow, A. (1999). "Ecological and Economic Consequences of Hypoxia: Topic 2 Report for the Integrated Assessment of Hypoxia in the Gulf of Mexico" *NOAA Coastal Ocean Program Decision Analysis Series No. 16.* NOAA Coastal Ocean Program, Silver Spring, MD. 45 pp.

Earth System Research Laboratory (ESRL) (2009). "Trends in Carbon Dioxide." <http://www.esrl.noaa.gov/gmd/ccgg/trends/> (June 6, 2009).

Elmore, H. L. and West, W. F. (1961). "Effect of temperature on stream reaeration." *J. Sanit. Eng. Div.-ASCE*, 87(SA6), 59-72.

Feth, J. H. (1981). "Chloride in natural continental water – a review." *U.S. Geological Survey Water-Supply Paper* 2176, 30 p.

Finlayson, B. L. (1985). "Field calibration of a recording turbidity meter." *Catena*, 12(2-3), 141-147.

Gassman, P. W., Reyes, M. R., Green, C. H., and Arnold, J. G. (2007). "The Soil and Water Assessment Tool: Historical Development, Applications, and Future Research Directions." *T. ASABE*, 50(4), 1211-1250.

Gillain, S. (2005). "Diel turbidity fluctuations in streams in Gwinnett County, Georgia." *Proc., 2005 Georgia Water Resources Conference,* held April 25-27, 2005, at the University of Georgia. Kathryn J. Hatcher, ed., Institute of Ecology, The University of Georgia, Athens, GA.

Gippel, C. J. (1989). "The use of turbidimeters in suspended sediment research." *Hydrobiologia*, 176/177, 465-480.

Gippel, C. J. (1995). "Potential of turbidity monitoring for measuring the transport of suspended solids in streams." *Hydrol. Process.*, 9, 83-97.

Goolsby, D. A., Battaglin, W. A., Aulenbach, B. T., and Hooper, R. P. (2001). "Nitrogen input to the Gulf of Mexico." *J. Environ. Qual.*, 30(2), 329-336.

Goolsby, D. A., Battaglin, W. A., Lawrence, G. B., Artz, R. S., Aulenbach, B. T., Hooper, R. P., Keeney, D. R., and Stensland, G. J. (1999). *Flux and Sources of Nutrients in the Mississippi-Atchafalaya River Basin: Topic 3 Report for the Integrated Assessment on Hypoxia in the Gulf of Mexico*, *NOAA Coastal Ocean Program Decision Analysis Series No. 17.* NOAA Coastal Ocean Program, Silver Spring, MD. 130 pp.

Gray, J. S., Wu, R. S. S., and Or, Y. Y. (2002). "Effects of hypoxia and organic enrichment on the coastal marine environment." *Mar. Ecol. Prog. Ser.*, 238, 249-279.

Grayson, R. B., Finlayson, B. L., Gippel, C. J., and Hart, B. T. (1996). "The Potential of Field Turbidity Measurements for the Computation of Total Phosphorus and Suspended Solids Loads." *J. Environ. Manage.*, 47, 257-267.

Hach Environmental. (2005). *Hydrolab® DS5X, DS5, and MS5 Water Quality Multiprobes: User Manual*, Hach Company, Colorado.

Hamukuaya, H., O'Toole, M. J., and Woodhead, P. M. J. (1998). "Observations of severe hypoxia and offshore displacement of Cape hake over the Namibian shelf in 1994." *S. Afr. J. Mar. Sci./S.-Afr. Tydskr. Seewet.*, 19, 57-59.

Handler, N. B., Payran, A., Higgins, C. P., Luthy, R. G., and Boehm, A. B. (2006). "Human development is linked to multiple water body impairments along the California coast." *Est. Coast.*, 29(5), 860-870.

Harter, S. K. and Mitsch, W. J. (2003). "Patterns of Short-Term Sedimentation in a Freshwater Created Marsh." *J. Environ. Qual.*, 32, 325-334.

Herlihy, A. T., J. L. Stoddard, and C. B. Johnson. (1998). "The relationship between stream chemistry and watershed land cover data in the Mid-Atlantic region, U.S." *Water Air Soil Poll.*, 105, 377-386.

Hofmann, B. S., Brouder, S. M., and Turco, R. F. (2004). "Tile spacing impacts on Zea mays L. yield and drainage water nitrate load." *Ecol. Eng.*, 23(4-5), 251-267.

Hornberger, G. M. and Kelly, M. G. (1975). "Atmospheric reaeration in a river using productivity analysis." *J. Environ. Eng. Div.-ASCE*, 101(EE5), 729-739.

House, W. A., Leach, D., Warwick, M. S., Whitton, B. A., Pattinson, S. N., Ryland, G., Pinder, A., Ingram, J., Lishman, J. P., Smith, S. M., Rigg, E., and Denison, F. H. (1997). "Nutrient transport in the Humber rivers." *Sci. Total Environ.,* 194/195, 303-320.

Hurlbert, S. H. (1984). "Pseudoreplication and the design of ecological field experiments.*" Ecol. Monogr.*, 54(2), 187-211.

Hynes, H. B. N. (1970). *The Ecology of Running Waters*, University of Toronto Press, Toronto.

IIHR Hydroscience and Engineering (2009). "Hydrologic Information System – HIS." <http://his08.iihr.uiowa.edu/uicc/> (July 13, 2009).

Iowa Department of Natural Resources (Iowa DNR) (2007a). "Iowa Section 303(d) Impaired Waters Listings." <http://wqn.igsb.uiowa.edu/wqa/downloads/303d.html#2004> (Apr. 5, 2007).

Iowa Department of Natural Resources (Iowa DNR) (2007b). "IA DNR: water quality standards." <http://www.iowadnr.com/water/standards/criteria.html> (Apr. 24, 2007).

Iowa Department of Natural Resources (Iowa DNR) (2008). "Welcome to the NRGIS library – Iowa Geological Survey – DNR" <http://www.igsb.uiowa.edu/nrgislibx/gishome.htm> (June 23, 2008).

Iowa Environmental Mesonet (IEM) (2008a). "IEM | Hourly Precip Grid." <http://mesonet.agron.iastate.edu/cgi-bin/precip/catAZOS.py?date=2007-06-22> (May 15, 2008).

Iowa Environmental Mesonet (IEM) (2008b). "IEM | ASOS Data." <http://mesonet.agron.iastate.edu/ASOS/> (May 15, 2008).

Iowa Rivers Information System (IRIS) (2008). "IRIS: Species by River." <http://maps.gis.iastate.edu/iris/data/searchlocation.jsp?huc10=0708020904&search=Clear+Creek&stype=stream> (July 7, 2008).

IOWATER (2007). *IOWATER Volunteer Water Quality Monitoring Program Manual*, Iowa Department of Natural Resources, Iowa City, IA.

IOWATER (2008). "IOWATER monitoring sites data view." <http://www.iowater.net/database/viewdata.asp> (Jan. 30, 2008).

Jensen, J. N. (2003). *A Problem-Soling Approach to Aquatic Chemistry*, John Wiley and Sons, Inc., Hoboken, New Jersey.

Judd, C. M., McClelland, G. H., and Ryan, C. S. (2009). *Data Analysis: A Model Comparison Approach, 2nd Edition*, Routledge, New York.

Justić, D., Rabalais, N. N., Turner, R. E., and Wiseman, W. J. (1993). "Seasonal Coupling between Riverborne Nutrients, Net Productivity and Hypoxia." *Mar. Pollut. Bull.*, 26(4), 184-189.

Justić, D., Rabalais, N. N., and Turner, R. E. (1996). “Effects of climate change on hypoxia in coastal waters: A doubled CO_2 scenario for the northern Gulf of Mexico.” *Limnol. Oceanogr.* 41(5), 992-1003.

Kannel, P. R., Lee, S., Kanel, S. R., Lee, Y. S., and Ahn, K. H. (2007). "Application of QUAL2Kw for water quality modeling and dissolved oxygen control in the river Bagmati." *Environ. Monit. Assess.*, 125(1-3), 201-217.

Kosinski, R. J. (1984). “A comparison of the accuracy and precision of several open-water oxygen productivity techniques.” *Hydrobiologia*, 119, 139-148.

Kosmulski, M. (2006). “pH-dependant surface charging and points of zero charge III. Update.” *J. Colloid Interface Sci.*, 298, 730-741.

Lewis, J. (1996). “Turbidity-controlled suspended sediment sampling for runoff-event load estimation.” *Wat. Resour. Res.,* 32(7), 2299-2310.

Lick, W.J. (2009). *Sediment and Contaminant Transport in Surface Waters*, CRC Press, Boca Raton, FL.

Lohrenz, S. E., Fahnenstiel, G. L., Redalje, D. G., Lang, G. A., Chen, X. G., and Dagg, M. J. (1997). "Variations in primary production of northern Gulf of Mexico continental shelf waters linked to nutrient inputs from the Mississippi River." *Mar. Ecol. Prog. Ser.*, 155, 45-54.

Loperfido, J.V., Just, C. L., and Schnoor, J. L. (2009a). “High-frequency Diel Dissolved Oxygen Stream Data Modeled for Variable Temperature and Scale.” *J. Environ Eng.*, Accepted.

Loperfido, J.V., Just, C.L., Papanicolaou, A.N., and Schnoor, J.L. (2009b). “High-frequency sensing to understand diel turbidity cycles, suspended solids and nutrient transport in Clear Creek, Iowa.” *Water Resour. Res.*, In Review.

Martinez-Manez, R., Soto, J., Garcia-Breijo, E., Gil, L., Ibanez, J., and Llobet, E. (2005). "An "electronic tongue" design for the qualitative analysis of natural waters." *Sensor. Actuat B-Chem.*, 104(2), 302-307.

Matthews, W. J. (1998). *Patterns in Freshwater Fish Ecology*, Chapman & Hall, New York.

Mayer, L. M., Keil, R. G., Macko, S. A., Joye, S. B., Ruttenberg, K. C., and Aller, R. C. (1998). “Importance of Suspended Participates in Riverine Delivery of Bioavailable Nitrogen to Coastal Zones.” *Global Biogeochem. Cy.,* 12(4), 573-579.

McTammany, M. E., Webster, J. R., Benfield, E. F., and Neatrour, M. A. (2003). “Longitudinal patterns of metabolism in a southern Appalachian river.” *J. N. Am. Benthol. Soc.*, 22(3), 359-370.

Mee, L. D. (2001). “Eutrophication in the Black Sea and a basin-wide approach to its control.” *Science and Integrated Coastal Management,* B. von Bodungen and R. K. Turner, eds., Dahlem University Press, Berlin, 71-91.

Meybeck, M., Idlafkih, Z., Fauchon, N., and Andereassian, V. (1999). "Spatial and temporal variability of Total Suspended Solids in the Seine basin." *Hydrobiologia*, 410, 295-306.

Miller, J. R. and Russell, G. L. (1992). "The Impact of Global Warming on River Runoff." *J. Geophys. Res.*, 97(D3), 2757-2764.

Milly, P. C. D., Betancourt, J., Falkenmark, M., Hirsch, R. M., Kundzewicz, Z. W., Lettenmaier, D. P., and Stouffer, R. J. (2008). "Stationary is dead: whither water management?" *Science*, 319, 573-574.

Montgomery, J. L., Harmon, T., Haas, C. N., Hooper, R., Clesceri, N. L., Graham, W., Kaiser, W., Sanderson, A., Minsker, B., Schnoor, J., and Brezonik, P. (2007). "The WATERS Network: An Integrated Environmental Observatory Network for Water Research." *Environ. Sci. Technol.*, 41(19), 6642-6647.

Moore, W. G. (1942). "Field Studies on the Oxygen Requirements of Certain Fresh-Water Fishes." *Ecology*, 23(3), 319-329.

Morse, J. T., Anderson, S. M., and Wilch, T. I. (2002). "Developing a management plan for a small, rural watershed in South-Central Michigan through monitoring of stream flow, turbidity, and temperature." *Proc, The Geological Society of America 2002 Denver Annual Meeting,* Denver, Co., Paper No. 66-1.

National Climatic Data Center (NCDC) (2008). "National Climatic Data Center (NCDC)*." <http://www.ncdc.noaa.gov/oa/ncdc.html> (Sept. 12, 2008).

National Climatic Data Center (NCDC) (2009). "National Climatic Data Center (NCDC)*." <http://www.ncdc.noaa.gov/oa/ncdc.html> (June. 17, 2009).

Natural Resources Conservation Service (NRCS) (2007). "NCSS Web Soil Survey" <http://websoilsurvey.nrcs.usda.gov/app/> (May 7, 2007).

National Weather Service (NWS) (2009). "National Weather Service – Central Region Headquarters Home Page" <http://www.crh.noaa.gov/images/dvn/downloads/Clim_IA_01.pdf> (April 24, 2009).

Nordberg, K., Filipsson, H. L., Gustafsson, M., Harland, R., and Roos, P. (2001). "Climate, hydrographic variations and marine benthic hypoxia in Koljo Fjord, Sweden." *J. Sea Res.*, 46(3-4), 187-200.

O'Connor, D. J. and Di Toro, D. M. (1970). "Photosynthesis and oxygen balance in streams." *J. Sanit. Eng. Div.-ASCE*, 96(SA2), 547-571.

Odum, H. T. (1956) "Primary production in flowing waters." *Limnol. Oceanog.*, 1, 102-117.

Park, S. S., and Lee, Y. S. (2002). "A water quality modeling study of the Nakdong River, Korea." *Ecol. Model.*, 152(1), 65-75.

Parkos III, J. J., Santucci, Jr., V. J., and Wahl, D. H. (2003). "Effects of adult common carp (*Cyprinus carpio*) on multiple trophic levels in shallow mesocosms." *Can. J. Fish. Aquat. Sci.*, 60, 182-192.

Pelletier, G. J., Chapra, S. C., and Tao, H. (2006). "QUAL2Kw - A framework for modeling water quality in streams and rivers using a genetic algorithm for calibration." *Environ. Modell. Softw.*, 21(3), 419-425.

Pflieger, W. L. (1997). *The Fishes of Missouri, Revised Ed.,* Conservation Commission of the State of Missouri, Jefferson City, MO.

Piegorsch, W. W. and Bailer, A. J. (2005). *Analyzing Environmental Data,* John Wiley and Sons, Ltd, West Sussex, England.

Preston, S. D., Alexander, R. B., Woodside, M. D., and Hamilton, P. A. (2009). *SPARROW MODELING-Enhanced Understanding of the Nation's Water Quality*, USGS Fact Sheet 2009-3019, 6 p.

Pullar, D., and Springer, D. (2000). "Towards integrating GIS and catchment models." *Environ. Modell. Softw.*, 15(5), 451-459.

Pulliam, J. (2005). "Small Town Pollutes Tributary." *Daily Iowan*, July 5, Metro Section.

Quinn, J. M., Davies-Colley, R. J., Hickey, C. W., Vickers, M. L., and Ryan, P. A. (1992). "Effects of clay discharges on streams 2. Benthic invertebrates." *Hydrobiologia*, 248, 235-247.

Rae, R. and Vincent, W. F. (1998). "Phytoplankton production in subarctic lake and river ecosystems: development of a photosynthesis-temperature-irradiance model." *J. Plankton Res.*, 20(7), 1293-1312.

Rabalais, N. N., Turner, R. E., Justic´, D., Dortch, Q., and Wiseman Jr., W. J. (1999). "Characterization of Hypoxia: Topic 1 Report for the Integrated Assessment of Hypoxia in the Gulf of Mexico." *NOAA Coastal Ocean Program Decision Analysis Series No. 15.* NOAA Coastal Ocean Program, Silver Spring, MD. 167 pp.

Rabalais, N. N., Turner, R. E., and Wiseman, W. J. (2001). "Hypoxia in the Gulf of Mexico." *J. Environ. Qual.*, 30(2), 320-329.

Rabalais, N. N., Turner, R. E., and Wiseman, W. J. (2002). "Gulf of Mexico hypoxia, aka "The dead zone"." *Annu. Rev. Ecol. Syst.*, 33, 235-263.

Rabalais, N. N., Wiseman, W. J., Turner, R. E., SenGupta, B. K., and Dortch, Q. (1996). "Nutrient changes in the Mississippi River and system responses on the adjacent continental shelf." *Estuaries*, 19(2B), 386-407.

Ravisanger, V., Dennett, K. E., Sturm, T. W., and Amirtharajah, A. (2001). "Effect of sediment pH on resuspension of kaolinite sediments." *J. Environ. Eng.*, 127(6), 531-538.

Reynolds, W. W. and Casterlin, M. E. (1978a). "Behavioral thermoregulation and diel activity in white sucker (*Catostomus commersoni*)." *Comp. Biochem. Physiol.*, 59A, 261-262.

Reynolds, W. W. and Casterlin, M. E. (1978b). "Ontogenetic change in preferred temperature and diel activity of the yellow bullhead, *Ictalurus natalis*." *Comp. Biochem. Physiol.*, 59A, 409-411.

Rogers, K. R. (2006). “Recent advances in biosensor techniques for environmental monitoring.” *Anal. Chim. Acta.,* 568, 222-231.

Rosenberg, R. (1985). "Eutrophication-the future marine coastal nuisance?" *Mar. Pollut. Bull.*, 16(6), 227-231.

Royer, T. V., David, M. B., and Gentry, L. E. (2006). "Timing of riverine export of nitrate and phosphorus from agricultural watersheds in Illinois: Implications for reducing nutrient loading to the Mississippi River." *Environ. Sci. Technol.*, 40(13), 4126-4131.

Ryan, P. A. (1991). “Environmental effects of sediment on New Zealand streams: a review.” *N. Z. J. Mar. Freshwat. Res.*, 25, 207-221.

Schaetzl, R. J. and Anderson, S. (2005). *Soils: Genesis and Geomorphology*, Cambridge University Press, Cambridge, UK.

Schnoor, J. L. (1996). *Environmental Modeling: Fate and Transport of Pollutants in Water, Air, and Soil*, John Wiley & Sons, Inc., New York.

Schoellhamer, D. H. (2002). “Variability of suspended-sediment concentration at tidal to annual time scales in San Francisco Bay, USA.” *Cont. Shelf Res.*, 22, 1857-1866.

Schroth, B. K., and Sposito, G. (1997). “Surface charge properties of kaolinite.” *Clays Clay Miner.*, 45(1), 85-91.

Schwarz, G. E., Hoos, A. B., Alexander, R. B., and Smith, R. A. (2006). *The SPARROW Surface Water-Quality Model: Theory, Application and User Documentation*, USGS Techniques and Methods, Book 6, Section B, Chapter 3.

Snoeyink, V. L. and Jenkins, D. (1980). *Water Chemistry,* John Wiley & Sons., Inc, New York.

Sparks, B. L. and Strayer, D. L. (1998). “Effects of low dissolved oxygen on juvenile *Elliptio complanata* (Bivalvia:Unionidae).” J. N. Am. Benthol. Soc., 17(1), 129-134.

Streeter, H. W., and Phelps, E. B. (1925). “A study of pollution and natural purification of the Ohio River III: Factors concerned in the phenomena of oxidation and reaeration.” *Bulletin 146*, *U.S. Health, Educational and Welfare*, Public Health Service, Washington D.C.

Strock, J. S., Bruening, D., Apland, J. D., and Mulla, D. J. (2005). "Farm nutrient management practices in two geographically diverse watersheds in the cottonwood river watershed of Minnesota, USA." *Water Air Soil. Poll.*, 165(1-4), 211-231.

Suzuki, T. (2001). "Oxygen-deficient waters along the Japanese coast and their effects upon the estuarine ecosystem." *J. Environ. Qual.*, 30(2), 291-302.

Tränkler, H. R. and Kanoun, O. (2001) “Recent Advances in Sensor Technology.“ Proc. IEEE Instrum. Meas. Tech. Conf., Budapest, Hungary, May 21-23.

Thoning, K. W., Tans, P. P., and Komhyr, W. D. (1989). “Atmospheric Carbon Dioxide at Mauna Loa Observatory 2. Analysis of the NOAA GMCC Data, 1974-1985.” *J. Geophys. Res.*, 94(D6), 8549-8565.

Tomer, M. D., Meek, D. W., Jaynes, D. B., and Hatfield, J. L. (2003). "Evaluation of nitrate nitrogen fluxes from a tile-drained watershed in central Iowa." *J. Environ. Qual.*, 32(2), 642-653.

United States Environmental Protection Agency (US EPA) (2000). "Water Quality Conditions in the United States – A Profile from the 1998 National Water Quality Inventory Report to Congress." *Rep. No. EPA841-F-00-006,* Washington, D.C.

United States Environmental Protection Agency (US EPA) (2007a). "Task Force < Mississippi River Basin." <http://www.epa.gov/msbasin/taskforce/actionplan.htm> (May 21, 2007).

United States Environmental Protection Agency (US EPA) (2007b). "Water Quality Models and Tools | Water Science and Technology | US EPA" <http://www.epa.gov/waterscience/models/> (Apr. 24, 2007).

United States Geological Survey (USGS) (2008a). "USGS Water data for the Nation" <http://waterdata.usgs.gov/nwis/ > (May 21, 2008).

United States. Geological Survey (USGS). (2008b). "USGS Surface Water data for USA: USGS Surface-Water Annual Statistics." <http://waterdata.usgs.gov/nwis/annual/?referred_module=sw> (Jan. 30, 2008).

Wang, H., Hondzo, M., Xu, C., Poole, V., and Spacie, A. (2003). "Dissolved oxygen dynamics of streams draining an urbanized and an agricultural catchment." *Ecol. Model.*, 160, 145-161.

Washington State Department of Ecology (2007). "Environmental Assessment Program – Models for TMDLs." < http://www.ecy.wa.gov/programs/eap/models.html> (April. 24, 2007).

WATERS Network (2009). "WATERS Network | Home." <http://www.watersnet.org/> (May 4, 2009).

Wilcock, R. J., Nagels, J. W., McBride, G. B., Collier, K. J., Wilson, B. T., and Huser, B. A. (1998). "Characterisation of lowland streams using a single-station diurnal curve analysis model with continuous monitoring data for dissolved oxygen and temperature." *New Zeal. J. Mar. Fresh.*, 32, 67-79.

Wiley, M. J., Osborne, L. L., and Larimore, R. W. (1990). "Longitudinal structure of an agricultural prairie river system and its relationship to current stream ecosystem theory." *Can. J. Fish. Aquat. Sci.*, 47, 373-384.

Williams, R. J., White, C., Harrow, M. L., and Neal, C. (2000). "Temporal and small-scale spatial variations of dissolved oxygen in the Rivers Thames, Pang and Kennet, UK." *Sci. Total Environ.*, 251/252, 497-510.

Wool, T. A., Ambrose, R. B., Martin, J. L., and Comer, E. A.(2008). *Water Quality Analysis Simulation Program (WASP) Version 6.0, DRAFT: User's Manual*, US Environmental Protection Agency – Region 4, Atlanta, GA.

Zambrano, L. and Hinojosa, D. (1999). "Direct and indirect effects of carp (*Cyprinus carpo* L.) on macrophyte and benthic communities in experimental shallow ponds in central Mexico." *Hydrobiologia,* 408/409, 131-138.

Zimmerman, J. B., Mihelcic, J. R., and Smith, J. (2008) "Global Stressors on Water Quality and Quantity." *Environ*. *Sci*. *Technol*. 42(12), 4247-4254.